# *Glycals as probes for mechanistic studies of glycosylases*

by

Ellen Chui-Kwan Lai

B.Sc., The University of Waterloo, 1985
M.Sc., The University of Waterloo, 1987

A THESIS SUBMITTED IN PARTIAL FULFILMENT OF

THE REQUIREMENTS FOR THE DEGREE OF

DOCTOR OF PHILOSOPHY

in

THE FACULTY OF GRADUATE STUDIES

**Department of Chemistry**

We accept this thesis as conforming

to the required standard:

THE UNIVERSITY OF BRITISH COLUMBIA

November, 1994.

(Signature)

Department of _____CHEMISTRY_____

The University of British Columbia
Vancouver, Canada

Date _____Nov 21, 94_____

DE-6 (2/88)

# ABSTRACT

Several derivatives of D-*gluco*-heptenitol and D-glucal were synthesized and used to study the reaction mechanisms of three glycosylases (glycosyl mobilizing enzymes): glycogen phosphorylase, β-glucosidase, and β-*N*-acetylhexosaminidase. 1-Fluoro-D-*gluco*-heptenitol ($F_1$hept) and 1,1-difluoro-D-*gluco*-heptenitol ($F_2$hept) acted as competitive inhibitors of glycogen phosphorylase *b*, and collaborative X-ray crystallographic studies revealed that both $F_1$hept and $F_2$hept bind to the active site. Furthermore, $F_1$hept and phosphate bind simultaneously, allowing crystallographic investigation of a stable ternary complex.

Various glycals were examined as potential substrates (catalytically *hydrated* by the enzyme), or as potential inhibitors or inactivators (of the *hydrolysis* of a glucoside substrate), of *Agrobacterium* β-glucosidase. Both heptenitol and methylglucal acted as substrates of this enzyme. Enzymatic protonation of the double bond of methylglucal occurred from below the ring. $F_1$hept and $F_2$hept acted as noncompetitive (or uncompetitive) inhibitors, as did heptenitol (at concentrations < 8 m$M$).

α,β-Unsaturated glucals, which might act as Michael acceptors for a nucleophilic residue in the active site of a glycosylase, were investigated as a new class of potential inactivators of *Agrobacterium* β-glucosidase. 1-Nitroglucal functioned as a time-dependent inactivator, probably as a result of a Michael addition reaction between 1-nitroglucal and a nucleophilic residue in the active site. However, protein mass spectrometry revealed that in most cases more than one equivalent of 1-nitroglucal bound to the enzyme. Unfortunately, other α,β-unsaturated glucals that were examined [1-cyano-, 1-(methyl carboxylate)-, sodium 1-(carboxylate)-, and 2-cyano- derivatives of glucal] only acted as reversible inhibitors.

Three β-*N*-acetylhexosaminidases (human placenta, jack bean, and bovine kidney) were also studied, and shown to hydrolyze an *N*-acetylglucosaminide substrate with net retention of anomeric configuration. All three enzymes hydrated 2-acetamido-D-glucal, yielding *N*-acetyl-D-glucosamine as the product in each case. This is the first time that proton transfer has been shown to occur from the top face during the hydration of a glycal by a 'retaining' β-glycosidase. 2-Acetamido-D-glucal bound tightly to the human, bovine, and jack bean enzymes, with $K_i$ values of 8.5, 25, and 29 μ$M$, respectively.

# TABLE OF CONTENTS

# LIST OF TABLES

# LIST OF FIGURES

# LIST OF REACTION SCHEMES

## ABBREVIATIONS AND SYMBOLS

| | |
|---|---|
| $A_{280}^{0.1\%}$ | The absorbance (per unit pathlength) of a 0.1% (1 mg/mL) solution at 280 nm. |
| $A\lambda$ | Absorbance at wavelength $\lambda$ (where $\lambda$ is given in nm). |
| ADP | Adenosine 5'-diphosphate. |
| AMP | Adenosine 5'-monophosphate. |
| Asn | L-Asparagine [(+)-3-aminobutanedioic acid 1-amide]. |
| Asp | L-Aspartatic acid [(+)-2-aminobutanedioic acid]. |
| ATP | Adenosine 5'-triphosphate. |
| ax | Axial. |
| BES | $N$, $N$-(Bis-2-hydroxyethyl)-2-aminoethanesulfonic acid. |
| BSA | Bovine serum albumin. |
| $C$-terminal | Carboxy terminal (end of a peptide or protein). |
| conj. | Conjugate. |
| Cp | Cyclopentadienyl. |
| $Cp_2TiCl_2$ | Titanocene dichloride. |
| $Cp_2TiMe_2$ | Dimethyl titanocene. |
| DCI | Desorption chemical ionization. |
| $1d\beta Glc\phi$ | 1-Deoxy-$\beta$-D-glucosylbenzene. |
| $\alpha$DKIE | $\alpha$-Secondary deuterium kinetic isotope effect. |
| DMF | Dimethylformamide. |
| DTT | Dithiothreitol. |
| E | Enzyme. |
| E.C. | Enzyme Commission (classification number) of the International Union of Biochemistry. |
| EDTA | Ethylenediaminetetraacetic acid. |
| $\epsilon\lambda$ (epsilon) | Molar extinction coefficient at wavelength $\lambda$. |
| eq | Equatorial. |
| ES | Enzyme-substrate complex. |
| $F_1hept$ | 1-Fluoroheptenitol. |
| $F_2hept$ | 1,1-Difluoroheptenitol. |
| FAB | Fast atom bombardment. |
| $2F\beta GlcDNP$ | 2',4'-Dinitrophenyl 2-deoxy-2-fluoro-$\beta$-D-glucopyranoside. |
| $G_n$ (or $G_{n+1}$) | Glycogen. |
| $\alpha$G1P | $\alpha$-D-Glucose-1-phosphate ($\alpha$-D-glucopyranosyl phosphate). |
| $\beta$GlcDNP | 2',4'-Dinitrophenyl $\beta$-D-glucopyranoside. |
| GlcNAc | $N$-Acetyl-D-glucosamine. |
| $\beta$GlcNAcMu | 4'-Methylumbelliferyl 2-deoxy-2-acetamido-$\beta$-D-glucosaminide. |
| $\beta$GlcNAcPNP | 4'-Nitrophenyl $N$-acetyl-$\beta$-D-glucosaminide. |
| $\beta$GlcPNP | 4'-Nitrophenyl $\beta$-D-glucopyranoside. |
| Glu | L-Glutamic acid [(+)-2-aminopentanedioic acid]. |
| Gly | Glycine [aminoethanoic acid]. |
| H-NAGase | $\beta$-$N$-Acetylhexosaminidase isolated from human placenta. |
| HEPES | $N$-[2-Hydroxyethyl]piperazine-$N'$-[2-ethanesulfonic acid]. |
| His | L-Histidine [$(S)$-2-amino-3-(4-imidazolyl)propionic acid]. |
| HMPA | Hexamethyl phosphoramide, $(Me_2N)_3PO$. |
| HMPT | Tris(dimethylamino)phosphine, $(Me_2N)_3P$. |
| HPLC | High-pressure liquid chromatography. |
| I | Inhibitor. |
| IR | Infrared (spectroscopy). |

| | |
|---|---|
| $J$ | Coupling constant. |
| J-NAGase | $\beta$-$N$-Acetylhexosaminidase isolated from jack bean. |
| K-NAGase | $\beta$-$N$-Acetylhexosaminidase isolated from bovine kidney. |
| $k_{cat}$ | Catalytic rate constant (turnover number). |
| $k_i$ | Maximum first-order rate constant for inactivation. |
| $k_{obs}$ | Pseudo first-order rate constant for inactivation. |
| $K_i$ | Dissociation constant for an enzyme-inhibitor complex. |
| $K_m$ | Michaelis constant of a substrate. |
| $K_{m,app}$ | Apparent Michaelis constant of a substrate (in the presence of an inhibitor). |
| $\lambda_{max}$ | Wavelength (nm) of maximum absorbance. |
| Lys | L-Lysine [$(S)$-2,6-diaminohexanoic acid]. |
| ManNAc | $N$-Acetyl-D-mannosamine. |
| min | Minutes. |
| $M_r$ | Relative molecular mass. |
| MS | Mass spectrometry. |
| $N$-terminal | Amino terminal (end of a peptide or protein). |
| $\beta$NADP | $\beta$-Nicotinamide adenine dinucleotide phosphoric acid. |
| NAGase | $\beta$-$N$-Acetylhexosaminidase. |
| NAGlucal | 2-Acetamido-D-glucal. |
| NBS | $N$-Bromosuccinimide. |
| NMR | Nuclear magnetic resonance. |
| NOE | Nuclear Overhauser effect. |
| $v$ (nu) | Wavenumber. |
| Nu | Nucleophile. |
| p | Negative logarithm of (e.g., equilibrium constant, p$K$). |
| p (or P) | Phosphate. |
| P | Product. |
| pABG5 | *Agrobacterium* $\beta$-glucosidase (cloned and expressed in *E. coli*). |
| PL | Pyridoxal. |
| PLP | Pyridoxal 5'-phosphate. |
| $R_f$ | Retardation factor. |
| Red Al® | Sodium bis(2-methoxyethoxy) aluminum hydride. |
| *RF* | Range-finding (or approximate). |
| Ser | L-Serine [$(S)$-2-amino-3-hydroxypropionic acid]. |
| TBAF | Tetra($n$-butyl)ammonium fluoride. |
| TBDMS | $t$-Butyldimethylsilyl. |
| TEA | Triethanolamine. |
| THF | Tetrahydrofuran. |
| ~ (tilde) | Approximately. |
| TLC | Thin-layer chromatography. |
| U | Units of enzyme activity. |
| UV | Ultraviolet (light). |
| v | Volume. |
| $v$ | Reaction velocity. |
| $V_{max}$ | Maximal reaction velocity. |
| VIS | Visible (light). |

**In most cases, the following were not listed:**

(1) SI units and prefixes.
(2) Abbreviations and symbols used for systematic chemical nomenclature.

# ACKNOWLEDGMENTS

**DEDICATION**

*With thankfulness to God for my dear parents,*

*Lai Wai Hum and Chung Sau Chun.*

**CHAPTER 1: GENERAL INTRODUCTION**

*1.1. GLYCOSYLASES AND THE REACTIONS THEY CATALYZE.*

Carbohydrates play central roles in energy metabolism, cell-cell recognition, and a variety of other important biological processes, and glycosyl hydrolysis and glycosyl transfer are important biochemical reactions. Glycosylases (or glycosyl mobilizing enzymes) are enzymes that utilize a glycoside (such as glycogen, α- or β-glucosides, or β-N-acetylhexosaminides) as a substrate, and yield a product that contains a glycosyl residue. In the general reaction mechanism of these enzymes the aglycone moiety is replaced by either water (for hydrolytic reactions) or some other glycosyl acceptor (i.e., in transfer reactions) to yield the product (see Scheme 1.1).
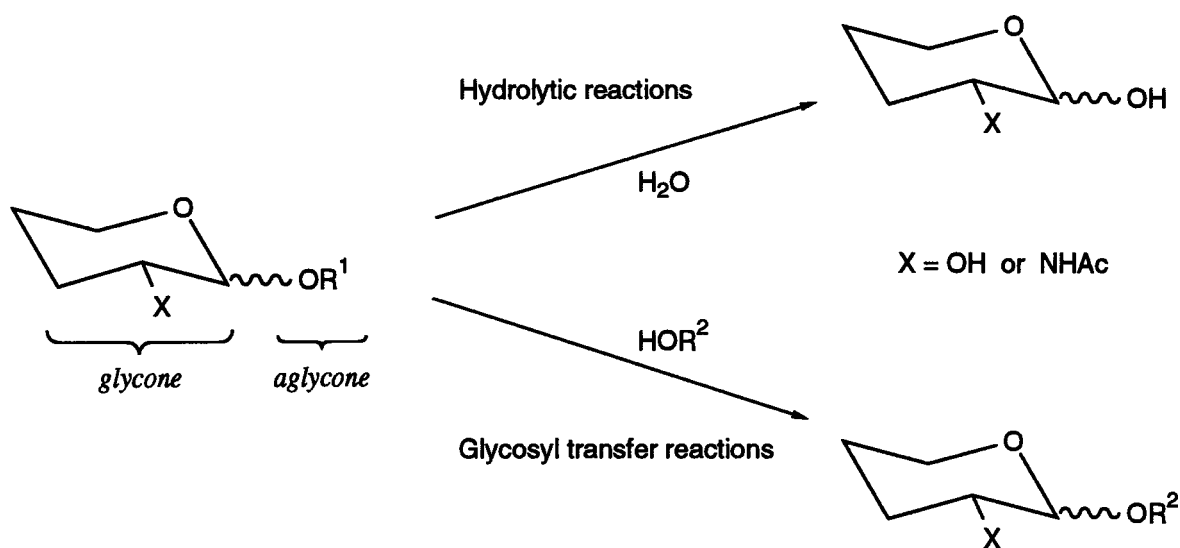


**Scheme 1.1.** The hydrolytic and glycosyl transfer reactions catalyzed by glycosylases.

For the enzymes studied in this thesis, the natural substrate substituents are:

β-glucosidase:             $R^1$ = glucose (in cellobiose) or some other aglycone
glycogen phosphorylase:    $R^1$ = glycogen         $R^2$ = phosphate
β-N-acetylhexosaminidase:  $R^1$ = a ganglioside     X = NHAc (a 2-acetamido group)

The reaction mechanisms of three glycosylases were studied in this thesis: glycogen phosphorylase, β-glucosidase, and β-N-acetylhexosaminidase (NAGase). Briefly, glycogen phosphorylase catalyzes the interconversion of glucosyl-phosphate linkages (in α-glucose-1-phosphate, or αG1P) and glucosidic linkages (in glycogen, a highly branched homopolysaccharide of D-glucose units that is the major form of storage carbohydrate in animal cells). β-Glucosidase catalyzes the hydrolysis of β-glucosides (e.g., cellobiose) to yield glucose. NAGase catalyzes the hydrolytic removal of the N-acetylglucosamine (GlcNAc) residue from gangliosides (oligosaccharide-containing ceramide lipids). Some of the functions and specific features of each enzyme will be discussed in subsequent chapters of this thesis.

## 1.2. THE CLASSIFICATION OF GLYCOSYLASES.

Glycosylases can be divided into several different classes based on several different characteristics. These enzymes can be classified as "retaining" or "inverting" according to the relative anomeric configurations of the substrate cleaved and the product formed (see Scheme 1.2). Another classification is based on the sugar (glycone) moiety of the glycoside that the enzyme can accept as a substrate (e.g., glucosidases are most reactive towards glucosides). Finally, these enzymes can be classified as "α" or "β" depending on the anomeric configuration of the glycoside that the enzyme can accept as a substrate.
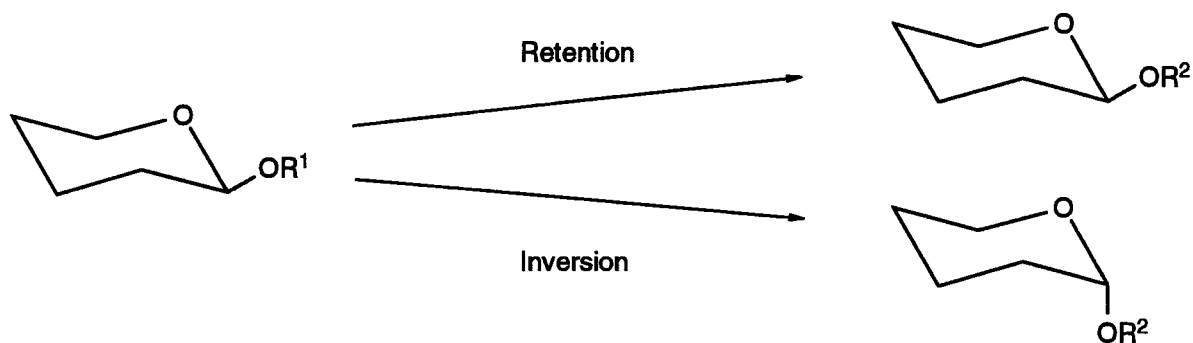


Scheme 1.2. The distinction between "retaining" and "inverting" glycosylases.

Of the enzymes studied in this thesis, glycogen phosphorylase is classified as an α-retaining glycosylase, whereas β-glucosidase from *Agrobacter sp.* is β-retaining. In most cases the stereochemical outcome of the hydrolysis of β-*N*-acetylglycosaminides by NAGases is not reported, and a determination of the stereochemistry of this reaction was in fact one of the objectives of this work.
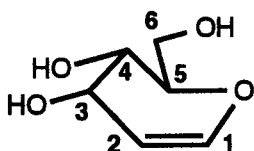


[1.1]
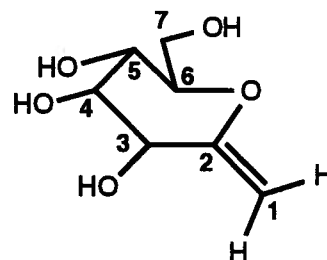
[1.2]

The *anomeric* specificity of glycosylases is typically absolute, e.g., a β-glucosidase exhibits no enzymatic activity towards an α-glucoside. However, certain compounds *without* a glycosidic bond—and therefore lacking the appropriate α- or β-aglycone group—can act as substrates for either α- or β-glycosylases (or both). Examples of such nonglycosidic substrates are glycals (e.g., 1,5-anhydro-2-deoxy-D-hex-1-enitol, see 1.1 above) and heptenitols (e.g., 2,6-anhydro-1-deoxy-D-*gluco*-hept-1-enitol, see 1.2 above) (Hehre et al., 1977). Examples of the corresponding reactions include the ability of glycogen phosphorylase to convert heptenitol (and phosphate) to 1-deoxy-D-*gluco*-heptulose-2-phosphate, and the ability of β-glucosidase to hydrate heptenitol to form 1-deoxy-D-*gluco*-heptulose, and to hydrate D-glucal to form 2-deoxy-D-glucose. Glycosylases stereospecifically catalyze these reactions with nonglycosidic substrates. The same stereochemical outcome (α or β product) is obtained from catalytic reactions with a glycal and with a natural substrate. A detailed account of the glycosylase-catalyzed reactions of glycals is provided later in this chapter.

## *1.3. GENERAL FEATURES OF THE CATALYTIC MECHANISM OF RETAINING GLYCOSYLASES.*

### 1.3.1. Overview.

Koshland (1953) was the first to propose that catalysis by retaining glycosylases involves a double-displacement reaction mechanism. This mechanism has subsequently received considerable experimental support, and is now believed to include the following general features (see Scheme 1.3):
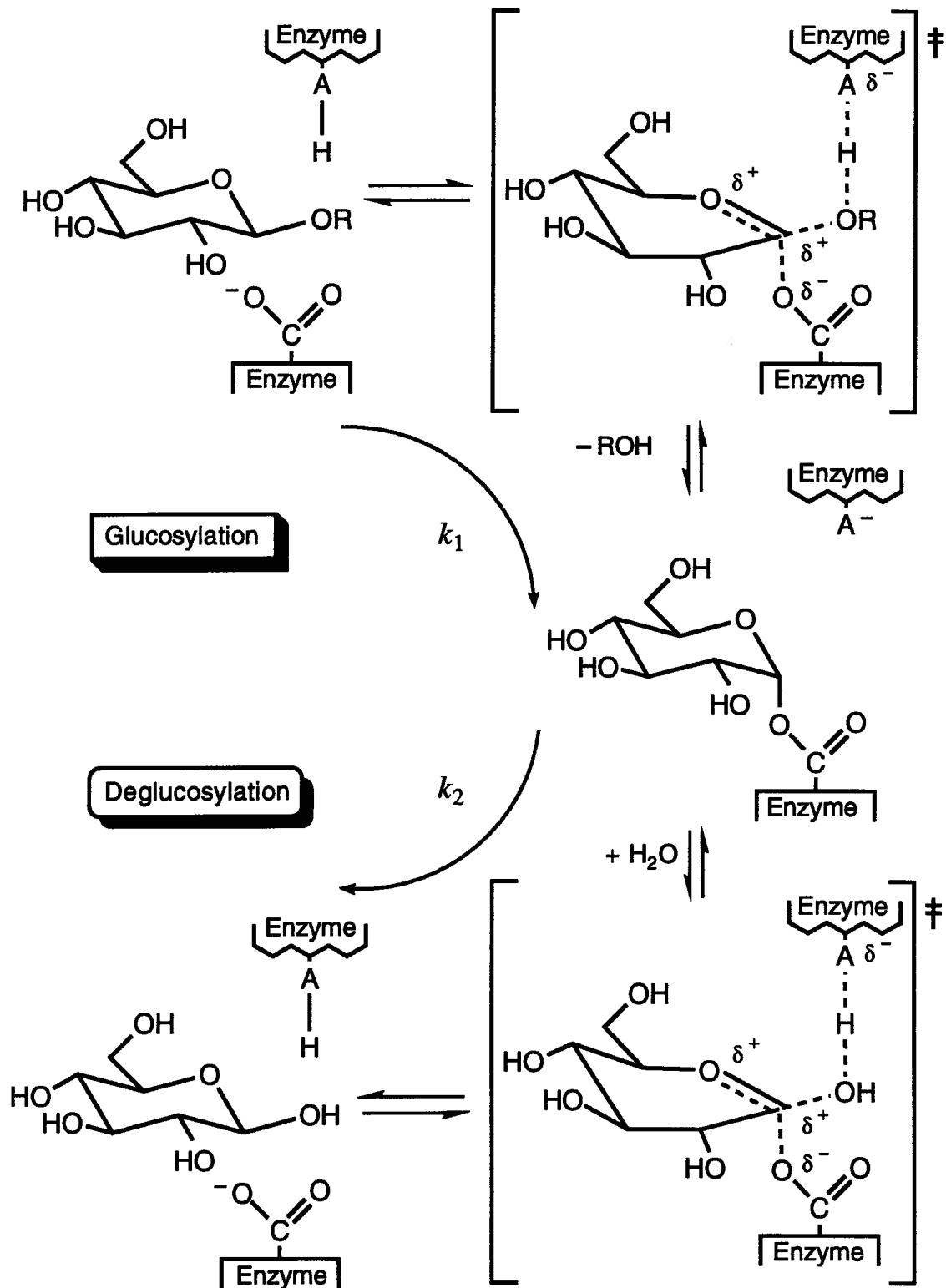
**Scheme 1.3.** The proposed mechanism for β-glucosidase-catalyzed hydrolysis of β-glucosides.

(i) *Acid catalysis* promotes the departure of the aglycone group of certain substrates.

(ii) In the active site of the enzyme, the *carboxylate group* of an acidic amino acid residue of the protein is located next to the anomeric centre of the glycoside substrate. This carboxylate group is on the opposite side of the sugar ring relative to the aglycone.

(iii) A *covalent glycosyl-enzyme intermediate* forms between the carboxylate of the enzyme and C-1 of the sugar.

(iv) *Oxocarbonium ion-like transition states* may be involved in both the formation and breakdown of the covalent glycosyl-enzyme intermediate.

(v) Various *noncovalent interactions* accelerate the rate of the reaction.

## 1.3.2. General acid catalysis.

The departure of the aglycone leaving group is believed to be catalyzed by protonation of the sugar by the side chain of an acidic amino acid residue in the enzyme's active site. In hen egg white lysozyme, Glu 35 has been identified as a catalytically important acidic residue by X-ray crystallography (Imoto et al., 1972). However, the acidic residue may not need to be a carboxyl side chain.

Additional evidence for the role of general acid catalysis was obtained from studies of the glycosylase-catalyzed hydration of glucal and heptenitol (Hehre et al., 1977; Schlesselmann et al., 1982). These studies found that an acidic residue is essential for the protonation of the enolic double bond in such substrates, and that this protonation event is a prerequisite for subsequent nucleophilic attack by water (in hydration reactions catalyzed by $\beta$-glucosidase) or phosphate (in glycosyl transfer reactions catalyzed by glycogen phosphorylase) (Klein et al., 1982).

The importance of general acid catalysis in the reaction mechanism of glycosylases is variable, and in some cases it may not occur at all. For example, it is structurally impossible to protonate glycosyl pyridinium salts. Yet these compounds are hydrolyzed by glycosylases, and the observed rate increases for the hydrolysis of these compounds by $\beta$-galactosidase is $10^8$-$10^{13}$-fold compared with the rate of spontaneous hydrolysis (Sinnott, 1979). Clearly these dramatic rate increases are effected by a reaction mechanism that does not require general acid catalysis.

### 1.3.3. The carboxylate group in the active site.

*a. X-ray structural studies.*

The first evidence for the presence of a strategically placed carboxylate group in the active site was provided by X-ray crystallographic studies of lysozyme, a glycosylase that catalyzes the hydrolysis of polysaccharides in the glycopeptide layer of bacterial cell walls (Scheme 1.4). X-ray diffraction methods have been used to determine the structures of the lysozymes of bacteriophage T4 and hen egg white (Anderson et al., 1981; Imoto et al., 1972), and strategically placed carboxylate groups were observed in the active sites of both enzymes (the side chains of Asp 20 and Asp 52, respectively).
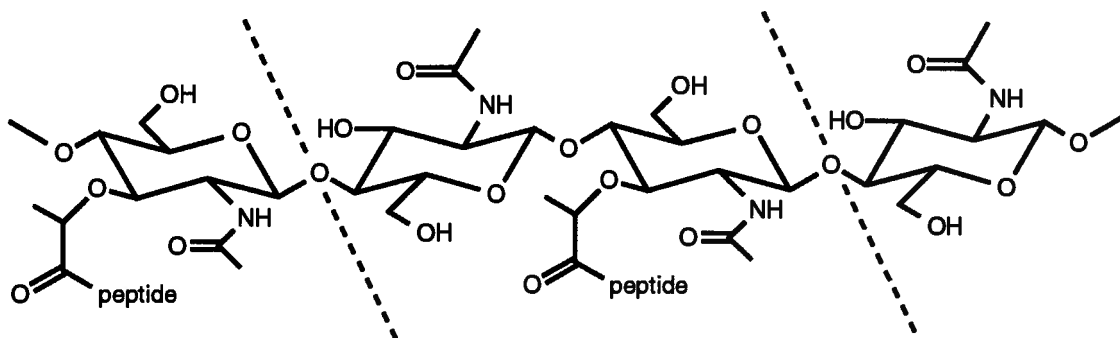


**Scheme 1.4.** Bacterial cell wall hydrolysis catalyzed by lysozyme.

The glycosidic bond that is cleaved is indicated by the dotted lines.

*b. Fluoro sugars.*

Direct evidence for the role of a carboxylate group during catalysis was provided by Withers et al. (1990), who devised a novel class of inhibitors (exemplified by 2',4'-dinitrophenyl 2-deoxy-2-fluoro-β-D-glucopyranoside, 2FβGlcDNP, see **1.3** below) to trap and identify the amino acid residue involved. These "mechanism-based" inhibitors cause the enzyme to catalyze its own inactivation. The normal catalytic activity

of the target enzyme results in the formation of a covalent bond between the inhibitor molecule and a catalytically reactive residue in the enzyme's active site.

The substitution of an electron-withdrawing fluorine atom at C-2 in 2FβGlcDNP, immediately adjacent to the reaction centre at C-1, inductively destabilizes *both* transition states (see Scheme 1.3). This decreases both the rate of formation ($k_1$) and the rate of hydrolysis ($k_2$) of the glycosyl-enzyme intermediate. The presence of a highly reactive leaving group (2,4-dinitrophenol) in the glycoside *increases $k_1$ only* (it does not affect $k_2$). The combination of the inductive and leaving-group effects results in the accumulation of the glycosyl-enzyme intermediate. Thus when the radiolabeled, mechanism-based inhibitor [1-$^3$H]-2FβGlcDNP was used with *Agrobacterium* β-glucosidase, it identified Glu 358 as an active-site nucleophile of this enzyme (Withers et al., 1990).



[1.3]          [1.4]          [1.5]
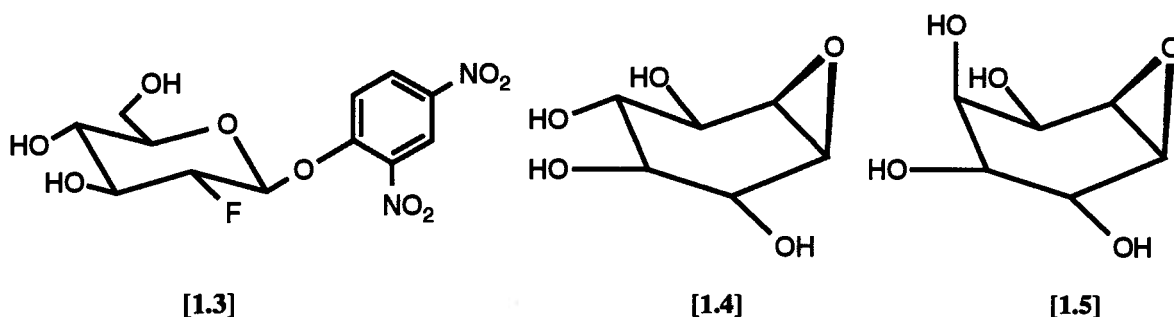
*c. Conduritol epoxides.*

Similar evidence identifying the active-site nucleophile as a carboxylate moiety has been obtained using another class of inactivators of glycosylases. Conduritol epoxides (with the appropriate configuration, e.g., 1.4, conduritol B epoxide) are a class of synthetic mechanism-based inactivators that have been used in the affinity labeling of active-site residues (an aspartate residue in each case) in three different retaining β-glucosidases: enzymes isolated from the fungus *Aspergillus wentii*, bitter almonds, and lysosomes from human placenta (Bause & Legler, 1974; Dinur et al., 1986; Legler & Harder, 1978). D-Glucal has also been used to label the active-site nucleophile of *Aspergillus wentii* β-glucosidase, and this study identified the same aspartate residue as the active site nucleophile as was determined using conduritol B epoxide (Legler et al., 1979).

Conduritol C *cis*-epoxide **(1.5)** was used to identify Glu 461 as a residue that was thought to be the active-site nucleophile of *E. coli* β-galactosidase (Herrchen & Legler, 1984). However, a subsequent study using the tritiated, mechanism-based inhibitor [1-$^3$H]-2FβGalDNP identified Glu 537 as the active-site nucleophile in this enzyme (Gebler et al., 1992). This latter study concluded that Glu 461 acts instead as a general acid-base catalyst during the reaction mechanism.

Conduritol epoxides exploit the normal catalytic features of glycosylases to inactivate these enzymes (see Scheme 1.5). In the active site the side chain of an acidic amino acid (AH) transfers a proton to the oxirane ring of the inactivator. A carboxylate group of an amino acid in the enzyme's active site then forms an ester bond with the activated oxirane, yielding a covalent enzyme-inactivator complex.
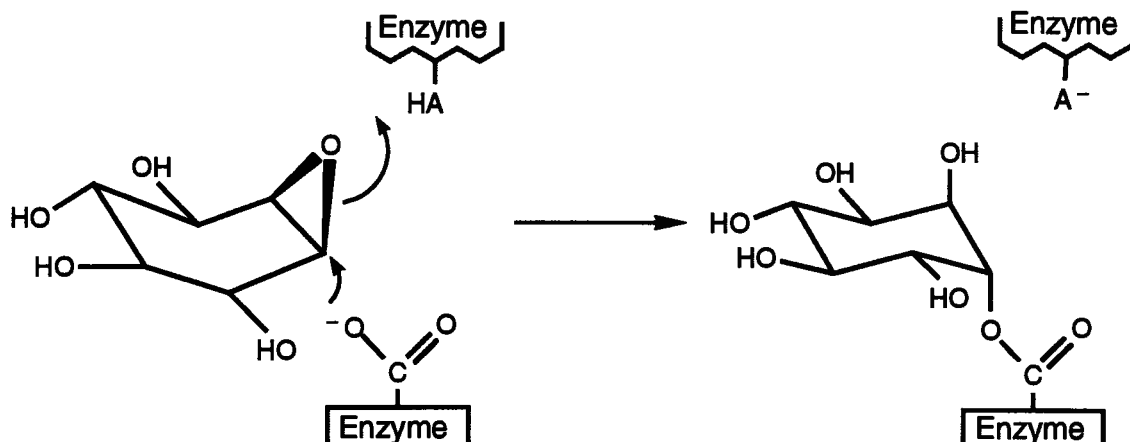


**Scheme 1.5.** The proposed mechanism for the inactivation of β-glucosidases by conduritol epoxides.

*d. Cyclophellitol.*

Cyclophellitol **(1.6)** is a natural product that was initially isolated from culture filtrates of the mushroom *Phellinus sp.* (Atsumi et al., 1990a), and subsequently prepared synthetically by Tatsuta et al. (1990). The structure of cyclophellitol differs from conduritol B epoxide **(1.4)** in that the former has a hydroxymethyl group at C-5, and is therefore more similar to the structure of a β-glucoside. Preliminary kinetic studies showed

that cyclophellitol acts as an inhibitor of β-glucosidases (Atsumi et al., 1990a, 1990b). More detailed kinetic studies with several α- and β-glucosidases showed that cyclophellitol is a highly stereospecific covalent inactivator of β-glucosidases from almond and *Agrobacter sp.*, with inactivation constants of [$K_i$ = 0.34 m$M$, $k_i$ = 2.38 min$^{-1}$] and [$K_i$ = 0.055 m$M$, $k_i$ = 1.26 min$^{-1}$], respectively (Withers & Umezawa, 1991). By comparison, conduritol B epoxide (1.4), which inactivates almond β-glucosidase B with inactivation constants of $K_i$ = 1.7 m$M$, $k_i$ = 0.13 min$^{-1}$, is 92-fold less effective than cyclophellitol based on relative $k_i/K_i$ values (Legler & Hasnain, 1970). Due to the very high stereochemical specificity of cyclophellitol, no time-dependent inactivation of yeast α-glucosidase is observed, and only extremely slow inactivation ($t_{1/2}$ > 5 hours) of *E. coli* β-galactosidase can be detected (Withers & Umezawa, 1991).



[1.6]
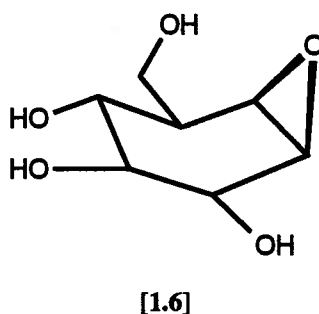
*e. N-Acetylconduramine B trans-epoxide.*

The successful inactivation of various glycosylases by conduritol epoxides inspired the use of *N*-acetylconduramine B *trans*-epoxide (1.7) in an attempt to inactivate NAGases from various sources (Legler & Bollhagen, 1992). Although this compound strongly inhibits NAGases isolated from bovine kidney, jack bean, and the gastropod *Helix pomatsia* (with $K_i$ values of 0.50 to 1.6 μ$M$, i.e., 500-8,000-fold lower than the $K_i$ for *N*-acetylglucosamine), no covalent inactivation is observed. An interesting phenomenon occurs when either of the first two of these NAGases is used at a reaction pH ≤ 5. Under these conditions the rate of substrate hydrolysis in the presence of 1.7 *increases* with time. A proposed explanation for this result is given in Scheme 1.6. At a reaction pH ≤ 5, these two NAGases catalyze the rapid conversion of the strong inhibitor 1.7 into an oxazoline (1.8; which has similar inhibitory potency to 1.7); however, 1.8 undergoes acid-catalyzed hydrolysis

to form the much less inhibitory compound *N*-acetylinosamine (**1.9**), and hence the rate of substrate hydrolysis in the presence of **1.7** *increases* with time (Legler & Bollhagen, 1992).
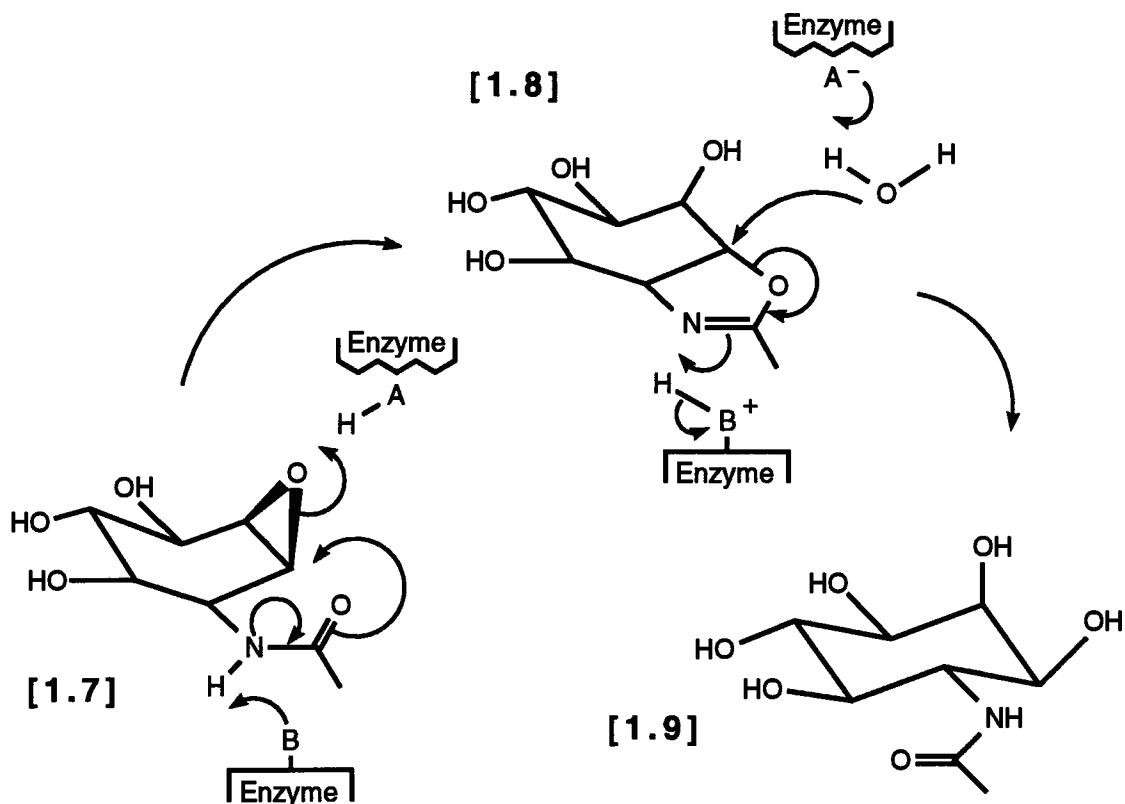


**Scheme 1.6.** The mechanism for the reaction of *N*-acetylconduramine B *trans*-epoxide with NAGase.

*f. Other inhibitors of NAGases.*

Some indirect evidence for the participation of a catalytic carboxyl group in the reaction mechanism of bovine kidney NAGase A was obtained from inhibition studies using *N*-acetylglucono-1,5-lactone (**1.10**) and *N*-acetylglucono-1,5-lactam (**1.11**) (Legler et al., 1991). Both the lactone and the lactam are good inhibitors of the enzyme, with $K_i$ values of 0.036 and 0.67 $\mu M$, respectively. The lactam displays a normal approach to the inhibition equilibrium, whereas the lactone displays a slow approach. After the lactone is preincubated with the substrate, 4'-methylumbelliferyl 2-acetamido-2-deoxy-$\beta$-D-glucopyranoside ($\beta$GlcNAcMu), the addition of the

enzyme catalyzes substrate hydrolysis at a rate that decreases slowly with time to a final value. The $K_i$ for the *initial* inhibition is about 50-fold higher than the final $K_i$.



[1.10]          [1.11]          [1.12]
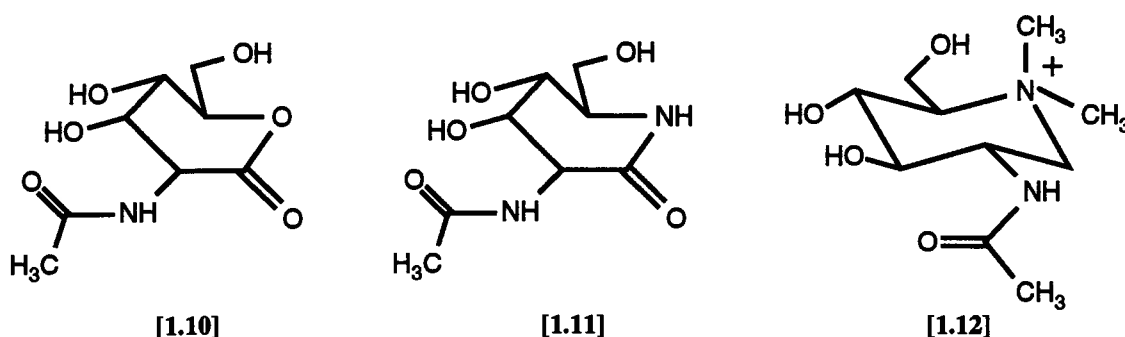
An explanation for (i) the much stronger inhibition displayed by the lactone (19 times stronger than the lactam), and (ii) the slow approach to the inhibition equilibrium of the lactone (1.10) compared with the lactam (1.11), has been proposed by Legler et al. (1991). They proposed that the lactone (1.10) is a better acceptor of the enzyme's nucleophilic carboxylate group than the lactam (1.11). Thus the slow approach to the inhibition equilibrium arises because of the formation of an orthocarboxylic acid derivative in the active site of the enzyme as a result of the attack on the lactone by a nucleophilic carboxylate group (see Scheme 1.7). However, no direct proof of the existence of such a nucleophilic carboxylate group in the active site of NAGase has been obtained (e.g., by labeling and isolation), and the slow approach to the inhibition equilibrium may be due to reasons other than the formation of a covalent bond between the enzyme and the inhibitor (as discussed later in this chapter).
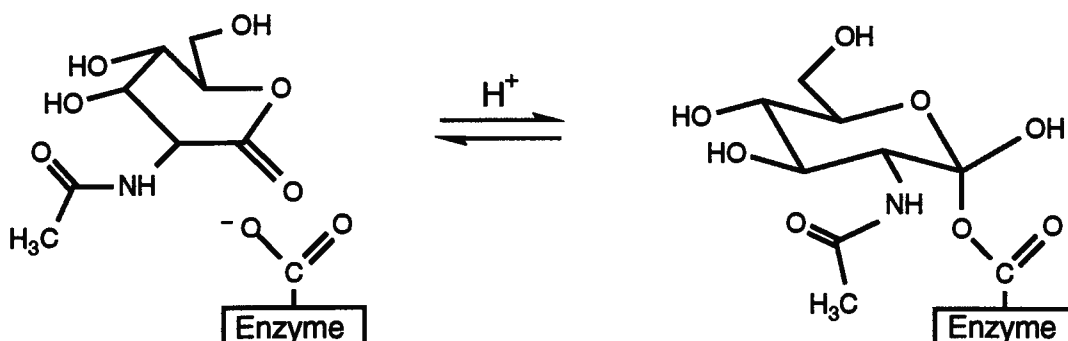


**Scheme 1.7.** The proposed mechanism for the slow inhibition of NAGase by *N*-acetylglucono-1,5-lactone.

Legler et al. (1991) have also studied the pH-dependence of the inhibition of bovine kidney NAGase A by the cationic sugar 2-acetamido-1-deoxy-$N,N$-dimethylnojirimicin (**1.12**). The observed relationship between log $K_i$ and pH suggests that inhibition depends on the deprotonation of a functional group with a pK$_a$ near 5.0. This is probably a carboxylate group of a catalytic amino acid in the enzyme's active site. However, no direct proof of the existence of such a nucleophilic group has been obtained (e.g., by labeling and isolation). Compound **1.12** is useful for studying deprotonation of an active-site moiety because **1.12** possesses a quaternary amine. This removes any ambiguity as to whether the deprotonation event is attributable to a catalytically important amino acid residue of the enzyme, or a functional group on the inhibitor.

### 1.3.4. The nature of the glycosyl-enzyme intermediate.

*a. Evidence from lysozyme and Agrobacterium β-glucosidase (pABG5).*

A fundamental question concerning the nature of the glycosyl-enzyme intermediate is whether it involves an ion pair or a transient, covalent adduct. Based on evidence from X-ray structural studies of hen egg white lysozyme, Blake et al. (1967) suggested that a negatively charged Asp 52 carboxylate ion could stabilize a positively charged oxocarbonium ion intermediate, and that the lifetime of this ion pair could be long enough for a water molecule (or an alcohol) to attack the oxocarbonium ion. However, it is questionable whether the ion pair could last long enough for the departed leaving group to diffuse away and allow a glycosyl acceptor to approach the active site and then react with the oxocarbonium ion.

Convincing evidence that the reaction mechanism of glycosylases involves the formation of a covalent glycosyl-enzyme intermediate has been obtained from studies of the inactivation of *Agrobacterium* β-glucosidase (pABG5) with a novel class of mechanism-based inactivators, 2-deoxy-2-fluoro-β-D-glycosides, e.g., 2FβGlcDNP (Street, 1988). The reaction of pABG5 with 2FβGlcDNP permits the isolation of a 2-fluoroglycosyl-enzyme intermediate whose half-life is over 500 hours. This covalent intermediate is stable enough to be characterized by various kinetic experiments and structural studies. ^{19}F NMR studies of the 2-fluoromannosyl-enzyme intermediate formed by 2FβManDNP and pABG5 showed that the sugar was covalently bonded to the enzyme through an axial (α-) glycosidic linkage (Withers & Street, 1988).

*b. Evidence from β-galactosidase.*

Additional evidence that the reaction mechanism of glycosylases involves the formation of a covalent glycosyl-enzyme intermediate has been obtained from α-secondary deuterium kinetic isotope effect (αDKIE) studies using *E. coli* β-galactosidase and a series of aryl galactosides (Sinnott, 1978). Reactions where the glycosylation step is rate-limiting yield αDKIEs with $k_H/k_D \approx 1.05$, and reactions where the deglycosylation step is rate-limiting yield αDKIEs with $k_H/k_D \approx 1.2$-$1.25$. A normal αDKIE indicates that there is an increase in $sp^2$ character at the α-carbon as the substrate changes from its $sp^3$ ground state to the transition state, whereas an inverse αDKIE indicates that there is an increase in $sp^3$ character at the α-carbon as the substrate changes from its $sp^2$ ground state to the transition state. Therefore the αDKIE results of both types of studies (where the glycosylation or the deglycosylation step is rate-limiting) indicate that a covalent intermediate is formed, and then hydrolyzed, *via* oxocarbonium ion-like transition states.

*c. Evidence from glycogen phosphorylase.*

A glucosyl-enzyme covalent intermediate has yet to be isolated for the glucosyl transfer reaction catalyzed by glycogen phosphorylase. The complexity of the reaction mechanism—which requires the enzyme to form a ternary complex with both substrates (glycogen as well as phosphate or αG1P)—and the rapid turnover of the enzyme make it difficult to accumulate sufficient amounts of the putative glucosyl-enzyme intermediate. To overcome this problem, Kokesh & Kakuda (1977) used α-cyclodextrin (cyclohexaamylose, a cyclic oligosaccharide composed of six glucose residues) as a substrate for potato phosphorylase. Although α-cyclodextrin activates the enzyme ternary complex, it cannot act as a glucosyl acceptor due to the absence of a free hydroxyl group at C-4. This reduces the rate of turnover of any reaction intermediate that may be formed. The use of α-cyclodextrin as a substrate analogue for potato phosphorylase allowed Kokesh & Kakuda (1977) to detect enzyme-catalyzed exchange between the bridging and nonbridging phosphoryl oxygen atoms of $^{18}$O-labeled αG1P. This result is evidence for the involvement of a covalent glucosyl-enzyme intermediate in the proposed catalytic mechanism (see Scheme 1.8).
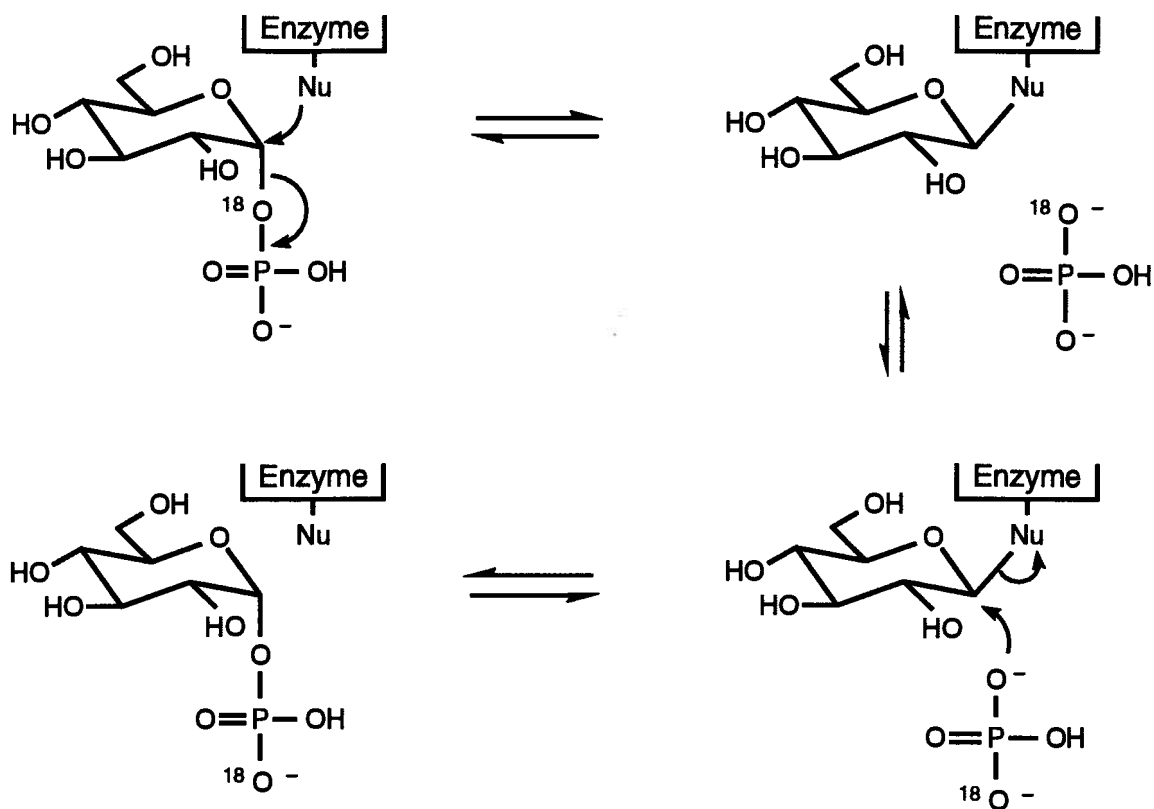
**Scheme 1.8.** Isotope exchange between bridging and nonbridging oxygens through an enzyme intermediate.

Withers & Rupitz (1990) have demonstrated the mechanistic similarity between potato phosphorylase and rabbit muscle phosphorylase. This study used a series of deoxy- and deoxyfluoro-αG1P substrates in a linear free-energy study of the nature of the transition state of each enzyme. The reaction catalyzed by rabbit muscle phosphorylase therefore probably involves the formation of a covalent glucosyl-enzyme intermediate.

### 1.3.5. The oxocarbonium ion-like transition states of glycosylase substrates.

*a. α-Secondary deuterium kinetic isotope effects.*

The results of α-secondary deuterium kinetic isotope effect (αDKIE) studies indicate that both transition states in the proposed reaction mechanism of glycosylases have oxocarbonium ion-like character (see

Scheme 1.3). As mentioned previously, these studies provide insights into the changes in the hybridization at the reactive centre (the α-carbon) as it proceeds from the ground state to the transition state of the reaction. The results of Sinnott (1978) and Kempton & Withers (1992)—obtained using a series of aryl galactosides and *E. coli* β-galactosidase, or a series of aryl glucosides and *Agrobacterium* β-glucosidase, respectively—showed that the (normal) αDKIEs observed when the deglycosylation step is rate-limiting are greater than those obtained when the glycosylation step is rate-limiting. Thus the second transition state has more oxocarbonium ion-like character (i.e., involves a process that is less $S_N2$-like) than the first transition state.

*b. Properties of transition-state analogues.*

A transition-state analogue is a tight-binding, reversible inhibitor whose structure resembles the transition state of the enzyme-catalyzed reaction under study. The ability of transition-state analogues to bind more tightly to the enzyme's active site when compared with the binding of the normal substrate is a phenomenon that agrees well with the hypothesis that the structure of the enzyme's active site is more complementary to the transition state than to the ground state of the substrate (Pauling, 1948).

Studies performed using transition-state analogues have also provided evidence that the transition states of glycosylase-catalyzed reactions have oxocarbonium ion-like character. The oxocarbonium ion form of the parent glycoside substrate can be distinguished from the latter in two ways. In the oxocarbonium ion form of the glycoside (i) the O-5 and C-1 atoms share a full positive charge, and (ii) the C-5, O-5, C-1, and C-2 atoms are coplanar (Sinnott, 1987). Compounds whose structures possess these properties have been shown to act as reversible inhibitors of glycosylases, and are classified as transition-state analogues for these enzymes (see Table 1.1).

*c. Examples of transition-state analogues.*

An aldonolactone (or aldonolactam) is structurally similar to a glycosyl cation due to its half-chair conformation and the partial positive charge carried by the ring oxygen as a result of the contribution of the resonance structure shown in Fig. 1.1. Glucono-1,5-lactone and glucono-1,5-lactam are transition-state

analogues that bind to *A. wentii* β–glucosidase 100- to 300-fold more strongly than the corresponding aldoses

(see Table 1.1).
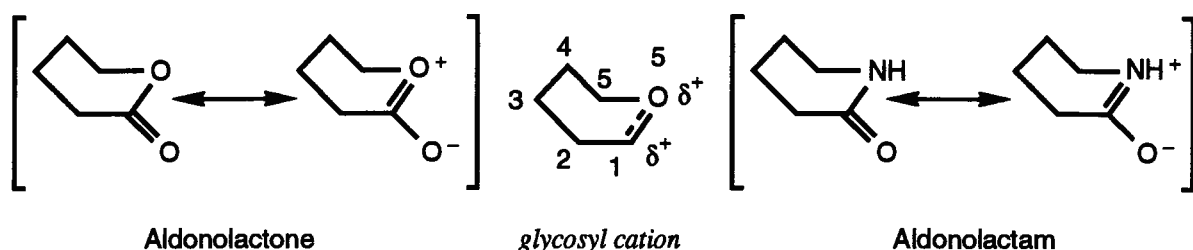


**Figure 1.1.** The structural similarities between the glycosyl cation and aldonolactones and aldonolactams.

Nojirimycin and related compounds are transition-state analogues that are among the tightest-binding glycosylase inhibitors known (Niwa et al., 1970). These compounds contain a positively charged ring nitrogen. Nojirimycin may exist in different forms (see Scheme 1.9), each of which is able to act as a glycosylase inhibitor by forming an ion pair with a negatively charged residue in the active site (presumably an amino acid side chain carboxylate) (Legler, 1990).
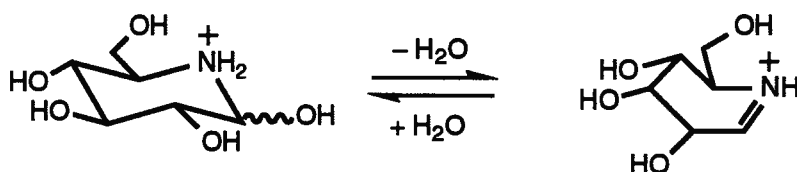


**Scheme 1.9.** The two forms of nojirimycin in aqueous solution at neutral pH.

Several transition-state analogues have been examined as inhibitors of bovine kidney NAGase A (Legler et al., 1991). When compared with GlcNAc ($K_i = 1.97$ m$M$), NAGase A was inhibited 2,600-fold more strongly by *N*-acetyldeoxynojirimycin (**1.14**); 2,900-fold more strongly by *N*-acetylglucono-1,5-lactam (**1.11**);

55,000-fold more strongly by $N$-acetylglucono-1,5-lactone (**1.10**); and about $10^6$-fold more strongly by $N$-acetylnojirimycin (**1.13**).



[1.13]       [1.14]       [1.15]       [1.16]
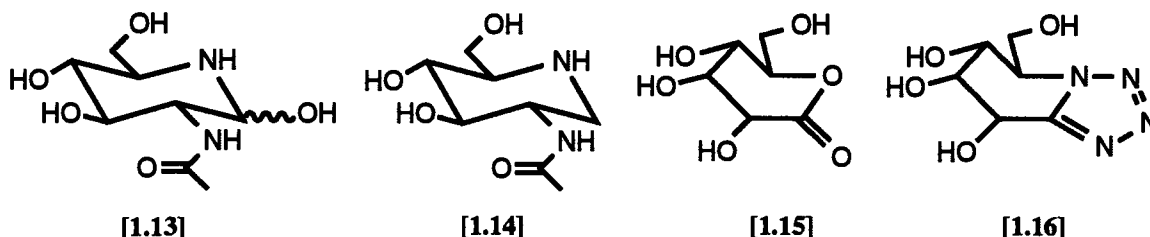
The transition-state analogues D-glucono-1,5-lactone (**1.15**) and nojirimycin tetrazole (**1.16**), with $K_i$ values of 25 and 14 $\mu M$, respectively, bind approximately 100-fold more strongly than glucose ($K_i = 2$ m$M$) to the complex formed by glycogen phosphorylase, glycogen, and orthophosphate (Gold et al., 1971; Withers & Rupitz, unpublished results). The strong binding of these compounds suggests that the reaction catalyzed by glycogen phosphorylase involves oxocarbonium ion-like transition states.

**Table 1.1.** The reversible inhibition of glycosylases by some transition-state analogues.

| Enzyme | Inhibitor | $K_i$ ($\mu M$) | Reference |
|---|---|---|---|
| β-glucosidase | glucose | 2800 | Legler et al., 1980 |
| *(A. wentii)* | β-glucosylamine | 1.6 | *ibid.* |
| | glucono-1,5-lactone | 9.6 | *ibid.* |
| | glucono-1,5-lactam | 36.0 | *ibid.* |
| | nojirimycin | 0.36 * | Legler & Julich, 1984 |
| β-$N$-acetylhexosaminidase A | $N$-acetylglucosamine | 1970 | Legler et al., 1991 |
| *(Bovine kidney)* | 2-acetamido-2-deoxyglucosylamine | 4.3 | *ibid.* |
| | $N$-acetylglucono-1,5-lactone (**1.10**) | 0.036 * | *ibid.* |
| | $N$-acetylglucono-1,5-lactam (**1.11**) | 0.67 | *ibid.* |
| | $N$-acetylnojirimycin (**1.13**) | 0.002 * | *ibid.* |
| | $N$-acetyldeoxynojirimycin (**1.14**) | 0.76 | *ibid.* |
| glycogen phosphorylase | glucose | 2000 | Gold et al., 1971 |
| *(Rabbit muscle)* | glucono-1,5-lactone (**1.15**) | 25 | *ibid.* |
| | nojirimycin tetrazole (**1.16**) | 14 | Withers & Rupitz, unpublished results |

An asterisk (*) denotes a slow approach to the inhibition equilibrium.

As was briefly mentioned earlier, the reaction of some glycosylases in the presence of certain inhibitors is characterized by a slow approach to the inhibition equilibrium (see Table 1.1). This phenomenon is more frequently observed with inhibitors that have a nitrogen atom in the sugar ring. When a slow approach to the inhibition equilibrium is observed, the $K_i$ for the initial inhibition is about 50- to 100-fold greater than the final $K_i$. One possible explanation for this phenomenon is that a loose complex is formed initially, which then undergoes a slow conformational change to form a tight enzyme-inhibitor complex (Legler, 1990). Another possible explanation is that the enzyme is capable of assuming two different conformations, characterized by either a high or low affinity for the inhibitor, and that these conformations are in equilibrium. When a slow approach to the inhibition equilibrium is observed, the inhibitor binds to the low-concentration, high-affinity conformer, which then shifts the conformational equilibrium towards the high-affinity state (Legler, 1990).

*d. The transition states of phosphorylase-catalyzed reactions.*

The transition states in the glycogen phosphorylase reaction have been studied using deoxy and deoxyfluoro analogues of the substrate αG1P (Street et al., 1989). These derivatives are turned over by the enzyme, but at greatly reduced rates (1,000- to 10,000-fold slower than αG1P). These rate reductions have been attributed to two effects: destabilization of transition states by the disruption of normal enzyme-ligand interactions, and inductive destabilization of electron-deficient transition states by the introduction of an electronegative fluorine atom adjacent to the reaction centre (as seen in the inactivation of *Agrobacterium* β-glucosidase by 2-deoxy-2-fluoro-β-D-glucosides).

A linear free-energy relationship, with a correlation coefficient $\rho = 0.90$, was obtained from a logarithmic plot of the rate constants for the enzyme-catalyzed reaction versus the nonenzymatic, acid-catalyzed hydrolysis of deoxy and deoxyfluoro analogues of αG1P (Street et al., 1989). This indicates that the electronic structures of the transition states of the two reactions are similar. The mechanism of the nonenzymatic, acid-catalyzed hydrolysis of αG1P has been shown to involve transition states with substantial oxocarbonium ion-like character (Bunton & Humeres, 1969). Thus the enzymatic reaction should also involve transition states with substantial oxocarbonium ion-like character, given the good correlation in the linear free-energy relationship for the enzyme-catalyzed and nonenzymatic reactions.

### 1.3.6. The binding energy attributable to noncovalent interactions.

Pauling (1946) was the first to propose that most of the catalytic power of an enzyme comes from noncovalent interactions between the transition state of the reaction and the enzyme's active site. Attempts to evaluate the importance of noncovalent interactions in the reaction mechanism of glycosylases have been carried out using various substrate analogues in which an individual hydroxyl group has been replaced by a hydrogen or a fluorine atom.

Noncovalent interactions between the C-2 hydroxyl group of the substrate and the active site of *A. wentii* β-glucosidase account for a $10^6$-fold increase in the rate of glucoside hydrolysis, whereas the same interactions involving the C-4 hydroxyl group account for a $10^4$-$10^5$-fold rate increase (Roeser & Legler, 1981). Similar studies by Namchuk (1993) using *Agrobacterium* β-glucosidase showed that the binding energy attributable to noncovalent interactions between the enzyme's active site and different hydroxyl groups of the substrate decreased in the order C-2 > C-3 > C-6 ~ C-4.

Deoxy derivatives of αG1P have been used as substrate analogues in a study of noncovalent interactions in the glucopyranose binding site of glycogen phosphorylase *b* (Street, 1988). This study showed that hydrogen-bonding interactions between C-3 and C-6 hydroxyl groups and the enzyme's active site are important in the stabilization of the transition state. Stabilization of the transition state lowers the activation energy of the reaction and increases the reaction rate. The structure of the transition state of the reaction (not the ground state) has the highest complementarity to the enzyme's active site, and noncovalent interactions are clearly an important aspect of this complementarity.

## 1.4. THE REACTIONS OF GLYCALS WITH GLYCOSYLASES.

### 1.4.1. The enzyme-catalyzed hydration of glycals.

Glycals, with their half-chair conformations, bear a structural resemblance to the transition states for the enzymatic hydrolysis of glycosides (see Fig. 1.2). These compounds were once considered to be transition-state analogues, and they have been investigated as inhibitors of glycosylases. Indeed, D-galactal was found to be a very strong inhibitor ($K_i$ = 18-90 μM) of several β-D-galactosidases (Lee, 1969). However, a close inspection of

the structures of glycals and the transition states of glycosylase substrates shows that their similarities are limited (Fig. 1.2). In addition to the absence of a hydroxyl group at C-2, glycals have their double bond located between C-1 and C-2, whereas the double bond of the transition state of a glycosylase substrate is located between C-1 and O-5. The stereochemistry of some of the ring substituents on each structure also differs (see Fig. 1.2).

These considerations prompted more detailed kinetic studies of the mechanism of the inhibition of *E. coli* β-galactosidase by D-galactal (Wentworth & Wolfenden, 1974). The extent of the steady-state inhibition ($K_i$ = 14 μ$M$) was interpreted as the result of the slow formation of a covalent, 2-deoxy-galactosyl-enzyme intermediate, and the subsequent hydrolysis of this adduct to form 2-deoxy-β-galactose ($k_{cat}$ ~ 0.004 s$^{-1}$). However, under pre-steady-state conditions unmodified (i.e., unreacted) D-galactal is only a weak inhibitor ($K_i$ > 1 m$M$). It is noteworthy that the 2-hydroxyl group of normal substrates seems to play an important role in increasing the rate of enzymatic hydrolysis (Namchuk, 1993).
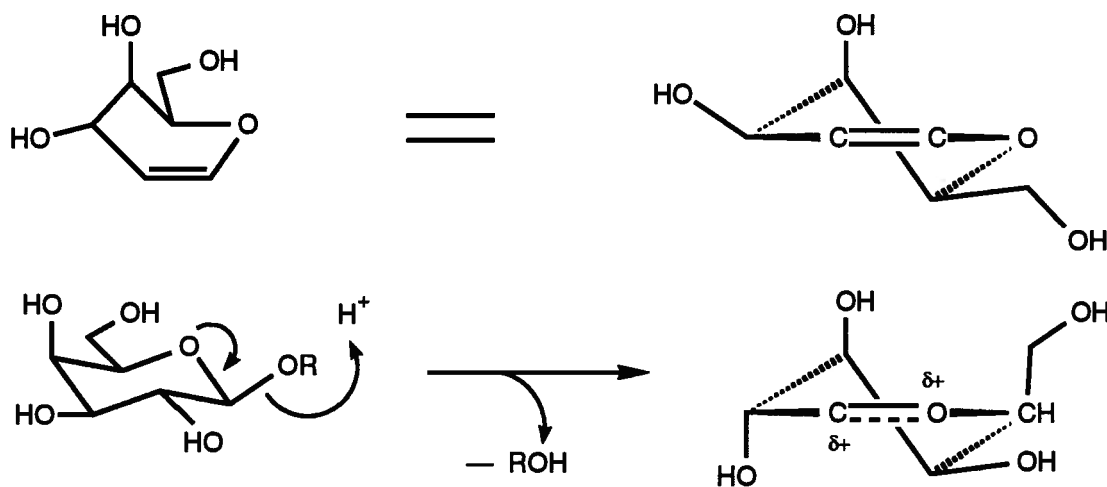


**Figure 1.2.** The structural similarities between galactal and the transition state of a β-galactoside.

Subsequent research has shown that glycals generally act as *substrates*, and that the hydration of the enolic double bond in glycals is catalyzed by both α- and β-glycosylases. Examples of this catalytic activity include the hydration of D-glucal by both *Candida tropicalis* α-glucosidase and sweet almond β-glucosidase

(Hehre et al., 1977), the hydration of maltal by sweet potato β-amylase (Hehre et al., 1986), and the hydration of cellobial by exo- and endo- type cellulases (Kanda et al., 1986).

The hydration of glycals (I) by glycosylases (E) can be represented by the following reaction scheme (Legler, 1990):

$$
E + I \underset{}{\overset{K_i'}{\rightleftharpoons}} E{\cdot}I \underset{k_{off}}{\overset{k_{on}}{\rightleftharpoons}} E{-}I \xrightarrow[k_{hydro}]{H_2O} E + \text{2-deoxyhexose}
$$
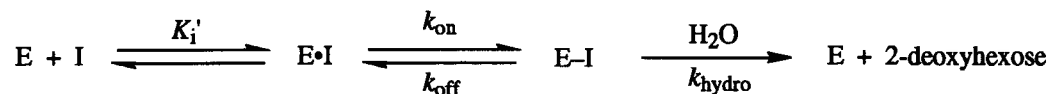
where $K_i'$ is the dissociation constant of a loose, rapidly formed, pre-steady-state complex (E•I). The inhibition constant for the steady state, $K_i$, is:

$$
K_i = \frac{K_i'}{\left\{ 1 + \dfrac{k_{on}}{(k_{off} + k_{hydro})} \right\}}
$$

and the rate constant for the approach to the steady state, $k_{appr}$, is:

$$
k_{appr} = \left( \frac{k_{on} \cdot [\,I\,]}{K_i' + [\,I\,]} + k_{off} + k_{hydro} \right)
$$

In the presence of substrate, (S), with a Michaelis constant, $K_m$, as defined in the case of inhibition studies, then:

$$
k_{appr} \left\{ 1 + \frac{[\,S\,]}{K_m} \right\} = \left( \frac{k_{on} \cdot [\,I\,]}{K_i' + [\,I\,]} + k_{off} + k_{hydro} \right)
$$

From the above scheme, depending on the magnitude of the kinetic parameters $k_{on}$, $k_{off}$, and $k_{hydro}$, different combinations of glucal–glycosylase interactions are possible.

For *A. wentii* β-glucosidase the sum of $k_{hydro}$ and $k_{off}$ is smaller than $k_{on}$, and this together with the use of [$^{14}$C]-labeled D-glucal made it possible for Legler et al. (1979) to trap the covalent glucal-enzyme intermediate before glucal was turned over to 2-deoxyglucose. Before the enzyme had time to turn over the [$^{14}$C]-glucal the protein was rapidly denatured, and a catalytic aspartate residue was identified by subsequent proteolytic digestion and amino-acid sequencing of the radiolabeled peptide. The same nucleophilic aspartate residue that is involved in the catalytic hydration of glucal by β-glucosidase was also labeled by the irreversible

inhibitor conduritol B epoxide (Bause & Legler, 1974) and the slow substrate p-nitrophenyl-2-deoxy-β-D-glucopyranoside (Roeser & Legler, 1981).

The stereochemistry of the enzyme-catalyzed hydration and protonation at C-2 of glycals has been investigated with α- and β-glucosidases (Hehre et al., 1977) and with three "inverting" exo-α-glucanases (Chiba et al., 1988). These reactions result in the production of 2-deoxy-α-glucose by α-glucosidases, whereas 2-deoxy-β-glucose is produced by β-glucosidases and inverting exo-α-glucanases. These are the same stereochemical outcomes as observed with the glycosylase-catalyzed hydrolysis reactions of glycosides.

^{1}H NMR studies of the catalytic hydration of glycals in $D_2O$ (where exchangeable protons are replaced by deuterium) showed that retaining α-glucosidases protonate D-glucal from *above* the double bond, whereas β–glucosidases and inverting exo-α-glucanases protonate D-glucal from *below* the double bond. Thus the direction of protonation of the double bond in D-glucal is *opposite* from the direction that would be expected based on the known stereochemistry of the glycosylase-catalyzed hydrolysis reactions of glycosides.



*glycosylation*          *deglycosylation*
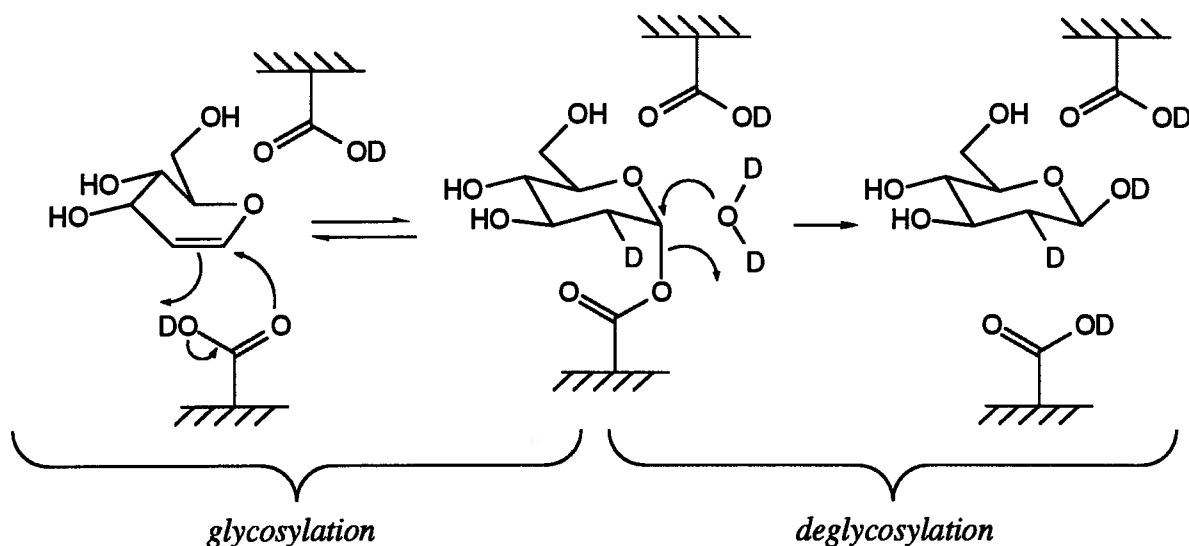
**Scheme 1.10.** The proposed mechanism for the hydration of D-glucal in $D_2O$ by β-glucosidase.

The available kinetic data on the glycosylase-catalyzed hydration reactions of glycals shows that although the initial protonation step appears to differ significantly from that seen in the glycosylase-catalyzed hydrolysis reactions of normal glycosides, the remainder of the reaction mechanism is the same, involving the same active site residues and yielding products with the same configuration. Thus in the proposed mechanism for the catalytic hydration of glycals (Legler et al., 1979), carboxylate groups act as both a general acid catalyst and a nucleophile (Scheme 1.10).

### 1.4.2. The enzyme-catalyzed hydration of heptenitols.

D-*gluco*-heptenitol (**1.2**) is a glycal with an exocyclic enolic double bond. In general, heptenitols do not inhibit glycosylases as effectively as hexenitol glycals (glycals with an endocyclic enolic double bond). Glycosylases are able to hydrate D-*gluco*-heptenitol to form 1-deoxy-D-*gluco*-heptulose (**1.17**). [Note that in both (**1.2**) and (**1.17**) the *exocyclic* carbon atom is designated as C-1.] However, if the reaction is performed in the presence of an alcohol, a glycoside may be formed. Thus β-galactosidase is able to synthesize glyceryl 2,6-anhydro-1-deoxy-β-D-*galacto*-heptuloside (**1.18**) from D-*galacto*-hept-1-enitol and glycerol. The initial anomeric configuration (i.e., prior to subsequent α/β equilibration) of the product of the catalytic hydration (or glycoside synthesis reaction) of a heptenitol is determined by the anomeric specificity of the glycosylase.
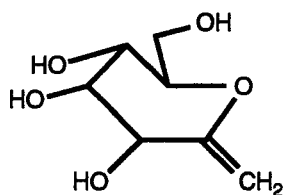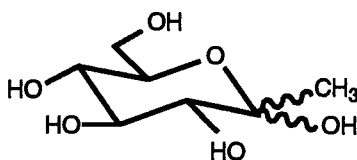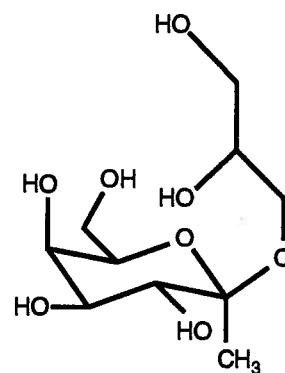


[1.2]          [1.17]          [1.18]

The greater catalytic activity of glycosylases towards heptenitols compared with hexenitol glycals has been attributed to the greater structural resemblance of heptenitols to the normal glycoside substrates of these

enzymes. In the three-dimensional structure of heptenitol there are four hydroxyl groups that can assume positions that are equivalent to the hydroxyls of α- or β-D-glucoside substrates, and this increased structural similarity may allow for better binding of heptenitols in the active site. In addition, the exocyclic double bond of a heptenitol occupies a position in the active site that is extremely close to the position normally occupied by the glycosidic bond of regular glycoside substrates, and hence the double bond of the heptenitol is susceptible to the same catalytically important protonation event (i.e., general acid catalysis).

The catalytic hydration of D-*galacto*-heptenitol by *E. coli* β-galactosidase has a Michaelis constant, $K_m$, of 50-70 m$M$, and a turnover number, $k_{cat}$, of 41 to 64 s$^{-1}$ (Brockhaus & Lehmann, 1977). Similar kinetic data have been obtained for the catalytic hydration of D-*gluco*-heptenitol by α-glucosidase from *C. tropicalis* (rice), sweet almond β-glucosidase, and an inverting exo-α-glucanase from *A. globiformis* (Hehre et al., 1980).

The stereochemistry of the hydration of heptenitols by retaining α-glucosidases has been studied using 2-[$^2$H]-D-*gluco*-octenitol. Enzymes from *A. niger* and *C. tropicalis* were used in this study, and both protonated the substrate from the top (*si, re*) face, the same direction of protonation that several α-glucosidases use to protonate D-glucal and D-galactal (Weiser et al., 1988), but the opposite direction of protonation used by α-glucosidases with normal glycoside substrates.
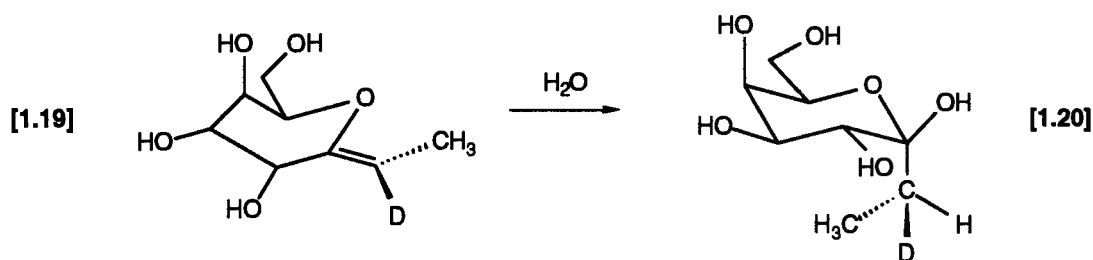


Scheme 1.11. The hydration of D-*galacto*-octenitol by β-galactosidase.

In contrast, when 2-[$^2$H]-D-*galacto*-octenitol (**1.19**) is hydrated by *E. coli* β-galactosidase, the stereochemistry for the protonation of the double bond is the same as that observed with normal glycoside substrates (Lehmann & Schlesselman, 1983). During the catalytic hydration of **1.19**, protonation is exclusively from above the ring, and the hydration reaction yields **1.20**, 1,2-dideoxy-2-deutero-D-*galacto*-octulopyranose

(see Scheme 1.11). The two different directions that can be taken for the protonation step implies that the protonating amino acid residue may be located on either face of the ring of a bound substrate in the active site of a particular glycosylase enzyme.

The results of stereochemical investigations of the glycosylase-catalyzed hydration of hexenitol and heptenitol glycals suggests that there are two mechanistically distinct and separately controlled aspects of these reactions (Chiba et al., 1988). In the so-called "plastic" aspect of the reaction, various glycosylases show considerable heterogeneity in the direction of protonation, a phenomenon that is substrate-dependent. In the so-called "conserved" aspect of the reaction, the creation of a product with a specific configuration is a consequence of the acceptor's direction of attack against the reaction centre. The latter phenomenon is mainly determined by the particular enzyme, with little influence by the substrate.

### 1.4.3. The reactions of glycals with glycogen phosphorylase.

Glycogen phosphorylase catalyzes the addition of D-glucal (as a 2-deoxyglucosyl residue) to the nonreducing end of a polysaccharide composed of glucose subunits:

$$\text{glucal} + (\text{glucose})_n \longrightarrow (2\text{-deoxyglucose})\text{-}(\text{glucose})_n$$
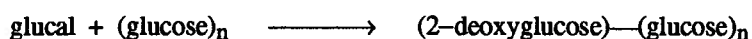
One of the products of the reaction is also 2-deoxy-$\alpha$G1P, which is probably formed by the enzymatic phosphorolysis of the modified polysaccharide (Klein et al., 1982). The maximum rate of utilization of D-glucal is approximately 20-30% of the rate of glycogen synthesis using $\alpha$G1P.

In the presence of arsenate (i.e., in place of orthophosphate), phosphorylase catalyzes the arsenolysis of D-*gluco*-heptenitol to form 1-deoxy-D-*gluco*-heptulose-2-arsenate, which undergoes rapid spontaneous hydrolysis with retention of configuration to form 1-deoxy-$\alpha$-D-*gluco*-heptulose. The rate of the phosphorylase-catalyzed formation of 1-deoxy-$\alpha$-D-*gluco*-heptulose (in the presence of arsenate) with 50 m$M$ heptenitol is 17-32% of the rate of arsenolysis of polysaccharides, depending on the source of the enzyme (Klein et al., 1986).

In the presence of orthophosphate, phosphorylase converts D-*gluco*-heptenitol to form 1-deoxy-$\alpha$-D-*gluco*-heptulose-2-phosphate (heptulose-2-phosphate, **1.21**), which binds tightly to the enzyme and acts as an inhibitor (with $K_i$ = 14 $\mu M$) (Klein et al., 1984). To date, heptenitol is the only known substrate of

phosphorylase that can be utilized in the absence of a polysaccharide primer. The rate of this reaction cannot be measured accurately due to the formation of the "dead end" inhibitor, heptulose-2-phosphate.

In the presence of *glycogen* and arsenate (i.e., with arsenate acting as a phosphate analogue), heptenitol acts as a competitive inhibitor (with $K_i = 4.3$ m$M$) of rabbit skeletal muscle phosphorylase $b$ (Klein et al., 1986). However, transfer of the heptulosyl residue to a polysaccharide acceptor is not detectable. Therefore heptenitol is used only as a substrate for the degradative pathway of the phosphorylase reaction.

**Table 1.2.** Comparison of the binding constants of some ligands of glycogen phosphorylase $b$.

| Ligand | $K_m$ (or $K_i$) $(\mu M)$ | Reference |
| --- | --- | --- |
| glucose-1-phosphate | 2,200 | Hu & Gold, 1978 |
| glucose-1,2-(cyclic phosphate) [1.22] | 500 | *ibid.* |
| 1-deoxy-heptulose-2-phosphate [1.21] *(also referred to as heptulose-2-phosphate)* | 14 | Klein et al., 1984 |
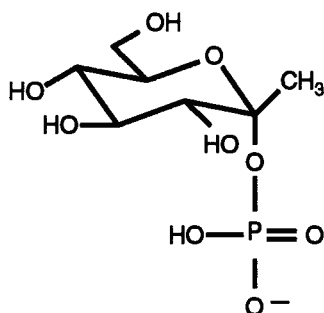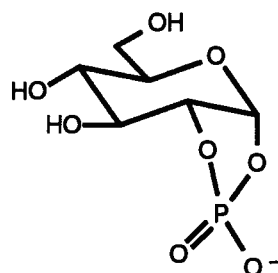


[1.21]          [1.22]

Heptulose-2-phosphate binds to phosphorylase $b$ with an affinity that is 100-fold greater than the substrate $\alpha$G1P (see Table 1.2). X-ray structural analysis of the (heptulose-2-phosphate)–[phosphorylase $b$] complex showed that the phosphate group of the inhibitor was located underneath the sugar ring, oriented towards the C-3 hydroxyl group, probably to avoid steric hindrance from the C-1 methyl group (McLaughlin et al., 1984).

Heptulose-2-phosphate (**1.21**) and glucose-1,2-(cyclic phosphate) (**1.22**) are considered to be transition-state analogues for the degradative reaction of glycogen phosphorylase because of their chemical structures and low $K_i$ values (Hu & Gold, 1978). The preferred orientation of the phosphate group of both compounds is under C-2 of the sugar ring, in contrast with αG1P with its phosphate group away from the ring (*trans* to C-2) (O'Connor et al., 1979).

The stereochemistry of the protonation of D-glucal by glycogen phosphorylase *b* is from below the sugar ring (Klein et al., 1982). Thus if the reaction is carried out in a deuterated buffer, deuterium is incorporated into the equatorial position at C-2—the *opposite* stereochemical outcome to that observed when hexenitol glucals are protonated by other α-retaining glycosylases. Klein et al. (1982) also found that in addition to an absolute requirement for phosphate (or arsenate), the catalytic reaction of D-glucal is also dependent on the dianionic form of the enzyme-bound cofactor, pyridoxal phosphate.



Y = P or As      B = nucleophile (or base)      PL = pyridoxal
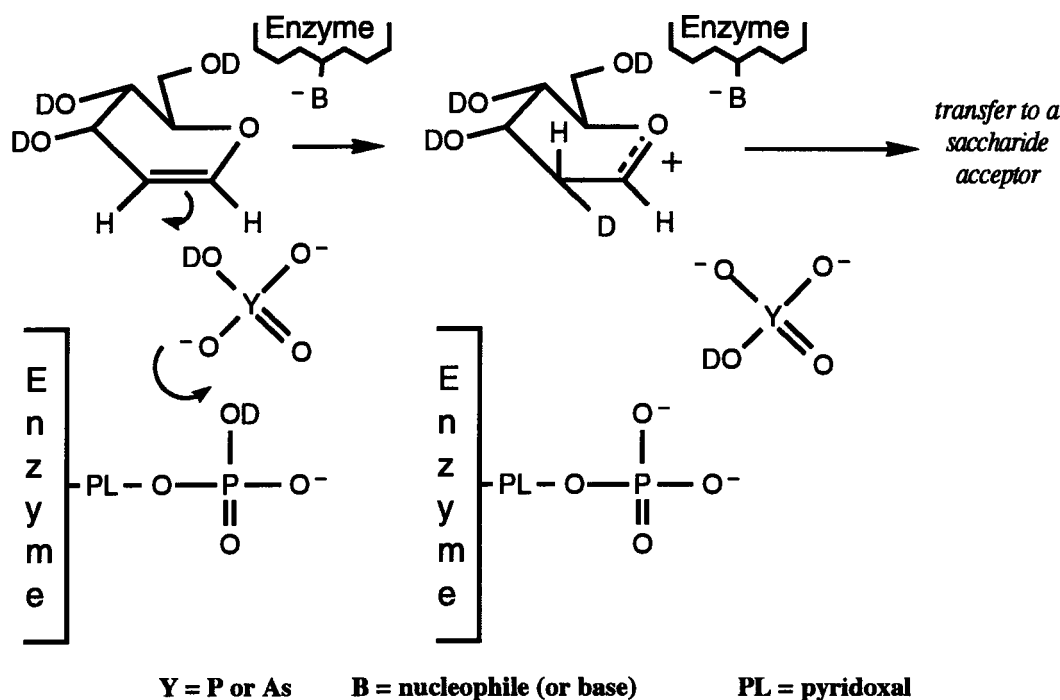
**Scheme 1.12.** The "proton transfer relay" for the deuteration of D-glucal by glycogen phosphorylase.

On the basis of these observations, Klein et al. (1982) have proposed that a "proton transfer relay" is a feature of the enzyme's reaction mechanism (Scheme 1.12). Orthophosphate (or arsenate) is located below the D-glucal ring, in a region of the active site that is adjacent to the phosphate group of the enzyme's cofactor. The enzyme-bound cofactor pyridoxal phosphate is believed to mediate a proton transfer relay between the enzyme and D-glucal as shown in Scheme 1.12.

## 1.5. THE AIMS OF THIS THESIS.

### 1.5.1. Research significance and objectives.

Both reversible and irreversible inhibitors (or inactivators) are useful in studies of enzyme reaction mechanisms and the properties of transition states. These compounds may also find applications as therapeutic drugs. Identification of catalytic residues in the enzyme's active site, and gaining an understanding of their specific roles in catalysis, are also possible using irreversible inhibitors. The aims of this thesis were to synthesize several derivatives of D-*gluco*-heptenitol and D-glucal, and examine the potential utility of these compounds as mechanism-based inhibitors of three glycosylases: glycogen phosphorylase, $\beta$-glucosidase, and $\beta$-$N$-acetylhexosaminidase.

### 1.5.2. Studies using fluorinated derivatives of D-*gluco*-heptenitol.

Withers et al. (1990) have shown that 2-fluoro-glucosides rapidly inactivate $\beta$-glucosidase, and that such compounds are useful probes for studying the reaction mechanism of this enzyme. The electron-withdrawing fluorine atom inductively destabilizes the oxocarbonium ion-like transition states, and the overall effect of these inhibitors is the covalent inactivation of the enzyme by the accumulation of the glucosyl-enzyme intermediate. Fluorinated heptenitols, with one or two electron-withdrawing fluorine atoms situated adjacent to the reaction centre, were therefore considered to be potential inactivators of glycosylases. One advantage of these compounds over 2-fluoro-sugars is that the former can be used to study the effect of *varying* the degree of withdrawal of electron density from the reaction centre. Hence difluoroheptenitol

(F$_2$hept) and monofluoroheptenitol (F$_1$hept) were synthesized, and kinetic studies of these compounds were carried out using glycogen phosphorylase and β-glucosidase.

Fluoroheptenitols also proved to be useful for structural studies of glycogen phosphorylase. It had previously been established that glycogen phosphorylase is able to convert heptenitol in the presence of phosphate to 1-deoxy-heptulose-2-phosphate (Klein et al., 1984). The synthesis of F$_2$hept and F$_1$hept— compounds that are not turned over by the enzyme as rapidly as heptenitol—assisted collaborators in the U.K., who performed X-ray structural studies using crystals of the enzyme containing either of the fluoroheptenitols. These studies yielded insights on the binding of phosphate in the enzyme's active site, studies that could not be performed with heptenitol.

### 1.5.3. Studies using derivatives of D-glucal.

An initial aim of this study was to determine whether methylglucal might act as a substrate, or possibly even an inhibitor or inactivator, of β-glucosidase. If promising results were obtained with the parent compound, the synthesis of fluorinated derivatives of methylglucal would be attempted, and their effects on the activity of the enzyme would also be studied to provide more insight into the role of inductive effects on glycal hydration, or possibly the utility of fluorinated glycals as inhibitors or inactivators.

Another aim of this study was to examine whether α,β-unsaturated glucals, which can act as Michael acceptors for the nucleophilic residue present in the active site of β-glucosidase, might constitute a new class of inactivators of this enzyme. 1-Nitroglucal and other α,β-unsaturated glucals [1-cyano-, 1-(methylcarboxylate)-, sodium 1-(carboxylate)-, and 2-cyano- glucal] were therefore examined as potential inhibitors of β-glucosidase.

Finally, 2-acetamidoglucal (NAGlucal) was used to study the reaction mechanism of the clinically important enzyme β-N-acetylhexosaminidase (NAGase). Stereochemical studies and other kinetic experiments were performed on NAGases isolated from jack bean, bovine kidney, and human placenta. The stereochemistry of the hydrolysis of the commonly used substrate βGlcNAcPNP (4'-nitrophenyl N-acetyl-β-D-glucosaminide) was also investigated.

## CHAPTER 2: KINETIC STUDIES USING GLYCOGEN PHOSPHORYLASE

### 2.1. INTRODUCTION.

#### 2.1.1. Biochemical role *in vivo*.

Glycogen phosphorylase (α-1,4-glucan-orthophosphate glucosyl transferase, E.C. 2.4.1.1) plays a key role in carbohydrate metabolism. It is found in all cell types, from microbial species to the various complex tissues of higher plants (starch phosphorylase) and mammals. Glycogen phosphorylase catalyzes the reaction shown below, where the terminal α(1-4) glucosidic linkage at the nonreducing end of a glycogen side chain undergoes phosphorolysis. The cleavage of the terminal glucosidic bond results in the removal of the terminal glucose residue as α-D-glucose-1-phosphate (αG1P), leaving behind a glycogen chain with one less glucose unit. Although glycogen phosphorylase catalyzes the formation and breakdown of glycogen, its primary function *in vivo* is to catalyze the breakdown of glycogen and provide a regulated supply of αG1P.
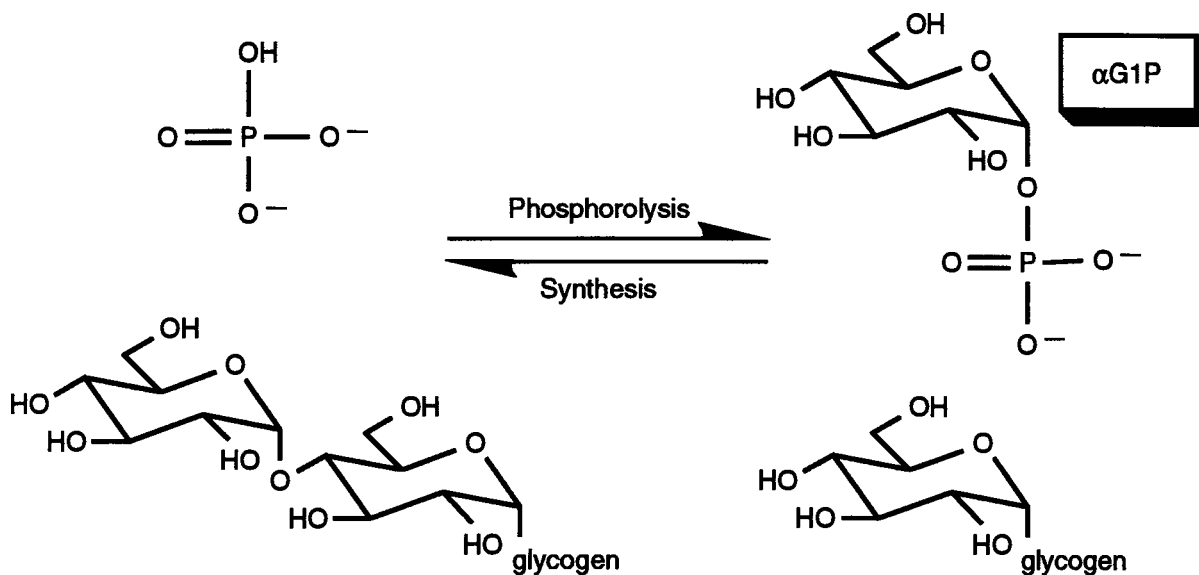
**Scheme 2.1.** The reaction catalyzed by glycogen phosphorylase.

### 2.1.2. Regulation.

Rabbit muscle glycogen phosphorylase was first isolated and characterized by Cori & Cori (1936). This enzyme has been studied extensively, and has been shown to be subject to complex regulatory mechanisms. The activity of this enzyme is carefully controlled by covalent modification (phosphorylation-dephosphorylation), as well as an allosteric regulatory mechanism (ligand-induced conformational changes).

Glycogen phosphorylase exists in two forms; the less active phosphorylase $b$ and the more active phosphorylase $a$. Phosphorylase $b$ is converted to the "$a$" form by phosphorylase kinase, which phosphorylates the enzyme at Ser 14 (Fischer & Krebs, 1955). A phosphoprotein phosphatase dephosphorylates the phosphate ester at Ser 14 in phosphorylase $a$, thereby converting the enzyme back to phosphorylase $b$ (Wosilait & Sutherland, 1956).

Phosphorylase $b$ assumes at least two conformations, the catalytically active R-conformation, and the inactive T-conformation. Phosphorylase $b$ is activated by adenosine-5'-monophosphate (AMP) and is subject to allosteric inhibition by adenosine-5'-triphosphate (ATP), glucose, adenosine-5'-diphosphate (ADP) and glucose-6-phosphate (Madsen & Shechosky, 1967). Phosphorylase $a$ exists mainly as the active R-conformer, and is not subject to allosteric regulation (Madsen & Withers, 1986).

### 2.1.3. Structural studies.

Glycogen phosphorylase can exist as a tetramer or a dimer *in vivo*, but the catalytically active R-states of phosphorylase $a$ or $b$ exist as dimers (Metzger et al., 1967). Each monomer has an $M_r$ of 97,444, and consists of 842 amino acids (Johnson, 1992). The amino acid sequence of rabbit muscle phosphorylase was determined by Titani et al. (1977). The tertiary structure of the monomer can be divided into $N$-terminal (residues 1-489) and $C$-terminal (residues 490-842) domains. In each domain, approximately 45% and 25% of the amino acid residues are in $\alpha$-helical or $\beta$-sheet secondary structural elements, respectively.

The X-ray crystal structures of several forms of glycogen phosphorylase have been determined, and these studies have identified the primary ligand binding sites on the enzyme (Acharya et al., 1991; Sprang & Fletterick, 1979; McLaughlin et al., 1984). The catalytic site (site C) is located at the centre of the enzyme,
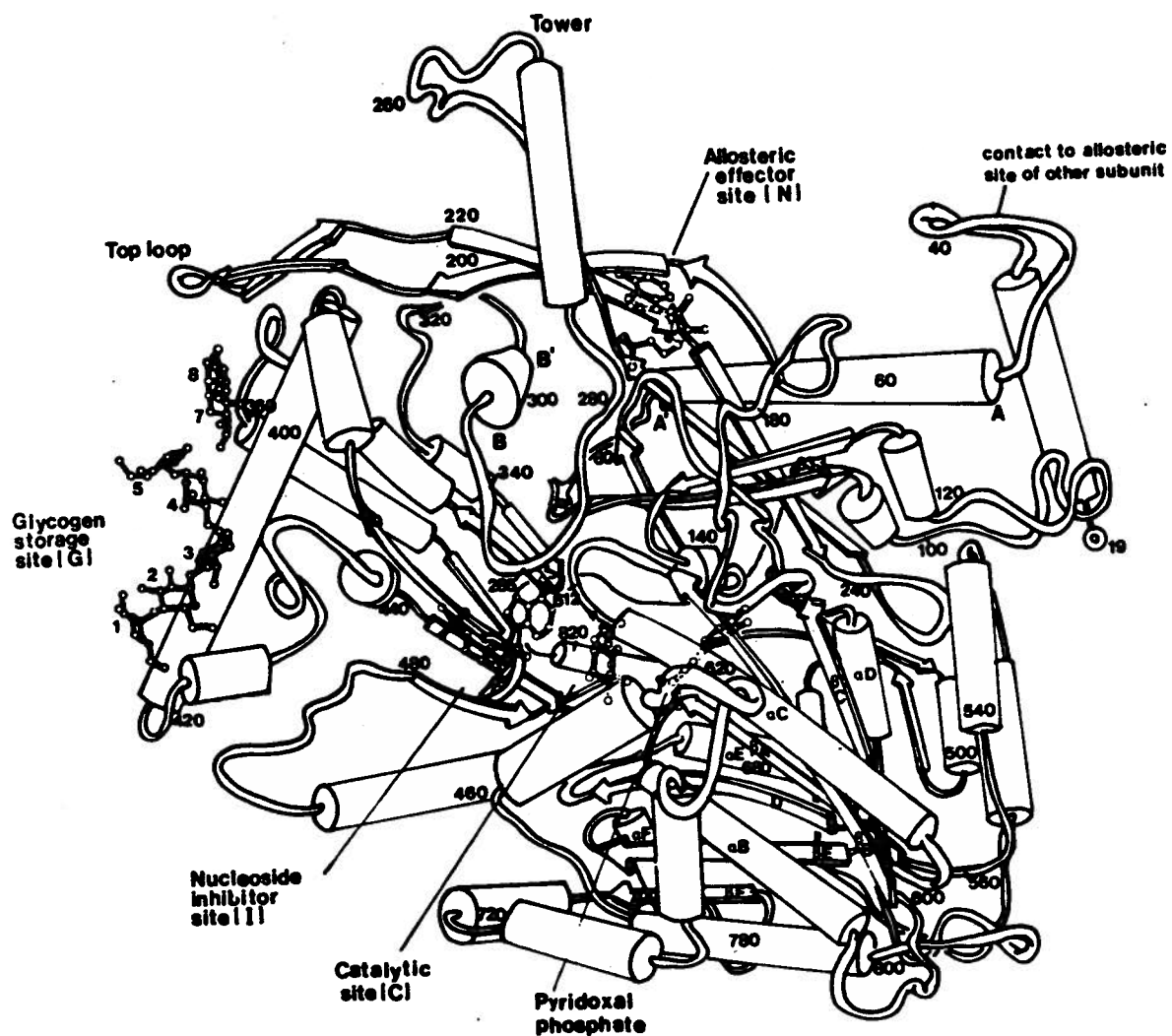
**Figure 2.1.** The structure of the glycogen phosphorylase *b* monomer.

The structure shown is from McLaughlin et al. (1984). α-Helices and β-strands are represented by cylinders and arrows, respectively. Please see the text for descriptions of the primary ligand binding sites.

near the boundary between the *N*-terminal and *C*-terminal domains (Madsen & Withers, 1986). The active site consist of the following elements:

1. A highly specific pocket for the glucopyranosyl moiety of the substrate, αG1P. The inhibitor glucose also binds here.

2. A phosphate subsite for the binding of the phosphate moiety of αG1P.

3. A cofactor subsite for the binding of pyridoxal-5'-phosphate (PLP). PLP is covalently bound to the enzyme *via* a Schiff base with Lys 680. The phosphate group of PLP is adjacent to the phosphate subsite of the substrate (Madsen & Withers, 1986).

At the entrance to the catalytic site there is an inhibitor binding site (site I) where aromatic inhibitors such as caffeine, and various nucleosides and nucleotides, bind to the enzyme. About 32 Å from site C, near Ser 14 and close to the subunit-subunit interface, there is an allosteric effector binding site (Site N) where AMP binds to the enzyme. The glycogen storage site (site G) is located on the surface of the *N*-terminal domain of the enzyme. Site G is located about 30 Å and 39 Å from the catalytic and allosteric effector sites, respectively. The enzyme attaches to the glycogen particle *via* site G, and smaller oligosaccharides such as maltoheptaose also bind strongly to this site (McLaughlin et al., 1984).

### 2.1.4. General features of the catalytic mechanism.

Phosphorylase is an α-retaining glycosylase, and hence the reaction it catalyzes is thought to involve a double-displacement mechanism (see Scheme 2.2). The main features of the proposed catalytic mechanism (in the direction of glycogen synthesis) include: general acid catalysis (to facilitate cleavage of the glucosyl-phosphate linkage); formation of a glucosyl-enzyme intermediate (either covalently or electrostatically); and general base catalysis to facilitate nucleophilic attack (by the 4-hydroxyl group of glycogen's terminal glucose residue) directed against the anomeric centre of the glucosyl-enzyme intermediate. These features of the reaction, and the experimental support for their occurrence, were reviewed in Chapter 1 of this thesis. Other important features of the catalytic mechanism of glycogen phosphorylase include the role of the cofactor, pyridoxal phosphate (PLP), and the fact that the enzyme catalyzes a two-substrate reaction.
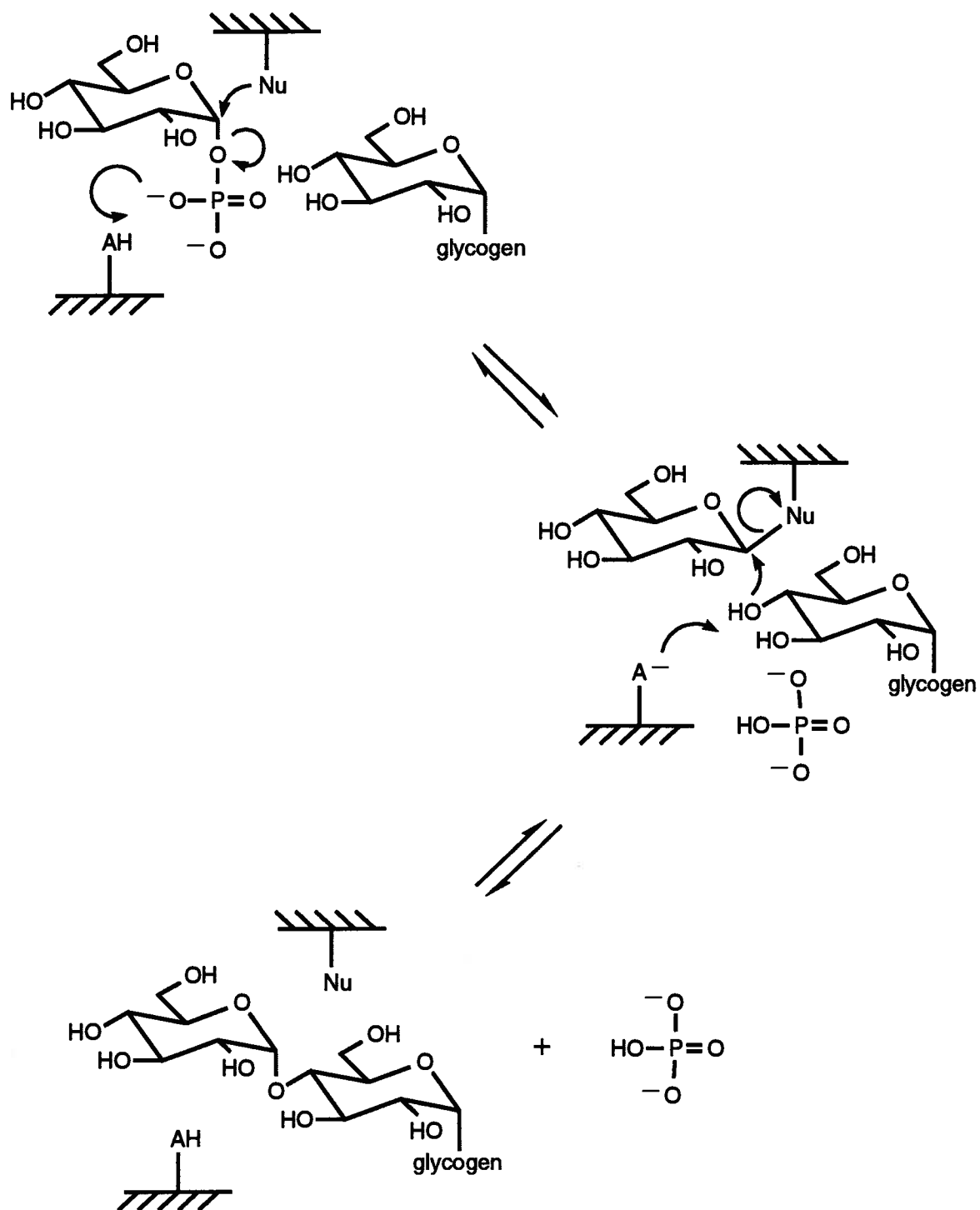
**Scheme 2.2.** The proposed catalytic mechanism of glycogen phosphorylase.

The flow of electrons is shown for the glycogen synthesis reaction only, but it should be noted that the reaction is reversible.

**2.1.5. The cofactor pyridoxal phosphate (PLP).**

*a. Structural and catalytic roles.*

One molecule of PLP is present in each phosphorylase monomer. PLP is attached to the enzyme by a Schiff base involving Lys 680, and this adduct plays an important role in maintaining the quaternary structure of the enzyme through subunit interactions (Kastenschmidt et al., 1968). PLP also plays an important role during catalysis. Removal of PLP yields the apo-enzyme, which has no catalytic activity, but catalytic activity can be restored by reconstitution (Illingworth et al., 1958).
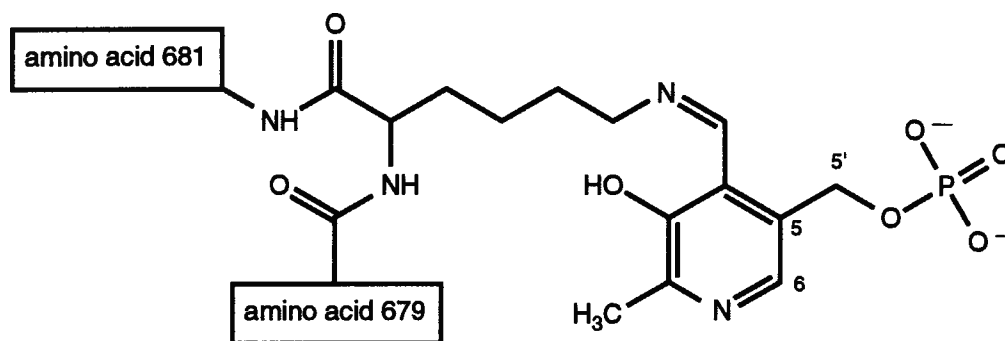


**Figure 2.2.** The Schiff base formed between Lys 680 and the cofactor pyridoxal phosphate (PLP).

In the proposed reaction mechanism of phosphorylase, the 5' phosphate group of PLP is believed to act as either a Brønsted acid catalyst (Klein et al., 1982, 1984; Palm et al., 1990) or as an electrophile, with the 5' phosphate of PLP remaining in the di-anionic form throughout the course of the reaction (Withers et al., 1982) (see Schemes 2.3 and 2.4 for the mechanistic details of how PLP might act as an acid catalyst or as an electrophile, respectively). Although researchers agree that PLP plays a crucial role during phosphorylase catalysis, there is a lack of agreement on the precise details of the role this cofactor plays during the reaction mechanism.
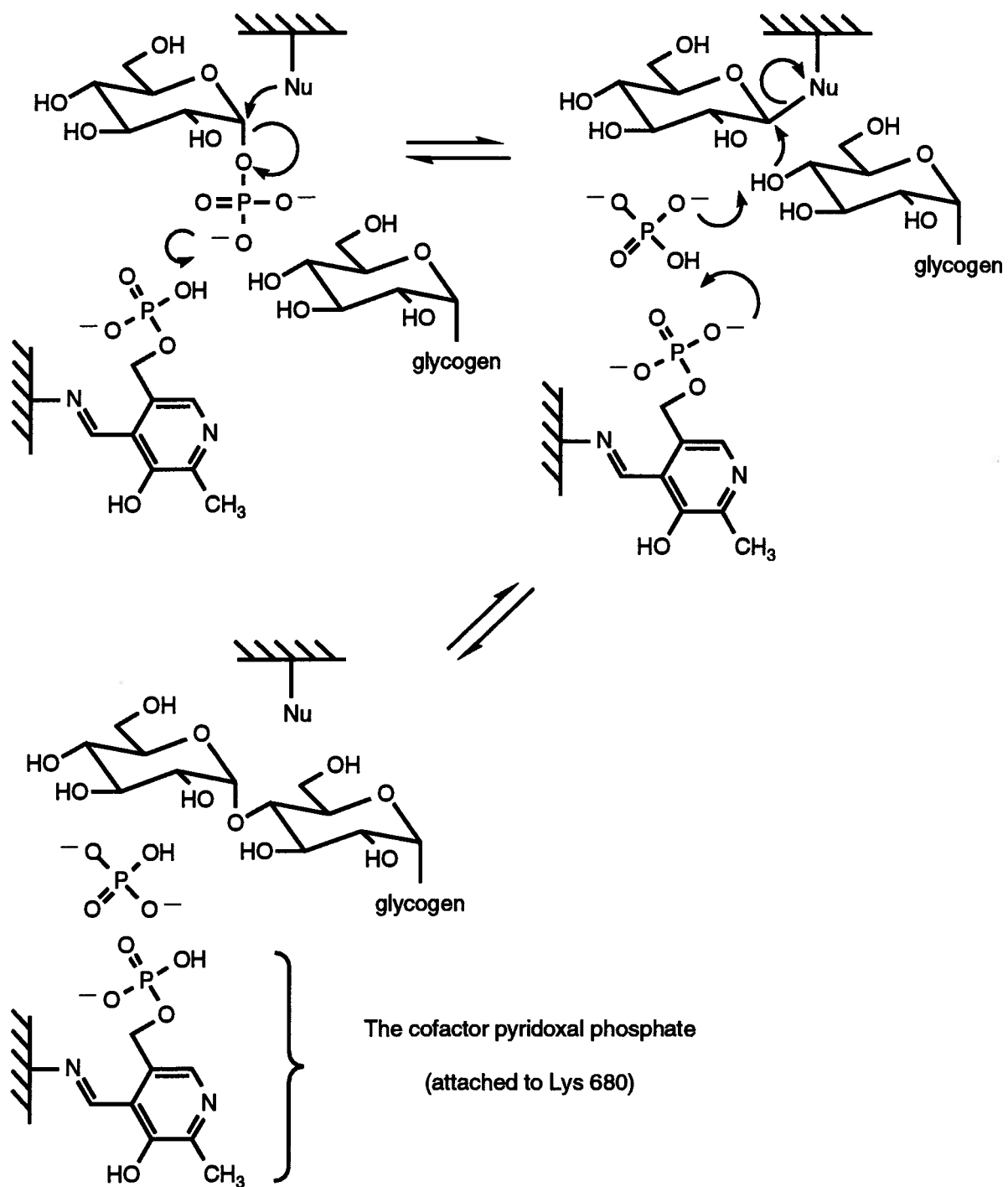
**Scheme 2.3.** The proposed role of the phosphorylase cofactor PLP as a Brønsted acid catalyst.

Adapted from Palm et al. (1990).

*b. The proposed role of PLP as a Brønsted acid catalyst.*

In this proposal, the phosphate group of PLP acts as a proton donor and acceptor, as shown in Scheme 2.3 (Helmreich, 1992; Palm et al., 1990). When the reaction proceeds in the direction of glycogen synthesis, the phosphate group of PLP first acts as an acid catalyst and protonates αG1P. This protonation event facilitates cleavage of the glucosidic bond, which in turn facilitates the general base-catalyzed attack against the glucosyl-enzyme intermediate by the 4-hydroxyl group of the terminal glucosyl residue of the glycogen particle.

When the reaction proceeds in the direction of glycogen phosphorolysis, the phosphate group of PLP protonates the bound phosphate substrate, which in turn protonates the glucosidic linkage at the terminal glucosyl residue of the glycogen particle. The phosphate group of PLP subsequently acts as a base catalyst that facilitates nucleophilic attack against the glucosyl-enzyme intermediate by phosphate. This mechanism probably involves oxocarbonium ion-like transition states (Helmreich, 1992).

*c. The proposed role of PLP as an electrophile.*

An alternative proposal for the role of the phosphorylase cofactor PLP is that this moiety acts as an electrophilic catalyst (reviewed in Madsen & Withers, 1984, 1986). This proposal states that in the active ternary complex the geometry of the 5' phosphate of PLP is distorted (by basic amino acid side chains) into a trigonal pyramidal configuration, with an empty apical position oriented towards the substrate phosphate (see Scheme 2.4). The interaction of the substrate phosphate with this PLP electrophile labilizes the glucosidic bond *via* the transient formation of a partial pyrophosphate bond. In the proposed mechanism the transition state involves both oxocarbonium ion-like sugar and trigonal bipyramidal phosphate species.

### 2.1.6. Glycogen phosphorylase catalysis as a rapid equilibrium, bireactant system.

Initial-rate, binding, and inhibition studies, as well as studies of isotopic exchange at equilibrium, have all demonstrated that glycogen phosphorylase is a two-substrate enzyme with a rapid equilibrium, random bi-bi reaction mechanism (Engers et al., 1969, 1970; Gold et al., 1970; Maddaiah & Madsen, 1966) (see Scheme 2.5).
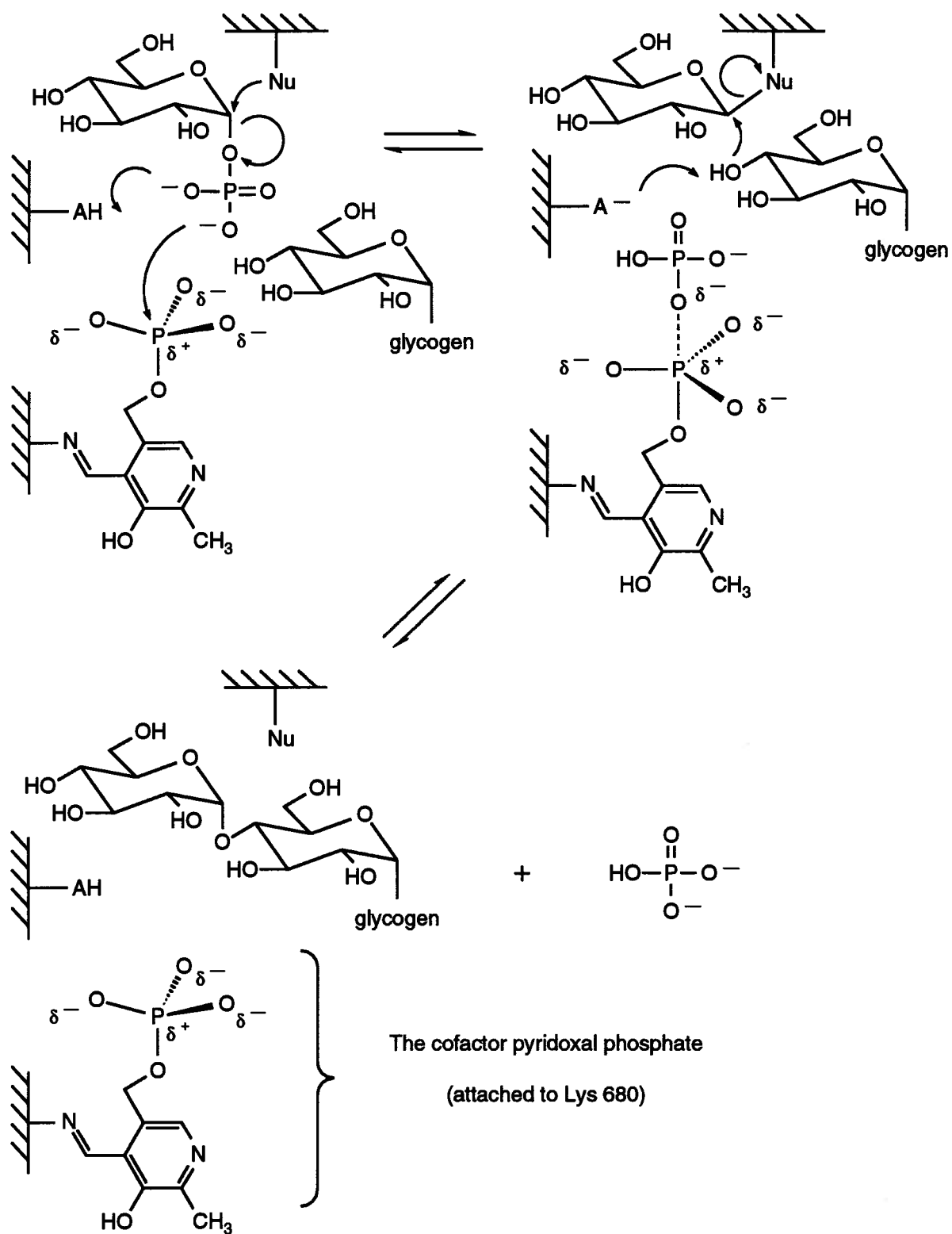
**Scheme 2.4.** The proposed role of the phosphorylase cofactor PLP as an electrophile.
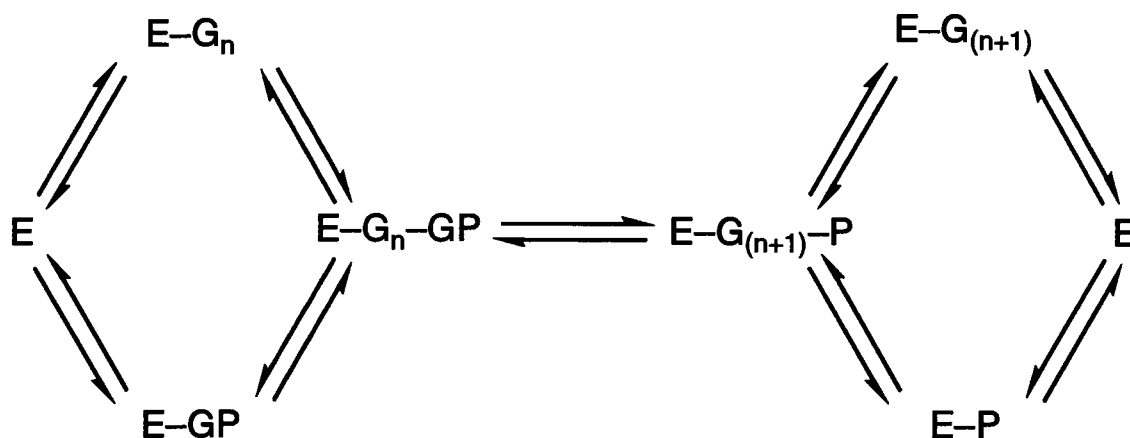
**Scheme 2.5.** The rapid equilibrium, random bi-bi mechanism for glycogen phosphorylase.

Adapted from Engers et al. (1969). The symbols are defined as follows:

| | | | | | |
|---|---|---|---|---|---|
| **E** | = | Enzyme | **E–Gₙ–GP** | = | ternary complex |
| **E–Gₙ** | = | Enzyme–glycogen complex | **E–G₍ₙ₊₁₎–P** | = | ternary complex |
| **E–GP** | = | Enzyme–αG1P complex | **E–P** | = | enzyme–phosphate complex |

In the *glycogen synthesis* direction of the proposed reaction mechanism, glycogen phosphorylase first binds to either one of its two substrates ($G_n$ or GP in Scheme 2.5). Either of these two binary complexes may then bind to the remaining substrate. The result is a ternary complex (E–$G_n$–GP in Scheme 2.5) that may be formed randomly in either of the two pathways shown (on the left-hand side of Scheme 2.5).

In the opposite direction—*glycogen phosphorolysis*—the enzyme first binds either of its two substrates ($G_{(n+1)}$ or P in Scheme 2.5), and then either of these two binary complexes may bind to the remaining substrate. The result is a ternary complex (E–$G_{(n+1)}$–P in Scheme 2.5) that may be formed randomly in either of the two pathways shown (on the right-hand side of Scheme 2.5).

Both of the ternary complexes (i.e., formed from either direction) are interconvertible (see Scheme 2.6), and this interconversion is the rate-limiting step of the reaction. The fact that the isomerization of the ternary complex is rate-limiting indicates that this step is slow compared with the formation of the product. However,

no product may be formed until after the ternary complex has formed. To simplify matters, in most kinetic studies (including those reported herein) one of the substrates (e.g., glycogen) is kept at saturating concentrations, and under these conditions the model reduces to a single-substrate system.

**E–G$_n$–GP**

glycogen

*Synthesis mode*

**E–G$_{(n+1)}$–P**

glycogen

*Phosphorolysis mode*
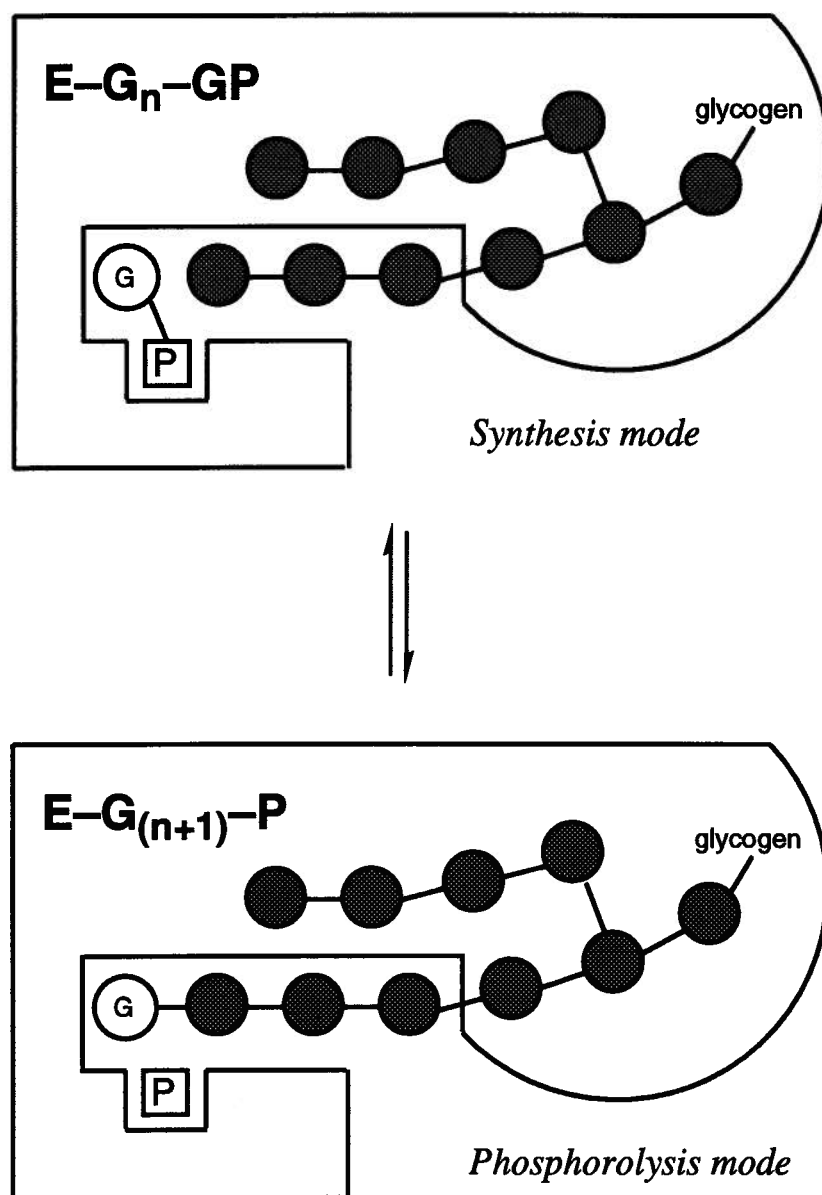
**Scheme 2.6.** Schematic representation of the ternary complexes of glycogen phosphorylase.

The two modes of glycogen binding are mutually exclusive. Circles represent glucosyl residues. Other symbols are defined in Scheme 2.5. Adapted from Segel (1975).

## 2.2. THE AIMS OF THIS STUDY.

Glycogen phosphorylase is known to be extremely specific for its substrate, and very few substrate analogues have been found that are turned over by this enzyme. One such substrate analogue is heptenitol (see Chapter 1 of this thesis). Heptenitol acts as a substrate analogue for glycogen phosphorylase exclusively in the degradation reaction (McLaughlin et al., 1984).

As was mentioned in the first Chapter, 2-deoxy-2-fluoroglycosides with the appropriate anomeric configuration rapidly inactivate $\beta$-retaining glycosidases, and these compounds also partially inactivate some $\alpha$-glycosidases (Withers et al., 1988). Fluorinated heptenitols, with one or two electron-withdrawing fluorine atoms situated adjacent to the reaction centre, were therefore considered to be potential inactivators (irreversible inhibitors) of glycosylases. One advantage of these compounds over 2-deoxy-2-fluoro sugars is that the former can be used to study the effect of *varying* the degree of withdrawal of electron density from the reaction centre, while maintaining interactions between the 2-hydroxyl of the sugar and the enzyme. Hence difluoroheptenitol ($F_2$hept), (2.1), and monofluoroheptenitol ($F_1$hept), (2.2), were synthesized, and kinetic studies of these compounds were carried out using two glycosylases, glycogen phosphorylase and $\beta$-glucosidase. The results of the kinetic studies performed with $\beta$-glucosidase will be discussed in Chapter 3.
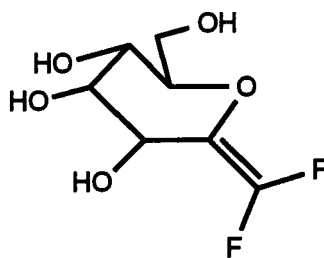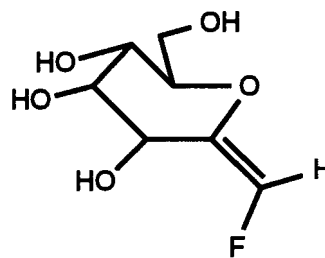


**[2.1]**                **[2.2]**

The fluorinated heptenitols studied herein have the same basic structure as heptenitol, except that one or both of the vinylic hydrogens is replaced by fluorine. These fluorinated heptenitols were therefore expected to bind to the active site of glycogen phosphorylase. One or both of these fluoroheptenitols might act as a *substrate* of phosphorylase (which would be expected if both glycosylation and deglycosylation of the enzyme

were rapid). If either of the fluoroheptenitols acted as a substrate, the influence of inductive effects on the reaction mechanism could be studied.

Alternatively, one or both of these fluoroheptenitols might act as an irreversible inhibitor (inactivator) by forming a covalent glucosyl-enzyme intermediate (which would be expected if the rate of glycosylation exceeded the rate of deglycosylation), or act as a reversible inhibitor. Enzyme inhibitors are useful for studies of reaction mechanisms, and often yield insights into the nature of the binding interactions between the inhibitor and the active site. Such information may be obtained from kinetic or structural studies (e.g., X-ray crystallography). Fluorinated inhibitors are especially useful in enzyme kinetic studies because fluorine substitution provides an active-site probe for the spectroscopic analysis of trapped glycosyl-enzyme intermediates (e.g., by $^{19}$F NMR). If either of the fluoroheptenitols acted as an inhibitor, then a stable analogue of heptenitol (one that is not turned over) would be particularly useful for X-ray structural studies of the phosphorylase-inhibitor complex.

## 2.3. RESULTS AND DISCUSSION.

### 2.3.1. Syntheses of fluorinated heptenitols.

F$_2$hept was synthesized using a procedure that was briefly described by Motherwell et al. (1989). The first step in this procedure is a Wittig-type reaction using persilylated glucono-1,5-lactone (2.3) (see Scheme 2.7). F$_1$hept was obtained by selective reduction of the appropriately persilylated F$_2$hept derivative (2.5) using Red Al$^®$ [sodium bis(2-methoxyethoxy) aluminum hydride] according to the procedure of Hayashi et al. (1979).

The original, briefly described procedure of Motherwell et al. (1989) for the difluoromethylenation of persilylated glucono-1,5-lactone (2.3) involves refluxing the starting material (in anhydrous THF) together with 5 equiv. of each of the following reagents: (i) tris(dimethylamino)phosphine (HMPT, [Me$_2$N]$_3$P); (ii) dibromodifluoromethane (CF$_2$Br$_2$); and (iii) zinc dust. Unfortunately, there are serious problems associated with this procedure. It requires the use of the toxic reagent HMPT, and a byproduct of the reaction is the oxide (Me$_2$N)$_3$PO (HMPA, hexamethyl phosphoramide), one of the most potent carcinogens known. The reaction is also plagued by variable and generally poor yields (Houlton et al., 1993).
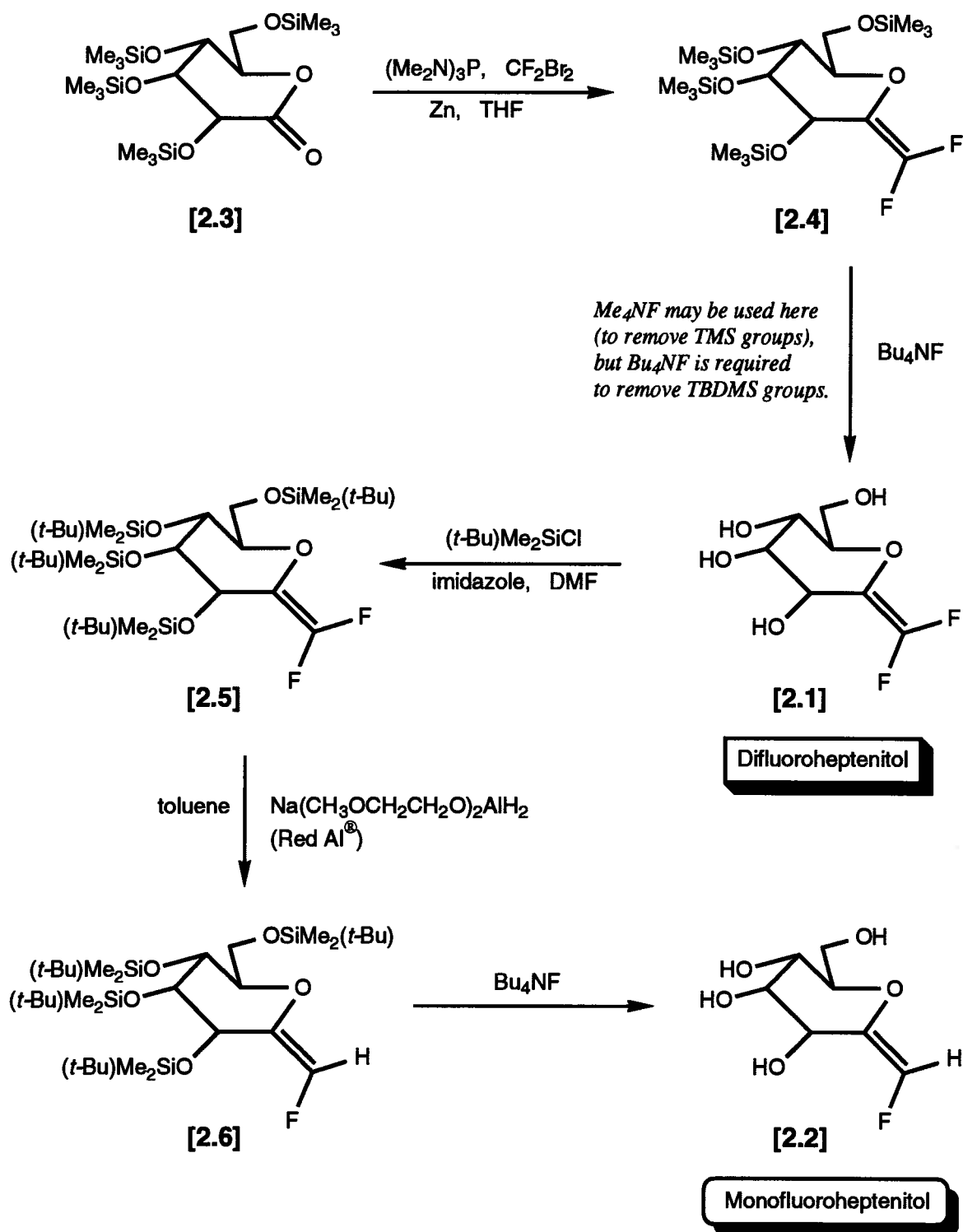
**Scheme 2.7.** The syntheses of F₂hept and F₁hept.

Professor Motherwell's research group has recently published a complete, detailed experimental protocol for the difluoromethylenation of persilylated carbohydrates such as **2.3** (Houlton et al., 1993). The authors attributed the poor reproducibility and low yields of the original version of this procedure (Motherwell et al., 1989) to the use of a heterogeneous system employing zinc dust, which may lead to the decomposition of reaction intermediates.

The deprotection of **2.4** to yield the desired product, $F_2$hept (**2.1**), presented several problems. Regardless of whether $Me_4NF$ or $Bu_4NF$ was used to effect the deprotection, it was found that $F_2$hept co-migrated with the tetraalkylammonium salt during TLC analysis. The tetraalkylammonium salt could not be removed even after repeated column chromatography (27:2:1 ethyl acetate:methanol:water) of the deprotection reaction mixture.

Several cation-exchange resins were then examined to see if they could remove the tetra($n$-butyl)-ammonium ion and allow for the purification of $F_2$hept. These resins (and their counterions) were:

1. Dowex® 50WX$_{12}$    (Na$^+$)        5. Dowex® MR-3X8    (Li$^+$, $^-$OH)

2. Biorex® 70          (Na$^+$)        **6. Dowex® 50WX$_{12}$**    **(Li$^+$)**

3. Dowex® 50 WX$_2$    (Na$^+$)        **7. Dowex® 50 WX$_2$**    **(Li$^+$)**

4. Amberlite® IR 120    (Li$^+$)

Of the resins examined, only #6 and #7, i.e., those containing the lithium salt form of Dowex® 50WX, were able to remove the tetra($n$-butyl)ammonium ion and allow for the purification of $F_2$hept. Resin #7, Dowex® 50 WX$_2$ (Li$^+$), gave the best results of the resins examined, and after cation-exchange, the LiF salt could be easily removed from the crude deprotection reaction mixture by subsequent column chromatography using silica gel.

Difluoroalkenes can be selectively reduced to monofluoroalkenes using the procedure of Hayashi et al. (1979). They found that monofluorinated alkenes (such as 1-fluoro-1-octene and 2-fluoro-1-phenylethene) could be successfully prepared from the corresponding difluorinated derivatives using Red Al® [sodium bis(2-methoxyethoxy) aluminum hydride] as a reducing agent. Hayashi et al. (1979) found that the strong

reducing agent LiAlH$_4$ was nevertheless sluggish and impractical for use in these reactions. Unfortunately, it was found that the difluoroheptenitol derivative **2.4** could not be used as a starting material for the selective reduction reaction because the trimethylsilyl protecting groups were unstable under the reaction conditions. It was therefore necessary to explore the use of alternative protecting groups. Triethylsilyl and *t*-butyldimethylsilyl ethers are about 100 and 10,000 times more stable than trimethylsilyl ethers, respectively (Greene & Wuts, 1991), thus these groups were suitable candidates. Unfortunately, all attempts to persilylate glucono-1,5-lactone with TBDMS chloride were unsuccessful, and if glucono-1,5-lactone was first persilylated with Et$_3$SiCl, the difluoromethylenation reaction (i.e., analogous to **2.3** → **2.4**) was unsuccessful. It was therefore necessary to proceed as shown in Scheme 2.7, first synthesizing the TMS-protected difluoroheptenitol, then replacing the protecting groups.

The purified persilylated F$_1$hept (**2.6**) yielded only one spot after TLC. However, NMR spectroscopy ($^1$H and $^{19}$F) showed that two isomers of persilylated F$_1$hept were formed in a ratio of 28:1 (from the ratio of integrated H-1 resonances in the $^1$H NMR spectra). The spectral ($^1$H, $^{13}$C, and $^{19}$F NMR as well as MS) data for the major isomer (*trans* F$_1$hept and its persilylated precursor) are reported in the Materials and Methods Section.

The selective reduction of difluoroalkenes to monofluoroalkenes using the procedure of Hayashi et al. (1979) generally yields a mixture of the *trans* (major) and *cis* (minor) isomers. Hayashi et al. (1979) found that although the ratio of *trans* and *cis* isomers varied, they obtained substantial amounts ($\geq$ 20% of the product) of the *cis* isomer in each of the reactions studied, except for the synthesis of 2-fluoro-1-phenylethene, where only 7% of the product was the *cis* isomer. Hence it was noteworthy that the synthesis of F$_1$hept yielded only 3.5% of the product as the *cis* isomer.

In most cases the stereochemistry of monofluoroalkenes can be easily identified by the value of the $^{19}$F or $^1$H NMR coupling constant, $^3J_{H,F}$. The $^3J_{H,F}$ values for fluorine and *vicinal* vinylic hydrogens are 40 and 20 MHz for *trans* and *cis* coupling, respectively (Gordon & Ford, 1972). However, the fluorine atom in F$_1$hept lacks a vicinal hydrogen, and hence it was impossible to use $^3J_{H,F}$ values to determine the stereochemistry of F$_1$hept.

## 2.3.2. The stereochemistry of $F_1$hept.

*a. The trans and cis isomers of $F_1$hept.*

The *trans* and *cis* isomers of $F_1$hept are shown below:
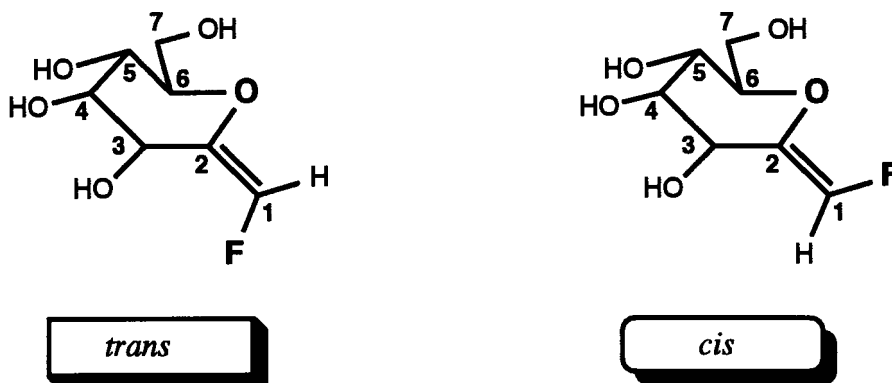


Various NMR experiments were performed in order to confirm the stereochemistry of the major isomer of $F_1$hept.

*b. $^{13}C$ NMR experiments.*

In the $^1$H-decoupled, $^{13}$C NMR spectrum of TBDMS-protected $F_2$hept (**2.5**, see Scheme 2.7), C-1 and C-2 each resonated as a doublet of doublets, and the multiplicity of these resonances arose from coupling with the two fluorine atoms. There was one other doublet in the spectrum (at $\delta = 66.9$ ppm, $J \approx 2$ Hz), and this resonance was assigned to C-3, the multiplicity presumably arising from *trans* allylic coupling with one of the fluorine atoms (see Fig. 2.3a). The other resonances in the $^1$H-decoupled, $^{13}$C NMR spectrum of TBDMS-protected $F_2$hept were singlets (see the Materials and Methods Section for detailed analytical data).

In the $^1$H-decoupled, $^{13}$C NMR spectrum of TBDMS-protected $F_1$hept (**2.6**, see Scheme 2.7) C-3 resonated at $\delta = 65.2$ ppm as a singlet (see Fig. 2.3b and Materials and Methods). It is known that the coupling constant arising from *trans* allylic coupling between a fluorine atom and a carbon atom in a given molecule is greater than the coupling constant that would arise from *cis* allylic coupling between two such atoms in the same allylic moiety of the molecule in question (or a structurally related molecule) (Gaudemer, 1977). The absence of

$\delta$ (ppm)
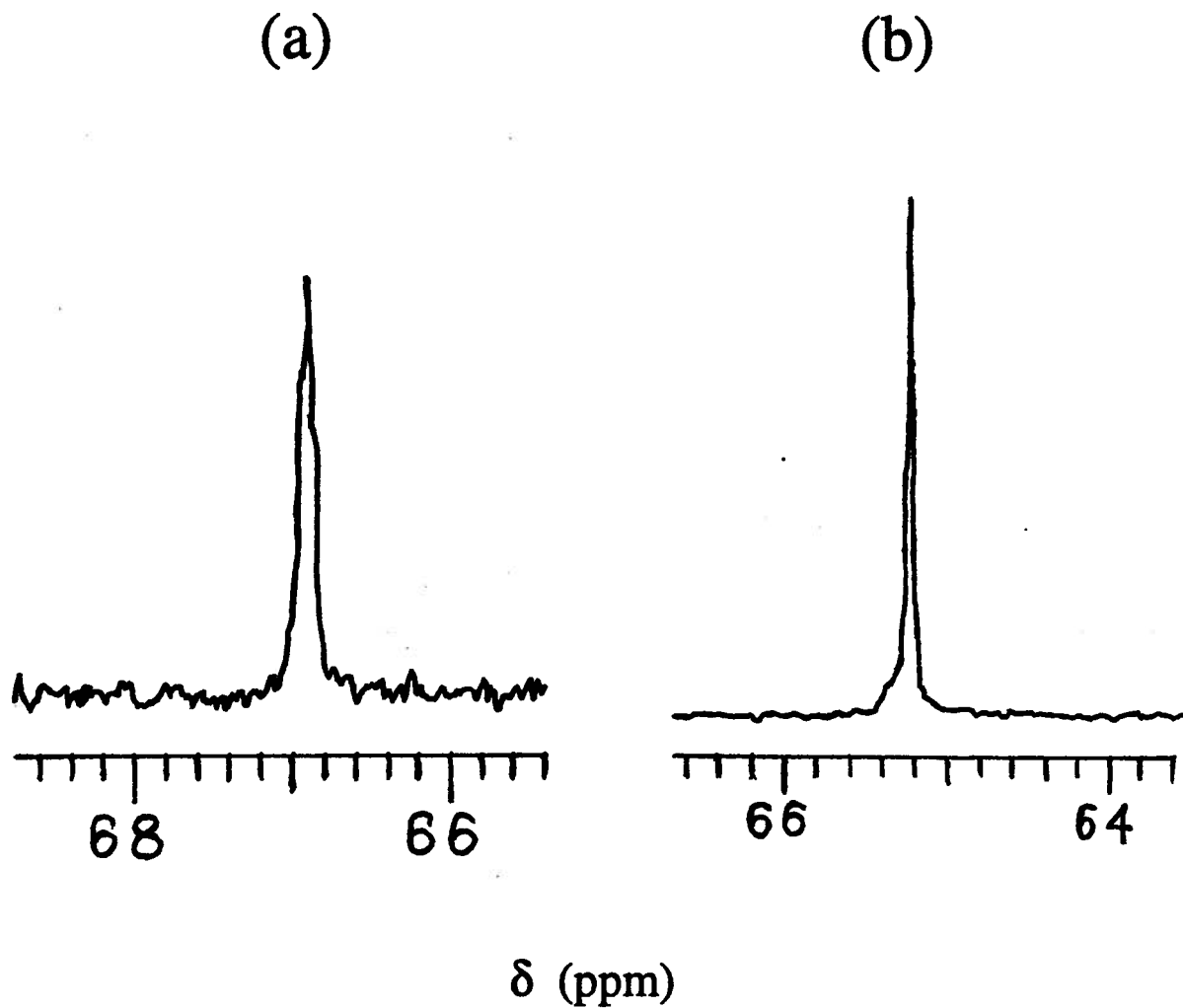
Figure 2.3. $^{13}$C NMR determination of the stereochemistry of the major isomer of $F_1$hept.

75 MHz, $^1$H-decoupled, $^{13}$C NMR spectra were obtained using the samples (in $CDCl_3$) indicated below. Only the relevant regions of the spectra are shown, which contain the signal attributable to C-3 as indicated below.

(a) TBDMS-protected $F_2$hept ($\delta = 66.9$ ppm, $d$, $J = 2$ Hz, C-3).
(b) TBDMS-protected $F_1$hept ($\delta = 65.2$ ppm, $s$, C-3).

coupling in the C-3 resonance ($\delta$ = 65.2 ppm) in the $^{13}$C NMR spectrum of TBDMS-protected $F_1$hept ruled out a *trans* allylic relationship between the fluorine atom and C-3, for if this was the case, a doublet would have been observed. Hence the geometric relationship between the fluorine atom and C-3 in $F_1$hept is *cis*, and therefore O-5 is *trans* with respect to the fluorine atom.

*c. An NOE experiment on TBDMS-protected $F_1$hept.*

The nuclear Overhauser effect (NOE; reviewed in Derome, 1988) frequently yields information on the internuclear distance between atoms. When an NOE experiment on TBDMS-protected $F_1$hept was performed, no enhancement of the vinylic hydrogen (H-1) signal (at $\delta$ = 6.8 ppm) was observed when the H-3 signal (at $\delta$ = 4.57 ppm) was irradiated, and *vice versa* (note that only one peak of the doublet attributable to the vinylic hydrogen could be irradiated at a time due to the magnitude of the coupling constant, $J_{1,3}$ = 80 Hz). This result indicated that the vinylic hydrogen and H-3 are *not* very close to each other. These two hydrogens are most likely *trans* with respect to each other, and hence O-5 is most likely *trans* with respect to F-1. This result agreed with the $^{13}$C NMR data that showed that the predominant isomer of $F_1$hept was the *trans* isomer. However, the *absence* of an NOE does *not* provide definitive proof for the stereochemistry of a molecule.

*d. $^1$H and $^{19}$F NMR experiments.*

The $^1$H NMR spectrum of $F_1$hept provided compelling evidence for the stereochemistry and abundance of the major (*trans*) and minor (*cis*) isomers of this compound. Two doublets attributable to H-1 were observed in this spectrum; one each at $\delta$ = 7.02 and 6.58 ppm, with integration ratios of 28:1, respectively. The more abundant H-1 signal was downfield ($\delta$ = 7.01 ppm) relative to the less abundant H-1 signal ($\delta$ = 6.58 ppm). An exhaustive compilation of experimental data obtained from olefinic compounds (see Table 5 of Gaudemer, 1977) has shown that an olefinic proton that is *cis* to an O-alkyl group resonates downfield from an olefinic proton that is *trans* to the same O-alkyl group. Hence the H-1 atom of the *major* isomer must have been *cis* to the oxygen atom of the sugar ring, which is exactly what one would expect if the major and minor isomers were *trans* and *cis*, respectively.

The $^{19}$F NMR spectrum of F$_1$hept also provided evidence for the stereochemistry of the major (*trans*) and minor (*cis*) isomers of this compound. Two doublets attributable to F-1 were observed in this spectrum; a minor doublet at $\delta$ = -163.78 ppm and a major doublet at $\delta$ = -169.71 ppm. Here the less abundant F-1 signal was downfield ($\delta$ = -163.78 ppm) relative to the more abundant F-1 signal ($\delta$ = -169.71 ppm). Hence the F-1 atom of the *minor* isomer must have been *cis* to the oxygen atom of the sugar ring, which again is exactly what one would expect if the major and minor isomers were *trans* and *cis*, respectively.

The above results are consistent with the assignment of $^1$H and $^{19}$F NMR signals arising from stereoisomeric H-1 and F-1 atoms in the *cis* (**2.7**) and *trans* (**2.8**) monofluoroalkenes shown below (Houlton et al., 1993). In the *cis* isomer (**2.7**), a compound whose stereochemistry has been determined by X-ray crystallography, the vinylic H-1 and F-1 atoms give rise to NMR signals of $\delta$ = 6.37 and -160 ppm in the $^1$H and $^{19}$F spectra, respectively (Houlton et al., 1993). However, in the *trans* isomer (**2.8**), the vinylic H-1 atom gives rise to a signal of $\delta$ = 7.00 (downfield from $\delta$ = 6.37 ppm) in the $^1$H NMR spectrum, and the vinylic F-1 atom gives rise to a signal of $\delta$ = -177.4 (upfield from $\delta$ = -160 ppm) in the $^{19}$F NMR spectrum (Houlton et al., 1993). These data are what one would expect based on the geometric relationship of the stereoisomeric H-1 and F-1 atoms to the ring oxygen.



**[2.7]** *(cis)*          **[2.8]** *(trans)*
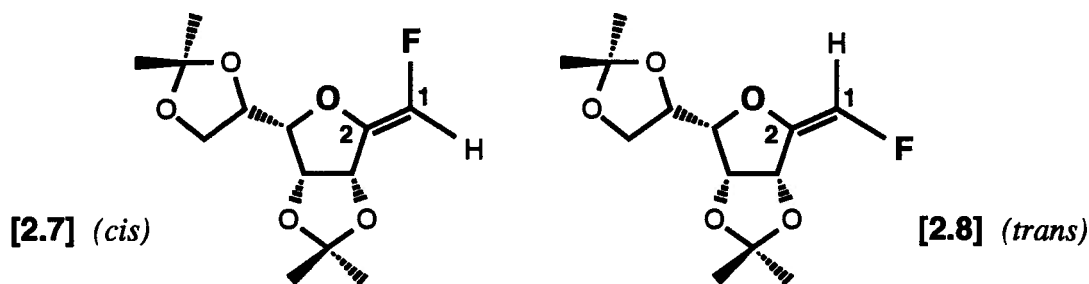
### 2.3.3. Substrate and inactivation tests using F$_2$hept.

F$_2$hept was tested as a substrate of phosphorylase *b* in the glycogen phosphorolysis reaction. In this experiment, 17 m*M* F$_2$hept was incubated with 100 m*M* KCl, 1 m*M* EDTA, 1 m*M* DTT, 50 m*M* triethanolamine hydrochloride (pH 6.8), 1% glycogen, 5 m*M* orthophosphate, 1.5 m*M* AMP, and 0.6 mg of enzyme. After five days at room temperature there was no detectable turnover of F$_2$hept as measured by TLC and $^{19}$F NMR.

The substrate test was run in parallel with a control reaction *without* $F_2$hept but otherwise containing the same reaction components. During the course of the above test, small aliquots (10 μL) were removed from the substrate test and the control reaction, and then added to fresh tubes, each of which contained 0.500 mL of a reaction mixture containing a saturating concentration (16 m$M$) of αG1P, 1 m$M$ AMP, 1% glycogen, 100 m$M$ KCl, 1 m$M$ EDTA, 1 m$M$ DTT, and 50 m$M$ triethanolamine hydrochloride (pH 6.8). Initial reaction rates were then assayed in the direction of glycogen synthesis as described (Engers et al., 1970). No significant decrease in phosphorylase activity was observed over 5 days when the results obtained using aliquots from the substrate test were compared with those from the parallel control reaction.

### 2.3.4. Inhibition studies using $F_2$hept and $F_1$hept.

Inhibition studies were performed using phosphorylase acting in either direction of the reaction. In the glycogen synthesis direction, the experiments were performed using a constant concentration (1%) of glycogen, 5 different concentrations of αG1P, and 4-5 different concentrations of the inhibitor (as well as in the absence of the inhibitor). About 2.5 μg of phosphorylase $b$ (from rabbit muscle) was used in each reaction. The exact reaction conditions are given in the legends to Figs. 2.4 and 2.5. A standard assay (Engers et al., 1970) was used to determine the amount of inorganic phosphate released during the reaction.

When the data for Figs. 2.4a and 2.5a were plotted as double-reciprocal or Dixon plots, curved lines were obtained, indicating that the fluoroheptenitols bind to and stabilize the T-state conformation of phosphorylase. Straight lines were obtained from Hill plots ($\ln[v/(V_{max} - v)]$ vs. $\ln[S]$) with both inhibitors (Figs. 2.4a and 2.5a). The values of the inhibition constants were determined from replots of the apparent $K_m$ values ($K_{m,app}$) versus the inhibitor concentrations (Figs. 2.4b and 2.5b). $F_2$hept and $F_1$hept both acted as competitive inhibitors of phosphorylase. These conclusions were based on the fact that for both compounds— over the range of inhibitor concentrations studied—the $V_{max}$ was constant, while the $K_m$ value showed an apparent increase of a factor of ($1 + [I]/K_i$) (Segel, 1975). The $K_i$ values of $F_2$hept and $F_1$hept for the glycogen synthesis reaction were $4.9 \pm 0.4$ and $4.0 \pm 0.4$ m$M$, respectively. The values of the kinetic parameters for these compounds and other substrates and inhibitors of phosphorylase are summarized in Table 2.1.
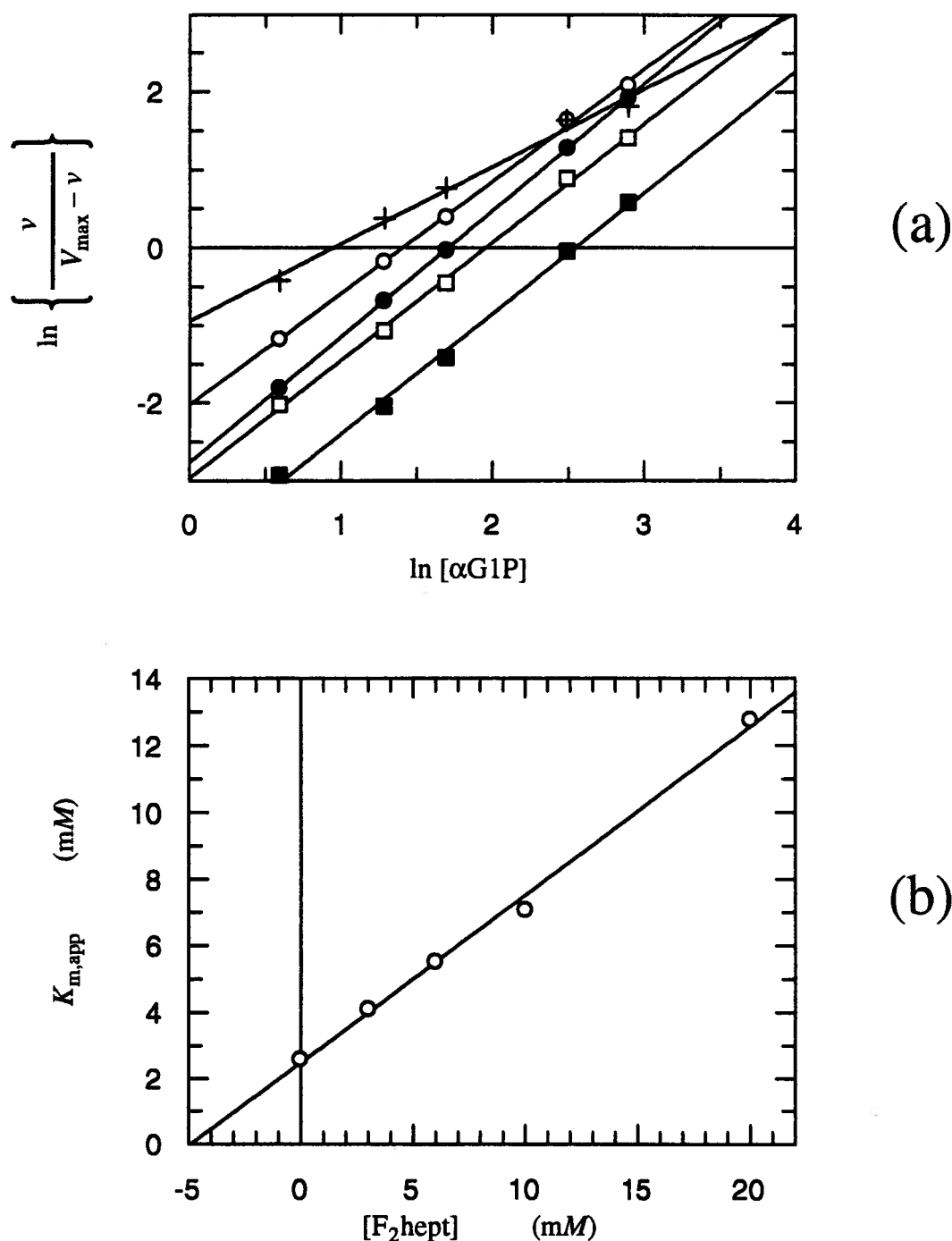
**Figure 2.4.** Kinetic parameters for the inhibition by $F_2$hept of phosphorylase-catalyzed glycogen synthesis.

(a) Hill plots used to determine $K_{m,app}$ for the inhibition by $F_2$hept of phosphorylase $b$-catalyzed utilization of αG1P. Reactions (0.500 mL) were performed at 30 °C and contained 100 m$M$ KCl, 50 m$M$ TEA-HCl (pH 6.8), 1 m$M$ EDTA, 1 m$M$ DTT, 1 m$M$ AMP, 1% glycogen, and 2.5 μg of rabbit muscle phosphorylase $b$. Initial rates for the 5-min reactions were determined using a standard phosphate assay (Engers et al., 1970). The concentrations of $F_2$hept in the reactions were 0 {+}, 3.0 {o}, 6.0 {●}, 10 {□}, and 20 {■} m$M$.

(b) A replot of data obtained from panel (a) in order to estimate the value of the $K_i$ by visual inspection. The following values of $K_{m,app}$ were determined from panel (a): 2.6, 4.1, 5.5, 7.1, and 13 m$M$.
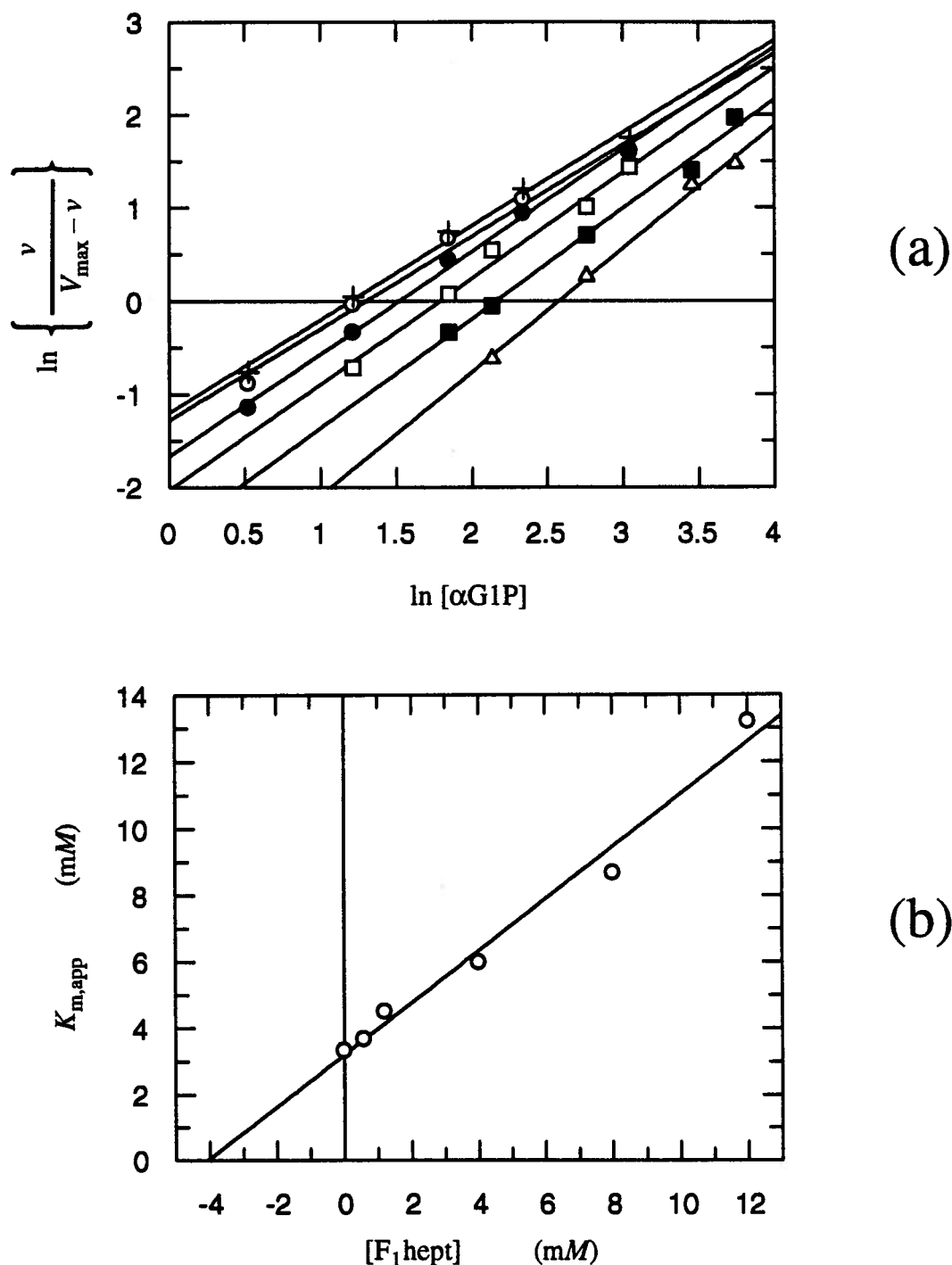
**Figure 2.5.** Kinetic parameters for the inhibition by $F_1$hept of phosphorylase-catalyzed glycogen synthesis.

(a) Hill plots used to determine $K_{m,app}$ for the inhibition by $F_1$hept of phosphorylase $b$-catalyzed utilization of $\alpha$G1P. Reactions were performed as described in Fig. 2.4 except that the concentrations of $F_1$hept in the reactions were 0 {+}, 0.60 {o}, 1.2 {●}, 4.0 {□}, 8.0 {■}, and 12 {△} m$M$.

(b) A replot of data obtained from panel (a) in order to estimate the value of the $K_i$ by visual inspection. The following values of $K_{m,app}$ were determined from panel (a): 3.3, 3.7, 4.5, 6.0, 8.7, and 13 m$M$.
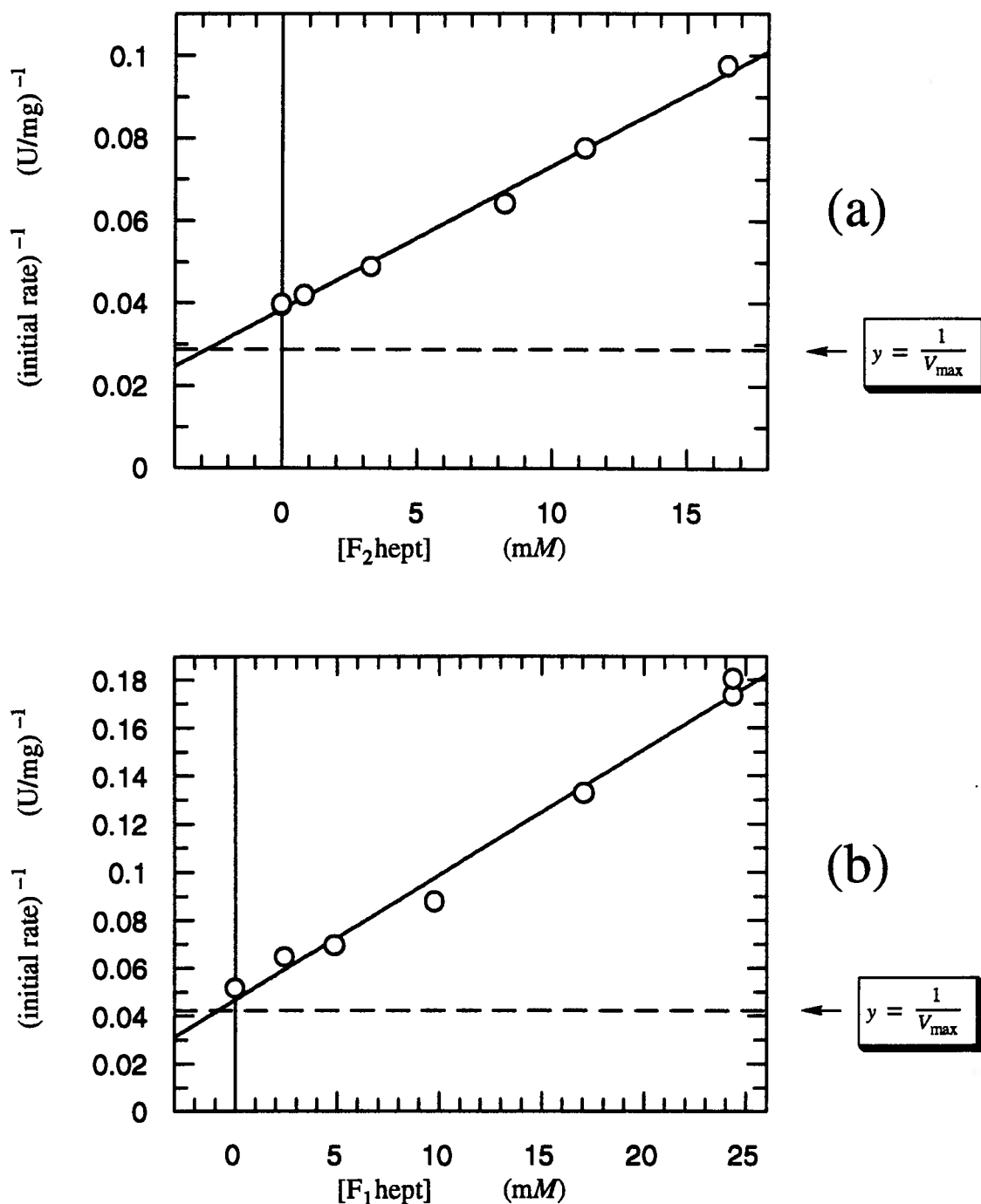
**Figure 2.6.** The inhibition by fluoroheptenitols of phosphorylase-catalyzed glycogen phosphorolysis.

Initial rates were measured by quantitating the reduction of NADP spectrophotometrically (Engers et al., 1969). Reactions (0.205 mL, 30 °C, and pH 6.8) contained 0.15 μg of rabbit muscle phosphorylase *b*, 35 m$M$ imidazole, 20 m$M$ sodium glycerophosphate, 10 m$M$ Mg(OAc)$_2$, 5 m$M$ DTT, 1 m$M$ EDTA, 1 m$M$ AMP, 0.5% glycogen, 1 m$M$ βNADP, 15 U/mL phosphoglucomutase, and 3.4 U/mL of glucose-6-phosphate dehydrogenase.

(a) Inhibition by F$_2$hept. The concentrations of F$_2$hept in the reactions were 0, 0.83, 3.3, 8.3, 11.2, and 16.5 m$M$.
(b) Inhibition by F$_1$hept. The concentrations of F$_1$hept in the reactions were 0, 2.4, 4.9, 9.8, 17.1, and 24.4 m$M$.

**Table 2.1.** Dissociation constants of fluoroheptenitols and substrates with phosphorylase $b$.

| Compound | $K_i$ or $K_m$ (mM) | | Reference |
|---|---|---|---|
| | glycogen synthesis | glycogen phosphorolysis | |
| F$_2$hept | 4.9 ± 0.4 | ~2.8 | this work |
| F$_1$hept | 4.0 ± 0.4 | ~0.9 | *ibid.* |
| αG1P | 1.5 | — | Engers et al., 1969 |
| D-glucose | 2.0 | — | Street et al., 1986 |
| heptenitol | — | 4.3[a] | Klein et al., 1986 |
| orthophosphate | — | 1.1[b] | Engers et al., 1969 |

Except as noted in (b) below, data were obtained from reactions with 1 m$M$ AMP and a saturating concentration of glycogen (1%).

(a) Obtained using arsenate in lieu of phosphate.
(b) A value of 15 m$M$ was obtained with 1 m$M$ AMP and a *nonsaturating* concentration of glycogen.

"Range-finding" (or approximate) $K_i$ values ($RF$ $K_i$ values) for F$_2$hept and F$_1$hept were determined for the glycogen phosphorolysis reaction (Fig. 2.6). In these experiments, initial rates were determined using a single concentration of the substrate orthophosphate (21 m$M$), and 5 different inhibitor concentrations (as well as with no inhibitor). As before, glycogen was present in all phosphorolysis reactions at a saturating concentration (1%). Initial rates were determined using a *phosphoglucomutase/glucose-6-phosphate dehydrogenase* coupled assay (Engers et al., 1969). The approximate $K_i$ values for F$_2$hept and F$_1$hept were determined from the appropriate Dixon plot (1/$v$ vs. [I]) (Fig. 2.6).

The linear plots obtained in this case (Fig. 2.6) suggest that in the presence of orthophosphate, F$_2$hept and F$_1$hept were able to bind to the R-state conformation of the enzyme. Similar behaviour has been observed previously with glucono-1,5-lactone and nojirimycin tetrazole (Gold et al., 1971; Withers & Rupitz, unpublished results). The approximate $K_i$ values for F$_2$hept and F$_1$hept were 2.8 and 0.9 m$M$, respectively, for the glycogen

phosphorolysis reaction. The dissociation constants ($K_i$ or $K_m$) of the fluoroheptenitols, their parent compound (heptenitol), and other substrates in either direction of the reaction catalyzed by phosphorylase $b$ are given in Table 2.1.

The monosaccharides listed in Table 2.1 all exhibited similar affinities for the enzyme's active site (i.e., $K_i$ or $K_m$ values in the 5 m$M$ range). These monosaccharides have closely related glycone moieties (glucose or *gluco*-heptenitol structures), but quite different aglycone moieties. However, the monosaccharides listed in Table 2.1 all have aglycone moieties that are either negatively charged (e.g., the phosphate moiety in αG1P), or uncharged but electron-rich (e.g., C=C moiety in the heptenitols). This suggests that there must be one or more positively charged (or electron-accepting) amino acid side chains adjacent to the anomeric carbon atom of the monosaccharide substrate (or inhibitor) in the enzyme's active site.

### 2.3.5. X-ray crystallographic studies.

X-ray crystallography has been used to study the binding of heptenitol (and heptulose-2-phosphate) by glycogen phosphorylase $b$ (Hajdu et al., 1987; Johnson et al., 1990), and these studies have yielded insights into the catalytic mechanism of the enzyme. As an example, the high-resolution crystal structure of the heptulose-2-phosphate-enzyme complex provided considerable experimental support for the "proton transfer" role of the cofactor PLP (McLaughlin et al.,1984; see also Johnson et al., 1990).

Another example of the utility of X-ray crystallographic studies is the work of Hajdu et al. (1987), who used a synchrotron radiation source and fast data-collection techniques to "observe" the progress of the catalytic conversion of heptenitol to heptulose-2-phosphate in crystals of phosphorylase $b$. Their objective was to detect the transient accumulation of a ternary complex (involving the enzyme, heptenitol, and phosphate) prior to the formation of the product (heptulose-2-phosphate). They did indeed obtain data indicating occupancy of the phosphate-binding site, as well as occupancy of the sugar-binding site, at early stages of the reaction. Occupancy of the phosphate-binding site increased with time, and its electron density eventually became contiguous with that of the reaction centre on the sugar, consistent with the formation of the product, heptulose-2-phosphate. However, the enzyme has a much higher affinity for the product, heptulose-2-phosphate ($K_i$ = 14 μ$M$; Klein et al.,1984), than for phosphate ($K_i$ = 15 m$M$ for AMP-activated phosphorylase; Engers

et al., 1969). It is therefore debatable whether the crystal structure observed at the early stages of the reaction in question represents a ternary complex (involving the enzyme, heptenitol, and phosphate) or a mixture of two binary complexes: (i) the enzyme and heptenitol, as well as (ii) the enzyme and heptulose-2-phosphate (Hajdu et al., 1987).

Hence even with the fastest available X-ray crystallographic data-collection methods, it is still necessary to reduce the phosphorylase reaction rate as much as possible in order to detect phosphate bound in the enzyme's active site (i.e., prior to the formation of any product). Part of the reason for this is that the rate-limiting step in data accumulation is the diffusion of the ligands into the crystal. Thus it is necessary to reduce the reaction rate to below the rate of diffusion of small ligands into the crystal. The use of fluorinated heptenitols proved to be especially useful for this purpose. The results of the kinetic studies reported herein showed that fluoroheptenitols are not turned over by the enzyme. Furthermore, it is known that in the absence of heptenitol, phosphate alone cannot bind in the active site of phosphorylase $b$ (E. Duke, pers. comm.). However, from the data discussed below, it appears that the binding of $F_1$hept promotes the binding of phosphate, and allows for the detection of phosphate bound in the active site, since in this case there is no detectable formation of a product.

X-ray crystallographic studies of each of the fluoroheptenitols bound at the active site of glycogen phosphorylase $b$ were carried out in collaboration with Dr. E. Duke and Prof. L. N. Johnson of the Laboratory of Molecular Biophysics at Oxford University. Crystals of T-state phosphorylase $b$ were soaked in a solution of 50 m$M$ fluoroheptenitol, 50 m$M$ phosphate, 10 m$M$ Mg(OAc)$_2$, 2.5 m$M$ AMP, in 10 m$M$ BES-NaOH, pH 6.7. Each crystal was soaked for a minimum of 30 min to allow for diffusion of the ligands into the crystal.

The three-dimensional electron-density map of the phosphorylase–$F_1$hept co-crystal showed a weak but readily detectable region of electron density attributable to the binding of phosphate (Fig. 2.7a). Phosphate was bound in a region of the active site directly below (i.e., on the α-face of) the sugar ring of $F_1$hept, close to the fluorine atom of $F_1$hept and also adjacent to the 5' phosphate of the cofactor PLP (Fig. 2.7a). The structural data from the phosphorylase–$F_1$hept co-crystal agree with the results of mechanistic studies which postulated that the bound substrate phosphate and the 5' phosphate of PLP are very close together in the active site of

**Figure 2.7.** The structure of $F_1$hept or $F_2$hept bound in the active site of glycogen phosphorylase $b$.

Co-crystals of T-state glycogen phosphorylase $b$ and either $F_1$hept (a) or $F_2$hept (b) were prepared as described in the text. Data were collected to 2.3 Å resolution by Dr. E. Duke in Prof. L. N. Johnson's laboratory at Oxford. Contours of electron density are indicated.
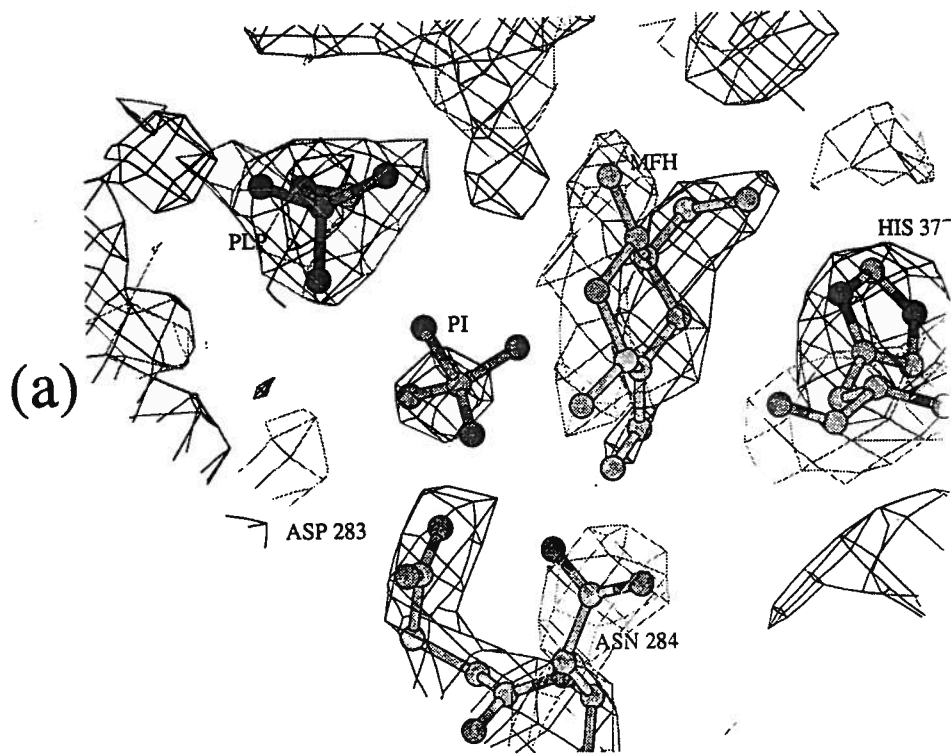
(a) $F_1$hept–phosphorylase. Electron density for phosphate was observed below the sugar ring. This perspective of the structure does not permit a clear view of the oxygen atom of the C-4 hydroxyl group.

(b) $F_2$hept–phosphorylase. No electron density for phosphate was observed. *For the purpose of comparison only,* this electron density map shows the location of the phosphate bound in the phosphorylase–**$F_1$hept** co-crystal.

Asp 283

Asn 284

Pi

PLP

Difluoroheptenitol : cyan

Monofluoroheptenitol : yellow

His 377
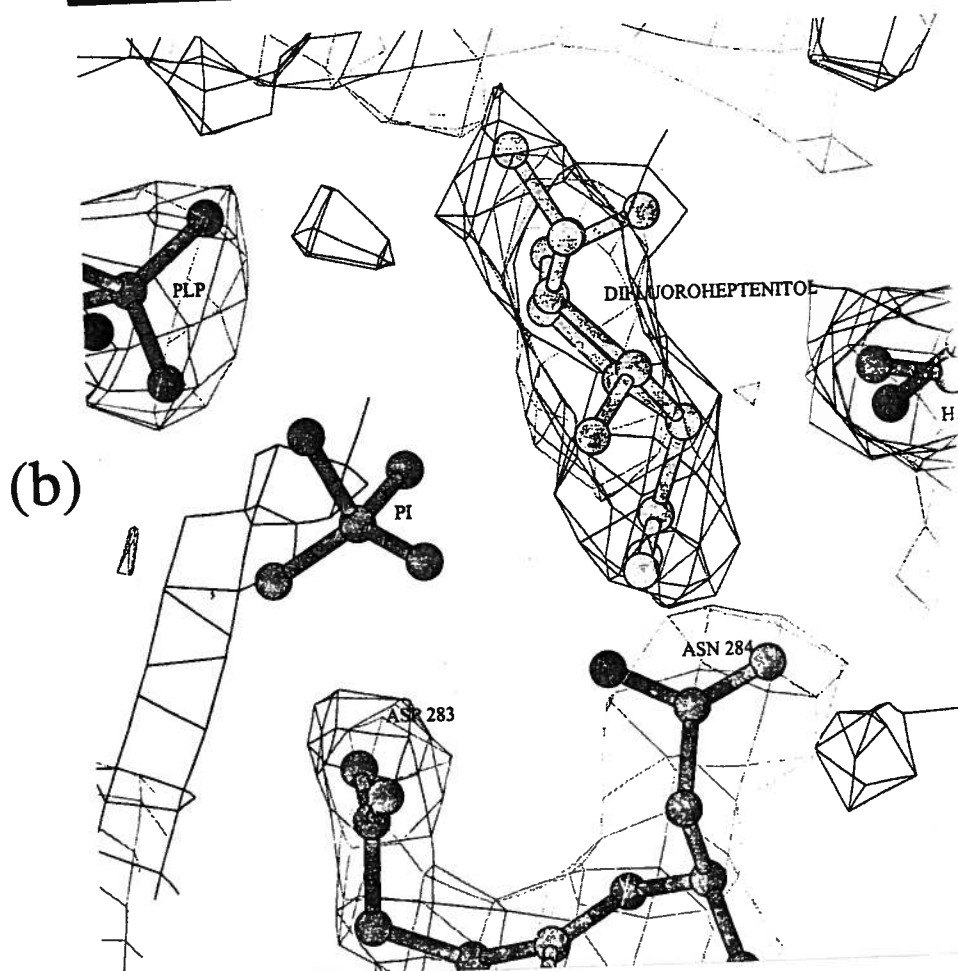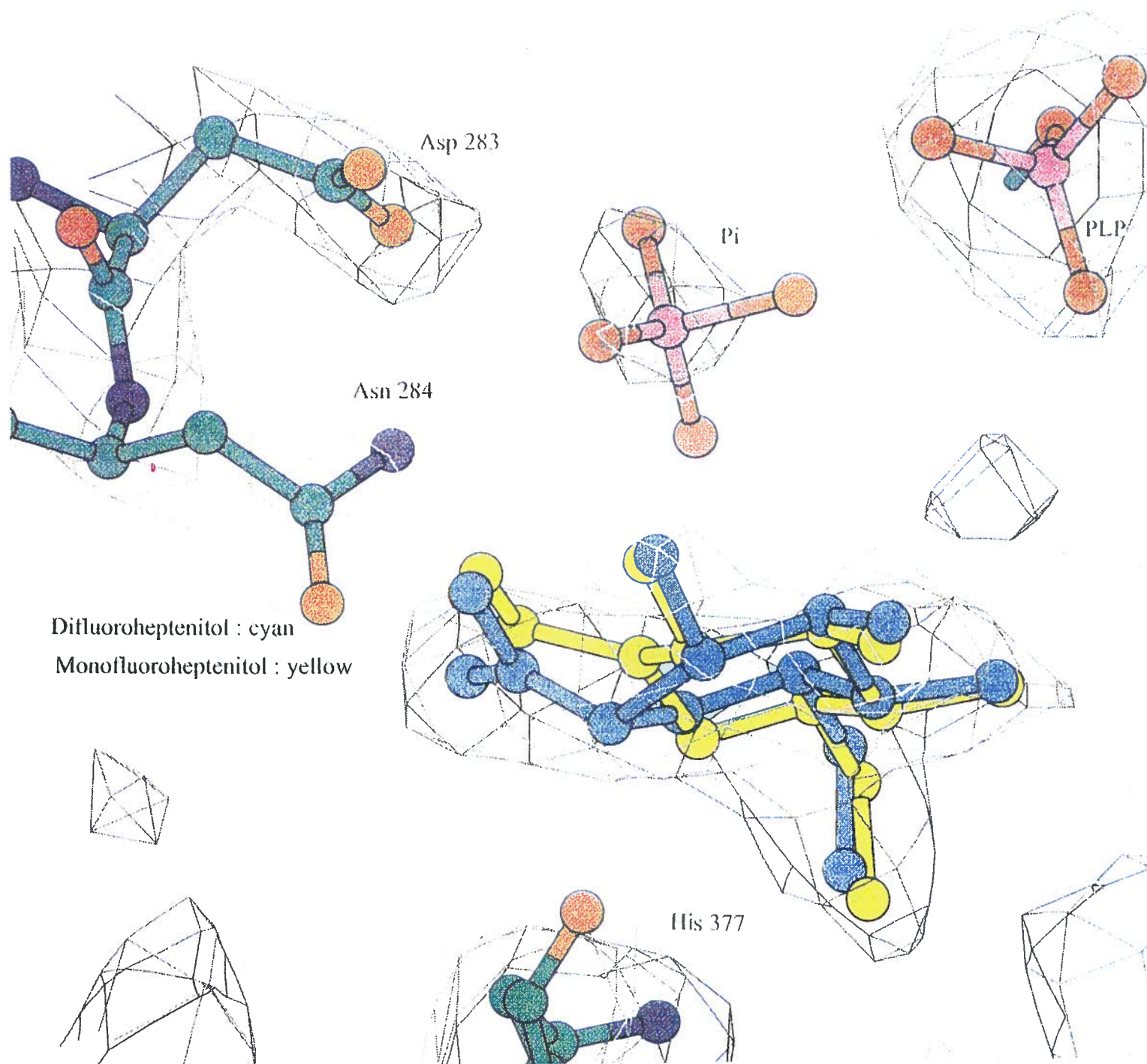
**Figure 2.8.** Composite electron-density map of fluoroheptenitols bound in the active site of phosphorylase $b$.

This electron density map is a composite of two separate maps of either $F_1$hept (yellow) or $F_2$hept (blue) bound in the active site of T-state glycogen phosphorylase $b$ (see Fig. 2.7). The electron density attributable to phosphate is from the $F_1$hept-phosphorylase co-crystal only.

phosphorylase, and that their interaction with each other is the major source of the catalytic power of the enzyme (Helmreich, 1992; Madsen & Withers, 1984, 1986; Palm et al., 1990).

The three-dimensional electron-density map of the phosphorylase–$F_2$hept co-crystal did not show any region of electron density attributable to the binding of phosphate in the active site (Fig. 2.7b). For the purpose of comparison, this electron density map shows the location of the phosphate *bound in the phosphorylase–$F_1$hept co-crystal*, but it is clear that in the *same* region of the electron density map of the phosphorylase–$F_2$hept co-crystal there is *no* corresponding electron density (compare the electron-density contours of Figs. 2.7a and 2.7b in this region). It may be that the presence of *two* electron-rich fluorine atoms at the C-1 position of a heptenitol derivative bound at the active site destabilizes the enzyme-substrate interactions necessary for the binding of a negatively charged phosphate immediately adjacent to these fluorine atoms.

Both $F_1$hept and $F_2$hept bound to the same location in the active site of phosphorylase *b* as heptenitol, and all three heptenitols appeared to exploit the same binding interactions with the same amino acid residues of the enzyme (Fig. 2.8; see also McLaughlin et al., 1984 for the binding of heptenitol in the enzyme's active site). Extra lobe(s) of electron density representing the fluorine atoms were evident (Figs. 2.7-2.8). When the electron density maps of the fluoroheptenitol-enzyme co-crystals were compared with that of the enzyme alone, it appeared that the position of the Asn 284 side chain had moved slightly in order to accommodate the fluorine atom(s) in each case (E. Duke, pers. comm.).

Interestingly, closer examination of the structures shown in Fig. 2.8 suggested that the two bound sugars adopted different conformations. $F_1$hept appeared to bind in a full-chair conformation, as had been found previously for heptenitol (Hajdu et al., 1987), whereas $F_2$hept appeared to adopt a structure resembling a half chair (E. Duke, pers. comm.). However, the resolution of the data (2.3 Å) is insufficient to place much confidence in these interpretations.

Only one isomer (*trans*) of $F_1$hept was observed in the X-ray structure of the phosphorylase–$F_1$hept co-crystal, as evidenced by the single lobe of electron density due to fluorine at C-1 (see Fig. 2.7a). Prior to the X-ray crystallographic studies, analytical data for $F_1$hept already had indicated the formation of one major

(>96%) isomer. The results of various NMR experiments (reported earlier in this chapter) indicated that the major isomer was *trans* $F_1$hept, and hence the X-ray crystallographic and NMR results were in good agreement.

## 2.4 CONCLUSIONS.

The $^1$H NMR spectrum of $F_1$hept showed that the major (>96%) isomer formed during the selective reduction of $F_2$hept was the *trans* isomer, and that a minor (<4%) but detectable amount of the *cis* isomer was also formed. The assigned stereochemistry of the major isomer of $F_1$hept was confirmed by $^1$H, $^1$H NOE, $^{13}$C, and $^{19}$F NMR experiments.

Both $F_2$hept and $F_1$hept were found to be competitive inhibitors of phosphorylase, binding to the active site in the absence of phosphate and stabilizing the (inactive) T-state of the enzyme, as seen with glucose analogues (Martin et al., 1991; Street et al., 1986).

The binding constants of $F_2$hept, $F_1$hept and αG1P in the glycogen synthesis direction are all similar (1-5 m$M$; see Table 2.1). The inhibition constants of $F_2$hept, $F_1$hept and heptenitol in the glycogen phosphorolysis direction are also similar (1-4 m$M$; see Table 2.1). These results indicate that fluorine substitution did not significantly affect the affinity of the enzyme for the heptenitol derivatives under study.

As was discussed in Chapter 1, heptenitol acts as a "suicide substrate" for phosphorylase in the glycogen degradation reaction. Heptenitol is rapidly turned over by the enzyme to form 1-deoxy-D-*gluco*-heptulose-2-phosphate, which acts as a tight-binding inhibitor (Klein et al., 1984). Given that heptenitol and $F_2$hept possess similar affinities for glycogen phosphorylase *b*, the inability of $F_2$hept to act as either a substrate or an inactivator must be due to a very slow rate of hydration ($k_1$). This slow rate of hydration of $F_2$hept is probably attributable to the inductive effect of the electron-withdrawing fluorine atoms at the C-1 position, which would destabilize any development of positive charge at the reaction centre. Hence the kinetic results are in agreement with the proposal that the reaction mechanism of phosphorylase involves oxocarbonium ion-like transition states.

The synthesis of fluoroheptenitols also proved to be a valuable contribution to X-ray crystallographic studies of glycogen phosphorylase carried out by collaborators in Great Britain. These studies yielded important

insights into the binding of phosphate in the enzyme's active site. In particular, they provided the first proof that a heptenitol derivative and phosphate can bind simultaneously, something which was not clear from earlier work performed with heptenitol (due to conversion to the product). Phosphate was bound in a region of the active site directly below (i.e., on the $\alpha$-face of) the sugar ring of *trans* $F_1$hept, close to the fluorine atom and also adjacent to the 5' phosphate of the cofactor PLP (see Fig. 2.7a). Both *trans* $F_1$hept and $F_2$hept bound to the same location in the active site of phosphorylase $b$ as heptenitol, and all three heptenitols appeared to exploit the same binding interactions with the same amino acid residues of the enzyme. Finally, the assigned stereochemistry of the major isomer of $F_1$hept (*trans*) was confirmed by the results of the X-ray crystallographic studies of the $F_1$hept-phosphorylase co-crystal.

Since fluoroheptenitols possess no anomeric configuration, they may also prove useful for kinetic and structural studies of other $\alpha$- or $\beta$-glucosyl mobilizing enzymes. These fluoroheptenitols might act as reversible or possibly even irreversible inhibitors of these enzymes. Indeed, the next chapter of this thesis shows that these compounds also reversibly inhibit *Agrobacterium* $\beta$-glucosidase.

## CHAPTER 3: KINETIC STUDIES USING β–GLUCOSIDASE

*3.1. INTRODUCTION.*

### 3.1.1. Importance and general properties of β-glucosidases.

*a. Catalytic activity and role in the microbial cellulase complex.*

β-Glucosidase (β-D-glucoside glucohydrolase or cellobiase, E.C. 3.2.1.21) is an enzyme that catalyzes the hydrolysis of various compounds with β-D-glucosidic linkages. Cleavage of the bond between the anomeric carbon and the glucosidic oxygen yields glucose as the product, as well as the free aglycone moiety. β-Glucosidases also catalyze reactions with nonglycosidic substrates, such as hydrolytic cleavage of the C—F bond in glucosyl fluorides, and hydration of the double bond of glucals.

β-Glucosidases are widely distributed in nature, and have been isolated from bacteria (Han & Srinivasan, 1969), yeast (Duerksen & Halvorson, 1958) and other fungi (Berghem & Pettersson, 1974), and plants (Hultson, 1964). As a component of the cellulase complex, β-glucosidase catalyzes the hydrolysis of cellobiose and cellodextrins (formed by the action of endo- and exo-glucanases) to form glucose. Since cellobiose acts as an inhibitor of both endo- and exo-glucanases, β-glucosidase plays an important role in the degradation of cellulose (Berghem et al., 1975).

*b. Catalytic activity and role in lysosomal glycolipid metabolism in humans.*

Glucosylceramide is an important glycolipid in animal cells. It is the substrate of lysosomal (or acid) β-glucosidase, which hydrolyzes the β-D-glucosidic linkage of this glycolipid (Fig. 3.1). In humans, the hereditary metabolic disorder known as Gaucher disease is a result of a deficiency of lysosomal β-glucosidase (glucosylceramidase, E. C. 3.2.1.45). Defective activity of this enzyme may lead to one of several variants of Gaucher disease, which include the non-neuropathic (Type 1), neuropathic infantile (Type2), and neuropathic juvenile (Type 3) forms (Barranger & Ginns, 1989; Grabowski, 1993; Grabowski et al., 1990). Prominent symptoms of Gaucher disease include the accumulation of glucosylceramide in tissues, and enlargement of the spleen and liver.
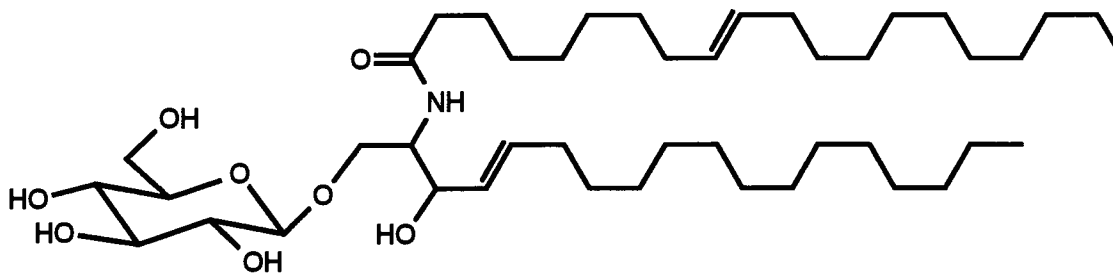
**Figure 3.1.** The structure of glucosylceramide.

Gaucher disease was the first lysosomal storage disease discovered (Gaucher, 1882), and it remains the most common type of lysosomal storage disease. It is also the first lysosomal storage disease to have been successfully treated by enzyme therapy (Barton et al., 1991; Beutler et al., 1991; Fallet et al., 1992). There are currently many studies in clinical and basic research directed at improved treatment and a possible cure for this important disorder of β-glucosidase function (Barton et al., 1991; Beutler et al., 1991; Grabowski, 1993).

### 3.1.2. *Agrobacterium* β-glucosidase.

The β-glucosidase used for this work is a protein from *Agrobacterium faecalis* (previously typed as *Alcaligenes faecalis*) (Han & Srinivasan, 1969). The purification and characterization of *Agrobacterium* β-glucosidase have been reported by Day & Withers (1986).

The *Agrobacterium* β -glucosidase monomer has a relative molecular mass of ~50,000. The catalytically active form of this enzyme is a dimer, with one active site per monomer (Day & Withers, 1986). The enzyme is β-retaining and has a "flexible" specificity for both the glycone and aglycone moieties of the substrate. *Agrobacterium* β-glucosidase hydrolyses a wide variety of different glycoside substrates, including β-glucosides, β-mannosides, β-galactosides, and cellobiose (Day & Withers, 1986). The substrate flexibility of the enzyme even includes the ability to hydrolytically cleave C—S, C—N, and C—F bonds.

The gene encoding *Agrobacterium* β-glucosidase has been cloned and expressed in *E. coli* (Wakarchuck et al., 1986). The expression product of the cloned gene is basically identical with the naturally occurring enzyme. Both proteins have the same amino acid sequence, and display the same kinetic behaviour (Wakarchuck et al., 1986). The β-glucosidase enzyme (commonly referred to as pABG5) used for this work was the expression product of the cloned gene.

## 3.2. THE AIMS OF THIS STUDY.

Various glycals were examined as potential substrates (catalytically *hydrated* by the enzyme), or as potential inhibitors or inactivators (of the *hydrolysis* of a glucoside substrate), of *Agrobacterium* $\beta$-glucosidase. One or more of these compounds might *inactivate* $\beta$-glucosidase by the formation of a covalent glycosyl-enzyme intermediate, which would be expected if the rate of glycosylation significantly exceeded the rate of deglycosylation, and this latter rate was extremely slow. Alternatively, one or more of these compounds might act as a *substrate*, which would be expected if both glycosylation and deglycosylation were rapid. Under these circumstances it might be possible to use a series of related substrates to study inductive effects on the reaction mechanism, or to study the stereochemistry of hydration of the substrate. Finally, these compounds should at least act as *inhibitors* of the catalytic hydrolysis of glucosides. The presence of the double bond in a glycal might result in increased affinity of these compounds for $\beta$-glucosidase, due to the flattening of the sugar ring towards the half-chair conformation of the transition state. Tight-binding enzyme inhibitors have frequently proven useful in basic and applied research.

D-Glucal is a hexenitol glycal with an endocyclic enolic double bond. This compound has been shown to act as a slow substrate of *Agrobacterium* $\beta$-glucosidase (Street, 1988). D-*Gluco*-heptenitol is a glycal with an exocyclic enolic double bond, and the effect of this compound on pABG5 activity has yet to be investigated. Such an investigation was part of this study, and hence heptenitol was synthesized for this work.

Both $F_2$hept and $F_1$hept were found to act as reversible inhibitors of glycogen phosphorylase *b*, an $\alpha$-glycosylase (see Chapter 2). Since heptenitols possess no anomeric configuration, the effects of $F_2$hept and $F_1$hept on *Agrobacterium* $\beta$-glucosidase activity were investigated. Methylglucal was also synthesized, and its effects on $\beta$-glucosidase activity were examined. If promising results were obtained with the parent compound, the synthesis of fluorinated derivatives of methylglucal would be attempted, and their effects on the activity of the enzyme would also be studied to provide more insight into the role of inductive effects on glycal hydration.

$\alpha,\beta$-Unsaturated glucals, which might act as Michael acceptors for a nucleophilic residue in the active site of a glycosylase, were investigated as a new class of potential inactivators of *Agrobacterium* $\beta$-glucosidase. The first $\alpha,\beta$-unsaturated derivative of D-glucal that was examined was 1-nitro-D-glucal, which was generously

provided by Prof. A. Vasella of the University of Zurich. Other $\alpha,\beta$-unsaturated derivatives of D-glucal were synthesized (or in some cases generously provided by colleagues) and their effects on *Agrobacterium* $\beta$-glucosidase activity were also studied.

## 3.3. RESULTS AND DISCUSSION.

### 3.3.1. The synthesis of heptenitol.

In 1977, Brockhaus & Lehmann published a multistep procedure for the synthesis of D-*galacto*-heptenitol. Later, Prof. Lehmann's group and their collaborators used a similar, multistep synthetic procedure to prepare D-*gluco*-heptenitol as part of a study of the catalytic hydration of this compound by $\alpha$- and $\beta$-glucosidases and exo-$\alpha$-glucanases (Hehre et al., 1980).



**[3.1]**                    **[3.2]**                    **[3.3]**
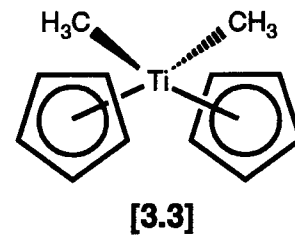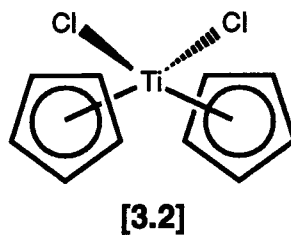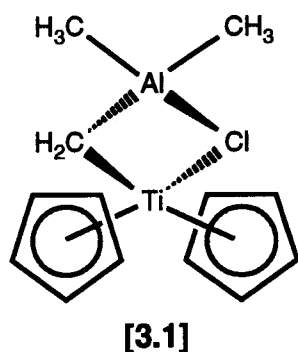
RajanBabu & Reddy (1986) have also reported the synthesis of D-*gluco*-heptenitol. They used persilylated D-glucono-1,5-lactone as a starting material, and Tebbe's reagent (3.1) (Tebbe et al., 1977) to effect the methylenation. However, there are several difficulties associated with the use of Tebbe's reagent. In addition to being very expensive, Tebbe's reagent has a short shelf-life, and its use requires special techniques and equipment due to its extreme sensitivity to air and water.

Dimethyltitanocene (3.3) has been used for the methylenation of several carbonyl compounds, including esters and lactones (Petasis & Bzowej, 1990). In this procedure titanocene dichloride ($Cp_2TiCl_2$, where $Cp$ = cyclopentadienyl) (3.2) is used to prepare dimethyltitanocene ($Cp_2TiMe_2$) (Claus & Bestian, 1962), which is used immediately to effect the methylenation of carbonyl compounds *via* a Wittig-type reaction. In this

work the procedure of Petasis & Bzowej (1990) was used for the one-step conversion of persilylated

glucono-1,5-lactone to persilylated D-*gluco*-heptenitol (Scheme 3.1). The reaction was relatively simple

(compared with the reaction using Tebbe's reagent) and efficient (with an 80% yield for the reaction shown in

Scheme 3.1). Triethylsilyl ethers were used to protect hydroxyl groups during the synthesis of

D-*gluco*-heptenitol. These ethers were stable enough for the reaction conditions, yet the silyl groups could be

easily removed later using tetra(*n*-butyl)ammonium fluoride (TBAF).
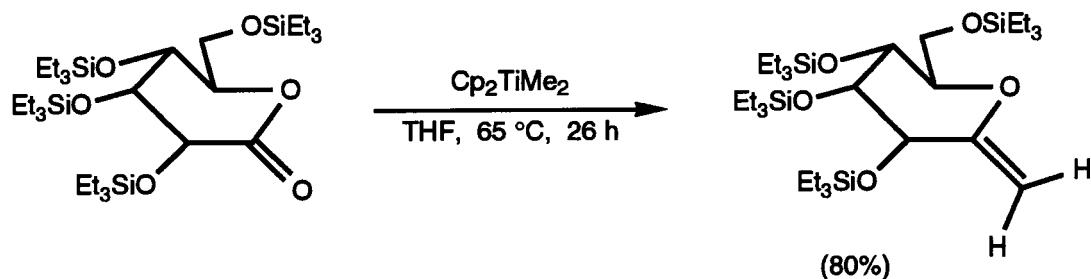


**Scheme 3.1.** The synthesis of heptenitol from glucono-1,5-lactone using dimethyltitanocene.

### 3.3.2. Kinetic studies using heptenitol.

*a. Heptenitol as a substrate of pABG5.*

Thin-layer chromatography provided the first evidence that heptenitol was catalytically hydrated by the

cloned β-glucosidase, pABG5. The enzymatic hydration product appeared to be identical to a sample of

1-deoxy-D-*gluco*-heptulose that had been prepared by the quantitative (nonenzymatic) hydration of heptenitol in

0.025 $N$ $H_2SO_4$ after 10 min at 100 °C. $^1H$ NMR was then used to determine which anomer of

1-deoxy-D-*gluco*-heptulose was formed initially during the enzymatic reaction. This determination was based

on the assignment of axial and equatorial methyl protons of 1-deoxy-D-*gluco*-heptulose reported by Hehre et al.

(1980).
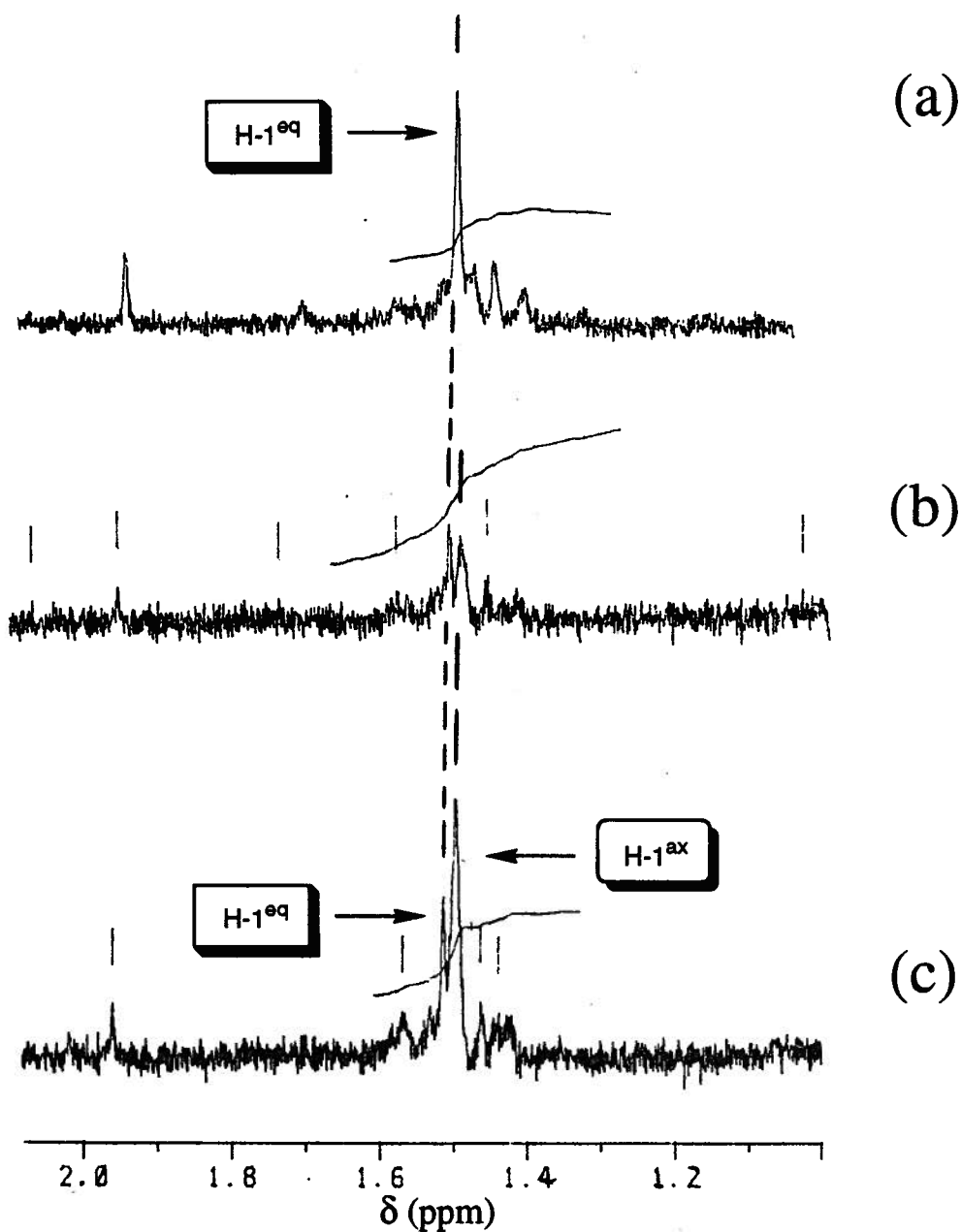
**Figure 3.2.** ^{1}H NMR determination of the stereochemistry of pABG5-catalyzed hydration of heptenitol.

400 MHz ^{1}H NMR spectra were obtained using the samples indicated below. Only the relevant regions of the spectra are shown, which contain the signals attributable to equatorial ($\delta$ = 1.52 ppm) or axial ($\delta$ = 1.50 ppm) methyl protons of the product, 1-deoxy-D-*gluco*-heptulose (Hehre et al., 1980). In all cases 18 m$M$ heptenitol was incubated in 50 m$M$ deuterated sodium phosphate buffer (pD 6.8) and 0.1% BSA at room temperature.

(a) Nonenzymatic hydration at 8.5 hours. No enzyme was added.
(b) Catalytic hydration at 13-27 minutes. pABG5 (0.32 mg/mL) was present.
(b) Catalytic hydration at 51-66 minutes. pABG5 (0.32 mg/mL) was present.
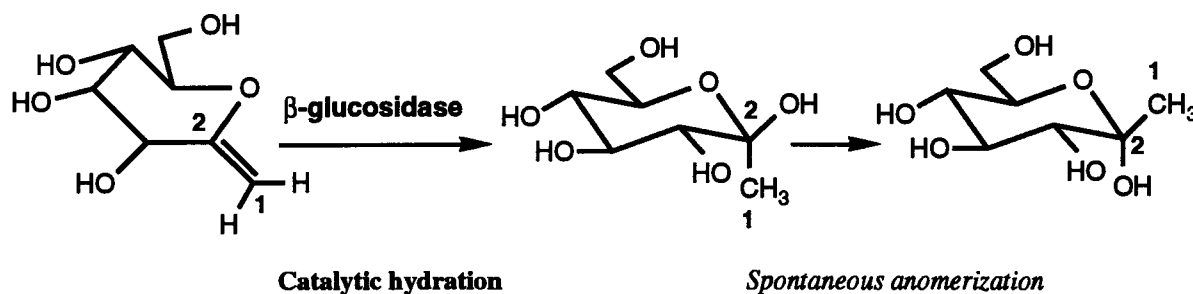
**Scheme 3.2.** The β-glucosidase-catalyzed hydration of heptenitol to form 1-deoxy-D-*gluco*-heptulose.

In a control reaction without enzyme, heptenitol was incubated for 8.5 hours at room temperature. During this time some spontaneous hydration occurred. In the $^1$H NMR spectrum (Fig. 3.2a) of this reaction mixture the only signal attributable to methyl protons was the signal at δ = 1.52 ppm (assigned to protons of an equatorial C-1 methyl group) (Hehre et al., 1980). Hence only the more stable α-anomer of 1-deoxy-D-*gluco*-heptulose was formed as a result of the nonenzymatic hydration of heptenitol.

When heptenitol was briefly incubated with pABG5 (for 13-27 min at room temperature), the $^1$H NMR spectrum (Fig. 3.2b) of this reaction mixture showed two distinct methyl $^1$H resonances, one at δ = 1.50 ppm (assigned to protons of an axial C-1 methyl group), and another at δ = 1.52 ppm (assigned to protons of an equatorial C-1 methyl group). The signal at δ = 1.50 ppm increased as the duration of the enzymatic reaction increased to 51-66 min at room temperature (Fig. 3.2c; cf. Fig. 3.2b). Hence the β-anomer of 1-deoxy-D-*gluco*-heptulose was formed as the initial product of the pABG5-catalyzed hydration of heptenitol (Scheme 3.2). Presumably this product subsequently anomerized spontaneously to form the more stable α-anomer.

For kinetic studies the cuprimetric method described by Hehre et al. (1980) was used to measure the rate of formation of the product, $k_{cat}$, and the Michaelis constant, $K_m$. The enzyme hydrated heptenitol at a reasonable rate, with a $k_{cat}$ value of 640 ± 60 min$^{-1}$. This is about 7% of the rate of pABG5-catalyzed hydrolysis of βGlcPNP, but about 300 times faster than the rate of pABG5-catalyzed hydration of D-glucal ($k_{cat}$ = 2.28 min$^{-1}$, $K_m$ = 0.85 mM) (Street, 1988). The affinity between heptenitol and the enzyme's active site appeared to be very poor, as the $K_m$ measured by the cuprimetric method was 270 ± 40 mM (Fig. 3.3).

However, the substrate specificity for pABG5-catalyzed hydration of heptenitol, $k_{cat}/K_m = 2.4 \text{ min}^{-1}\text{m}M^{-1}$, was

about the same as that for pABG5-catalyzed hydration of D-glucal, $k_{cat}/K_m = 2.7 \text{ min}^{-1}\text{m}M^{-1}$ (Street, 1988).
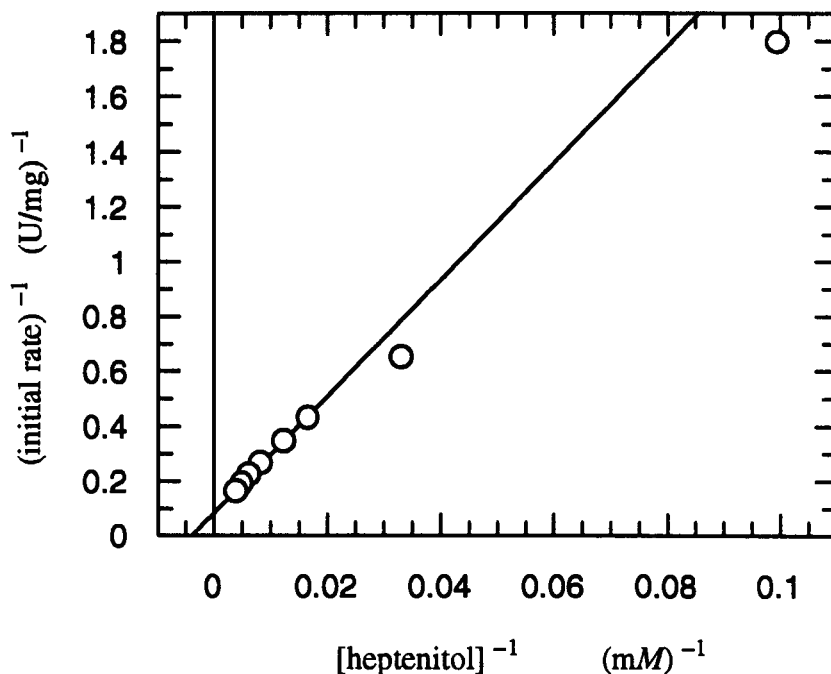


**Figure 3.3.** Determination of $K_m$ and $V_{max}$ for pABG5-catalyzed hydration of heptenitol.

Reactions (0.500 mL) were performed at 37 °C in 50 m$M$ sodium phosphate buffer (pH 6.8) with 30 μg of pABG5. Heptenitol concentrations were 10, 30, 60, 80, 121, 161, 201, and 251 m$M$.

*b. Heptenitol as an inhibitor of pABG5.*

As a further probe of this apparently poor binding, a reversible inhibition test was performed using heptenitol, the enzyme, and the substrate βGlcPNP. The resulting double-reciprocal plot indicated a very complicated pattern of binding (Fig. 3.4a). The results suggested that heptenitol acts as a mixed-type inhibitor of pABG5-catalyzed hydrolysis of βGlcPNP. The change (from uncompetitive or noncompetitive to competitive) in the type of inhibition observed as heptenitol concentration increased can be seen clearly in a Dixon plot (Fig. 3.4b).
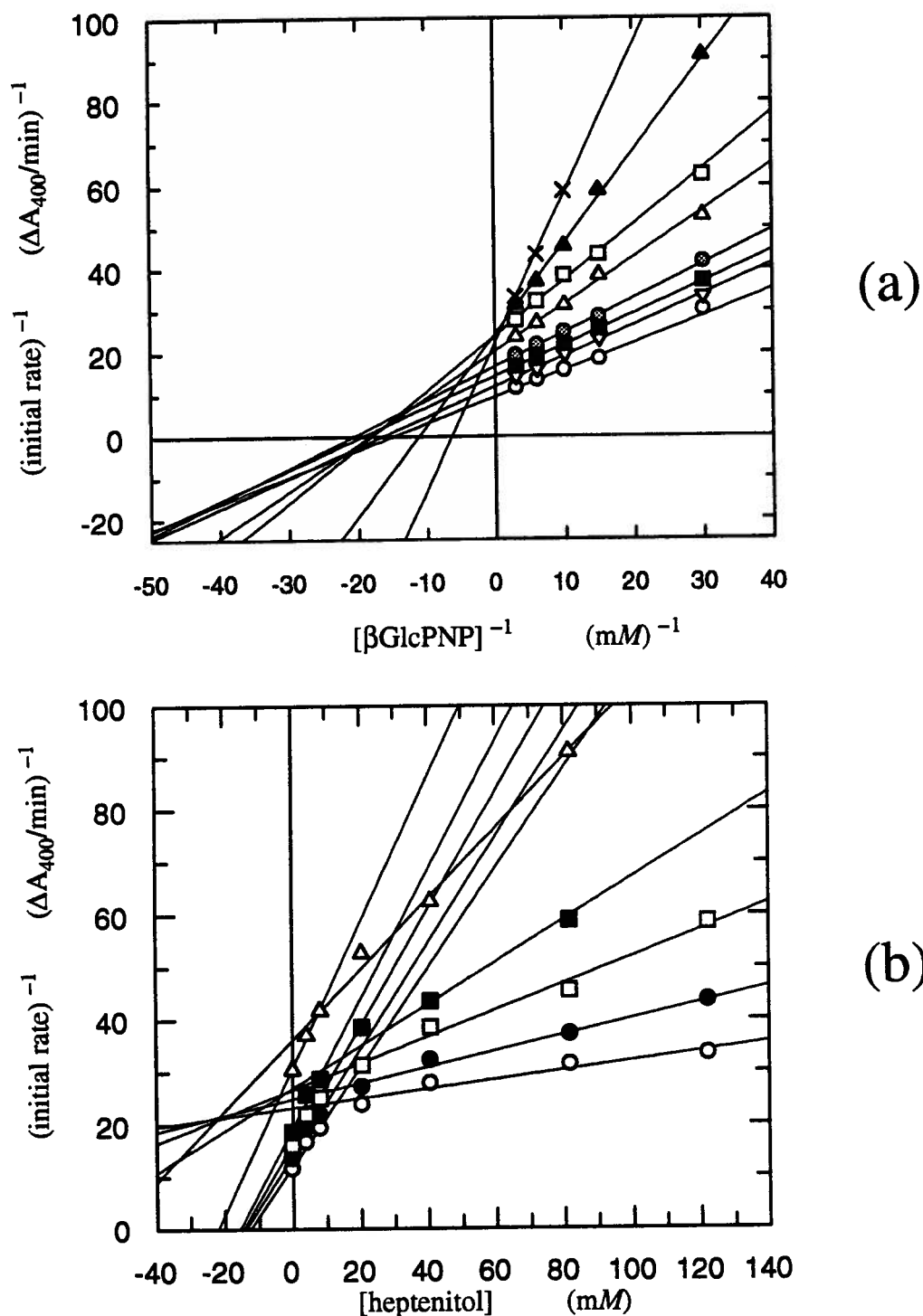
**Figure 3.4.** Determination of kinetic parameters for the inhibition of pABG5 by heptenitol.

(a) Double-reciprocal plot of kinetic data. Reactions (0.500 mL) were performed at 37 °C in 50 m$M$ sodium phosphate buffer (pH 6.8) with 0.06 μg of pABG5 and 0.1% BSA. The concentrations of heptenitol in the reactions were 0 {o}, 1.6 {▽}, 4.1 {■}, 8.2 {●}, 20.4 {△}, 40.8 {□}, 81.6 {▲}, and 122 {×} m$M$.

(b) Dixon plot of data obtained from panel (a). The concentrations of βGlcPNP in the reactions were 0.33 {o}, 0.17 {●}, 0.10 {□}, 0.067 {■}, and 0.033 {△} m$M$.

These results suggest that at low inhibitor concentrations, heptenitol occupies a binding site other than the active site, and acts as a noncompetitive inhibitor ($K_i = 13 \pm 1$ m$M$). This $K_i$ value was obtained by fitting the data from low inhibitor concentrations (0, 1.6, 4.1, and 8.2 m$M$) to equations describing different types of enzyme inhibition, using the computer program GraFit™ (Leatherbarrow, 1990). The best fit of the data was obtained for noncompetitive inhibition. The next best fit was obtained for uncompetitive inhibition, which would have yielded a value of $K_i = 8.5 \pm 0.7$ m$M$.

As the concentration of heptenitol increased, the $K_i$ increased also. It appeared that at higher inhibitor concentrations, heptenitol may also act as a competitive inhibitor, binding to the enzyme's active site. This explanation might account for the large difference in the values of the dissociation constants obtained from the substrate test ($K_m = 270$ m$M$) and the reversible inhibition test ($K_i = 13$ m$M$).

*c. Inactivation tests using heptenitol.*

Heptenitol was examined as a potential inactivator of pABG5 by incubating the enzyme with 10 m$M$ heptenitol and the appropriate reaction buffer for 20 hours at 37 °C (see Materials and Methods). At various time intervals small aliquots were removed and residual enzyme activity was assayed using the substrate βGlcPNP. No time-dependent inactivation of pABG5 was detected during these tests when compared with parallel control reactions.

### 3.3.3. Kinetic studies using fluoroheptenitols.

*a. Inactivation tests using fluoroheptenitols.*

F$_2$hept and F$_1$hept were examined as potential inactivators of pABG5 by incubating the enzyme with 10 m$M$ of either fluoroheptenitol and the appropriate reaction buffer for 19 hours at 37 °C (see Materials and Methods). At various time intervals small aliquots were removed and residual enzyme activity was assayed using the substrate βGlcPNP. No time-dependent inactivation of pABG5 was detected during these tests when compared with parallel control reactions.

*b. Substrate tests using fluoroheptenitols.*

TLC and ^{19}F NMR were used to determine if $F_2$hept or $F_1$hept acted as a substrate of pABG5. Either potential hydration product (1,1-difluoro- or 1-fluoro- derivative of 1-deoxy-D-*gluco*-heptulose) was expected to yield a TLC spot with an $R_f$ lower than that of the precursor fluoroheptenitol. The ^{19}F NMR spectrum of either potential hydration product was also expected to differ from that of the precursor fluoroheptenitol.

There were no detectable differences in the thin-layer chromatograms and ^{19}F NMR spectra obtained using aliquots taken over a period of 3 days from a 0.500-mL reaction mixture containing 17 m$M$ $F_2$hept, 0.6 mg of pABG5, 0.1% BSA, and 50 m$M$ deuterated phosphate buffer (pH 6.8). Comparable results were obtained in another experiment using the same conditions, but where $F_2$hept was replaced by 10 m$M$ $F_1$hept. These results indicated that neither $F_2$hept nor $F_1$hept acted as either substrates or inactivators of pABG5.

*c. Fluoroheptenitols as inhibitors of pABG5.*

Reversible inhibition tests were performed using either $F_2$hept or $F_1$hept. In each case, an approximate value of the inhibition constant (a range-finding $K_i$ or $RF$ $K_i$) was determined by measuring initial hydrolysis rates using a single substrate concentration (85 $\mu M$ $\beta$GlcPNP) and 5 or 6 inhibitor concentrations. Dixon plots of the respective data yielded $RF$ $K_i$ values. Inhibition constants for either $F_2$hept or $F_1$hept were then determined accurately. This involved measuring initial rates using 5 substrate concentrations bracketing the $K_m$ value (determined in the absence of inhibitor), and carrying out a set of reactions at each substrate concentration using 5-7 inhibitor concentrations bracketing the respective $RF$ $K_i$ value determined earlier.

The initial-rate data obtained at each substrate and inhibitor concentration were then fitted to equations describing different types of enzyme inhibition, using the computer program GraFit™ (Leatherbarrow, 1990). The data fit very well to equations describing noncompetitive and uncompetitive inhibition. The fit to the equation describing uncompetitive inhibition yielded $K_i$ values of 0.37 ± 0.01 m$M$ and 2.1 ± 0.1 m$M$ for $F_2$hept and $F_1$hept, respectively, while the fit to the equation describing noncompetitive inhibition yielded $K_i$ values of 0.57 ± 0.03 m$M$ and 3.2 ± 0.2 m$M$ for $F_2$hept and $F_1$hept, respectively.

Double-reciprocal plots were used to illustrate the nature of the observed inhibition (see Figs. 3.5a and 3.6a for the $F_2$hept and $F_1$hept plots, respectively). These plots showed that neither $F_2$hept nor $F_1$hept acted as a

competitive inhibitor of pABG5. In each case it appeared that uncompetitive (or noncompetitive) behaviour was observed. Thus both $F_2$hept and $F_1$hept displayed similar inhibitory behaviour to that observed earlier with low concentrations of heptenitol. This behaviour was clearly evident in Dixon plots (see Figs. 3.5b and 3.6b for the $F_2$hept and $F_1$hept plots, respectively), and by a comparison of these plots with that of heptenitol (Fig. 3.4b).

The theory, mathematical expressions, and graphical methods for the determination of different types of inhibition have been reviewed by Segel (1975) (see also Appendix II). By definition a *competitive* inhibitor is one that competes with the substrate for binding to the active site of the free enzyme. Although other models have been proposed to describe this phenomenon, the classical model postulates that *competitive* inhibition involves a single site that can bind either a substrate or an inhibitor molecule, but not both.

By definition, both *noncompetitive* and *uncompetitive* inhibition involve two sites on the enzyme, one that is specific for the substrate (the active site), and a second, distinct site that is specific for the inhibitor (Segel, 1975). In *noncompetitive* inhibition, the inhibitor (I) can bind to either the free enzyme or the enzyme-substrate (ES) complex; in either case, however, the result is either the formation of (i) an inactive ternary complex, i.e., ES + I→(ESI), or (ii) a binary complex (EI) which (in the forward direction of the reaction) can only lead to the formation of such an inactive complex, i.e., EI + S→(ESI). An *uncompetitive* inhibitor cannot bind to the free enzyme, but can only bind to and inhibit the enzyme-substrate complex, i.e., ES + I→(ESI).

Although heptenitol acted as a mixed-type inhibitor, and $F_2$hept and $F_1$hept acted as uncompetitive (or noncompetitive) inhibitors, it was quite surprising that none of these heptenitols acted as competitive inhibitors of pABG5. These heptenitols all possess a pyranosyl ring that is structurally similar to that found in normal substrates. The pyranosyl ring of these heptenitols contains all of the hydroxyl groups found in normal substrates, thus these heptenitols are presumably able to exploit all of the noncovalent interactions involving the glycone that contribute to the stability of binding of normal substrates in the enzyme's active site.

Noncompetitive and uncompetitive inhibition are most commonly observed in steady-state multisubstrate systems, but are only rarely observed in unisubstrate enzymes like pABG5. However, noncompetitive inhibition of a β-glucosidase has been reported, since D-glucal is a mixed competitive/noncompetitive inhibitor of *Aspergillus wentii* β-glucosidase (Legler et al., 1979).
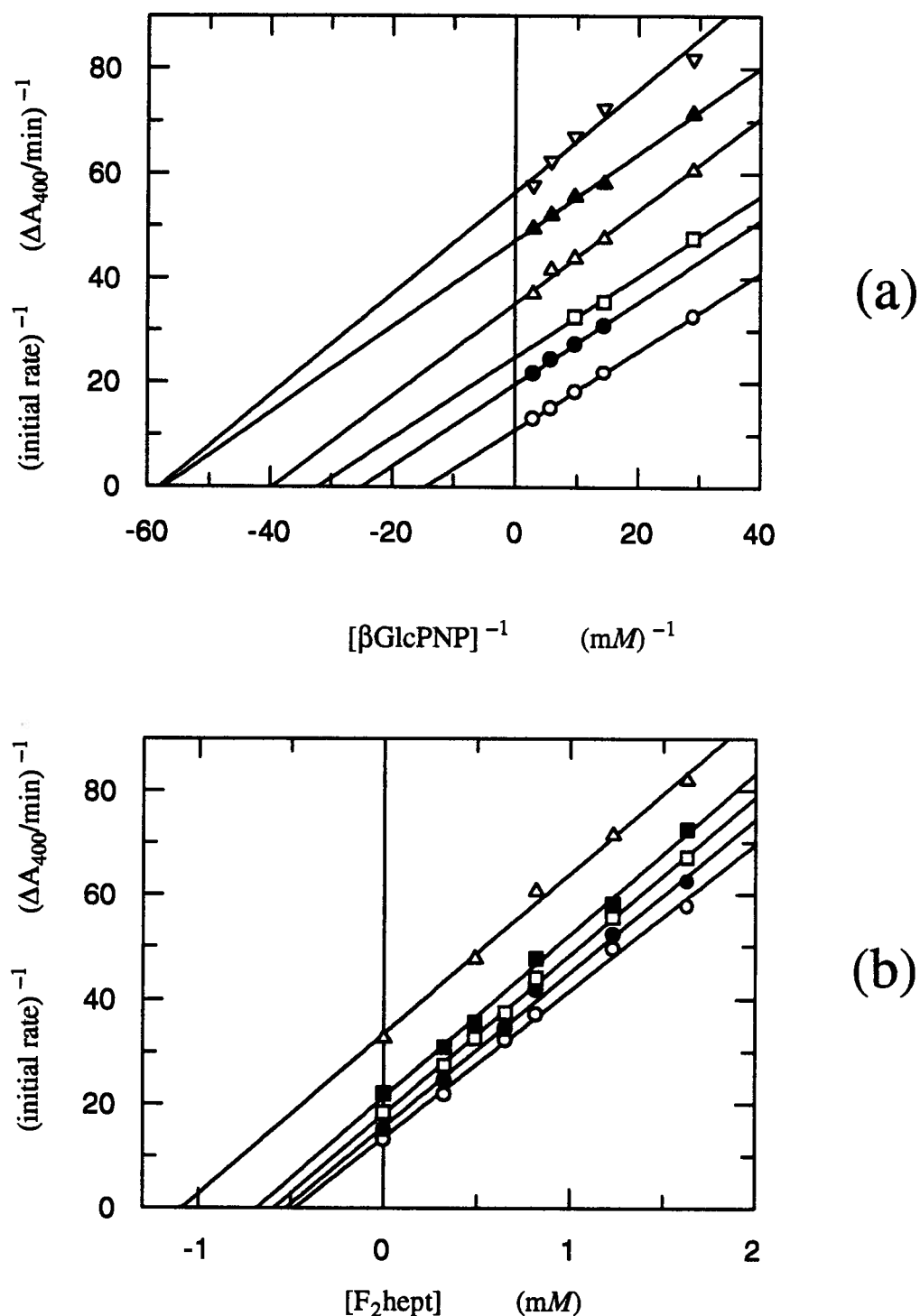
**Figure 3.5.** Determination of kinetic parameters for the inhibition of pABG5 by $F_2$hept.

(a) Double-reciprocal plot of kinetic data. Reactions (0.500 mL) were performed at 37 °C in 50 m$M$ sodium phosphate buffer (pH 6.8) with 0.051 μg of pABG5 and 0.1% BSA. The concentrations of $F_2$hept in the reactions were 0 {o}, 0.33 {●}, 0.49 {□}, 0.82 {△}, 1.2 {▲}, and 1.6 {▽} m$M$.

(b) Dixon plot of data obtained from panel (a). The concentrations of βGlcPNP in the reactions were 0.34 {o}, 0.17 {●}, 0.10 {□}, 0.069 {■}, and 0.034 {△} m$M$.
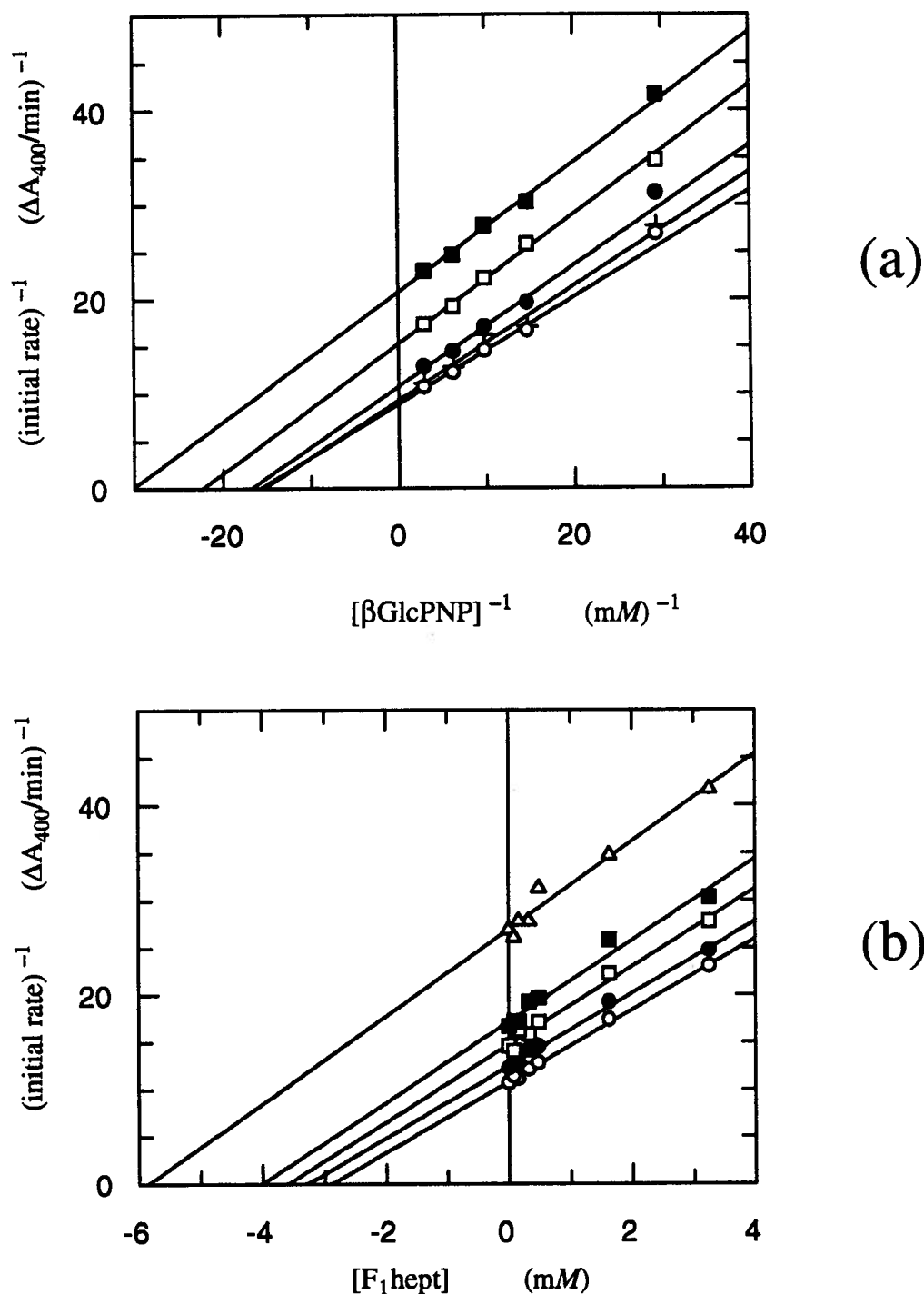
**Figure 3.6.** Determination of kinetic parameters for the inhibition of pABG5 by F₁hept.

(a) Double-reciprocal plot of kinetic data. Reactions (0.500 mL) were performed at 37 °C in 50 m$M$ sodium phosphate buffer (pH 6.8) with 0.053 μg of pABG5 and 0.1% BSA. The concentrations of F₁hept in the reactions were 0 {o}, 0.16 {+}, 0.49 {•}, 1.6 {□}, and 3.3 {■} m$M$.

(b) Dixon plot of data obtained from panel (a). The concentrations of βGlcPNP in the reactions were 0.34 {o}, 0.16 {•}, 0.10 {□}, 0.068 {■}, and 0.034 {△} m$M$.

### 3.3.4. Kinetic studies using methylglucal.

*a. The synthesis of methylglucal.*

Methylglucal was synthesized from persilylated glucal according to the procedure of Lesimple et al. (1986). This reaction involved deprotonation at C-1 of protected D-glucal, and then reaction of the lithio anion with methyl iodide to afford the protected methylglucal (Scheme 3.3). Tetra($n$-butyl)ammonium fluoride (TBAF) was used for the deprotection of silylated hydroxyl groups.
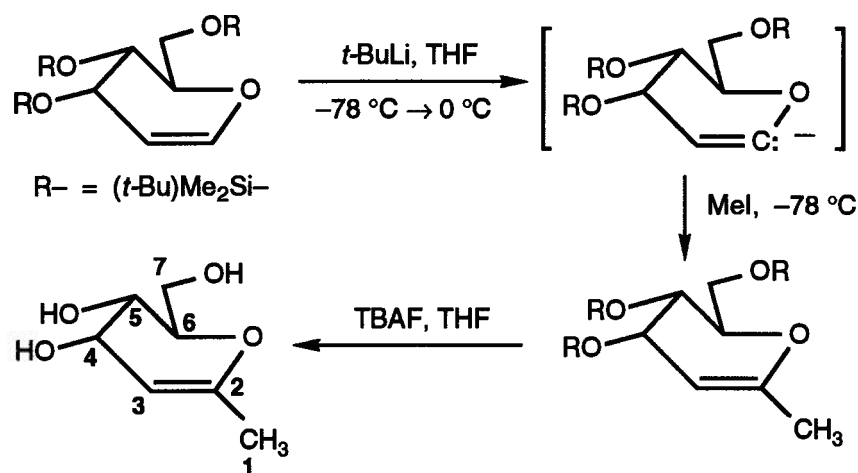


**Scheme 3.3.** The synthesis of methylglucal.

The low yield of the reaction was probably attributable to the use of $t$-butyldimethylsilyl ethers to protect the hydroxyl groups, which may have led to the formation of α-silyl carbanions (Friesen et al., 1991). The use of $t$-butyldiphenylsilyl or tri-isopropylsilyl ethers as hydroxyl protecting groups is now thought to be a more appropriate synthetic approach for reactions such as the one shown in Scheme 3.3 (Friesen et al., 1991).

*b. Methylglucal as a substrate of pABG5.*

TLC provided initial evidence (the appearance of a spot with an $R_f$ lower than that of the starting material) that methylglucal was hydrated by pABG5. However, methylglucal was unstable in the 50 m$M$ phosphate buffer (pH 6.8) that is normally used for kinetic studies with pABG5. The phosphate buffer in the reaction mixture was replaced with 10 m$M$ HEPES-NaOH (pH 7.0), as both the enzyme and methylglucal were

relatively stable in this buffer. As a control, the values of kinetic parameters for the hydrolysis of the substrate

βGlcPNP were obtained using the 10 m$M$ HEPES-NaOH buffer ($K_m$ = 75 µ$M$, $k_{cat}$ = 8400 min⁻¹), and these

values agreed well with those obtained using the 50 m$M$ phosphate buffer ($K_m$ = 78 µ$M$, $k_{cat}$ = 9500 min⁻¹).

The product was clearly identified by ¹H NMR spectroscopy as 1,3-dideoxy-D-*gluco*-heptulose, the

signal attributable to the methyl hydrogens of the product (δ = 1.43 ppm) being clearly distinguishable from the

signal attributable to the methyl hydrogens of the substrate methylglucal (δ = 1.74 ppm) (see Figs. 3.7 and 3.8).

The initial rate of the hydration reaction was determined after a very lengthy incubation period (110 h).

The activity of the enzyme (in control reactions without methylglucal) was checked periodically throughout this

period, and after 120 hours the enzyme retained over 91% of its initial activity. Reactions were performed using

5 different concentrations of methylglucal. Each 0.500-mL reaction also contained 0.65 mg of pABG5, 0.1%

BSA, and 10 m$M$ HEPES-NaOH (pH 7.0). At the end of the incubation period, the ¹H NMR spectrum of each

D₂O-exchanged reaction solution was determined and then the rate of formation of the product was calculated

from the ¹H NMR data (see Materials and Methods Section).

The values of $K_m$ and $k_{cat}$ were determined by fitting the data to the Michaelis-Menten equation using

the computer program GraFit™ (Leatherbarrow, 1990). The Lineweaver-Burk plot for this data is shown in

Fig. 3.9. Methylglucal was found to be a very poor substrate for pABG5, with a $K_m$ of 57 ± 8 m$M$ and a $k_{cat}$ of

0.056 ± 0.004 min⁻¹. Given these results, the original intention of proceeding with the synthesis and kinetic

analysis of fluorinated derivatives of methylglucal was abandoned.

*c. The stereochemistry of the catalytic hydration of methylglucal by pABG5.*

The stereochemistry of the enzyme-catalyzed addition of a proton (or deuteron) to C-3 of methylglucal

was determined by ¹H NMR analysis of the hydration product derived from methylglucal after reaction with

pABG5 in a D₂O-containing solution. This reaction (0.500-mL) contained 14 m$M$ methylglucal and 0.62 mg of

pABG5 in HEPES buffer (pH 7.0). All of these solutes were dissolved in D₂O; substrates and buffers having

been lyophilized from (or in the case of the enzyme, dialysed using) D₂O. The reaction mixture was incubated

for 10 days (241 h) at 37 °C, lyophilized, resuspended in D₂O, and then the stereochemistry of deuterium

incorporation was determined by ¹H NMR spectroscopy (Figs. 3.7c and 3.8c).
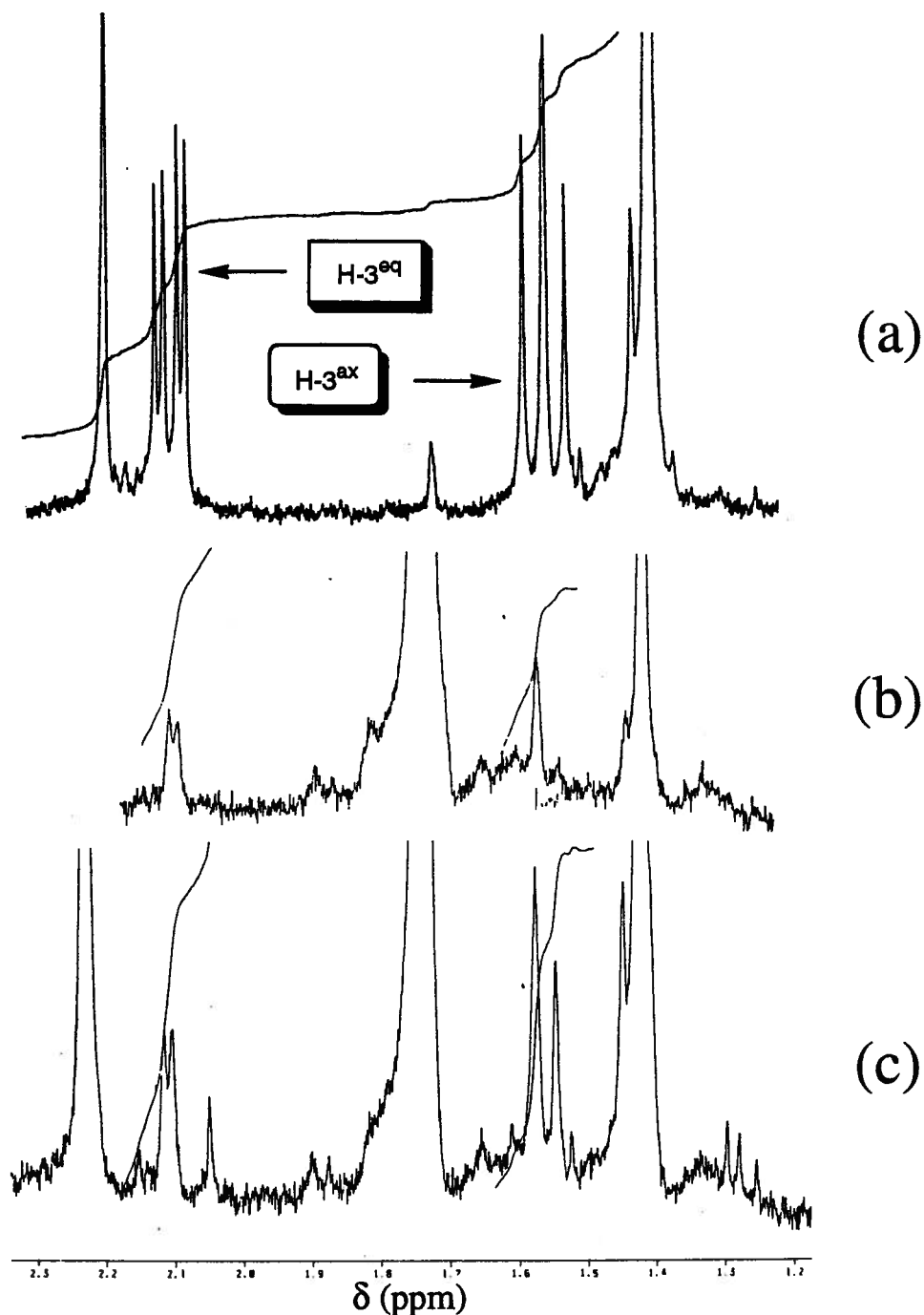
**Figure 3.7.** $^1$H NMR determination of the stereochemistry of pABG5-catalyzed hydration of methylglucal.

400 MHz $^1$H NMR spectra were obtained using the samples indicated below. Spectra were recorded using a sweepwidth of 5 kHz and signals were averaged over 1,000 transients. Only the relevant regions of the spectra are shown, which contain the signals attributable to equatorial ($\delta = 2.10$ ppm, $dd$) or axial ($\delta = 1.56$ ppm, $t$) H-3 protons of the hydration reaction product, 1,3-dideoxy-D-$gluco$-heptulose. Samples (b) and (c) were obtained after incubation of 14 m$M$ methylglucal with or without 0.31 mg/mL pABG5 for 10 days at 37° C in fully deuterated reaction mixtures containing 10 m$M$ HEPES buffer (pH 7.0).

(a) A sample of 1,3-dideoxy-D-$gluco$-heptulose obtained after incubation of methylglucal for 8 days at 37° C in 50 m$M$ sodium phosphate buffer (pH 6.8). The spectrum was recorded with solvent suppression.

(b) Sample without enzyme (nonenzymatic hydration only).

(c) Sample with pABG5 (enzymatic and nonenzymatic hydration).
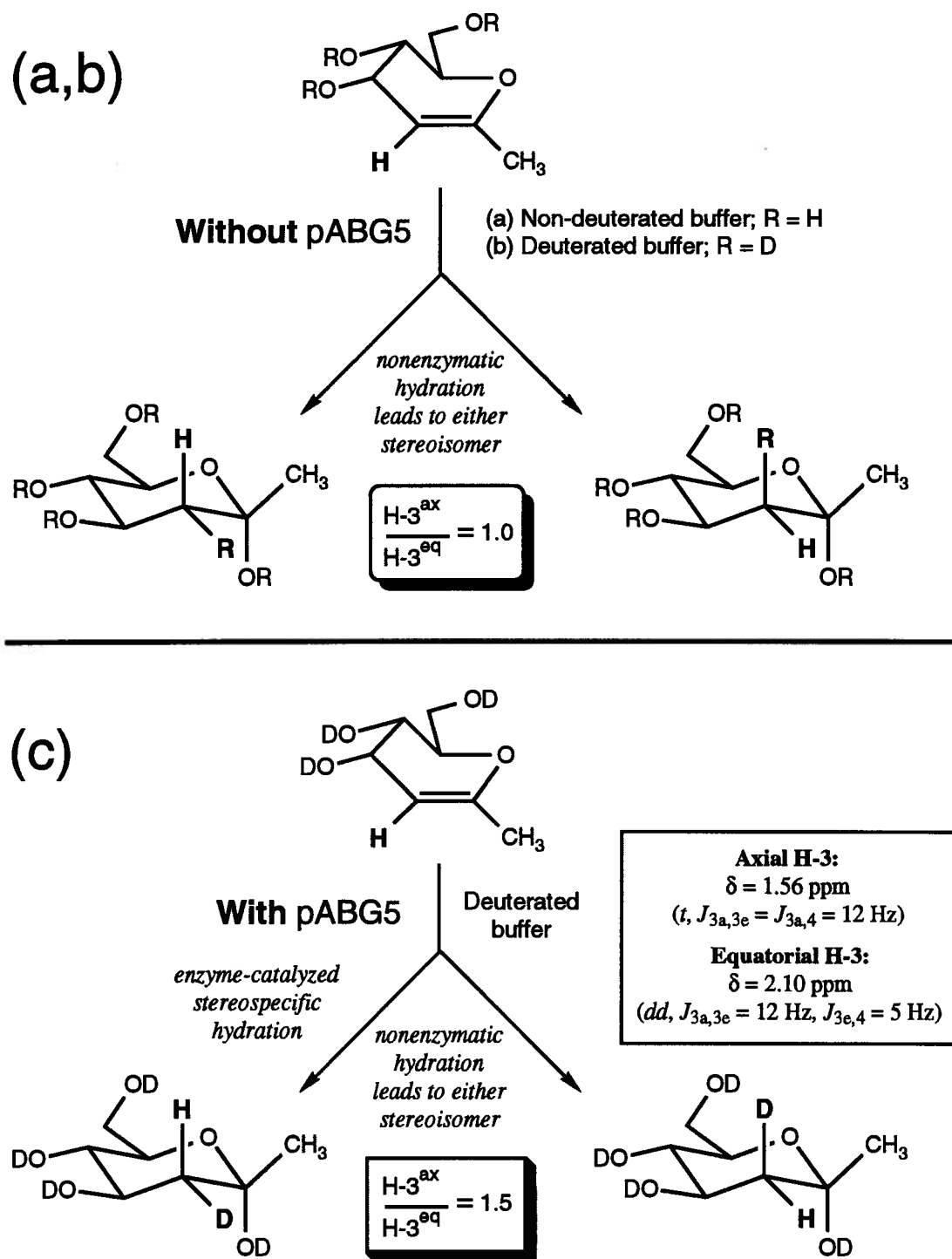
**Figure 3.8.** Interpretation of $^1$H NMR evidence for the stereochemistry of methylglucal hydration.

Panels (a,b) and (c) represent interpretations of the relevant $^1$H NMR results obtained from the corresponding reactions described in the legend of Fig. 3.7.
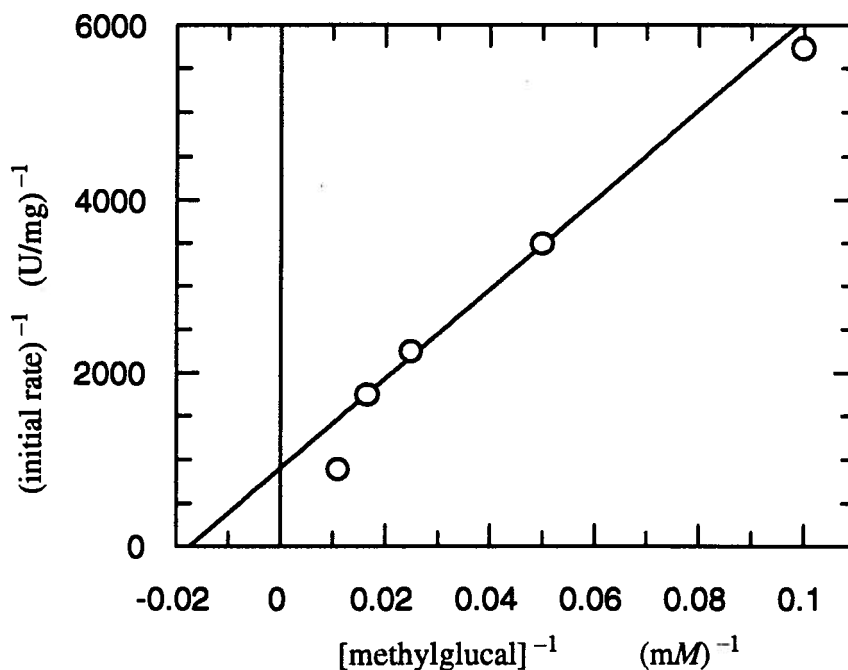
**Figure 3.9.** Determination of $K_m$ and $V_{max}$ for pABG5-catalyzed hydration of methylglucal.

---

Reactions (0.500 mL) were performed at 37 °C in 10 m$M$ HEPES buffer (pH 7.0) with 0.65 mg of pABG5 and 0.1% BSA. Methylglucal concentrations were 10, 20, 40, 60, and 90 m$M$.

---

Two control reactions were also carried out. In one control reaction, methylglucal was incubated for 8 days at 37 °C in an $H_2O$-containing, *phosphate* buffer (Figs. 3.7a and 3.8a). These conditions resulted in the nonenzymatic hydration of methylglucal to form 1,3-dideoxy-D-*gluco*-heptulose. At the end of this control reaction, water was removed by lyophilization, and after several rounds of resuspension in $D_2O$ and lyophilization, the $^1H$ NMR spectrum was taken (Fig. 3.7a). Chemical shifts and $^1H$–$^1H$ coupling constants obtained from this spectrum were used to assign resonances that were specific for the axial (H-3$^{ax}$) and equatorial (H-3$^{eq}$) protons at C-3 of the product (see Figs. 3.7 and 3.8).

Another control reaction contained no enzyme (Figs. 3.7b and 3.8b), but was otherwise identical to (and was run in parallel with) the enzymatic reaction described previously. This control reaction (no enzyme, 10 days, in $D_2O$-containing buffer) yielded a $^1H$ NMR spectrum containing resonances attributable to both H-3$^{ax}$ and H-3$^{eq}$ protons. In this spectrum the integration ratio of these two signals was 1:1, indicating that the nonenzymatic hydration of methylglucal was not stereospecific (Figs. 3.7b and 3.8b).

The parallel, enzymatic reaction (10 days, in $D_2O$-containing buffer) yielded a $^1H$ NMR spectrum that also contained resonances attributable to both H-3$^{ax}$ and H-3$^{eq}$ protons. In this spectrum the integration ratio of these two signals (H-3$^{ax}$ : H-3$^{eq}$) was 3:2 (Figs. 3.7c and 3.8c). During the (very slow) enzymatic hydration reaction, spontaneous nonenzymatic hydration was unavoidable, and hence it was not surprising that the $^1H$ NMR spectrum contained resonances attributable to both H-3$^{ax}$ and H-3$^{eq}$ protons. However, the *extra* 1,3-dideoxy-[$^2H$-3$^{eq}$]-D-*gluco*-heptulose present in the enzymatic reaction must have resulted from the catalytic hydration of methylglucal by pABG5 in the $D_2O$-containing buffer, which led to the *increase* in the [$^1H$-3$^{ax}$] : [$^1H$-3$^{eq}$] ratio (from 1:1 to 3:2). Hence during the enzymatic hydration of methylglucal, the deuteron must have added from *below* the α-face of the sugar ring, the same stereochemistry that has been observed during the hydration of D-glucal by pABG5 (Street, 1988).

*d. Methylglucal as an inhibitor of pABG5.*

A reversible inhibition test was performed using methylglucal. Due to a shortage of methylglucal, only an approximate value of the inhibition constant (a range-finding $K_i$ or $RF$ $K_i$) was determined. A Dixon plot of the data (Fig. 3.10) yielded an $RF$ $K_i$ value of 40 m$M$, which differed from the $K_m$ value (57 $\pm$ 8 m$M$) determined earlier for methylglucal. However, the $K_m$ (determined using an NMR-based assay instead of a more accurate spectrophotometric assay) and the $RF$ $K_i$ (an approximation of the actual $K_i$ value) were both determined using methods of limited accuracy, and hence the agreement between the two values was satisfactory given the error limits involved in their determination.

$$y = \frac{1}{V_{max}}$$

**[methylglucal]** **(m$M$)**

---
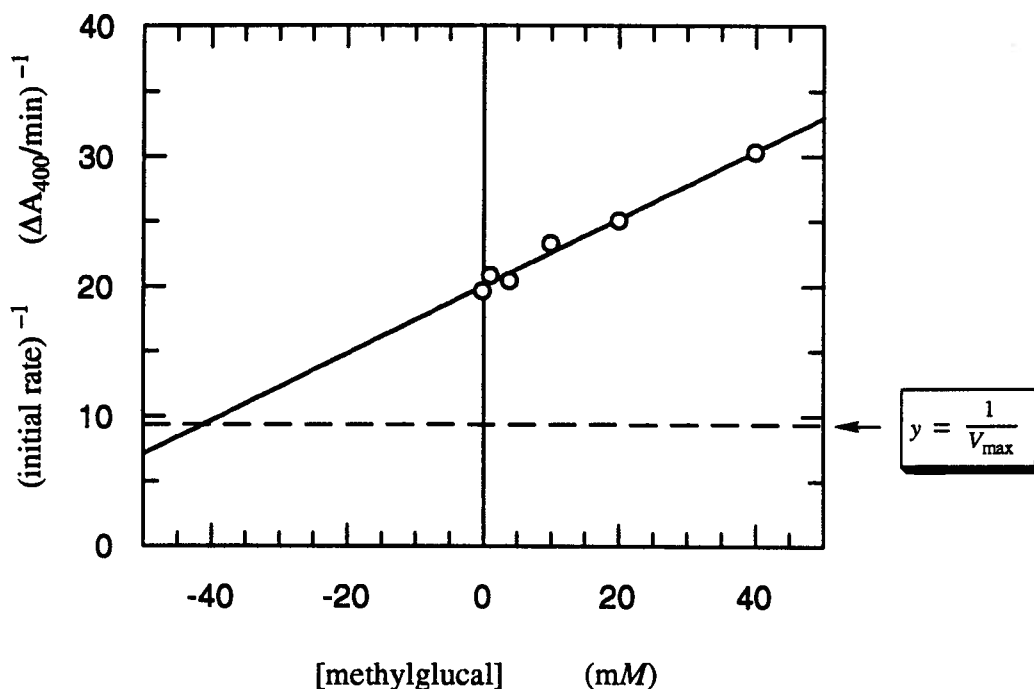
**Figure 3.10.** Estimation of the $K_i$ for the inhibition of pABG5 by methylglucal.

---

Reactions (0.500 mL) were performed at 37 °C in 10 m$M$ HEPES buffer (pH 7.0) with 0.10 µg of pABG5 and 0.1% BSA. The concentration of βGlcPNP in the reactions was 100 µ$M$. The concentrations of methylglucal in the reactions were 0, 1.0, 4.0, 10, 20, and 40 m$M$.

---

### 3.3.5. Kinetic studies using nitroglucal.

*a. Nitroglucal as an inactivator of pABG5.*

1-Nitroglucal (1,5-anhydro-2-deoxy-1-nitro-D-*arabino*-hex-1-enitol; also named as 1,2-dideoxy-1-nitro-D-*arabino*-hex-1-enopyranose by Beer et al., 1986) was the first α,β-unsaturated derivative of glucal examined. This compound (see below) was kindly provided by Prof. A. Vasella of the University of Zurich (see Beer et al., 1986; Baumberger et al., 1986).
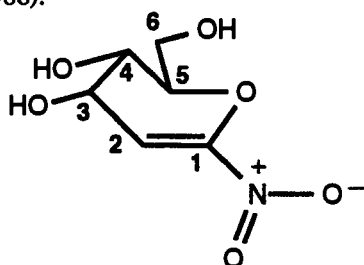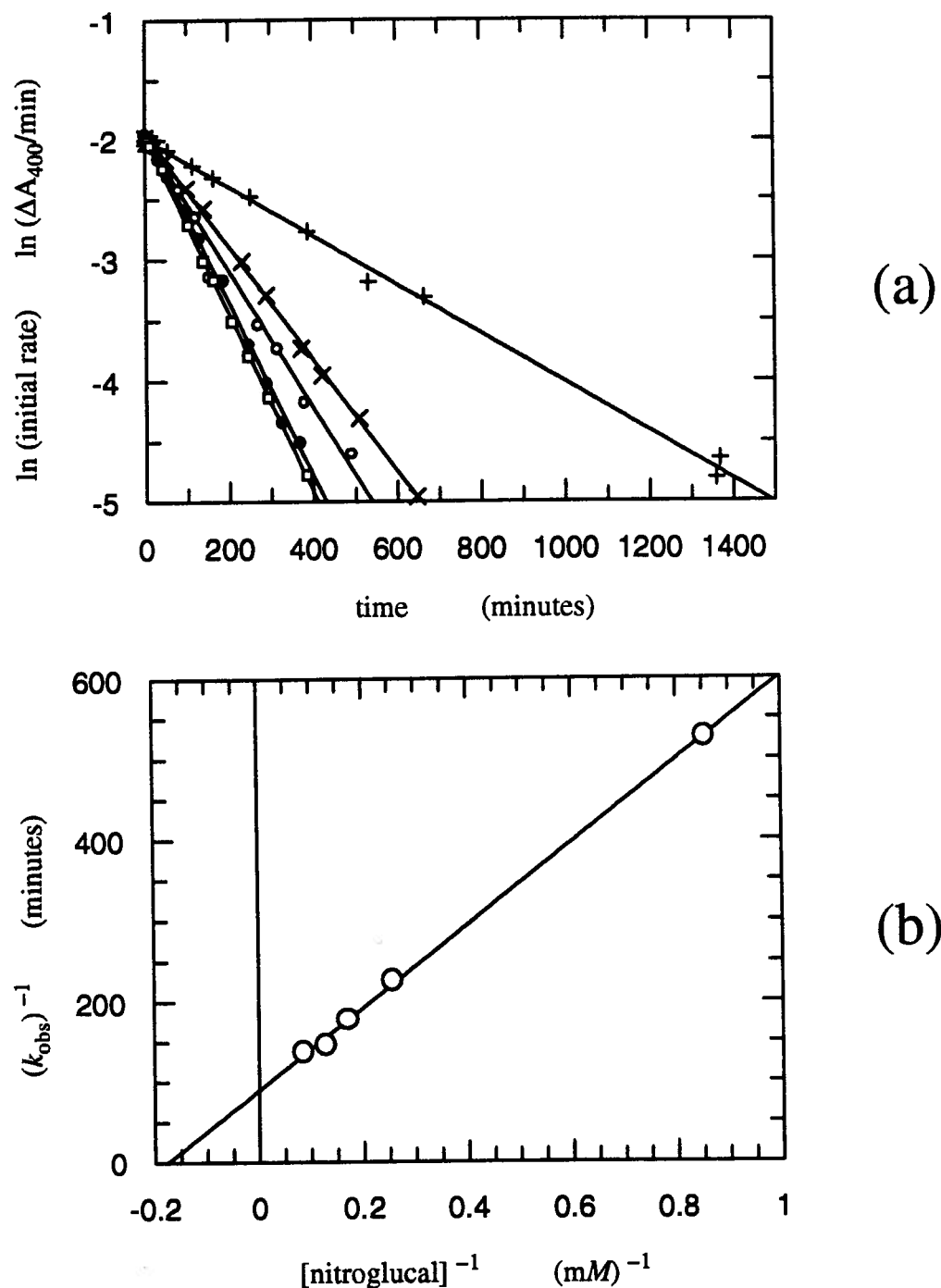
**Figure 3.11.** Determination of kinetic parameters for the inactivation of pABG5 by nitroglucal.

(a) Time-dependent decrease in pABG5 activity with increasing concentrations of nitroglucal. Inactivation reactions were performed at 37 °C in 50 m$M$ sodium phosphate buffer (pH 6.8) with a fixed concentration of pABG5 and 0.1% BSA. Residual activity assays were performed as described in the text. The concentrations of nitroglucal in the inactivation reactions were 1.2 {+}, 3.9 {×}, 5.9 {o}, 7.8 {•}, and 11.7 {□} m$M$, and the values of $k_{obs}$ were 0.0019, 0.0044, 0.0056, 0.0069, and 0.0073 min$^{-1}$, respectively.

(b) A double-reciprocal plot of the $k_{obs}$ values from panel (a), and the nitroglucal concentrations at which they were obtained.

When pABG5 was incubated with nitroglucal there was a *time-dependent* decrease in the activity of the enzyme (relative to a control reaction without nitroglucal) when aliquots were withdrawn and assayed with βGlcPNP (Fig. 3.11a). This *time-dependent* decrease in activity indicated that nitroglucal was covalently inactivating the enzyme, and hence experiments were performed as described below to determine the inactivation constants $k_i$ and $K_i$.

Inactivation constants were determined using reactions containing one of 5 different concentrations of nitroglucal (ranging from 1.2 to 12 m$M$) in 50 m$M$ phosphate buffer and 0.1% BSA. At different time intervals small aliquots of each reaction mixture were removed and then assayed for residual enzyme activity (see Materials and Methods Section) to determine if nitroglucal-mediated inactivation of pABG5 involved the formation of a covalent bond at the active site. In these assays (which contained 1.00 mL of 1 m$M$ βGlcPNP) each small aliquot of the inactivation mixture (10 μL) was diluted 100-fold into a solution containing a saturating concentration of the substrate. Under these conditions, any nitroglucal which was *not* covalently bound to the enzyme's active site would be competed out of the active site by the large excess of substrate. Hence *after* dilution, this fraction of the enzyme (previously containing noncovalently bound nitroglucal) would now be available for the catalysis of βGlcPNP hydrolysis.

The pseudo first-order rate constant ($k_{obs}$) obtained at each concentration of nitroglucal was fitted to the nonlinear form of the equation $k_{obs} = k_i \cdot [I]/\{K_i + [I]\}$ using the computer program GraFit™ (Leatherbarrow, 1990). This equation was used to calculate the binding constant, $K_i = 5.5 \pm 0.9$ m$M$, and the inactivation rate constant, $k_i = \{1.1 \pm 0.1\} \times 10^{-2}$ min$^{-1}$. A double-reciprocal plot of the data is shown in Fig. 3.11b.

*b. Determination of the site(s) of nitroglucal-mediated inactivation of pABG5.*

Another test for the active site-directed nature of an inactivator is whether the presence of a *competitive* ligand *decreases* the rate of inactivation at a fixed concentration of the inactivator. A competitive ligand binds to the active site of the free enzyme, thus it transiently protects the active site from inactivation, but since the binding is reversible, any active site-directed inactivation of the enzyme should eventually go to completion.

In the above-mentioned "protection" experiment that was used in this work, the competitive ligand was 1-deoxy-β-D-glucosylbenzene (1dβGlcφ), which binds to the active site of pABG5 with a $K_i = 3.4$ m$M$ (Street,

1988). The enzyme pABG5 was incubated at 37 °C in solutions containing a phosphate buffer (pH 6.8), 7.8 m$M$

nitroglucal, and either 0 or 9.9 m$M$ 1dβGlcφ. Residual activity assays were carried out at different time intervals

exactly as described earlier for the inactivation test.

At the concentration of 1dβGlcφ that was used (~3 × $K_i$), the rate of nitroglucal-mediated inactivation

of pABG5 was reduced approximately 2-fold compared to the rate in the absence of 1dβGlcφ (from 0.0069 to

0.0036 min$^{-1}$), as expected if the two ligands bind at the same site (Fig. 3.12).
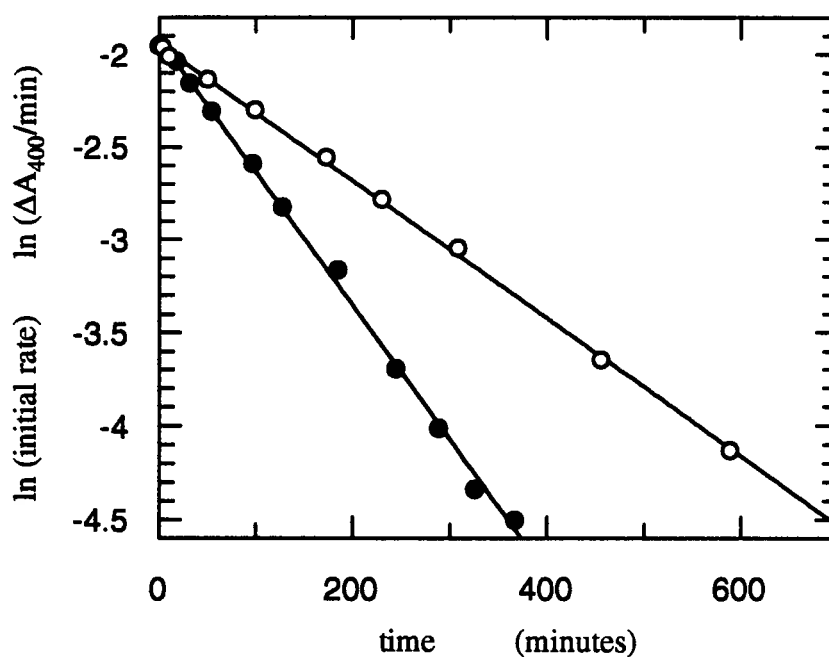


**Figure 3.12.** Competitive ligand-mediated protection against nitroglucal-mediated inactivation of pABG5.

Inactivation reactions were performed at 37 °C in 50 m$M$ sodium phosphate buffer (pH 6.8) with a fixed concentration of pABG5, 0.1% BSA, and 7.8 m$M$ nitroglucal. Residual activity assays were performed as described in the text. The concentrations of 1dβGlcφ in the inactivation reactions were 0 {●} or 9.9 {○} m$M$, and the values of $k_{obs}$ obtained were 0.0069 or 0.0036 min$^{-1}$, respectively.

*c. Mass spectrometry of nitroglucal-inactivated pABG5.*

Recent developments in protein mass spectrometry have made it possible to use this technique to identify a catalytically important amino acid residue in an enzyme's active site. Typically an active site-specific modifying reagent is used to covalently modify and label the amino acid in question, and enzyme inactivators are frequently ideal for such applications. Mass spectrometry is then used to determine the amino acid sequence of the modified tryptic peptide, and identify the modified amino acid. An example of this approach is the work of Miao et al. (1994), who used the inactivator 2',4'-dinitrophenyl-2-deoxy-2-fluoro-$\beta$-xylobioside to label and identify Glu 78 as an active-site nucleophile in the enzyme xylanase from *Bacillus subtilis.*

In this work, protein mass spectrometry data were collected using native pABG5 and the nitroglucal-inactivated enzyme, in collaboration with Dr. S. C. Miao and Prof. R. Aebersold of the University of British Columbia. The mass spectrum of the native enzyme indicated an $M_r$ of 51,205 ± 8. In contrast, the mass spectrum of the nitroglucal-inactivated enzyme showed that this sample consisted of many species. Each enzyme monomer was probably labeled with several molecules of nitroglucal, but the sample was so heterogeneous that the mass spectrometry data could not yield a meaningful estimate of the average number of equivalents of nitroglucal covalently bound per enzyme monomer.

Although disappointing, the above results were not surprising. Nitroglucal is a highly reactive $\alpha,\beta$-unsaturated glucal, and was probably able to react with several nucleophilic amino acid residues present in pABG5, including one located in the active site of the enzyme. Sample heterogeneity has also been observed in the mass spectrum of nitroglucal-inactivated glycogen phosphorylase *b* (Stirtan, 1993). Multiple-site modification of glycogen phosphorylase *b* by nitroglucal has also been detected by X-ray crystallographic studies. In these studies a covalently bound nitroglucal molecule was detected at the active site, and also at a second site near the surface of the enzyme (Stirtan, 1993). At the second site, a covalent bond had been formed between the C-2 position of the 2-deoxy-$\beta$-nitroglucosyl moiety and an imidazole nitrogen of the side chain of His 73.

*d. Is nitroglucal-inactivated pABG5 capable of reactivation?*

Street (1988) showed that if pABG5 was inactivated with 2FβGlcDNP, there was a slow return of enzymatic activity when the inactivated enzyme was removed from excess inactivator. Under these conditions the covalent inactivator-enzyme intermediate slowly completed the deglycosylation step of the catalytic reaction mechanism, and liberated the free enzyme. Transglycosylation acceptors such as 1dβGlcφ and cellobiose were found to increase the rate of reactivation of 2FβGlcDNP-inactivated pABG5 (Street, 1988). Transglycosylation acceptors bind at the "second binding site" immediately adjacent to the occupied active site of β-glucosidase. If a compound such as 1dβGlcφ or cellobiose is present, a covalent inactivator-enzyme intermediate undergoes transglycosylation (with a sugar as the acceptor) more rapidly than deglycosylation (with water as the acceptor), but the net result is still liberation of the free enzyme (Street, 1988).

In this work, reactivation of nitroglucal-inactivated pABG5 was attempted after the removal of excess inactivator by dialysis using 50 m$M$ phosphate buffer (pH 6.8). The "nitroglucal-free" retentate containing nitroglucal-inactivated pABG5 was divided into three equal-size aliquots. Each of these aliquots was in turn adjusted to the same volume using 50 m$M$ phosphate buffer (pH 6.8) and either (i) nothing else; or sufficient transglycosylation acceptor to give a final concentration of 21 m$M$ (ii) 1dβGlcφ; or (iii) cellobiose.

In all three cases there was no detectable reactivation of nitroglucal-inactivated pABG5 after an incubation period of 48 hours at 37 °C.

*e. Possible mechanisms for the inactivation of pABG5 by α,β-unsaturated glucals.*

Nitroglucal was one of several α,β-unsaturated glucals that were studied as potential inactivators of pABG5. Unfortunately, the conventional ring numbering systems used for *substituted* glycals makes it difficult to compare the results of these studies, and the results of work carried out using glycoside inactivators. This is because the C-1 position in an *unsubstituted* glycal does *not* maintain the designation "1" in a derivative that bears a substituent (at C-1 of the *unsubstituted* glycal) with one or more carbon atoms (e.g., in heptenitol, the *exocyclic* carbon atom is C-1; see Houlton et al., 1993). Hence for the purposes of the discussion *in this chapter*, it was deemed necessary to modify slightly the conventional ring numbering systems used for substituted glucals to allow for a clearer comparison of the results obtained in this work and in previous studies (Fig. 3.13).

*1-nitroglucal*          *1-cyanoglucal*          *1-(methyl carboxylate)glucal*

*sodium 1-(carboxylate)glucal*          *2-cyanoglucal*          *2-acetamidoglucal*
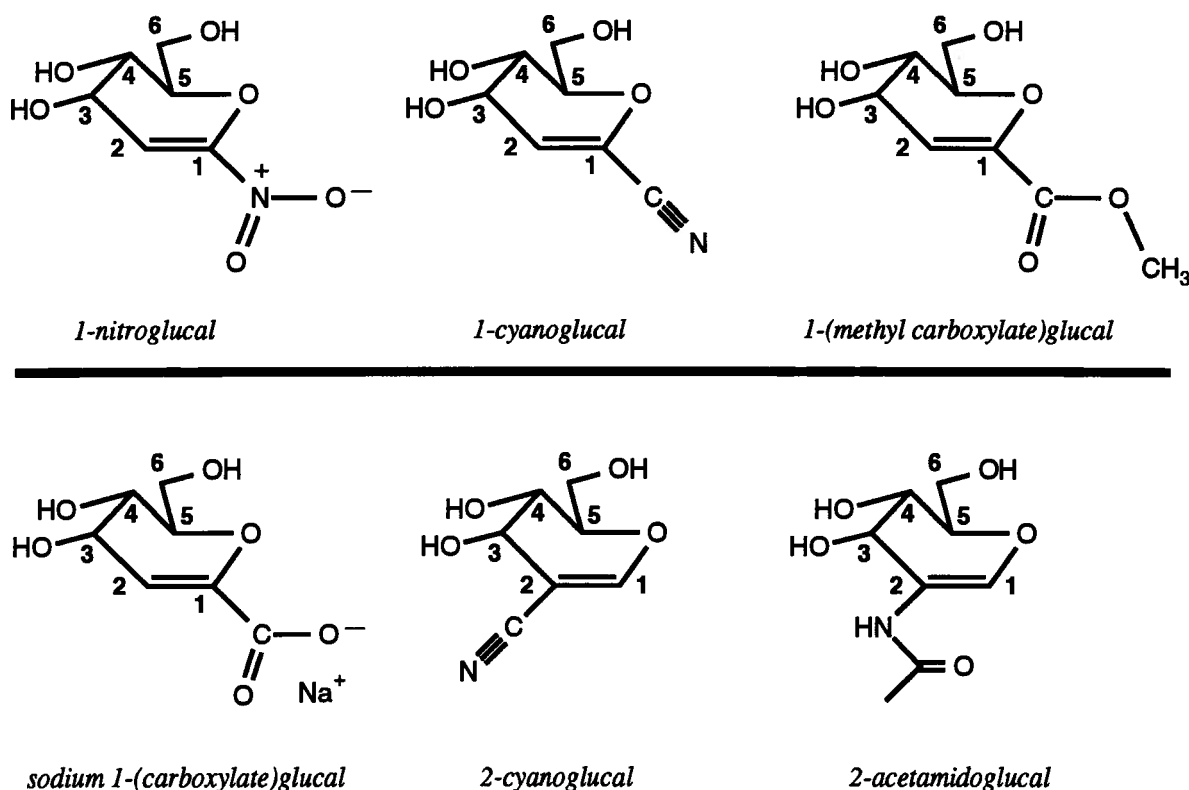
**Figure 3.13.** Ring numbering systems used *in this chapter* for substituted glucals.

*Conventional* ring numbering systems for substituted glycals that were part of this study are given in Figs. 5.1 and 5.2.

The structure and reactivity of α,β-unsaturated glucals suggest three possible ways for these compounds to inactivate pABG5 (see Scheme 3.4). One possible mechanism for inactivation would involve a Michael addition reaction between the α,β-unsaturated glucal and a nearby nucleophilic residue in the enzyme's active site. The reaction of *2-substituted* α,β-unsaturated glucals (e.g., *2-cyanoglucal*) in the active site may be favoured because with these compounds a Michael (or 1,4-) addition reaction involves C-1, and the formation of a covalent bond between C-1 of the glucal and the "normal" active-site nucleophile in pABG5 (Glu 358; see Withers et al., 1990) may be particularly facile. Furthermore, the reaction of *1-substituted* α,β-unsaturated glucals (e.g., *1-nitroglucal*) in the active site may also be possible. However, with these compounds a Michael

addition reaction involves C-2, thus although formation of a covalent bond between C-2 of the glucal and Glu 358 may be less likely, *another* active-site nucleophile in pABG5 may be close enough to react with C-2 in these compounds.

A second possible inactivation mechanism would involve a nucleophilic attack at the C-1 position of the glucal to give a glycosyl-enzyme intermediate. The electron-withdrawing nature of the C-1 or C-2 substituent in an α,β-unsaturated glucal should slow down the deglycosylation step (due to inductive destabilization of the transition state), resulting in accumulation of the intermediate. This mechanism is analogous to that proposed to explain the inactivation of β-glucosidase by 2-deoxy-2-fluoro-glucosides (Street, 1988).

There is a third possible mechanism for the inactivation of β-glucosidase by α,β-unsaturated glucals that possess a functional group with an electrophilic centre (e.g., a carbonyl group). This mechanism would involve a 1,2-addition reaction between an active-site nucleophile and the electrophilic centre of the substituent.

In contrast with the results obtained with 2FβGlcDNP-inactivated pABG5 (Street, 1988), it was not possible to reactivate nitroglucal-inactivated pABG5 (i.e., with 1dβGlcφ or cellobiose, see above). This suggests that the second of the above-mentioned mechanisms does not explain how nitroglucal inactivates pABG5. On the other hand, the bulky nitro group at the C-1 position may have prevented water or a transglycosylation acceptor from approaching close enough to attack the C-1 position of the inhibitor in the enzyme-nitroglucal intermediate. This steric hindrance would have left the nitroglucal bound to the enzyme's active site, and hence reactivation of pABG5 would not have been possible.

Another more likely explanation for the absence of any reactivation may have been that the mechanism of nitroglucal-mediated inactivation of pABG5 involved a Michael addition reaction at the C-2 position of the glucal, and that the resulting covalent bond in the glucosyl-enzyme intermediate was resistant to hydrolysis (or transglycosylation) due to its sheltered position in the enzyme's active site (Scheme 3.4). The results of the protein mass spectrometry of nitroglucal-inactivated pABG5 provided support for the hypothesis that the mechanism of inactivation involved a Michael addition reaction. These results were very similar to those obtained by Stirtan (1993) with nitroglucal-inactivated glycogen phosphorylase *b*.
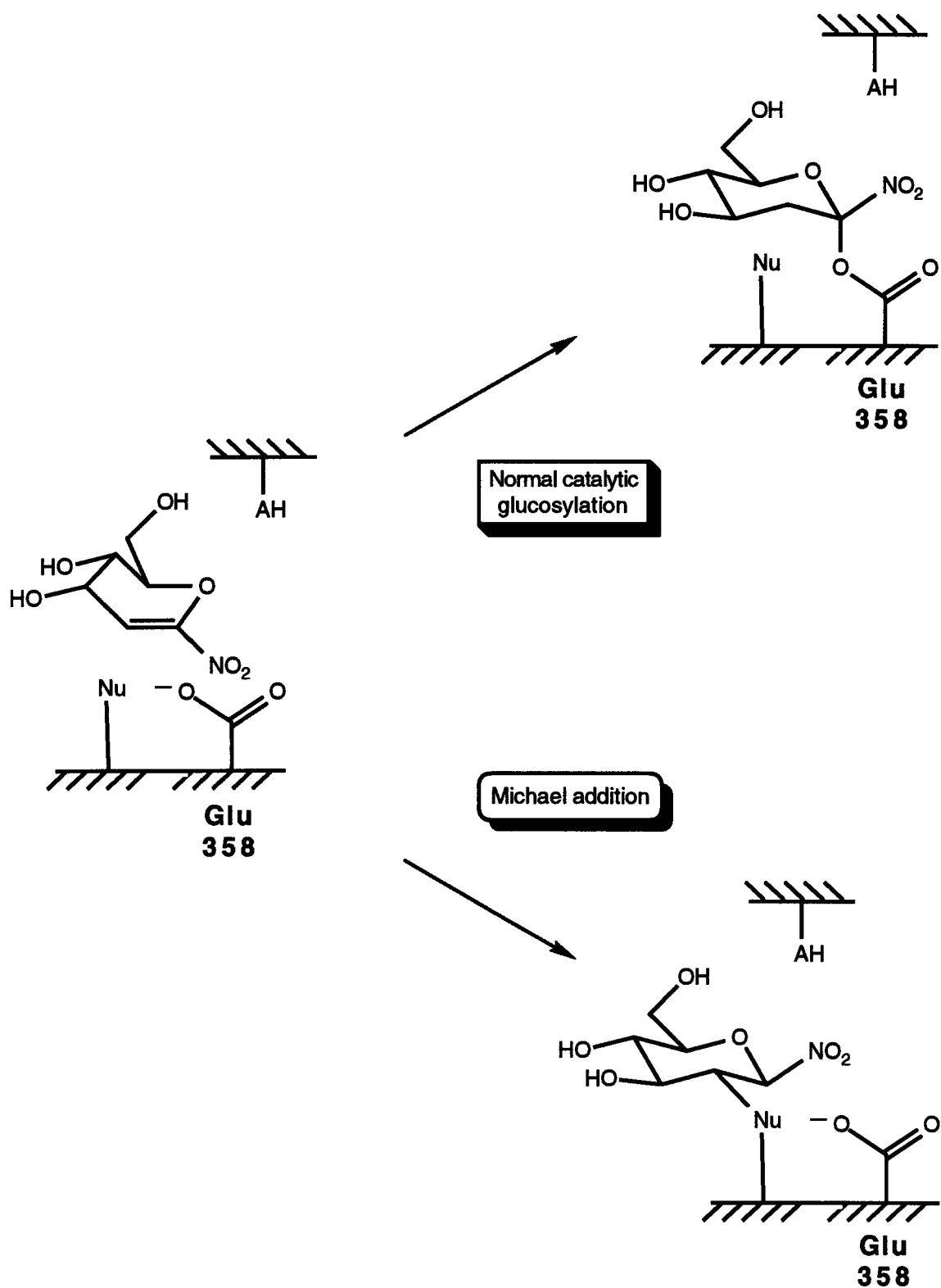
**Scheme 3.4.** Possible mechanisms for the inactivation of pABG5 by nitroglucal.

### 3.3.6. Kinetic studies using other α,β-unsaturated glucals.

*a. Other α,β-unsaturated glucals used in this study.*

The high reactivity of nitroglucal is attributable to the nitro substituent, which is probably the most activating group for Michael addition reactions (Shenhav et al., 1970). Other less reactive α,β-unsaturated derivatives of glucal (see Fig. 3.13) were therefore examined in an attempt to find an inactivator of pABG5 that would *selectively* label an active-site nucleophile. Two glucal derivatives (1-cyanoglucal and 2-cyanoglucal) were synthesized for this work. Two other compounds (methyl carboxylateglucal and sodium carboxylateglucal) were synthesized and kindly provided by Dr. William Stirtan of Prof. Withers' laboratory.

*b. The synthesis of 1-cyanoglucal.*

The synthesis of 1-cyanoglucal was accomplished using the multistep procedure shown in Scheme 3.5. The peracetylated glucosylcyanide (**3.5**) was obtained by heating a neat mixture of glucosyl bromide (**3.4**) and mercuric cyanide (Fuchs & Lehmann, 1975). This step gave a much higher yield (60%) than other routes that require the use of a solvent (e.g., 12%, Coxon & Fletcher Jr., 1963; 20%, Myers & Lee, 1984). Photobromination of **3.5** was accomplished using *N*-bromosuccinimide (Lichtenthaler & Jarglis, 1982), and this step was performed by Mr. K. Mok in Prof. Withers' laboratory. The product, 2,3,4,6-tetra-*O*-acetyl-α-bromo-β-D-glucosylcyanide (**3.6**), was formed stereospecifically.

Peracetylated 1-cyano-D-glucal (**3.7**) was prepared from **3.6** under aprotic conditions using zinc and one equivalent of pyridine. Somsák et al. (1990) published this procedure, and noted its superiority over the method involving zinc dust and acetic acid (Roth & Pigman, 1963). Use of the latter method to prepare **3.7** leads to a mixture of α- and β-glucosylcyanides as side products, and chromatographic separation of these anomers from the desired glucal is difficult (Somsák et al., 1990). Deacetylation of the base-sensitive compound **3.7** was accomplished using ammonia-saturated methanol under mild conditions (see Fritz et al., 1983).
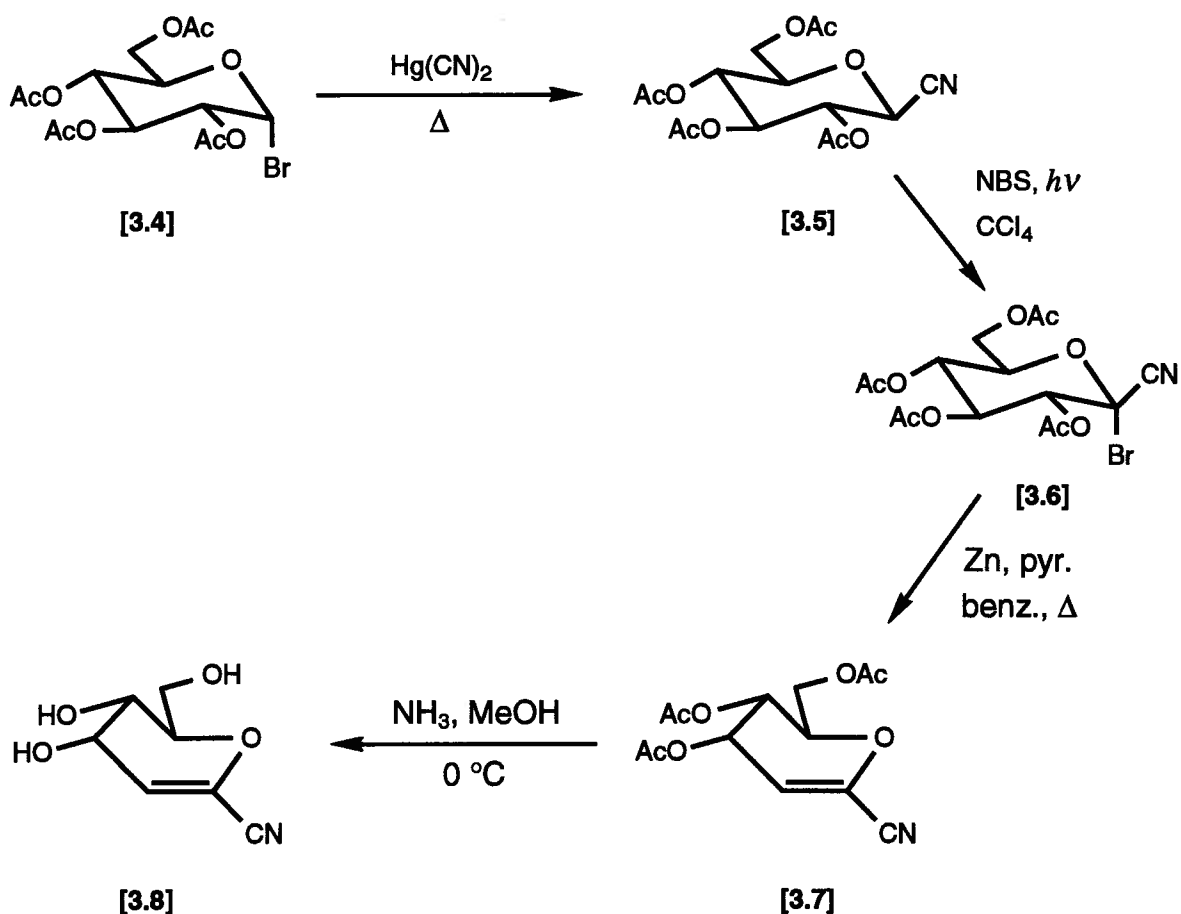
**Scheme 3.5.** The synthesis of 1-cyanoglucal.

---

*c. The synthesis of 2-cyanoglucal.*

Peracetylated 2-cyanoglucal was synthesized from peracetylated D-glucal (see Scheme 3.6) using chlorosulfonyl isocyanate and subsequent treatment with triethylamine (Hall & Jordaan, 1973). Deacetylation was accomplished as before using ammonia-saturated methanol under mild conditions (Fritz et al., 1983).

In the first step of the reaction sequence shown in Scheme 3.6, an N-chlorosulfonyl carboxamide derivative of glucal was probably formed initially, prior to the elimination of chlorosulfuric acid by triethylamine to yield the unsaturated nitrile. The low overall yield (27%) of the desired product was probably a consequence of the competing side-reaction shown. In this side-reaction the 3-acetoxy group of the starting material (peracetylated D-glucal) was probably cleaved with the assistance of the *trans* 4-acetoxy group, which

led to the formation of the dimer **3.9** (Hall et al., 1973). Hall & Jordaan (1973) found that a similar side-reaction was much less of a problem when peracetylated *galactal* was used to synthesize 2-cyanogalactal (which they obtained with a 60% overall yield), as in this case the C-3 and C-4 acetoxy groups were *cis* to one another, precluding *trans*-assisted dimer formation (i.e., analogous to **3.9**).
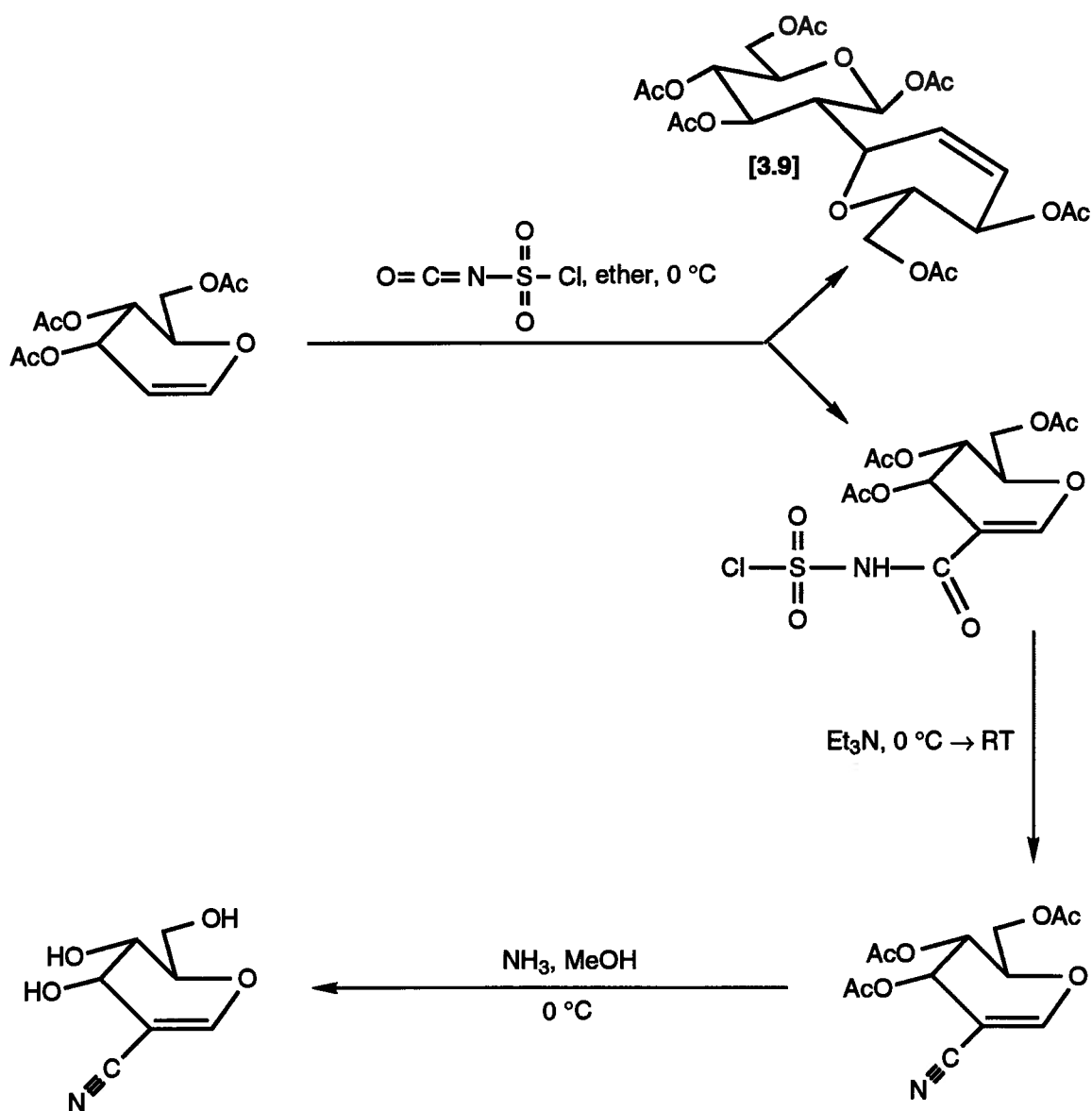


**Scheme 3.6.** The synthesis of 2-cyanoglucal.
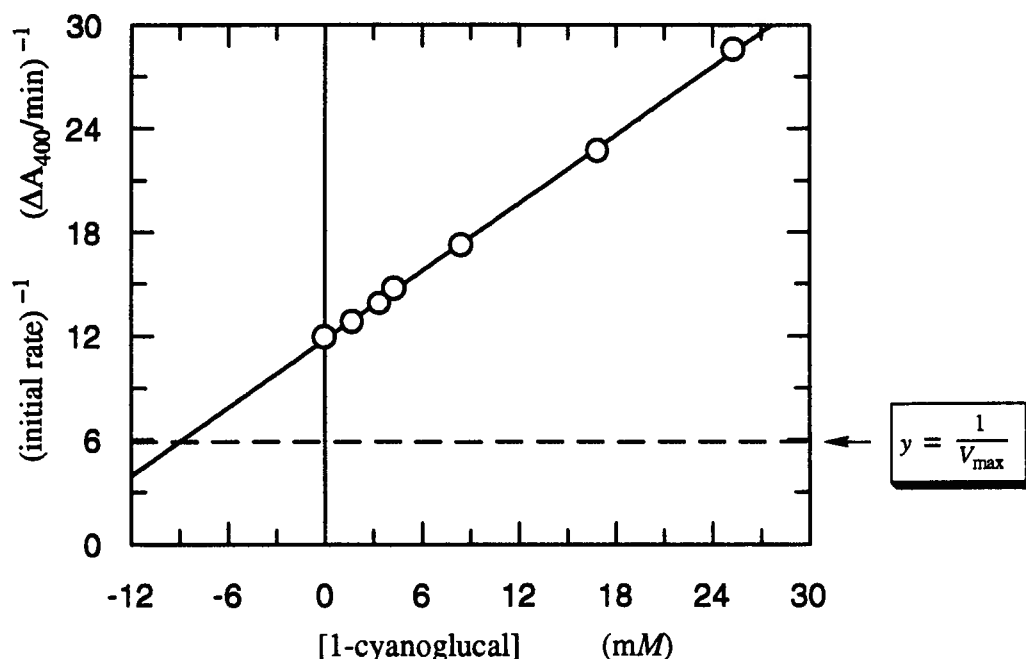
**Figure 3.14.** Estimation of the $K_i$ for the inhibition of pABG5 by 1-cyanoglucal.

---

Reactions (0.500 mL) were performed at 37 °C in 50 mM sodium phosphate buffer (pH 6.8) with 0.05 µg of pABG5 and 0.1% BSA. The concentration of βGlcPNP in the reactions was 83 µM. The concentration of 1-cyanoglucal in the reactions was 0, 1.7, 3.4, 4.3, 8.4, 16.9, and 25.3 mM.

---

*d. 1-Cyanoglucal as a reversible inhibitor of pABG5.*

1-Cyanoglucal was examined as a potential inactivator of pABG5 by incubating the enzyme with 33 mM 1-cyanoglucal and the appropriate reaction buffer for 8 hours at 37 °C (see Materials and Methods). At various time intervals small aliquots were removed and residual enzyme activity was assayed using the substrate βGlcPNP. No time-dependent inactivation of pABG5 was detected during these tests when compared with parallel control reactions. The 1-cyanoglucal remained unchanged (as determined by TLC) throughout this incubation period, which indicated that the compound was also not a substrate of the enzyme. Further kinetic studies showed that 1-cyanoglucal acted as a reversible inhibitor of pABG5-catalyzed hydrolysis of βGlcPNP. An approximate value for the inhibition constant, $K_i \sim 9.0$ mM, was obtained from a Dixon plot of the kinetic data (Fig. 3.14).
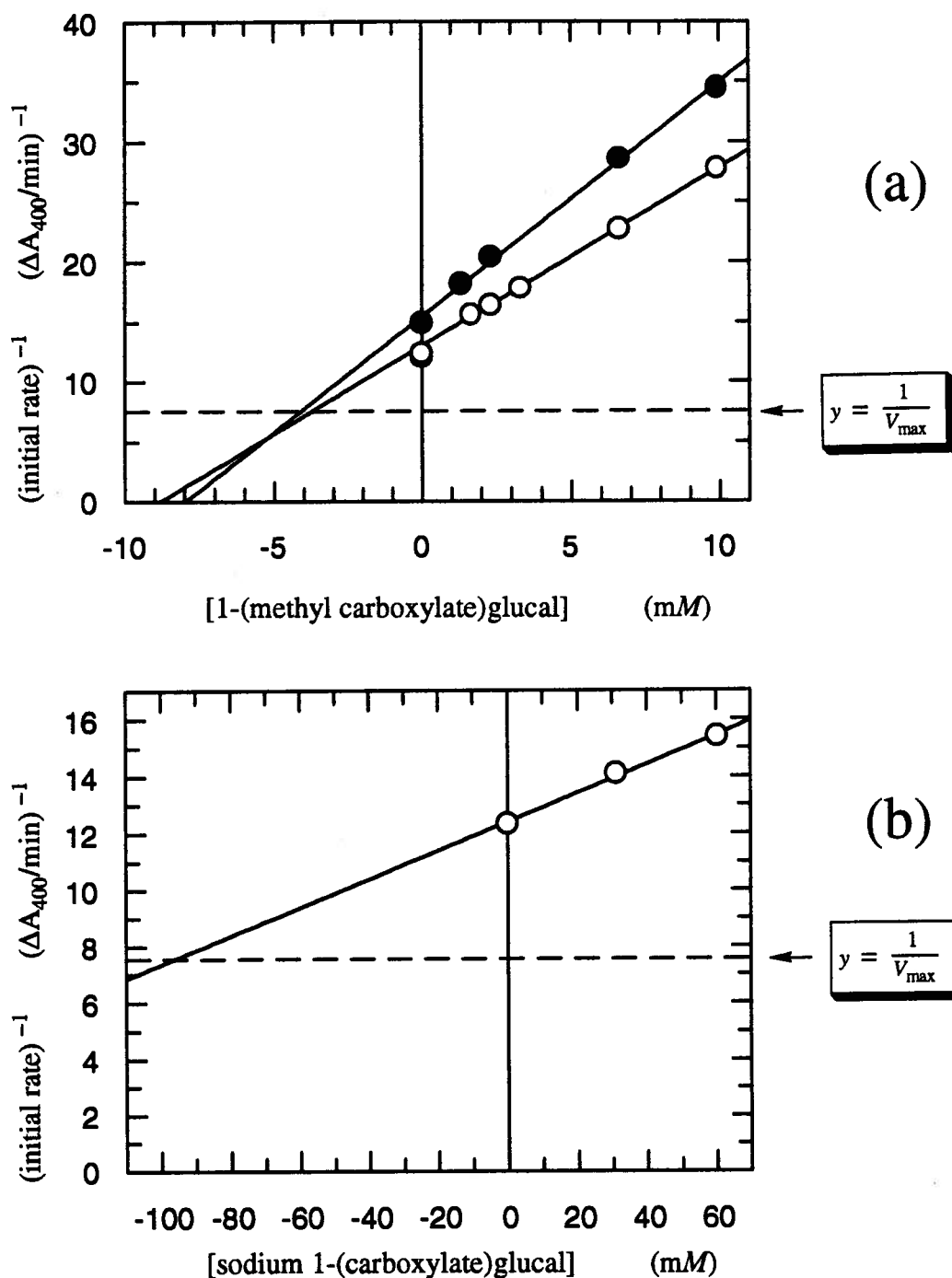
**Figure 3.15.** Estimation of the $K_i$ values for methylcarboxylate glucal and sodium carboxylate glucal.

In both cases reactions were performed as described in Fig. 3.14 and as specified further below:

(a) *RF* $K_i$ determination for the inhibition of pABG5 by methylcarboxylate glucal. The concentration of βGlcPNP in the reactions was 67 {•} or 101 {o} μ*M*. The concentration of methylcarboxylate glucal in the reactions was 0, 1.7, 2.3, 3.3, 6.6, and 9.9 m*M*.

(a) *RF* $K_i$ determination for the inhibition of pABG5 by sodium carboxylate glucal. The concentration of βGlcPNP in the reactions was 101 μ*M*. The concentration of sodium carboxylate glucal in the reactions was 0, 30, and 60 m*M*.

*e. Other α,β-unsaturated glucals as reversible inhibitors of pABG5.*

1-(Methyl carboxylate)glucal and sodium 1-(carboxylate)glucal are α,β-unsaturated derivatives of glucal that bear a carboxyl substituent at the C-1 position of the ring (see Fig. 3.13). Each compound was examined as a potential inactivator of pABG5 by incubating the enzyme with 10 or 11 m*M* methyl carboxylateglucal or sodium carboxylateglucal, respectively, and the appropriate reaction buffer for 24 hours at 37 °C (see Materials and Methods). At various time intervals small aliquots were removed and residual enzyme activity was assayed using the substrate βGlcPNP. No time-dependent inactivation of pABG5 was detected during these tests when compared with parallel control reactions. Both of these α,β-unsaturated derivatives of glucal remained unchanged (as determined by TLC) throughout their respective incubation periods, which indicated that neither compound acted as a substrate of the enzyme.
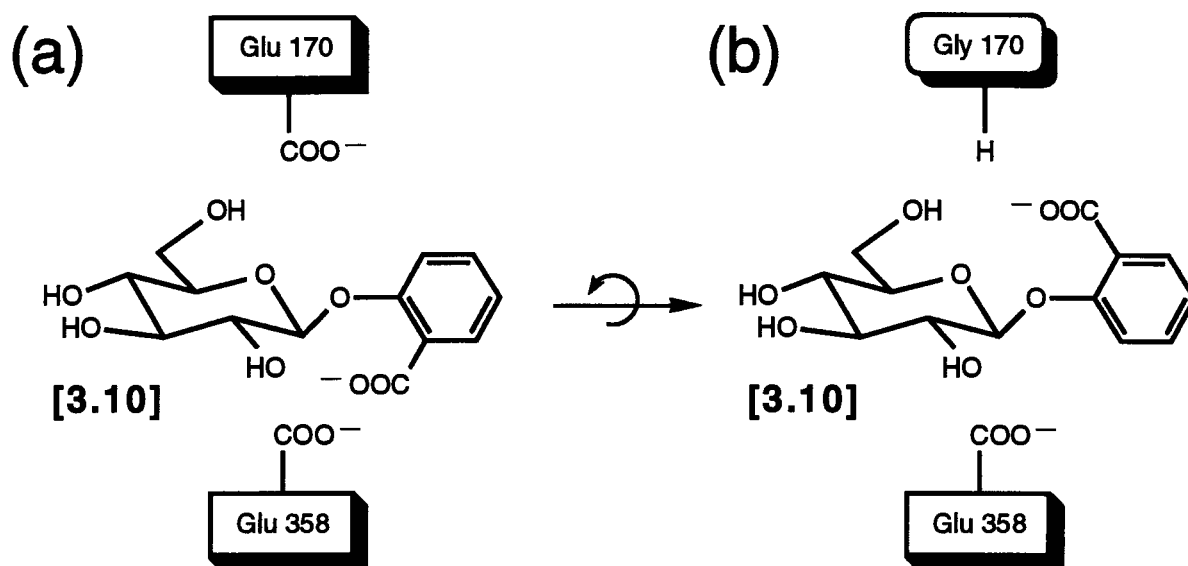


**Figure 3.16.** Minimization of electrostatic repulsion in the active site of the E170G variant form of pABG5.

Shown above are possible orientations of the aglycone moiety of **3.10**, 2'-carboxyphenyl β-D-glucoside, in the active site of (a) wild-type, and (b) the site-directed E170G variant, of pABG5 β-glucosidase (Q.P. Wang, pers. comm.). Carboxylate groups are shown in their fully ionized forms.

Reversible inhibition tests were then performed using either methyl carboxylateglucal or sodium carboxylateglucal (Fig. 3.15). Methyl carboxylateglucal bound to the enzyme with an inhibition constant, $K_i$, of ~3.2 m$M$ (Fig. 3.15a). Sodium carboxylateglucal bound very poorly to the enzyme, with an inhibition constant, $K_i$, of ~96 m$M$ (Fig. 3.15b).

The finding that sodium carboxylateglucal bound very poorly to pABG5 agreed well with unpublished results recently obtained by Dr. Qingping Wang of Prof. Withers' laboratory. Glycosides with an aglycone moiety bearing a negatively charged carboxylate group (such as 3.10) bound very poorly to pABG5 (Q.P. Wang, pers. comm.). Kinetic studies have shown that although 3.10 binds very poorly to the active site of wild-type pABG5 ($K_i$ = 60 m$M$), this glycoside binds about 65 times more strongly ($K_i$ = 0.92 m$M$) to a variant form of the enzyme obtained by site-directed mutagenesis (Q.P. Wang, pers. comm.). In the site-directed mutant protein (E170G) an active-site glutamate residue (Glu 170) had been replaced by a glycine residue, which removed one negative charge from the active site of this variant of pABG5 (see Fig. 3.16). Hence the very poor binding of negatively charged compounds such as sodium carboxylateglucal and 3.10 to wild-type pABG5 appears to be a consequence of electrostatic repulsion between the carboxylate group on the sugar and catalytically important carboxylate residues in the active site of the enzyme.

*f. 2-Cyanoglucal as a reversible inhibitor of pABG5.*

When the C-1 derivatized α,β-unsaturated glucals (1-nitro-, 1-cyano-, methyl carboxylate-, and sodium carboxylate- glucal) under study were tested as inactivators of pABG5 they were not reactive enough, or in one case (1-nitroglucal) too reactive, to act as specific labeling reagents for an active-site nucleophile in the enzyme. In most cases *C-1 derivatized* α,β-unsaturated glucals might not function as inactivators because the mechanism involves a Michael addition reaction, one that would require the formation of a covalent bond between the enzyme and the *C-2 position* of the sugar (see Scheme 3.4). Perhaps *C-1 derivatized* α,β-unsaturated glucals have difficulty binding to the enzyme in such a manner as to bring the C-2 position of the sugar close enough to a potentially reactive nucleophile in the active site, and hence only exceptionally reactive *C-1 derivatized* α,β-unsaturated glucals (such as 1-nitroglucal) are able to react.

Hence for steric reasons *C-2 derivatized* α,β-unsaturated glucals might be better able to act as Michael

acceptors for an active-site nucleophile in pABG5. In this case a Michael addition reaction would involve attack

by an active-site nucleophile of pABG5 at the "usual", *C-1 position* of the glucal. However, this would require

that a bulky substituent at C-2 be accommodated in the active site. Nevertheless it was worth investigating.

Several attempts were made to synthesize 2-nitroglucal using the procedure of Holzapfel et al. (1988), but only

the peracetylated form of this compound was stable. Unfortunately, even under the mildest deprotection

conditions, 2-nitroglucal was simply too reactive, and decomposed spontaneously into several different

compounds.
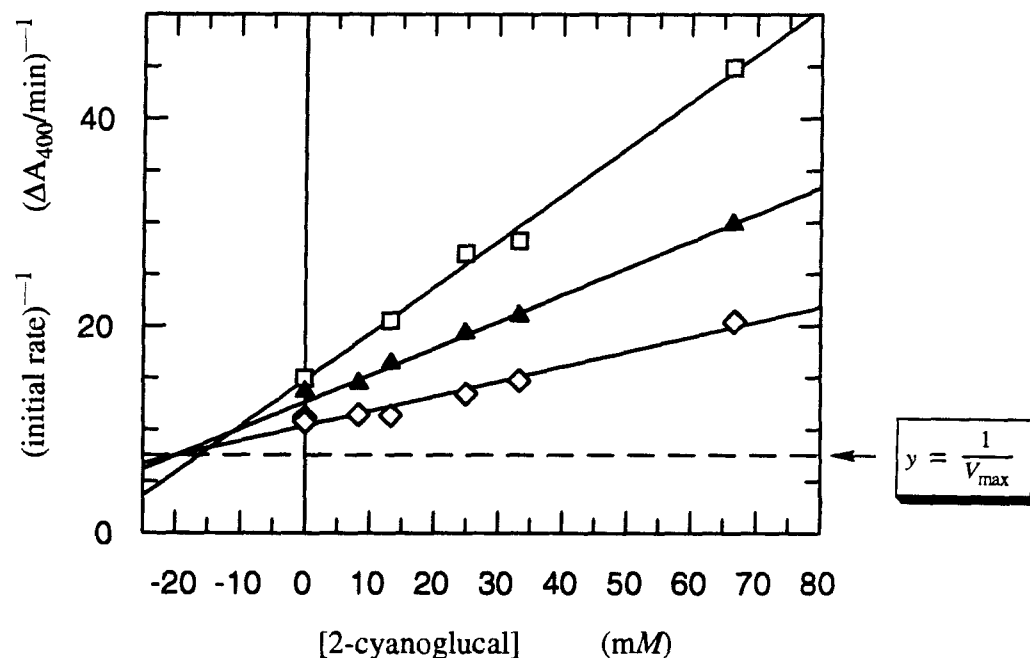


**Figure 3.17.** Estimation of the $K_i$ for the inhibition of pABG5 by 2-cyanoglucal.

Reactions were performed as described in Fig. 3.14 and as specified further below. The concentrations of βGlcPNP in the reactions were 67 {□}, 101 {▲} or 170 {◇} $\mu M$. The concentrations of 2-cyanoglucal in the reactions were 0, 8.3, 13, 25, 33, and 67 m$M$.

2-Cyanoglucal was therefore synthesized, and then tested as a potential inactivator of pABG5 by incubating the enzyme with 33 m$M$ 2-cyanoglucal and the appropriate reaction buffer for 20 hours at 37 °C (see Materials and Methods). At various time intervals small aliquots were removed and residual enzyme activity was assayed using the substrate βGlcPNP. No time-dependent inactivation of pABG5 was detected during these tests when compared with parallel control reactions. The 2-cyanoglucal remained unchanged (as determined by TLC) throughout this incubation period, which indicated that the compound was also not a substrate of the enzyme.

Reversible inhibition tests were then performed using 4-5 different concentrations of 2-cyanoglucal and 3 different concentrations of the substrate βGlcPNP. The initial-rate data obtained at each substrate and inhibitor concentration were fitted to equations describing different types of enzyme inhibition, using the computer program GraFit™ (Leatherbarrow, 1990). The best fit of the data was to the equation describing competitive inhibition, which yielded a $K_i$ value of 26 ± 3 m$M$. The Dixon plot obtained from the data is shown in Fig. 3.17, and this graphical approximation method yielded a similar value for the $K_i$. Although 2-cyanoglucal acted as a competitive inhibitor of pABG5, it bound poorly to the enzyme's active, and its $K_i$ = 26 ± 3 m$M$ represented even poorer binding to the enzyme than was observed with 1-cyanoglucal ($RF$ $K_i$ = 9.0 m$M$). The poorer affinity of 2-cyanoglucal for the active site of pABG5 must have been a consequence of either the size, geometry, or properties of the nitrile group at the C-2 position of this sugar. In many ways this is not surprising given the known specificity of this enzyme for interactions at the C-2 position (Namchuk, 1993).

### 3.3.7. Kinetic studies using 2-acetamidoglucal.

*a. The selective deprotection of peracetylated 2-acetamidoglucal.*

The peracetylated precursor (3.11) of 2-acetamidoglucal was synthesized from GlcNAc by John McCarter of Prof. Withers' laboratory, using the procedure of Pravdić et al. (1975). In this study the peracetylated precursor was first purified by column chromatography. Deacetylation of 3.11 using sodium methoxide in methanol (Pravdić & Fletcher Jr., 1967) selectively removed one of the two $N$-acetyl groups and all three $O$-acetyl groups to yield the desired product (3.12).
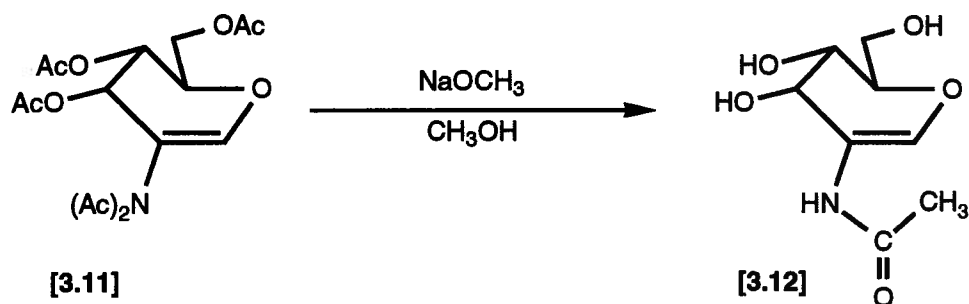
**Scheme 3.7.** The selective deprotection of peracetylated 2-acetamidoglucal.

*b. The inability of 2-acetamidoglucal to bind to pABG5.*

Inactivation tests and reversible inhibition tests were performed using 2-acetamidoglucal and pABG5. This compound did not inactivate or even bind to the enzyme, even at 2-acetamidoglucal concentrations as high as 33 m$M$. The reversible inhibition tests also showed that there was no effect on enzyme activity, even at 2-acetamidoglucal concentrations as high as 33 m$M$.

The inability of 2-acetamidoglucal to bind to pABG5 was probably due to the presence of the $N$-acetyl group at the C-2 position. Comparable results have been reported for the interaction between 2-deoxy-2-acetamidoglucose and sweet almond β-glucosidase (Dale et al., 1985). An inhibition constant, $K_i$, of > 900 m$M$ was obtained, and this extremely poor affinity was attributed to the polar nature of the acetyl group (Dale et al., 1985). Sweet almond β-glucosidase displays much greater affinity for compounds such as 2-deoxy-2-[($p$-chlorobenzyl)amino]glucose ($K_i$ = 3.0 m$M$) and 2-deoxy-2-[($p$-methoxybenzyl)amino]glucose ($K_i$ = 5.9 m$M$), where the acetyl group has been replaced by a nonpolar benzyl group (Dale et al., 1985).

*3.4. CONCLUSIONS.*

Heptenitol and two fluorinated derivatives ($F_2$hept and $F_1$hept) were synthesized and kinetic studies were performed using a cloned *Agrobacterium* β-glucosidase, pABG5. Heptenitol showed a mixed inhibition pattern. $F_2$hept and $F_1$hept both acted as uncompetitive (or noncompetitive) inhibitors, and there was no detectable binding of either $F_2$hept or $F_1$hept in the active site of pABG5. There were no changes in the

thin-layer chromatograms or ^{19}F NMR spectra of the reaction mixtures after prolonged incubation of pABG5 with either of the fluoroheptenitols. The fluoroheptenitols did not act as substrates or inactivators of pABG5.

A comparison of $K_i$ values showed that heptenitol, with two olefinic hydrogen atoms at C-1, did not bind to pABG5 as strongly as the more polar $F_1$hept and $F_2$hept (Table 3.1), whose only structural difference(s) with the parent compound are the presence of one or two olefinic fluorine atoms at C-1, respectively. Fluorine is not only the more polar of the olefinic C-1 substituents in these compounds (and thus more likely to strengthen interactions between the compound and a polar environment in the enzyme); fluorine is also, unlike hydrogen, capable of acting as a hydrogen-bond acceptor. Hydrogen bonding involving such an acceptor and a hydrogen-bond donor on the enzyme may in part account for the increased affinity of pABG5 for fluoroheptenitols compared with heptenitol.

Heptenitol was catalytically hydrated by pABG5 to yield 1-deoxy-β-D-*gluco*-heptulose as the initial product. Although this hydration reaction was reasonably fast ($k_{cat}$ = 640 min$^{-1}$, or ~7% of the rate of βGlcPNP hydrolysis), the affinity of heptenitol for the active site of pABG5 was extremely low ($K_m$ = 270 m$M$).

Heptenitols have been tested as substrates with other β-glycosidases. As an example, *E. coli* β-D-galactosidase hydrates D-*galacto*-heptenitol with a $K_m$ = ~50-70 m$M$ and a $k_{cat}$ = 2460-3840 min$^{-1}$, or ~1-2% of the rate of β-galactoside hydrolysis by the same enzyme (Brockhaus & Lehmann, 1977). However, this author is unaware of any studies that have tested heptenitols as inhibitors of β-glycosidases. Hence it was not possible to compare the type of inhibition of pABG5 displayed by heptenitol with published results obtained using other β-glycosidases. It is therefore unclear if heptenitol (and the other heptenitol derivatives studied herein) would have the same effects on β-glucosidases from other sources as these compounds had on pABG5. Further kinetic studies using β-glucosidases and α-glucosidases (given the lack of an anomeric carbon at the C-1 position of heptenitols) from other sources would help to answer these questions.

Methylglucal acted as a very poor substrate of pABG5, yielding 1,3-dideoxy-D-*gluco*-heptulose as the product of the hydration reaction. A $K_m$ of 57 m$M$ and a $k_{cat}$ of 0.056 min$^{-1}$ were obtained, thus methylglucal was ~2400- or [1.2 × 10$^8$]- fold less effective as a substrate compared with heptenitol or βGlcPNP, respectively (based on the ratio of their $k_{cat}/K_m$ values). Methylglucal itself was unstable, and the rate of its spontaneous

hydration was quite significant, especially in phosphate-containing buffers. Presumably the poor turnover of methylglucal is a consequence of several factors. Firstly, methylglucal lacks a C-3 hydroxyl group, and enzyme-substrate interactions involving *the comparable position in a glycoside* (in this case the C-2 hydroxyl) have been shown to contribute 8 kcal/mol or more to transition-state stabilization in the reactions catalyzed by pABG5 (Namchuk, 1993) and other enzymes (McCarter et al., 1992). Secondly, the C-1 methyl group may hinder approach of the nucleophile at C-2 (in methylglucal; *the comparable position in a glycoside being C-1*), or it may interact unfavourably with other active-site groups upon conversion to the glycosyl-enzyme intermediate. Thirdly, the apolar C-1 methyl group may not fit well into the generally polar "aglycone pocket" (adjacent to the active site) expected in a glycosidase.

1-Nitroglucal, an α,β-unsaturated glucal, acted as an inactivator of pABG5. Kinetic studies showed that inactivation occurred at the active site, most likely as a result of a Michael addition reaction between an active-site nucleophile and C-2 of the inactivator. The mass spectrum of nitroglucal-inactivated pABG5 showed that the sample was quite heterogeneous, indicating that on average several equivalents of nitroglucal were covalently bound to the enzyme. The synthesis of radiolabelled nitroglucal may prove useful in future studies directed at identifying active-site amino-acid residues of glycosylases, and thereby confirm that a Michael addition reaction provides the mechanistic basis for the inactivation behaviour of reactive α,β-unsaturated glucals.

Unfortunately, the other α,β-unsaturated glucals that were tested (1-cyano-, methyl carboxylate-, sodium carboxylate-, and 2-cyano- glucal) did not act as inactivators or substrates of pABG5. These compounds only acted as relatively poor-binding, reversible inhibitors of the enzyme.

For a summary of the kinetic data obtained using pABG5, please see Table 3.1.

**Table 3.1.** Summary of kinetic data obtained using a cloned β-glucosidase, pABG5.

| Compound | Structure | Inhibition | Inactivation | Substrate |
|---|---|---|---|---|
| βGlcPNP | A | | | $K_m = 78\ \mu M$ <br> $k_{cat} = 9{,}500\ \text{min}^{-1}$ |
| heptenitol | B <br> $R_1 = R_2 = H$ | $K_i = 13 \pm 1\ mM$ <br> (for noncompetitive) | no | $K_m = 270 \pm 40\ mM$ <br> $k_{cat} = 640 \pm 60\ \text{min}^{-1}$ |
| F$_2$hept | B <br> $R_1 = R_2 = F$ | $K_i = 0.67 \pm 0.04\ mM$ <br> (for noncompetitive) | no | no |
| F$_1$hept | B <br> $R_1 = H$ <br> $R_2 = F$ | $K_i = 3.2 \pm 0.2\ mM$ <br> (for noncompetitive) | no | no |
| methylglucal | C <br> $R_3 = H$ <br> $R_4 = CH_3$ | $K_i \sim 40\ mM$ | no | $K_m = 57 \pm 8\ mM$ <br> $k_{cat} = 0.056\ \text{min}^{-1}$ <br> $\pm 0.004\ \text{min}^{-1}$ |
| 1-nitroglucal | C <br> $R_3 = H$ <br> $R_4 = NO_2$ | $K_i \sim 4.8\ mM$ | $K_i = 5.5 \pm 0.9\ mM$ <br> $k_i = 0.011\ \text{min}^{-1}$ <br> $\pm 0.001\ \text{min}^{-1}$ | no |
| 1-cyanoglucal | C <br> $R_3 = H$ <br> $R_4 = CN$ | $K_i \sim 9.0\ mM$ | no | no |
| 1-(methyl carboxylate) glucal | C <br> $R_3 = H$ <br> $R_4 = COOCH_3$ | $K_i \sim 3.2\ mM$ | no | no |
| sodium 1-(carboxylate) glucal | C <br> $R_3 = H$ <br> $R_4 = COO^- Na^+$ | $K_i \sim 96\ mM$ | no | no |
| 2-cyanoglucal | C <br> $R_3 = CN$ <br> $R_4 = H$ | $K_i = 26 \pm 3\ mM$ <br> (competitive) | no | no |
| 2-acetamidoglucal | C <br> $R_3 = NHCOCH_3$ <br> $R_4 = H$ | no | no | no |
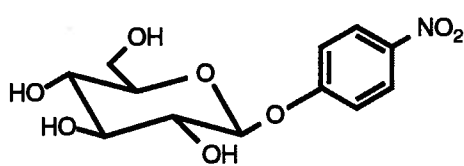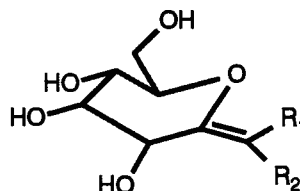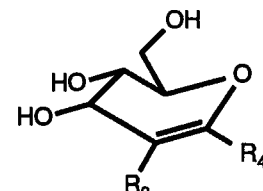


**A**    **B**    **C**

## CHAPTER 4: KINETIC STUDIES USING β-N-ACETYLHEXOSAMINIDASE (NAGase)

*4.1. INTRODUCTION.*

### 4.1.1. Some general properties of β-N-acetylhexosaminidase.

β-N-Acetylhexosaminidase (2-acetamido-2-deoxy-β-D-hexoside acetamidodeoxyhexohydrolase, E.C. 3.2.1.52)—abbreviated herein as NAGase—is an enzyme that is widely distributed in nature, and can be isolated from microbial, plant, and animal sources (Stirling, 1983). The enzyme possesses both β-N-acetylglucos-aminidase and β-N-acetylgalactosaminidase activities, and the former activity was first discovered by Helferich & Iloff (1933) in an emulsion prepared from almonds. A β-N-acetylglucosaminidase activity was first detected in mammalian tissue by Watanabe (1936).

Mammalian lysosomal NAGases are dimeric enzymes, consisting of α- or β-subunits held together by noncovalent forces. The relative molecular mass of each α and β subunit is in the $[5\text{-}7] \times 10^4$ range (Conzelmann & Sandhoff, 1987). There are three isozymes of human lysosomal NAGase; NAGase A is an αβ heterodimer, whereas the two homodimeric isozymes, NAGase B and NAGase S, are composed of ββ and αα subunits, respectively. NAGase S is unstable and appears to have only negligible enzymatic activity. NAGase A and NAGase B have isoelectric points near pH 5 and between pH 7.0-7.5, respectively, and hence are referred to as the acid and neutral forms of the enzyme (Conzelmann & Sandhoff, 1987). This difference in isoelectric points has been exploited in biochemical procedures (ion-exchange chromatography and isoelectric focusing) for the purification of these two clinically important isozymes of NAGase (Dance et al., 1970; Sandhoff, 1968).

NAGase A and NAGase B have different substrate specificities, and they also differ in their ability to withstand elevated temperatures (Okada & O'Brien, 1969). NAGase B is a heat-stable enzyme that is most active towards neutral substrates such as globoside, glycoproteins, glycosaminoglycans, and oligosaccharides. NAGase A is less stable at elevated temperatures, and is most active towards $G_{m2}$ gangliosides (see Fig. 4.1), as well as acidic substrates such as glucuronic acid-containing oligosaccharides, and even 6-sulfo-glucosaminides (Bearpark & Stirling, 1978; Ludolph et al., 1981). However, *in vitro* studies by Legler et al. (1991) have shown

that NAGase A and NAGase B display similar kinetic properties and pH-activity profiles, with the exception that NAGase B is inactive towards acidic substrates, e.g., the 6-sulfate ester of $N$-acetyl-$\beta$-glucosaminide.
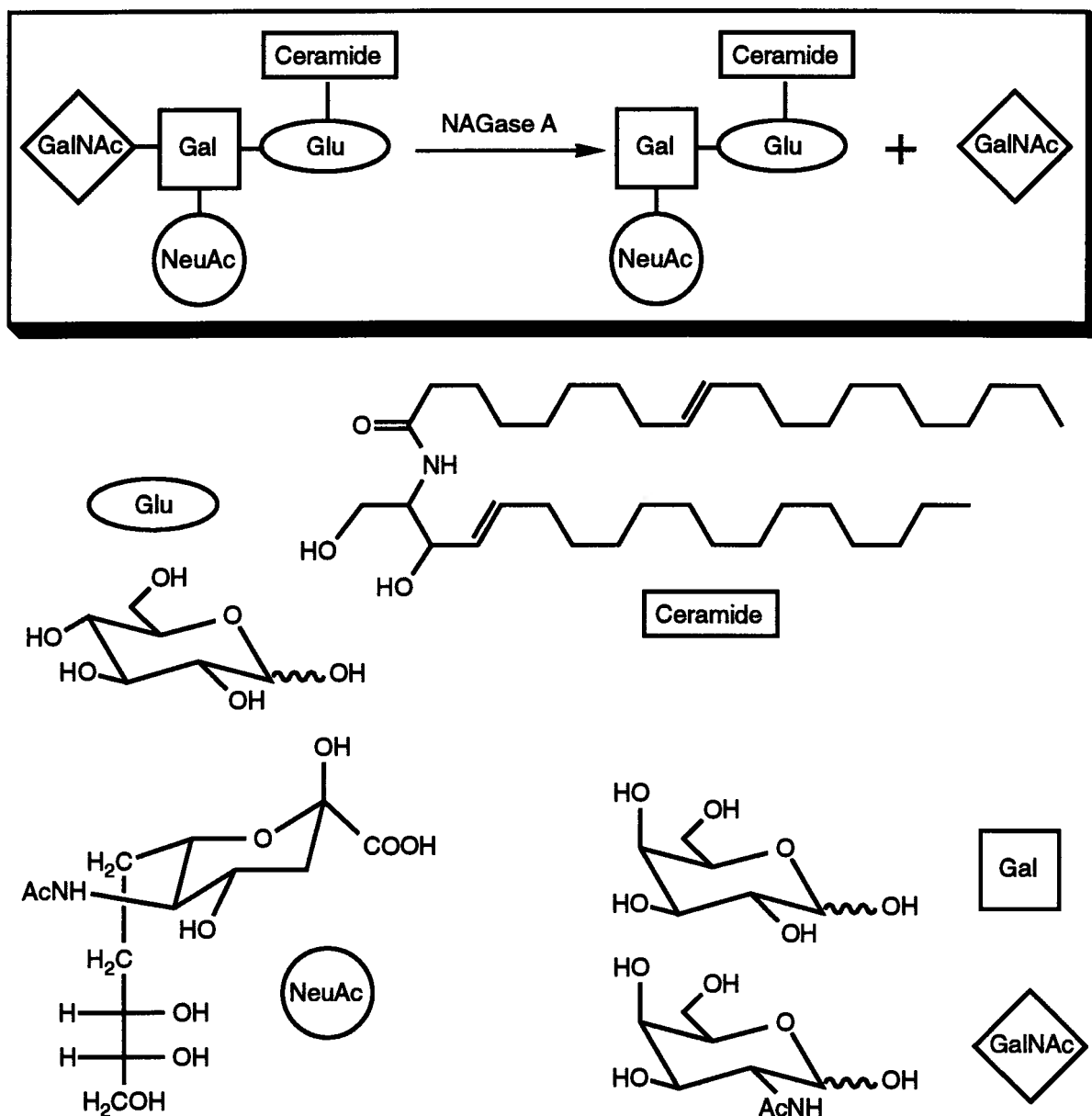


Figure 4.1. The catalytic removal of the GalNAc residue from ganglioside $G_{m2}$ by NAGase A.

The ability of NAGase A to remove the $N$-acetylgalactosamine residue from $G_{m2}$ gangliosides is particularly important (see Fig. 4.1). Gangliosides are sugar-containing lipids found in high concentrations in the nervous system (especially in gray matter), and they are important constituents of neuronal membranes. Inside lysosomes (a type of subcellular organelle) gangliosides are enzymatically degraded by the sequential removal of their sugars, and disorders of ganglioside breakdown can have extremely serious clinical consequences.

*In vivo*, the interaction between the water-soluble enzyme NAGase A and its membrane-bound glycolipid substrate is mediated by the noncatalytic activity of the $G_{m2}$-activator protein (Conzelmann et al., 1982). This activator protein binds to the $\alpha$-subunit of the enzyme, but not to the $\beta$-subunit. The amphipathic $G_{m2}$-activator protein is sufficiently hydrophilic to bind to NAGase A, yet it is also sufficiently lipophilic to bind membrane-bound $G_{m2}$ gangliosides and solubilize them as [$G_{m2}$-activator protein]–lipid complexes.

### 4.1.2. The clinical significance of $\beta$-$N$-acetylhexosaminidases.

*a. Tay-Sachs disease and Sandhoff disease.*

In the hereditary disorder known as Tay-Sachs disease there is a deficiency in NAGase A activity due to a defect in the production of the $\alpha$-subunit (Okada & O'Brien, 1969). The symptoms of Tay-Sachs disease are usually evident before an affected infant is one year old. Weakness and retarded psychomotor development are typical early symptoms. By the age of two, the child is demented and blind, and death before the age of four is the inevitable clinical outcome. The ganglioside content of the brain of an infant with Tay-Sachs disease is greatly elevated due to the deficiency of NAGase A activity.

Sandhoff disease is a hereditary disorder that is similar to but much rarer than Tay-Sachs disease. In Sandhoff disease there are deficiencies in both NAGase A and NAGase B activities due to a defect in the production of the $\beta$-subunit (Sandhoff et al., 1968). Both of these neuronal lipid storage diseases have similar symptoms and clinical outcomes, but Sandhoff disease is also characterized by the abnormal accumulation of globosides, glycopeptides, and oligosaccharides in extraneural tissues.

*b. Abnormal levels of NAGase activity in cancer cells.*

Some serum glycosylases, and especially NAGases, are produced at elevated levels and secreted into the extracellular medium by many different tumor cell types *in vitro* (Bernacki et al., 1985). These observations have led to a great deal of interest in the use of glycosylase inhibitors as pharmaceuticals. 2-Acetamidoglucal (NAGlucal) is an example of a NAGase inhibitor that has been evaluated as a therapeutic drug for Lewis lung carcinoma in mice (Bernacki et al., 1985). The administration of 100 mg of NAGlucal/kg body weight/day intraperitoneally for five consecutive days (days 3-8 following the subcutaneous implant of a tumor in C57 B1/6J female mice) resulted in a 63% increase in the life span of drug-treated mice compared to untreated controls.

*4.2. AIMS OF THIS STUDY.*

Several kinetic studies have been performed using various glycosylases and glycal derivatives (see Chapter 1). However, very few studies have been performed using NAGases and glycal derivatives such as NAGlucal. As mentioned above, Bernacki et al. (1985) noted the potential efficacy of NAGlucal as a chemotherapeutic agent. Another report briefly mentioned that 2-acetamidoglucal and 2-acetamidogalactal are reversible inhibitors of NAGase from boar epididymis, with inhibition constants, $K_i$, of 58 and 40 $\mu M$, respectively (Pokorny et al., 1975).

NAGase-catalyzed reactions probably follow the same mechanism as those catalyzed by other $\beta$-retaining glycosylases. However, no X-ray structural data is available for NAGases, and thus no information is available about catalytically important amino acids in the active sites of these enzymes. Furthermore, although some metal ions (such as $Ag^+$ and $Hg^{2+}$) are known to inactivate NAGases (Li & Li, 1970), no mechanism-based inactivators appear to have been discovered for these clinically important enzymes. Legler & Bollhagen (1992) did find that *N*-acetylconduramine B *trans* epoxide (see Scheme 1.6) acts as a reversible inhibitor of NAGases from various sources, with $K_i$ values of 0.5 to 1.6 $\mu M$. However, in contrast to the interaction of other glycosidases with cyclohexane polyol epoxides with the appropriate configuration (see Chapter 1), no covalent, irreversible inhibition is observed.

In this thesis, three different NAGases—isolated from jack bean, bovine kidney, or human placenta (J-, K-, and H-NAGase, respectively)—were studied. It was felt that NAGlucal might *inactivate* one of these NAGases, in the same way that D-glucal inactivates *A. wentii* β-glucosidase (Legler et al. 1979). This would occur if the rate of deglycosylation is much slower than the rate of glycosylation (see Scheme 1.3). If this were the case, it might be possible to trap an *N*-acetylglucosaminyl-NAGase intermediate, and identify a nucleophilic residue in the enzyme's active site.

NAGlucal might instead act as a *substrate* of one of the NAGases under study. This would occur if the rates of both deglycosylation and glycosylation are reasonably fast. If this were the case, the stereochemistry of the hydration reaction could be studied. In addition, the effects of the 2-acetamido substituent on the kinetics of the hydration reaction could also be studied, and these results could be compared with those obtained using other glycal derivatives and glycosides.

NAGlucal should at least act as a reversible *inhibitor* of one of the NAGases under study (and reduce the rate of hydrolysis of an *N*-acetylglucosaminide substrate, βGlcNAcPNP). Kinetic and structural studies carried out using enzyme inhibitors often yield insights into the nature of the binding interactions between the inhibitor and the active site.

This study also determined the stereochemistry of the NAGase-catalyzed hydrolysis of βGlcNAcPNP (4'-nitrophenyl 2-acetamido-2-deoxy-β-D-glucosaminide), a commonly used substrate for the assay of NAGase activity.

## 4.3. RESULTS AND DISCUSSION.

### 4.3.1. A "direct" colorimetric assay for NAGase-catalyzed hydrolysis of βGlcNAcPNP.

In previously published studies NAGase activity has been assayed using fluorometric or colorimetric methods. In the fluorometric assay, 4'-methylumbelliferyl 2-acetamido-2-deoxy-β-D-glucosaminide (βGlcNAcMu) is used as a substrate, and fluorometry is used to determine the concentration of the aglycone product, 4-methylumbelliferone, liberated as a result of enzyme-catalyzed hydrolysis.

In the colorimetric assay of NAGase activity, a chromogenic substrate such as 4'-nitrophenyl 2-acetamido-2-deoxy-$\beta$-D-glucosaminide ($\beta$GlcNAcPNP) is used. The concentration of the aglycone product (p-nitrophenol) liberated as a result of the enzyme-catalyzed hydrolysis of $\beta$GlcNAcPNP is measured at a wavelength of 400 nm, where there is very little absorbance by the substrate. p-Nitrophenol has a $pK_a$ of 7.15, and it is only the p-nitrophenolate anion that absorbs 400-nm light. However, the pH optimum for NAGase activity is usually $\leq$ pH 5.0; thus the percentage of the liberated aglycone in the anionic, light-absorbing form is less than 1% of the total product at this pH, resulting in small absorbance changes. The colorimetric assay therefore requires the addition of an alkaline "stop" buffer to raise the pH well above the $pK_a$ of p-nitrophenol in order to determine the concentration of the product.

There are several disadvantages associated with a "stopped" colorimetric assay of enzyme activity. A "stopped" assay is not as convenient as a "direct" assay of the product. A "stopped" assay also requires that the reaction rate is linear over the time period in question, and any variation in the reaction rate during this period will seriously affect the results. For these reasons a "direct", continuous colorimetric assay of NAGase activity was developed for this work, based on the procedure of Kempton & Withers (1992).

This direct assay involved monitoring the reaction (carried out in a cuvette thermostatted at 25 °C) at a wavelength of 360 nm. This wavelength was chosen after recording the absorption spectrum of a standard solution of $\beta$GlcNAcPNP before and after hydrolysis at pH 5.0 (performed by adding a small volume of enzyme solution). At pH 5.0 the difference in the molar extinction coefficients of the product and the substrate of the reaction ($\varepsilon_p$ and $\varepsilon_s$, respectively) was greatest at 360 nm. The values of $\varepsilon_p$ and $\varepsilon_s$, and $\Delta\varepsilon = (\varepsilon_p - \varepsilon_s)$ at 360 nm were then calculated at pH 5.0 (for the assay of J-NAGase) and pH 4.25 (for the assay of K-NAGase and H-NAGase) using carefully prepared standard solutions of the product and the substrate. Because of the stoichiometry of the hydrolysis reaction, the concentration of the substrate consumed ($-\Delta C$) is equal to the concentration of the product formed ($\Delta C$) during the reaction, and hence (where l = path length of 1.00 cm):

$$\Delta A_{tot} = \text{change in } A_{360} \text{ during the reaction}$$

$$= \Delta A_p + \Delta A_s = \text{the change in } A_{360} \text{ due to the } formation \text{ of the product plus the change in } A_{360} \text{ due to the } consumption \text{ of the substrate.}$$

$$= \varepsilon_p \bullet (\Delta C) \bullet l + \varepsilon_s \bullet (-\Delta C) \bullet l$$

$$= [\varepsilon_p - \varepsilon_s] \cdot (\Delta C) \cdot l$$

$$= \Delta \varepsilon \cdot (\Delta C) \cdot l$$

and hence the initial rate of product formation, $v$, can be measured as follows:

$$v \qquad = (\Delta C)/\text{min}$$

$$= [\Delta A_{tot}/\text{min}] \div \{\Delta \varepsilon \cdot l\}$$

The kinetic parameters $K_m$ and $V_{max}$ describing βGlcNAcPNP hydrolysis were determined by fitting the initial-rate data to the nonlinear form of the Michaelis-Menten equation using the computer program GraFit™ (Leatherbarrow, 1990). The initial-rate data for the hydrolysis of βGlcNAcPNP by J-NAGase is shown in Lineweaver-Burk form in Fig. 4.2. The values of $K_m$ and $V_{max}$ for the hydrolysis of βGlcNAcPNP by each of the NAGases under study are given in Table 4.2. The values of kinetic parameters determined for other compounds using NAGase are also listed.
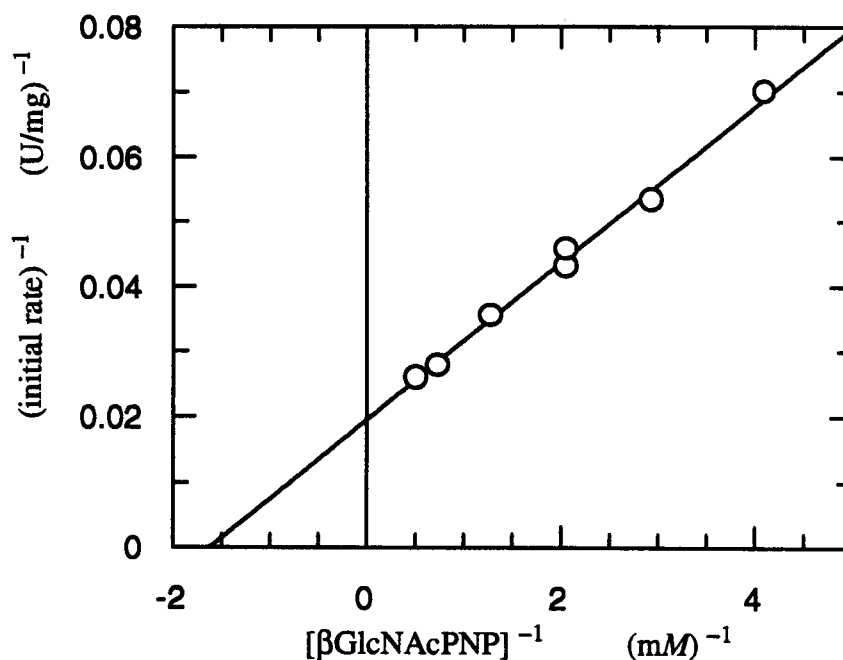


**Figure 4.2.** Determination of $K_m$ and $V_{max}$ for J-NAGase-catalyzed hydrolysis of βGlcNAcPNP.

Reactions were performed at pH 5.0 and 25 °C in 50 m$M$ citrate buffer containing 0.1% BSA, 100 m$M$ NaCl, and 1.0 µg/mL of β-$N$-acetylhexosaminidase from jack beans. The concentration of βGlcNAcPNP in the reactions was 0.24, 0.34, 0.49, 0.78, 1.36, and 1.95 m$M$.
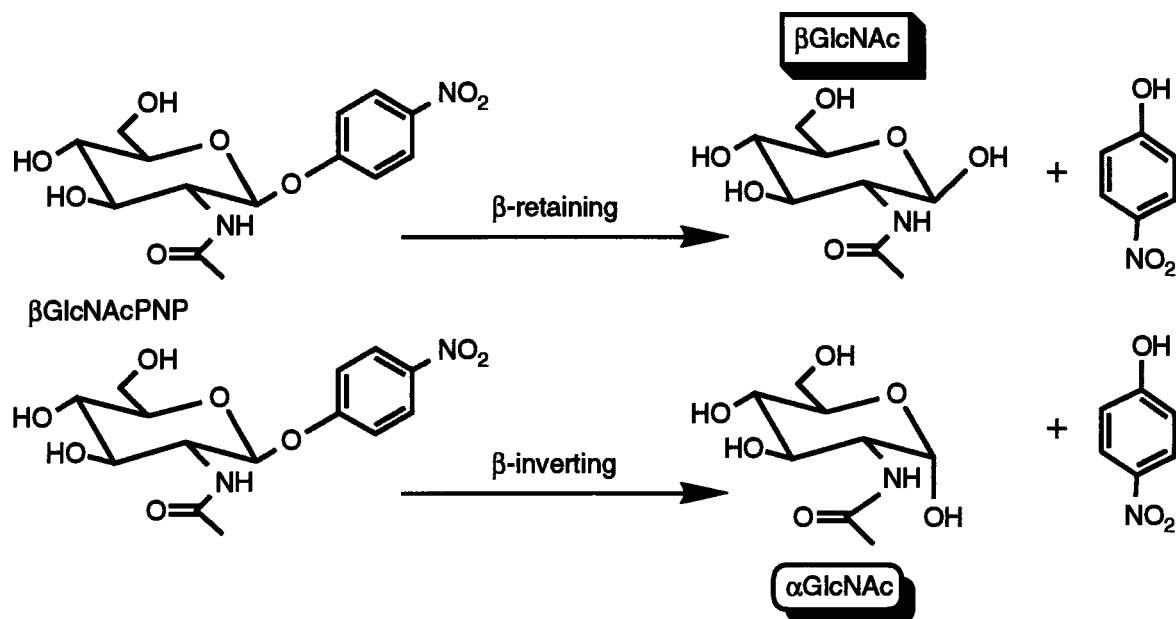
**Scheme 4.1.** The stereochemistry of βGlcNAcPNP hydrolysis by β-retaining and β-inverting NAGases.

The first β-*N*-acetylhexosaminidase studied was J-NAGase. The isolation, crystallization, and general properties of J-NAGase have been reported by Li & Li (1970). The $K_m$ value obtained for J-NAGase-catalyzed hydrolysis of βGlcNAcPNP using the "direct" colorimetric assay ($0.62 \pm 0.04$ m$M$) agrees well with the value obtained by Li & Li (1970) for the same reaction using a "stopped" assay ($0.64$ m$M$). The $V_{max}$ value obtained using the "direct" assay, $50 \pm 1$ U/mg, is also very close to the vendor's (Sigma Chemical Co.) specification for this enzyme-catalyzed reaction, 53 U/mg. It is therefore reasonable to conclude that the "direct" colorimetric assay yields reliable values for enzyme kinetic parameters.

**4.3.2. The stereochemistry of J-NAGase-catalyzed hydrolysis of βGlcNAcPNP.**

Koshland (1953) was the first to propose that there are important differences between the reaction mechanisms of retaining and inverting glycosidases. The reactions catalyzed by retaining glycosidases probably involve a double-displacement mechanism (see Scheme 1.3). In this reaction mechanism an amino acid residue acting as a nucleophile is involved in the formation of a glycosyl-enzyme intermediate, and this intermediate is

subsequently attacked by a water molecule. In contrast, the reactions catalyzed by inverting glycosidases probably involve a single-displacement mechanism, where a water molecule acts as the nucleophile that directly displaces the aglycone leaving group (Koshland, 1953).

Determination of the stereochemistry of catalysis by NAGase is a prerequisite to understanding the reaction mechanism. It appears that the stereochemistry of the hydrolysis of βGlcNAcPNP by jack bean NAGase has not been reported. Indeed only one NAGase, isolated from boar epididymis, has been subjected to such an analysis: Ya Khorlin et al. (1972) used $^1$H NMR to show that this NAGase is a β-retaining enzyme.

In this thesis, HPLC was used as an analytical tool to determine the stereochemistry of the hydrolysis of βGlcNAcPNP by J-NAGase. A DextroPak$^®$ column (operated at room temperature using 100% $H_2O$ as the eluant) was able to resolve the two anomers of 2-acetamido-2-deoxy-D-glucopyranose (GlcNAc). This column was used to determine which anomer was the initial product of the reaction (i.e., before α/β equilibration). When an *equilibrated* standard solution of GlcNAc was analyzed by HPLC, two peaks (with retention times of 3.38 and 3.55 minutes) eluted from the DextroPak$^®$ column (Fig. 4.3c). When a freshly prepared *anomerically pure* standard solution of αGlcNAc was analyzed by HPLC, a single peak (with a retention time of 3.55 minutes) eluted from the same column (not shown), identifying the first and second peaks as being attributable to the elution of the β– and α– anomers of GlcNAc, respectively. The anomeric configuration of the freshly prepared αGlcNAc standard (prepared in $D_2O$) was confirmed by $^1$H NMR (δ of H-1 = 5.2 ppm, $J_{1,2}$ = 3 Hz) and by determination of the melting point of the solid (203-205 °C; lit. mp 211 °C, Aldrich Chemical Co. Cat.). If the standard solution of αGlcNAc was left standing prior to HPLC analysis, the sample formed an equilibrium (α/β) mixture, and the β-anomer appeared as a shoulder of the α-anomer peak (as in Fig.4.3c). $^1$H NMR analysis of the equilibrium mixture indicated that the α-anomer was the major component.

When aliquots of an incubation mixture of βGlcNAcPNP and J-NAGase were analyzed by HPLC over time, the initial product observed was the β-anomer of GlcNAc, demonstrating that J-NAGase is a β-retaining enzyme (see Fig. 4.3a). This product subsequently anomerizes to form an equilibrium (α/β) mixture (Fig. 4.3b). The enzyme-catalyzed hydrolysis of βGlcNAcPNP by K-NAGase or H-NAGase also yielded the β-anomer of GlcNAc (not shown), thus all three of the NAGases examined are β–retaining enzymes.
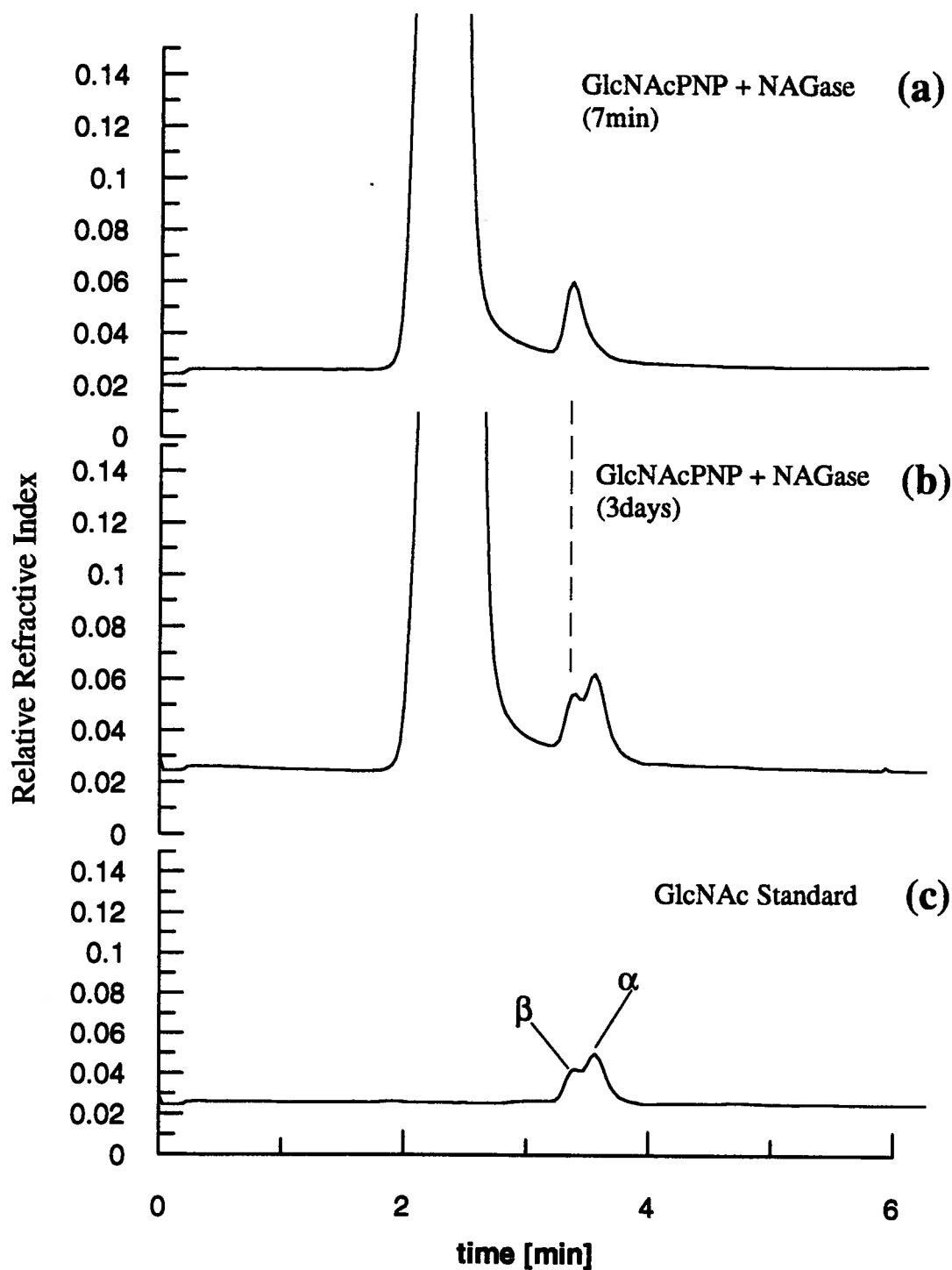
**Figure 4.3.** Determination of the stereochemistry of J-NAGase-catalyzed hydrolysis of βGlcNAcPNP.

Shown are the HPLC chromatograms obtained using a DextroPak® column (Waters®) and the indicated samples. The eluant was 100% $H_2O$. The initial (off-scale) peak in panels (a) and (b) represents the elution of the enzyme reaction buffer. The GlcNAc standard (panel c) was an equilibrium α/β mixture: the β-anomer eluted as a shoulder peak (with a retention time of 3.38 min) immediately before the α-anomer peak (with a retention time of 3.55 min).

### 4.3.3. NAGlucal as an inhibitor of NAGase.

*a. Tests for irreversible inhibition (inactivation).*

NAGlucal was examined as a potential inactivator of NAGase by incubating each of the enzymes under study with 10 m$M$ NAGlucal and the appropriate reaction buffer for 16 hours at 25 °C (see Materials and Methods). At various time intervals small aliquots were removed and residual enzyme activity was assayed using the substrate βGlcNAcPNP. No time-dependent inactivation of any of the NAGases under study was detected during these tests when compared with parallel control reactions.

*b. Tests for reversible inhibition.*

NAGlucal was then examined as a reversible inhibitor of J-NAGase-catalyzed hydrolysis of βGlcNAcPNP. The initial rates obtained at each concentration of substrate and inhibitor were fitted to equations describing different types of inhibition, using the computer program GraFit™ (Leatherbarrow, 1990). The best fit of the data was to the equation describing competitive inhibition, which yielded a value of $K_i = 29 \pm 2$ $\mu M$. A double-reciprocal plot of this data illustrates the competitive nature of the inhibition (Fig. 4.4a), and a replot of the $K_{m,app}$ values obtained at each inhibitor concentration (Fig. 4.4b) yielded an estimate of $K_i$ that was clearly in the same range as that obtained using numerical methods.

NAGlucal was then examined as a reversible inhibitor of each of the other two NAGases under study. In these cases, approximate values of $K_i$ ($RF$ $K_i$) were derived from Dixon plots of data obtained using different concentrations of NAGlucal and a fixed concentration of the substrate. The $RF$ $K_i$ values obtained for K-NAGase and H-NAGase were ~25 and ~8.5 $\mu M$, respectively. Thus in each case, the binding of NAGlucal to the NAGases under study was of high affinity, about 170-fold better than that of GlcNAc itself ($K_i = 5$ m$M$ for J-NAGase; Li & Li, 1970).
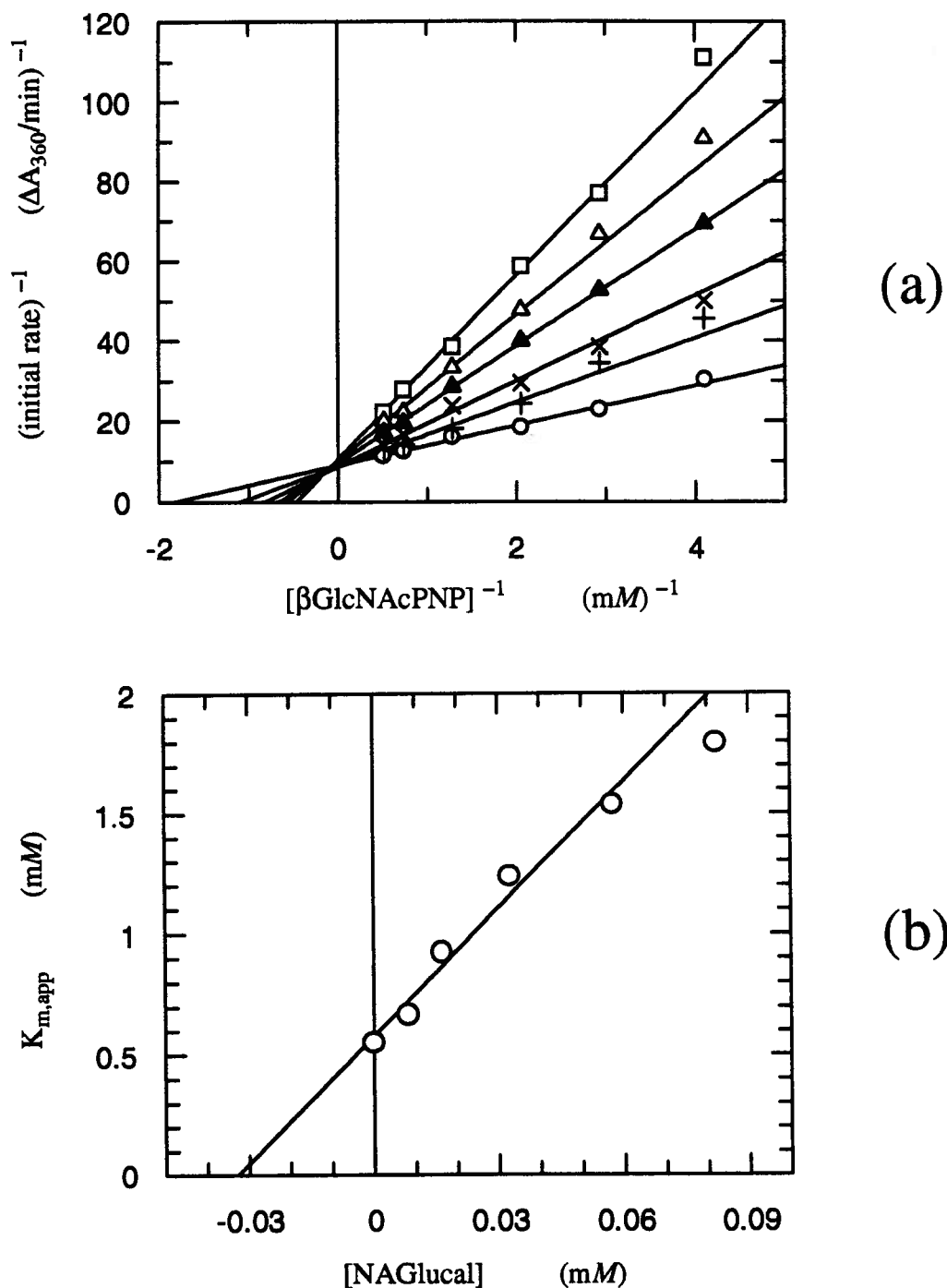
**Figure 4.4.** Determination of kinetic parameters for the inhibition of J-NAGase by NAGlucal.

(a) Determination of $K_{m,app}$ for the inhibition by NAGlucal of J-NAGase-catalyzed hydrolysis of βGlcNAcPNP. Reactions were performed as described in Fig. 4.2 except as noted. The concentrations of NAGlucal in the reactions were 0 {o}, 8.2 {+}, 16.4 {×}, 32.8 {▲}, 57.5 {△}, and 82.1 {□} μM.

(b) A graphical method—involving replotting data obtained from panel (a)—which allows the reader to estimate the value of the $K_i$ by visual inspection.
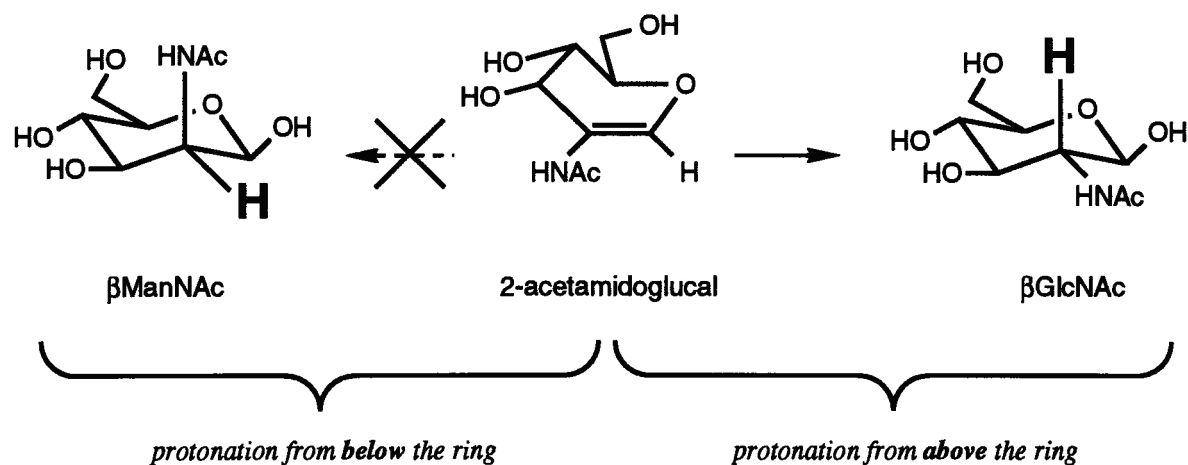
Scheme 4.2. The stereochemistry of the hydration of NAGlucal by NAGase.

### 4.3.4. NAGlucal as a substrate of NAGase.

*a. Preliminary TLC evidence.*

NAGlucal was not only found to be a good inhibitor of NAGase; preliminary TLC analysis using AgNO₃/NaOH for detection (Hough & Jones, 1962) indicated that NAGlucal was also hydrated by the enzyme. Control incubations of NAGlucal in buffer solution alone (i.e., without NAGase) showed no decomposition, even after extended incubation (3 days). Analysis of aliquots taken from the enzyme-catalyzed reaction mixture revealed that the NAGlucal spot decreased as the reaction progressed, while a product spot increased. This product spot co-migrated with GlcNAc and ManNAc standards.

*b. HPLC analysis of the stereochemistry of the hydration reaction.*

The hydration of NAGlucal should yield one of two possible products, depending on the stereochemistry of protonation of the double bond. If protonation of the double bond is from *below* the sugar ring, *N*-acetylmannosamine (ManNAc) should be formed, whereas if protonation of the double bond is from *above* the sugar ring, *N*-acetylglucosamine (GlcNAc) should be formed (see Scheme 4.2). Identification of the product was therefore important. The isomers GlcNAc and ManNAc could not be resolved by HPLC using a
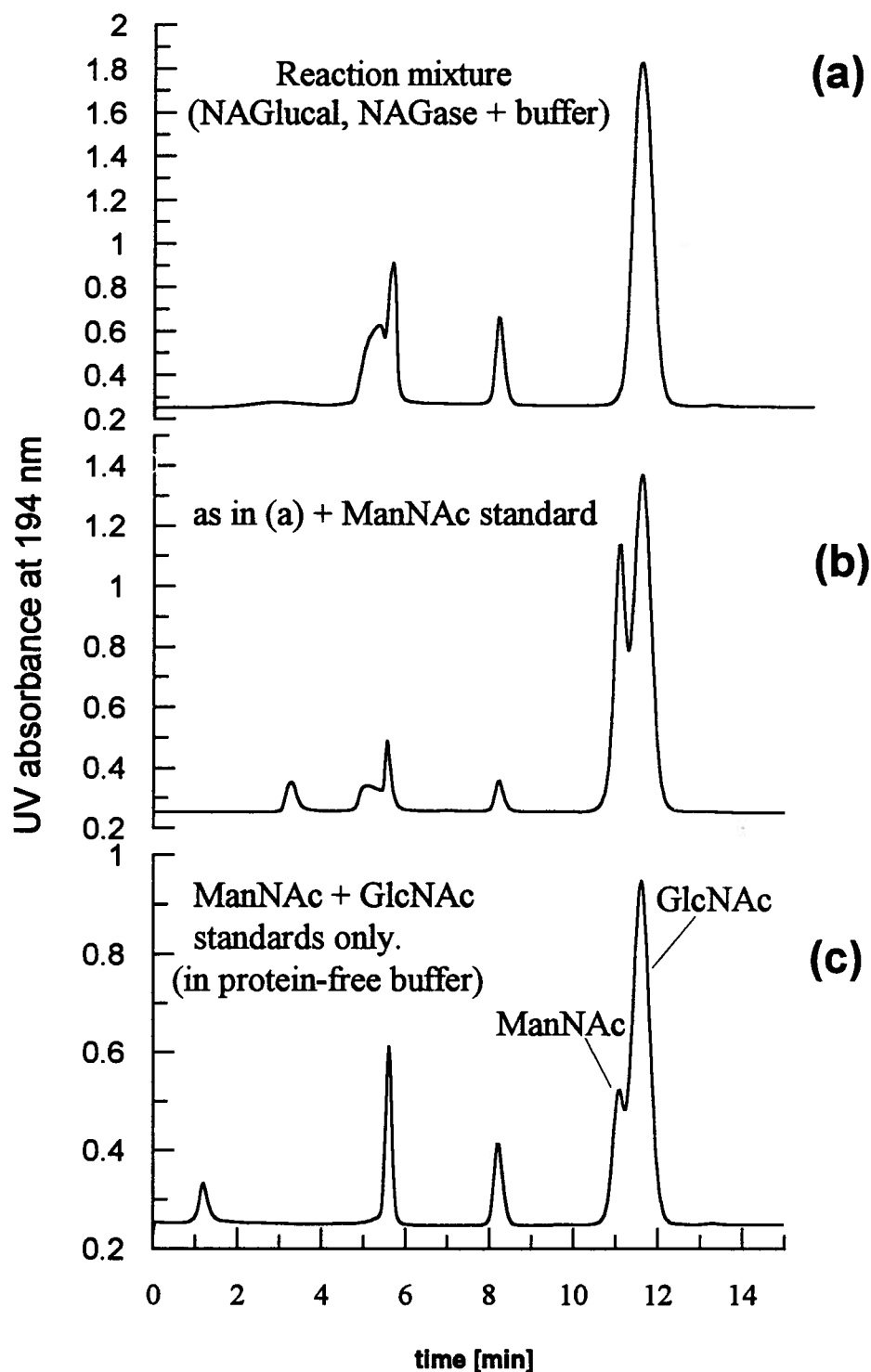
**Figure 4.5.** HPLC determination of the stereochemistry of J-NAGase-catalyzed hydration of NAGlucal.

Shown are the HPLC chromatograms obtained using an Aminex® HPX-87H column (Bio-Rad®). The eluant was 13 m*M* H₂SO₄. Peaks with retention times < 10 min represent the elution of components other than the product of the enzyme reaction (e.g., buffer, BSA, or NAGase). The ManNAc and GlcNAc standards eluted with retention times of 11.0 and 11.5 min, respectively, when 13 m*M* H₂SO₄ was used as the eluant.

DextroPak® column, as both compounds eluted as a doublet (i.e., an α/β equilibrium mixture) with the same retention time. However, an Aminex® HPX-87H column (Bio-Rad®) was able to separate GlcNAc and ManNAc, although their elution peaks were very close together (Fig. 4.5c). The ManNAc standard eluted from this column before the GlcNAc standard (with retention times of 11.0 and 11.5 minutes, respectively) when 13 m$M$ $H_2SO_4$ was used as the eluant.

When NAGlucal was incubated with J-NAGase (and the appropriate buffer) for several days, and aliquots of this reaction were analyzed by HPLC, the sole product observed was GlcNAc, which was identified by its elution at the same retention time (11.5 min) as that of an authentic sample (compare Fig. 4.5a and 4.5c). Furthermore, if the reaction product sample was spiked with an authentic ManNAc sample, HPLC analysis showed that the previously observed product peak acquired a prominent, leading shoulder (Fig. 4.5b), and thus ManNAc was *not* the product of the hydration reaction. GlcNAc was also the sole product of the hydration of NAGlucal by K-NAGase or H-NAGase (not shown). These results indicate that NAGase—a β-retaining glycosidase—protonates the double bond of NAGlucal from *above* the ring. In contrast (as described in Chapter 1), all other β-retaining glycosidases studied to date protonate the double bond of their glycal substrates from *below* the ring (Hehre et al., 1977; Legler, 1990).

## c. Determination of $K_m$ and $V_{max}$ for the hydration reaction.

The initial-rate data necessary to calculate $K_m$ and $V_{max}$ for the hydration of NAGlucal by J-NAGase could be obtained in two possible ways. One way was measurement of the rate of consumption of the substrate (NAGlucal), and the other would involve measurement of the rate of formation of the product (GlcNAc). However, the product of the hydration reaction does not absorb light very strongly; hence attempts were first made to measure the rate of consumption of the substrate by measuring the decrease in absorbance of 220-nm UV light. This wavelength was chosen after the absorption spectra were taken and the extinction coefficients calculated for NAGlucal and GlcNAc ($\lambda_{max}$ = 220 nm; $\varepsilon_{220}$ = 5.36 and 0.17 m$M^{-1}$cm$^{-1}$, respectively). However, at a wavelength of 220 nm there was too much interfering absorption from other components in the reaction (the buffer, BSA, and NAGase), and this approach was abandoned.

Several colorimetric methods are available for measuring the concentration of GlcNAc (e.g., Reissig et al., 1955). However, the results of the inhibition studies showed that NAGlucal binds very tightly to NAGase ($K_i = 29 \pm 2$ $\mu M$ for J-NAGase). Thus in order to determine the kinetic parameters $K_m$ and $V_{max}$ for the reaction, initial rates (i.e., with < 10% consumption of the substrate) of enzyme-catalyzed hydration had to be measured with substrate concentrations in the range of 10 to 100 $\mu M$. This meant that the concentration of GlcNAc formed would be in the 1 to 10 $\mu M$ range, concentrations well below the detection limits of most colorimetric methods. Another difficulty with existing colorimetric methods is that NAGlucal was found to react with the reagents used to detect GlcNAc.

As a result of these difficulties neither a cuprimetric method (Hehre et al., 1980), nor the colorimetric methods developed by Park & Johnson (1949) and Reissig et al. (1955) were able to accurately measure GlcNAc concentration with the required sensitivity. The same sensitivity problem was encountered in attempts to silylate the components of the stopped kinetic reactions, and then analyze them by gas chromatography using the procedure of Sweeley et al. (1963).

HPLC (with an Aminex® HPX-87H column) was eventually used to measure the concentration of GlcNAc. The instrumentation used was unable to accurately quantitate GlcNAc in the 1 to 10 $\mu M$ range. To overcome this difficulty the assay volume was scaled-up 10-fold, from 0.100 to 1.00 mL. These 1.00-mL reactions contained 20 to 200 $\mu M$ NAGlucal, citrate buffer (pH 5.0), and J-NAGase, and were incubated at 25 °C. Reactions were stopped by boiling for exactly 30 seconds, a procedure which was found to irreversibly denature the enzyme, but which did not result in significant decomposition of other components of the reaction. Water was removed by lyophilization, the residue remaining in each reaction tube was resuspended with 0.100 mL of double-deionized $H_2O$, and then 0.080 mL of each reaction was analyzed by HPLC. The lyophilization step effectively concentrated the GlcNAc 10-fold, and this permitted the quantitation of the reaction product by HPLC. The area of the GlcNAc peak was determined, and then corrected by subtracting the area of the GlcNAc peak in appropriate controls (reactions with the same concentrations of NAGlucal but without enzyme).
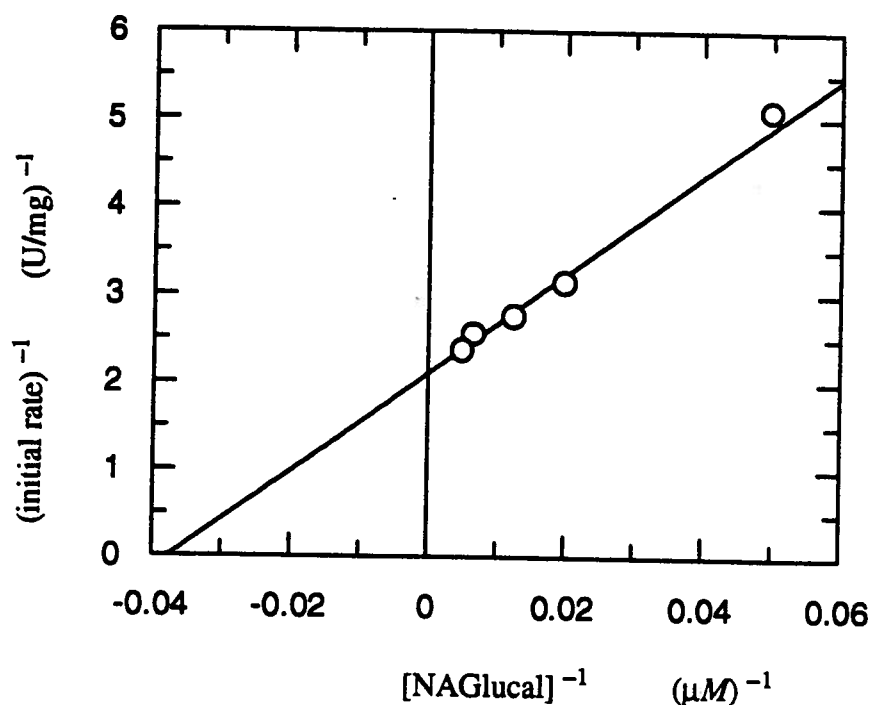
**Figure 4.6.** Determination of $K_m$ and $V_{max}$ for J-NAGase-catalyzed hydration of NAGlucal.

Reactions were performed at pH 5.0 and 25 °C in 5 m$M$ citrate buffer containing 0.01% BSA and 2.0 μg/mL of β-$N$-acetylhexosaminidase from jack beans. The concentration of NAGlucal in the reactions was 21, 50, 80, 150, and 200 μ$M$.

Fig. 4.6 shows the Lineweaver-Burk plot for the enzyme-catalyzed hydration of NAGlucal by J-NAGase. A $K_m$ of 27 ± 3 μ$M$ and a $V_{max}$ of 0.48 ± 0.01 U/mg were obtained by fitting the data to the nonlinear form of the Michaelis-Menten equation using the computer program GraFit™ (Leatherbarrow, 1990) (see Table 4.1). The $K_m$ for the J-NAGase-catalyzed hydration of NAGlucal (27 μ$M$) was in good agreement with the $K_i$ of 29 μ$M$ obtained for the inhibition of the enzyme by this compound.

The $K_m$ for the J-NAGase-catalyzed hydrolysis of βGlcNAcPNP (620 μ$M$; see Table 4.1) indicates that the affinity of NAGlucal for J-NAGase is about 20-fold greater than the affinity of βGlcNAcPNP for the enzyme. However, J-NAGase hydrated NAGlucal about 100-fold more slowly than the enzyme hydrolyzed βGlcNAcPNP (Table 4.1). Hence the overall substrate efficiency, $V_{max}/K_m$, for NAGlucal is about 4.5-fold

lower than that of βGlcNAcPNP. The kinetic parameters for the substrate activities of NAGlucal and βGlcNAcPNP with J-NAGase are summarized in Table 4.1. For comparison, the corresponding values for D-glucal and βGlcPNP with *Agrobacterium* β-glucosidase (pABG5) are also listed.

In contrast, *Agrobacterium* β-glucosidase binds D-glucal 10-fold less strongly and hydrates this compound about 4,400-fold more slowly than it binds to and hydrolyzes βGlcPNP. This means that D-glucal is about 48,000-fold less efficient as a substrate for pABG5 than βGlcPNP (based on their $V_{max}/K_m$ values). Clearly D-glucal, which lacks the C-2 hydroxyl group found on glycosides such as βGlcPNP, is a much poorer substrate for pABG5. Thus, even though NAGlucal was not as efficient a substrate for NAGase as βGlcNAcPNP, the difference between the efficiencies of these two substrates of NAGase was much less than the difference in the efficiencies of D-glucal and βGlcPNP as substrates of β-glucosidase. These results stress the importance of the 2-substituent for interactions in the active sites of glycosylases that are required for efficient catalysis.

**Table 4.1.** Kinetic parameters for glycosylase-catalyzed reactions of glucals and related glucosides.

| Enzyme | Substrate | $V_{max}$ (U/mg) | $K_m$ ($\mu M$) | $V_{max}/K_m$ (U/[mg·μM]) | Reference |
|---|---|---|---|---|---|
| J-NAGase | NAGlucal | $0.48 \pm 0.01$ | $27 \pm 3$ | $0.018 \pm 0.002$ | This work |
| | βGlcNAcPNP | $50 \pm 1$ | $620 \pm 40$ | $0.081 \pm 0.005$ | *ibid.* |
| *Agrobacterium* | D-glucal | 0.046 | 850 | $5.4 \times 10^{-5}$ | Street (1988) |
| β-glucosidase | βGlcPNP | 200 | 78 | 2.6 | Kempton & |
| (pABG5) | | | | | Withers (1992) |

**4.3.5. Kinetic studies with other glucal derivatives and glycosides.**

*a. Studies with D-glucal.*

A substrate test showed that J-NAGase did not hydrate D-glucal. A reversible inhibition test showed that D-glucal binds to J-NAGase very poorly, with an $RF\ K_i$ of 39 m$M$ (see Fig. 4.7). The affinity of J-NAGase for D-glucal is therefore 1,300-fold less than the affinity of the enzyme for NAGlucal ($K_i = 29$ $\mu M$).
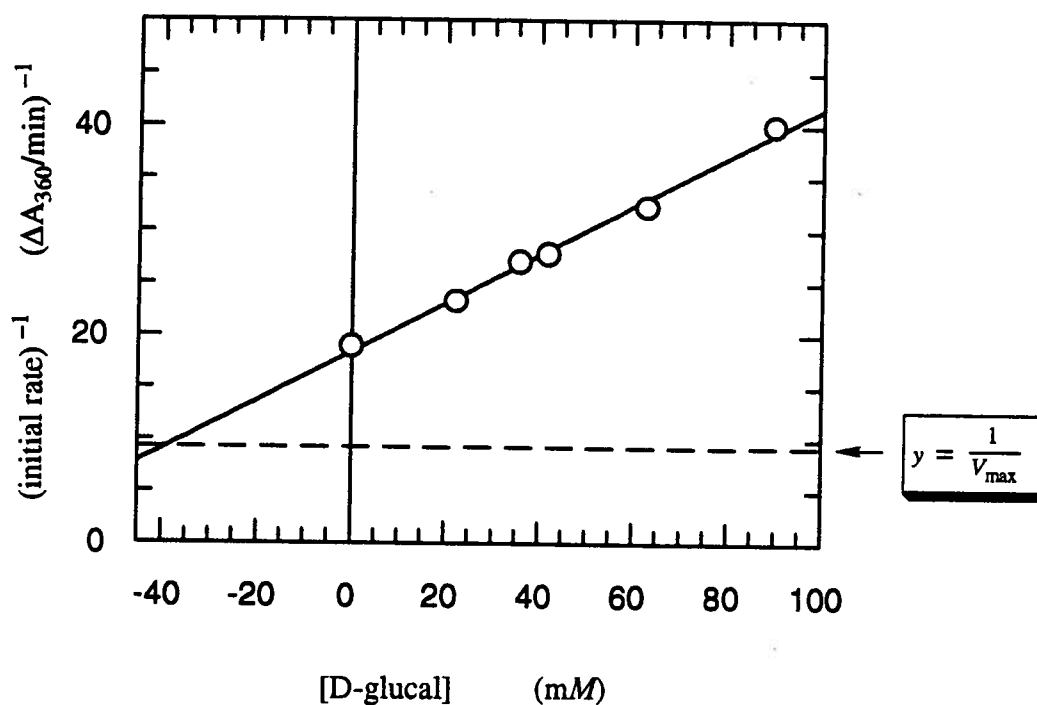
**Figure 4.7.** Estimation of the $K_i$ for the inhibition of J-NAGase by D-glucal.

---

Reactions were performed at pH 5.0 and 25 °C in 50 m$M$ citrate buffer containing 0.1% BSA and 1.0 μg/mL of β-$N$-acetylhexosaminidase from jack beans. The concentration of βGlcNAcPNP in the reactions was 0.58 m$M$. The concentrations of D-glucal in the reactions were 0, 22, 36, 42, 63, and 90 m$M$.

---

The 1,300-fold difference in the inhibition constants corresponds to a difference in binding energy[†] of 17.8 kJ/mol (or 4.2 kcal/mol) at 25 °C. This result, together with the results of the inhibition and substrate tests of NAGlucal, confirms the importance of the noncovalent interactions between the 2-acetamido group and the enzyme's active site. Indeed these interactions are likely much greater at the transition state, and would account for the relatively high rate of hydration of NAGlucal, and the lack of reaction with D-glucal.

---

[†] The free-energy difference, $\Delta\Delta G°$, is calculated from the expression $\Delta\Delta G° = RT\{\ln(K_{i,2}/K_{i,1})\}$, where $K_{i,2}$ and $K_{i,1}$ are the inhibition constants for the two inhibitors being compared, R is the gas constant, and T is the absolute temperature.

*b. Studies with 2-cyanoglucal.*

The results of the inhibition studies of J-NAGase using NAGlucal and D-glucal showed that *removing* the 2-acetamido group drastically reduced the affinity of the enzyme for the compound. It was therefore of interest to study the effect of *replacing* the 2-acetamido group with another C-2 substituent—in this case, the cyano group—to see if this resulted in improved binding in the enzyme's active site compared with D-glucal. 2-Cyanoglucal is also an α,β-unsaturated glucal, and thus it might act as a Michael acceptor for an active-site nucleophile and covalently inactivate NAGase.

2-Cyanoglucal was examined as a potential inactivator of NAGase by incubating each of the enzymes under study with 33 m$M$ 2-cyanoglucal and the appropriate reaction buffer for 17 hours at 25 °C (see Materials and Methods). At various time intervals small aliquots were removed and residual enzyme activity was assayed using the substrate βGlcNAcPNP. No time-dependent inactivation of any of the NAGases under study was detected during these tests when compared with parallel control reactions.

A reversible inhibition test showed that 2-cyanoglucal binds to J-NAGase very poorly, with a $K_i$ of ~57 m$M$, i.e., even worse binding than D-glucal ($K_i$ ~ 39 m$M$). Despite the fact that NAGlucal and 2-cyanoglucal both have a substituent at C-2, there is clearly a profound difference in the ability of the enzyme to accept these substituents. Either there is some steric repulsion (due to the linear geometry of the nitrile), or more likely, the nitrile is incapable of the hydrogen bonding that the $N$-acetyl group of NAGlucal exploits when it binds in the active site.

The configuration of the 2-acetamido substituent is also very important. Li & Li (1970) reported that ManNAc at concentrations up to 10 m$M$ does not inhibit J-NAGase. Furthermore, although $N$-acetyldeoxynojirimycin (4.1) acts as a potent competitive inhibitor of J-NAGase (with a $K_i$ = 0.23 μ$M$), the mannosamine analogue (4.2) of $N$-acetyldeoxynojirimycin does not act as a NAGase inhibitor (Fleet et al., 1986). These results show that NAGase binds very poorly to sugars if the 2-acetamido group is in the axial position, presumably because of repulsive steric interactions and/or the absence of hydrogen bonding.

**[4.1]**

**[4.2]**
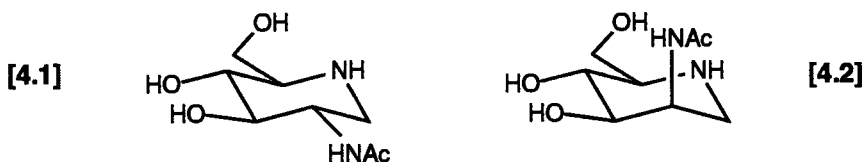
*c. Studies with 2FβGlcDNP and βGlcDNP.*

2FβGlcDNP inactivates β-retaining glucosidases very rapidly, and it does so by forming a 2-deoxy-2-fluoroglucosyl–enzyme intermediate whose rate of deglycosylation is extremely low (Withers et al., 1988). The stereochemical analysis of the hydrolysis of βGlcNAcPNP showed that J-NAGase is a β-retaining enzyme with a catalytic mechanism that is similar to that of a β-retaining glucosidase. Hence it was possible that 2FβGlcDNP might also act as an inactivator of NAGase, even though NAGase has very little affinity for sugars without a 2-acetamido group. The fluorine atom at C-2 in 2FβGlcDNP could possibly act as a hydrogen bond acceptor, thereby increasing the affinity of the enzyme for this compound, and the excellent leaving group could drive the glycosylation step.

2FβGlcDNP was examined as a potential inactivator of J-NAGase or K-NAGase by incubating either of these enzymes with 3 m$M$ 2FβGlcDNP and the appropriate reaction buffer for 48 hours at 25 °C (see Materials and Methods). At various time intervals small aliquots were removed and residual enzyme activity was assayed using the substrate βGlcNAcPNP. No time-dependent inactivation of any of the NAGases under study was detected during these tests when compared with parallel control reactions.

A substrate test was also performed with βGlcDNP and J-NAGase. Rates of βGlcDNP hydrolysis were determined using an assay that was similar to the one used for βGlcPNP. In both of these assays the reaction was monitored at 400 nm (whereas for βGlcNAcPNP the reaction was monitored at 360 nm), and the product formed during the reaction was quantitated spectrophotometrically (see Materials and Methods).

The results of the substrate test with βGlcDNP and J-NAGase showed that there was a very small amount of an unknown contaminant in the βGlcDNP preparation that appeared to act as a substrate of J-NAGase, but that βGlcDNP itself did not. Thus when βGlcDNP (6.5 and 1.5 m$M$ were tested) was incubated at 25 °C in a 0.200-mL reaction containing 50 m$M$ citrate (pH 5.0) and 6 μg of J-NAGase, there was a burst of product (DNP) formation, but the reaction rate decreased over time and eventually equaled the spontaneous (nonenzymatic) rate after 90 minutes. The amount of this contaminant "substrate" was estimated (from the initial burst of product formation) to be about 0.4% of the βGlcDNP used in the assay. After this burst of product formation had ended (i.e., about 90 min after the start of the assay), the addition of more J-NAGase

(6 μg) to the assay did not result in any additional product formation, despite the fact that over 99% of the initial

amount of βGlcDNP in the assay was still present. Only spontaneous (nonenzymatic) hydrolysis was observed

when more enzyme was added after the contaminant "substrate" had been consumed during the initial burst of

DNP formation.

βGlcDNP itself, then, did not act as a substrate for J-NAGase. The absence of hydrolytic activity by

J-NAGase towards βGlcDNP suggests that the failure of 2FβGlcDNP to inactivate NAGase was probably

attributable to an extremely low rate of cleavage of the glycosidic bond.

### 4.3.6. Substrate-enzyme interactions and the mechanism of NAGase-catalyzed reactions.

Each of the NAGases under study catalyzed the hydrolysis of βGlcNAcPNP with net retention of

anomeric configuration. This suggests that all three enzymes operate through a double-displacement mechanism

in which an $N$-acetylglucosaminyl-enzyme intermediate is formed and then hydrolysed. This mechanism was

originally proposed by Koshland (1953), and has subsequently received considerable experimental support

(reviewed in Sinnott, 1990).

The binding of NAGlucal to each NAGase was shown to be of high affinity, about 170-fold better than

that of GlcNAc itself ($K_i$ = 5 m$M$ for jack bean NAGase; Li & Li, 1970), which is particularly noteworthy given

the absence of an anomeric hydroxyl group on NAGlucal. There are two possible explanations for this tight

binding. It could genuinely be a case of tight binding, i.e., due to a resemblance of NAGlucal, with its planar

geometry around C-1, to the structure of an oxocarbonium ion-like transition state. Alternatively, the tight

binding could be a consequence of the accumulation of an $N$-acetylglucosaminyl-enzyme intermediate during

the hydration reaction, comparable to that which occurs during the inhibition of $E.$ $coli$ β-galactosidase by

D-galactal (Wentworth & Wolfenden, 1974), or the inhibition of $Aspergillus$ $wentii$ β-glucosidase by D-glucal

(Legler et al., 1979).
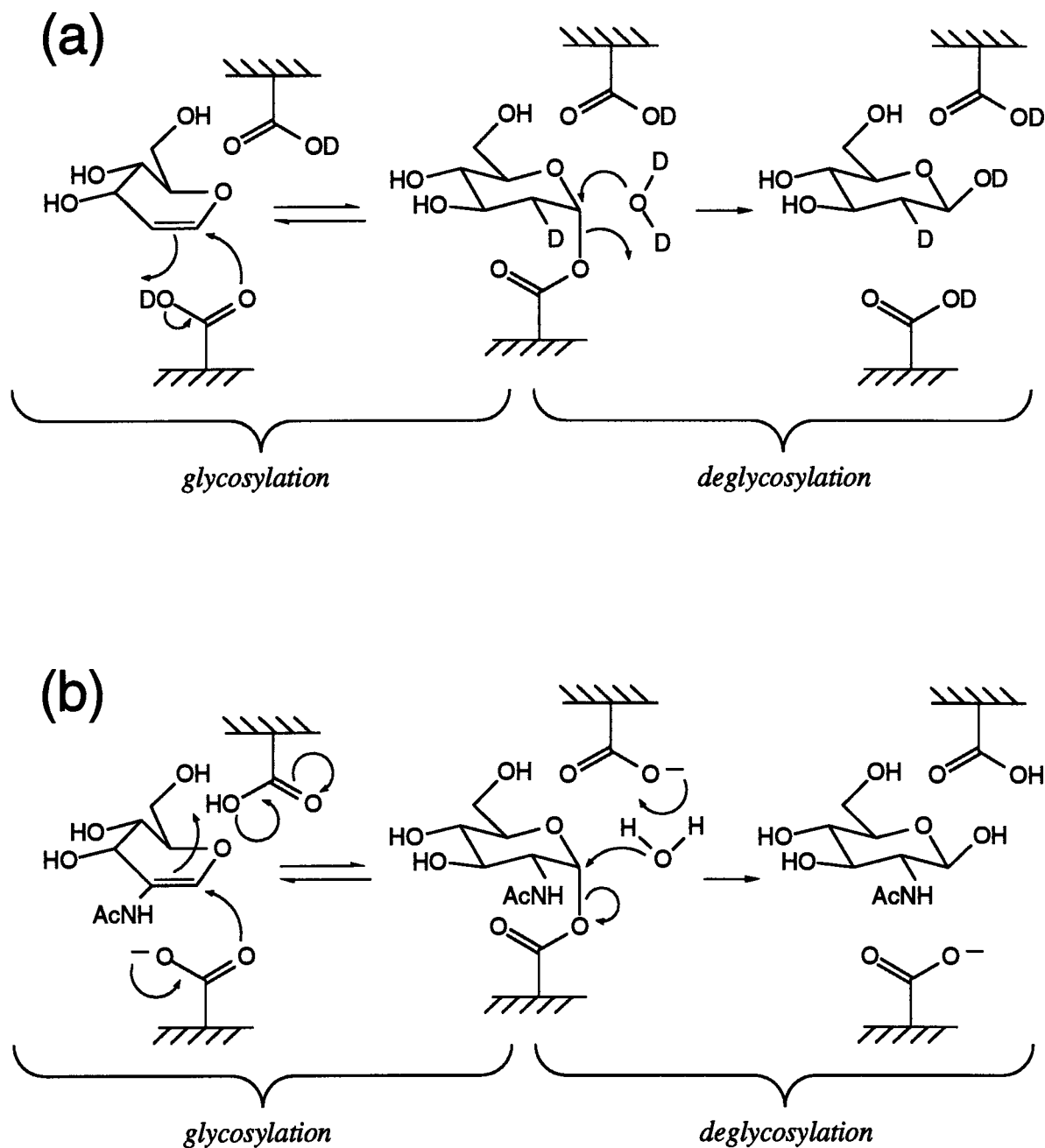
**Scheme 4.3.** Comparison of the proposed mechanisms of β-glucosidase and β-*N*-acetylhexosaminidase.

(a) β-Glucosidase-catalyzed hydration of D-glucal in D2O.
(b) β-*N*-Acetylhexosaminidase-catalyzed hydration of NAGlucal.

The latter hypothesis is unlikely given that the deglycosylation step for the reaction of NAGlucal is identical to that for the hydrolysis of βGlcNAcPNP (as both steps involve the hydrolysis of an $N$-acetylglucosaminyl-enzyme intermediate). The $V_{max}$ value for βGlcNAcPNP hydrolysis catalyzed by jack bean NAGase (50 µmol/min/mg) therefore represents a *minimum* estimate of the rate of the deglycosylation step. Since the $V_{max}$ value for NAGlucal hydration catalyzed by jack bean NAGase was only 0.48 µmol/min/mg, the second step cannot be rate-limiting for NAGlucal, and the value observed likely reflects the rate of formation of the intermediate.

The tight binding observed is therefore a genuine case of a high-affinity interaction, and is most likely a consequence of some critical structural features of the inhibitor resembling those of the transition state, and the consequent exploitation of transition-state binding interactions. Such tight, reversible binding of a glycal to a glycosidase has never been observed previously, presumably because in all cases examined the key 2-hydroxyl substituent was necessarily missing. In fact, glycals typically bind 10 to 100-fold worse to glycosidases than do the corresponding glycosides (Legler, 1990). Comparable behaviour was observed with D-glucal (which lacks the 2-acetamido substituent of NAGlucal) and jack bean NAGase. The binding of D-glucal to jack bean NAGase was about 8-fold worse than that of GlcNAc (Li & Li, 1970), and 1300-fold worse than that of NAGlucal.

The 1300-fold greater binding affinity of NAGlucal compared with D-glucal establishes the contribution of the 2-acetamido functionality to the binding affinity of NAGlucal as 4.2 kcal/mol, and in turn establishes, to at least some extent, the contribution of this substituent to transition-state stabilization in the normal reaction. NAGlucal is, at best, an imperfect transition-state analogue, given the absence of an anomeric oxygen atom and the imposed planarity around (O-5, C-1, C-2, and C-3) rather than (C-5, O-5, C-1, and C-2). The value of 4.2 kcal/mol therefore represents a *minimum* estimate of the contribution of the 2-acetamido group to transition-state stabilization, as indeed is reflected in the complete absence of reaction of the enzyme with D-glucal or βGlcDNP, despite the superiority of the leaving group in the latter substrate.

The stereochemistry of NAGase-catalyzed proton donation to C-2 of NAGlucal is without precedent in previous studies of 'retaining' β-glycosidases. Previously these enzymes have only been shown to effect proton

donation to glycals from the bottom face, most likely through the concerted process shown in Scheme 4.3a (Legler, 1990). In the absence of other constraints, this more commonly observed stereochemistry is presumably a consequence of the known preference for the reaction of acetals via oxocarbonium ion-like transition states to occur in a pre-associative process (Banait & Jencks, 1991). Such pre-association is most readily achieved in the concerted process shown in Scheme 4.3a. Furthermore, with unsubstituted glycals the intermediate formed involves a 2-deoxy sugar, thus the correct stereochemical orientation of a bulky substituent at C-2 is not a consideration. However, if proton donation came from the bottom face during the catalytic hydration of NAGlucal, it would result in the formation of an $N$-acetylmannosaminyl-enzyme intermediate in which the bulky C-2 substituent assumes the enzymatically unfavourable axial position. By contrast, protonation of NAGlucal at C-2 from the top face generates an $N$-acetylglucosaminyl-enzyme intermediate in which normal transition-state binding interactions with the equatorial 2-acetamido group can be exploited to assist the formation and subsequent hydrolysis of this intermediate (Scheme 4.3b). NAGase-catalyzed protonation of NAGlucal from the top face, as observed, is therefore quite reasonable and reflects both the constraints and benefits of having the correct substituent at C-2.

## *4.4. CONCLUSIONS.*

The direct colorimetric assay measuring the absorbance of 360-nm light proved to be a reliable, convenient method for assaying the hydrolysis of βGlcNAcPNP by NAGase. HPLC was used to determine the stereochemical outcome of this reaction for all three NAGases studied, all of which were found to be β-retaining enzymes that yielded βGlcNAc as the initial product of the hydrolysis reaction.

NAGlucal was found to be a reasonably good substrate for J-NAGase, with a $K_m = 27 \pm 3 \ \mu M$ and a $V_{max} = 0.48 \pm 0.01$ U/mg. Indeed, all three NAGases studied catalyzed the hydration of NAGlucal to form GlcNAc—not ManNAc—which indicated that the double bond was protonated from above the plane of the sugar ring. This is the first time that a β-retaining glycosidase has been shown to protonate an endocyclic double bond from the "correct" face. These results demonstrate firstly that the "incorrect" protonation observed

in other cases is the consequence of an alternative pathway adopted in the absence of the C-2 substituent, and secondly that protonation of glycals from the "correct" face is indeed possible.

Kinetic parameters for the NAGase-catalyzed hydration of NAGlucal, D-glucal, and various other glucal derivatives and glycosides were determined (see Table 4.2), and a comparison of the values of these parameters showed that the 2-acetamido group is extremely important for binding of NAGlucal by the enzyme. The relatively tight, reversible binding of NAGlucal suggests that glycals may indeed be regarded as transition-state analogues for glycosidases, but that the relatively low affinities generally observed are a consequence of their lack of the critical 2-substituent.

## 4.5. SUGGESTIONS FOR FUTURE WORK.

Bernacki et al. (1985) carried out studies using mice that showed that NAGlucal has promise as an antitumor and antimetastatic agent, and that these properties of the compound are attributable to its ability to act as an inhibitor of NAGase. A particularly noteworthy property of NAGlucal is its lack of cytotoxicity towards normal cells, a property that is very desirable for a chemotherapeutic agent (Bernacki et al., 1985).

The research described herein showed that NAGlucal has a low $K_i$ for human placental NAGase, and hence that it might be worthwhile to investigate the effect of this compound on the growth and spread of various types of human tumors *in vitro*. In addition, it might well be worth investigating analogues of NAGlucal that are substituted with a sugar at C-1; such compounds could have considerably higher affinity and specificity for NAGase.

At a more fundamental level, no mechanism-based inactivators of NAGase have been discovered. The synthesis and kinetic analysis of potential mechanism-based inactivators of $\beta$-$N$-acetylhexosaminidase would be very desirable, not only for possible practical applications, but also to provide more insights into the catalytic mechanism of this clinically important enzyme.

Table 4.2. Summary of kinetic data obtained using various β-N-acetylhexosaminidases.

| Parameter or compound | Structure | J-NAGase (jack bean) | K-NAGase (bovine kidney) | H-NAGase (human placenta) |
|---|---|---|---|---|
| Temperature (°C) | | 25 | 25 | 25 |
| pH | | 5.0 | 4.25 | 4.25 |
| βGlcNAcPNP | A | $K_m = 620 \pm 40\ \mu M$ $V_{max} = 50 \pm 1$ U/mg | $K_m = 1100 \pm 100\ \mu M$ $V_{max} = 24 \pm 2$ U/mg | $K_m = 580 \pm 60\ \mu M$ $V_{max} = 8.0 \pm 0.4$ U/mg |
| Stereochemistry | | β-retaining | β-retaining | β-retaining |
| NAGlucal | B $R_3 = NHAc$ $R_4 = H$ | $K_i = 29 \pm 2\ \mu M$ $K_m = 27 \pm 3\ \mu M$ $V_{max} = 0.48 \pm 0.01$ U/mg | $K_i \sim 25\ \mu M$ | $K_i \sim 8.5\ \mu M$ |
| Product from NAGlucal | | GlcNAc | GlcNAc | GlcNAc |
| D-glucal | B $R_3 = H$ $R_4 = H$ | $K_i \sim 39$ m$M$ | | |
| 2-cyanoglucal | B $R_3 = CN$ $R_4 = H$ | $K_i \sim 57$ m$M$ | not an inactivator | not an inactivator |
| 2FβGlcDNP | C $R_1 = F$ | not an inactivator | not an inactivator | |
| βGlcDNP | C $R_1 = OH$ | not a substrate | | |



A                              B                              C
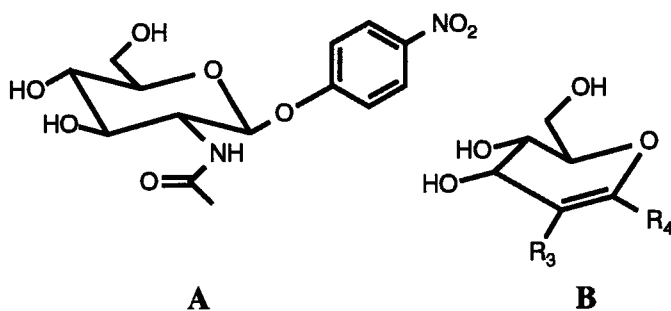
## CHAPTER 5: MATERIALS AND METHODS

*5.1. ORGANIC SYNTHESIS.*

### 5.1.1. Materials and routine experimental procedures.

*a. Analytical methods.*

Melting points (mp) were determined on a Laboratory Devices Mel-Temp II melting-point apparatus. Melting points were uncorrected.

$^1H$ Nuclear magnetic resonance (NMR) spectra were recorded on the following instruments at the indicated field strengths: a Brüker AC-200 at 200 MHz, a Varian XL-300 at 300 MHz, or a Brüker WH-400 at 400 MHz. When possible, tetramethylsilane (TMS) was used as an external reference ($\delta$ = 0.00 ppm). Spectra obtained in $D_2O$ were referenced externally to 2,2-dimethyl-2-silapentane-5-sulfonate ($\delta$ = 0.00 ppm). All chemical shifts were reported using the $\delta$ scale.

$^{19}F$ NMR spectra were recorded with proton coupling on a Brüker AC-200 instrument at a field strength of 188 MHz. Chemical shifts were reported using the $\delta$ scale referenced to $CFCl_3$ ($\delta$ = 0.00 ppm), although the external reference used was $CF_3COOH$ ($\delta$ = -76.53 ppm). Signals upfield of $CFCl_3$ were assigned negative values.

$^{13}C$ NMR spectra were recorded with proton decoupling on the following instruments at the indicated field strengths: a Brüker AC-200 at 50 MHz, a Varian XL-300 at 75 MHz, or a Brüker WH-400 at 125.76 MHz. The solvent peak (either $CDCl_3$ or $D_2O$) was used as a reference.

Low resolution electron-ionization mass spectra were recorded on a Kratos MS 50 mass spectrometer operating at 70 eV. Desorption chemical ionization (DCI) mass spectra were recorded on a Delsi Nermag R10-10C mass spectrometer using $NH_3$ as the chemical ionization gas. Fast atom bombardment (FAB) mass spectra were recorded on a AEI-MS 9 mass spectrometer with xenon as the FAB gun, operating at 7-8 kV and 1 mA current.

Microanalyses were performed by Mr. Peter Borda in the Microanalytical Laboratory, Department of Chemistry, at The University of British Columbia, Vancouver, B. C.

*b. Thin-layer chromatography and silica gel column chromatography.*

Thin-layer chromatography (TLC) was performed using analytical plates (silica gel 60 $F_{254}$, Merck). Compounds were visualized under UV light or after charring with 10% $H_2SO_4$ in methanol or iodine vapour.

Column chromatography was performed using Kieselgel 60 (230-400 mesh) silica gel.

*c. Solvents and reagents.*

Solvents and reagents were either reagent, certified, or spectral grade. Dry solvents and reagents were prepared as described below. Dichloromethane was first washed with concentrated sulfuric acid followed by water and sodium bicarbonate, predried over calcium chloride, and finally distilled over calcium hydride. Dimethyl formamide was stirred overnight over magnesium sulfate, then distilled under reduced pressure onto 4-Å molecular sieves. Diethyl ether and tetrahydrofuran were distilled over sodium metal and benzophenone. Methanol was distilled from magnesium methoxide (formed *in situ* by reaction of methanol with magnesium turnings in the presence of a catalytic amount of iodine). Pyridine was predried for several days by standing over pellets of NaOH, and then distilled over calcium hydride. Toluene was distilled over calcium hydride.

*d. Compounds synthesized and generously provided by colleagues.*

Some of the compounds used in this work were synthesized and generously provided by colleagues. With the exception of Prof. A. Vasella, all of the people mentioned were coworkers in Professor Withers' laboratory. Prof. A. Vasella of the University of Zurich provided 1-nitroglucal. Dr. Mark Namchuk provided 2FβGlcDNP {2',4'-dinitrophenyl 2-deoxy-2-fluoro-β-D-glucopyranoside} and βGlcDNP {2',4'-dinitrophenyl β-D-glucopyranoside}. Dr. William Stirtan provided 1-(methyl carboxylate)-D-glucal {methyl 2,6-anhydro-3-deoxy-D-*arabino*-hept-2-enolate} as well as sodium 1-(carboxylate)-D-glucal {sodium 2,6-anhydro-3-deoxy-D-*arabino*-hept-2-enolate}. John McCarter provided the peracetylated precursor of 2-acetamidoglucal {1,5-anhydro-2-deoxy-2-(*N*-acetylacetamido)-3,4,6-tri-*O*-acetyl-D-*arabino*-hex-1-enitol}. Ken Mok performed

the photobromination of 2,3,4,6-tetra-$O$-acetyl-$\beta$-D-glucopyranosyl cyanide to give 2,3,4,6-tetra-$O$-acetyl-1-$\alpha$-bromo-$\beta$-D-*gluco*-pyranosyl cyanide.

**5.1.2. Routine synthetic procedures.**

*a. Deacetylation with sodium methoxide in methanol.*

The following procedure was adapted from the work of Zemplen & Pacsu (1929). The acetylated sugar derivative (~1 g) was dissolved in ~50 mL of dry methanol. A catalytic amount of solid sodium methoxide (~1-2 mg per 50 mL) was added, and then the reaction mixture was stirred at room temperature until the reaction was complete. The sodium methoxide was removed by passing the reaction solution through a small column of silica gel. The column eluate was then evaporated to dryness *in vacuo*. The resulting oil was crystallized and then recrystallized from the solvents specified for the individual compounds.

*b. Deacetylation with ammonia-saturated methanol.*

The following procedure was adapted from the work of Fritz et al. (1983). The acetylated glycal (~1 g) was dissolved in ~30 mL of dry methanol. About 10 mL of cold (0 °C), dry MeOH was saturated with $NH_3$ by bubbling, and then the solution was poured into the reaction flask. The mixture was left at room temperature until the reaction was complete, and then the solvent was evaporated *in vacuo*. The resulting residue was crystallized and then recrystallized from the solvents specified for the individual compounds.

*c. Trimethylsilylation.*

The following procedure was adapted from the work of Horton & Priebe (1981). The starting material (~1 g) was dissolved in ~10 mL of dry pyridine and the resulting solution was cooled in an ice bath. Syringes were used to add one equiv. of hexamethyldisilazane ($Me_3SiNHSiMe_3$) and one-half equiv. of trimethylsilyl chloride ($Me_3SiCl$) for every hydroxyl group of the starting material. A white precipitate formed immediately. The ice bath was removed, and then the reaction was stirred at room temperature for ~25 min until the reaction was complete. The contents of the reaction flask were vacuum filtered through Celite in a fine porosity sintered glass funnel. The solvent in the filtrate was evaporated *in vacuo*, and then the resulting oil was purified further

by vacuum distillation. The trimethylsilyl group was not stable enough for the product to be purified by silica gel column chromatography.

*d. Triethylsilylation.*

The following procedure was adapted from the work of RajanBabu & Reddy (1986). The starting material (~0.5 g) was dissolved in ~5 mL of a 1:1 v:v mixture of dry pyridine and dry methylene chloride, and then a small amount of triethylamine (~0.5 mL) was added. Triethylsilyl chloride ($Et_3SiCl$, 1.1 equiv. for every hydroxyl group of the starting material) was added, followed by stirring at room temperature until the reaction was complete, and then pentane, saturated $KH_2PO_4$, and $H_2O$ were added. The product was isolated by repeated extraction into pentane, followed by washing of the combined pentane layer with saturated sodium bicarbonate and then $H_2O$. The pentane layer was dried over $MgSO_4$, and the solvent was evaporated *in vacuo*. The triethylsilyl group was stable enough for the product to be purified by silica gel column chromatography.

*e. Tert-butyldimethylsilylation.*

The following procedure was adapted from the work of Corey & Venkateswarlu (1972). The starting material (~0.4 g) was dissolved in ~10 mL of dry DMF. For every hydroxyl group of the starting material, 1.5-2.0 equiv. of ($t$-butyl)dimethylsilyl chloride (TBDMS chloride) and 2.5 equiv. of imidazole were added. The reaction was stirred at room temperature for 2 hours, a condenser was attached to the flask, and then the mixture was stirred at 45 °C for 10 hours until the reaction was complete. The product was extracted four times into ether, and then the combined ether layer was washed with saturated sodium bicarbonate and then $H_2O$. The ether layer was then dried over $MgSO_4$, and the solvent was evaporated *in vacuo*. The product was purified by silica gel column chromatography.

| [3.3] | | -R | | -R | -Ra | -Rb |
|---|---|---|---|---|---|---|
| | [2.3] | SiMe₃ | [1.2] | H | H | H |
| | [5.1] | SiEt₃ | [2.1] | H | F | F |
| | | | [2.2] | H | F | H |
| | | | [2.4] | SiMe₃ | F | F |
| | | | [2.5] | SiMe₂(t-Bu) | F | F |
| | | | [2.6] | SiMe₂(t-Bu) | F | H |
| | | | [5.2] | SiEt₃ | H | H |

**Figure 5.1.** Structures of $Cp_2TiMe_2$, heptenitol derivatives, and associated synthetic intermediates.

The numbering systems used for D-glucono-1,5-lactone and D-*gluco*-heptenitol derivatives are indicated.

### 5.1.3. Syntheses.

*a. The synthesis of heptenitol and its derivatives.*

**Dimethyltitanocene** ($Cp_2TiMe_2$, **3.3**) (see Claus & Bestian, 1962). Titanocene dichloride (**3.2**, $Cp_2TiCl_2$, obtained from Aldrich Chemical Co.) [1.4 g, 5.6 mmol] was dissolved in ~30 mL of dry ether. A dropping funnel was used to add 8.4 mL of a 1.4 $M$ solution of methyl lithium [2.1 equiv., 12 mmol] dropwise at -20 °C under $N_2$. The reaction mixture was stirred in the dark at -20 °C under $N_2$ for one hour. Ice was then added to quench the reaction, and the resulting solution was extracted three times with ether; during this procedure, the solution was kept < 15 °C and shielded from light. The combined ether layer was dried over $MgSO_4$, and the solvent was evaporated *in vacuo* at low temperature. The resulting bright orange solid [0.95 g, 81%] was dried over $P_2O_5$ in a dessicator *in vacuo* for 2 hours at room temperature to give **3.3** (mp 110-117 °C,

dec), which was stored shielded from light at -20 °C as 9.1 mL of a 0.5 $M$ solution in THF. $^1$H NMR data (300 MHz, THF): δ 5.75 ($s$, 10 H, Cp$_2$); –0.08 ($s$, 6 H, Me$_2$).

**2,3,4,6-Tetra-*O*-(triethylsilyl)-D-glucono-1,5-lactone (5.1)** (see RajanBabu & Reddy, 1986). Glucono-1,5-lactone (**1.15**, Sigma Chemical Co.) [0.50 g, 2.81 mmol] was persilylated as described above using triethyl silyl chloride (Et$_3$SiCl) [2.1 mL, 12 mmol, 4.4 equiv.], 5.6 mL of a 1:1 v:v mixture of dry pyridine and dry methylene chloride, and 0.5 mL of triethylamine. The product was stable enough to be purified by silica gel column chromatography (4:1 hex:CHCl$_3$) to give a colorless oil of **5.1** [1.63 g, 91%]. $^1$H NMR data (300 MHz, CDCl$_3$): δ 4.56 (*ddd*, 1 H, $J_{4,5}$ = 7.6 Hz, $J_{5,6'}$ = 4.2 Hz, $J_{5,6}$ = 2.7 Hz, H-5); 4.12 (*dd*, 1 H, $J_{2,3}$ = 3.6 Hz, $J_{2,4}$ = 0.9 Hz, H-2); 4.00 (*dt*, 1 H, $J_{3,4}$ = $J_{4,5}$ = 7.6 Hz, $J_{2,4}$ = 0.9 Hz, H-4); 3.92-3.86 (*m*, 2 H, H-6, H-3); 3.80 (*dd*, 1 H, $J$ = 10.8, 4.2 Hz, H-6'); 1.02-0.95 (*m*, 36 H, [{C$\underline{H}_3$CH$_2$}$_3$Si-O]$_4$); 0.70-0.58 (*m*, 24 H, [{CH$_3$C$\underline{H}_2$}$_3$Si-O]$_4$). $^{13}$C NMR data (75 MHz, CDCl$_3$): δ 169.9 (C=O); 81.4, 77.2, 73.7, 71.0 (C-2 to C-5); 61.7 (C-6); 6.76, 6.72, 6.67, 6.59 (12 C, [{C$\underline{H}_3$CH$_2$}$_3$Si-O]$_4$); 4.93, 4.58, 4.45 (12 C, [{CH$_3$C$\underline{H}_2$}$_3$Si-O]$_4$).

**2,6-Anhydro-1-deoxy-3,4,5,7-tetra-*O*-(triethylsilyl)-D-*gluco*-hept-1-enitol (5.2)** (see Petasis & Bzowej, 1990). The lactone **5.1** [0.62 g, 0.98 mmol] was dried overnight *in vacuo*. Dry THF [9 mL] was added and then the flask was fitted with a condenser. Cp$_2$TiMe$_2$ (**3.3**, prepared as described above) [2.1 equiv., 2.1 mmol] was added in the dark under N$_2$, and the mixture was refluxed at about 70 °C for 2 days. Heating was stopped, the solution was filtered through a bed of silica (stirred with 1% Et$_3$N in EtOAc), the product was eluted with 5% ether in hexane, and the solvent was evaporated *in vacuo*. The resulting residue was purified twice by column chromatography using 2% ether in hexane as the eluant. The solvent was evaporated *in vacuo* to give an oil [0.52 g, 84%] of **5.2**. $^1$H NMR data (300 MHz, CDCl$_3$): δ 4.38 (*s br*, 1 H, H-1); 4.11 (*ddd*, 1 H, $J_{5,6}$ = 9.0 Hz, $J_{6,7'}$ = 4.8 Hz, $J_{6,7}$ = 1.9 Hz, H-6); 4.02 (*s br*, 1 H, H-1'); 3.98 (*d*, 1 H, $J_{3,4}$ = 3.0 Hz, H-3); 3.85 (*dd*, 1 H, $J_{7,7'}$ = 11.3, $J_{6,7}$ = 2.0 Hz, H-7); 3.76-3.65 (*m*, 3 H, H-7', H-5, H-4); 1.04-0.93 (*m*, 36 H, [{C$\underline{H}_3$CH$_2$}$_3$Si-O]$_4$); 0.70-0.60 (*m*, 24 H, [{CH$_3$C$\underline{H}_2$}$_3$Si-O]$_4$).

**2,6-Anhydro-1-deoxy-D-*gluco*-hept-1-enitol (1.2).** After the heptenitol **5.2** [0.52 g, 0.82 mmol] had been purified by column chromatography it was dried overnight *in vacuo* and then dissolved in 6.6 mL [8 equiv., 6.6 mmol] of a 1 $M$ solution of TBAF in THF and then stirred for ~2 hours at room temperature. The solvent

was evaporated *in vacuo*, and then an excess of the Li$^+$ form of Dowex 50W X2 resin [~5-10 mL of solid

suspended in MeOH] was added to remove the ammonium salt (Bu$_4$N$^+$). The mixture was stirred overnight at

room temperature, and then the resin was filtered and washed with MeOH. The solvent was evaporated *in*

*vacuo*, and then the residue was purified by column chromatography (27:2:1 EtOAc:MeOH:H$_2$O) and

crystallized and recrystallized from MeOH, ether, and EtOAc to give white crystals [0.12 g, 85%] of **1.2** (mp

131-133 °C; mp 95-97 °C when recrystallized from 5:1 EtOAc:MeOH). $^1$H NMR data (400 MHz, D$_2$O): δ

4.78 (t, 1 H, $J_{1,1'}$ = $J_{2,1}$ < 1 Hz, H-1); 4.74 (t, 1 H, $J_{1,1'}$ = $J_{2,1'}$ < 1 Hz, H-1'); 3.95-3.89 (m, 2 H, H-3, H-7); 3.76

(dd, 1 H, $J_{7,7'}$ = 12.5 Hz, $J_{6,7'}$ = 5.3 Hz, H-7'); 3.55 (t, 1 H, $J_{3,4}$ = $J_{4,5}$ = 9.1 Hz, H-4); 3.45 (ddd, 1 H, $J_{5,6}$ = 9.9

Hz, $J_{6,7'}$ = 5.3 Hz, $J_{6,7}$ = 2.1 Hz, H-6); 3.41 (dd, 1 H, $J_{5,6}$ = 9.4 Hz, $J_{4,5}$ = 9.1 Hz, H-5). $^{13}$C NMR data (50

MHz, D$_2$O): δ 159.45 (C-2); 94.95 (C-1); 81.91, 77.45, 71.29, 69.98, 61.45 (C-3 to C-7). DCI MS data: *m/z*

177 (MH$^+$); 194 (M+NH$_4^+$). *Anal.* Calc. for C$_7$H$_{12}$O$_5$ (176.17): C, 47.72; H, 6.87. Found: C, 47.76; H, 6.84.

**2,3,4,6-Tetra-*O*-(trimethylsilyl)-D-glucono-1,5-lactone (2.3)** (see Horton & Priebe, 1981). Glucono-

1,5-lactone (**1.15**, Sigma Chemical Co.) [5.0 g, 28 mmol] was dissolved in 47 mL of dry pyridine and then

persilylated as described above using hexamethyldisilazane [23 mL, 110 mmol, 4 equiv.] and trimethyl silyl

chloride (Me$_3$SiCl) [58 mmol, 2 equiv.]. Vacuum distillation (bp = 128 °C, 0.4 Torr) yielded a colorless oil of

**2.3** [10.7 g, 82%]. $^1$H NMR data (300 MHz, CDCl$_3$): δ 4.18 (dt, 1 H, $J_{5,6}$ = $J_{5,6'}$ = 2.3 Hz, $J_{4,5}$ = 7.5 Hz, H-5);

4.00 (d, 1 H, $J_{2,3}$ = 8 Hz, H-2); 3.91 (t, 1 H, $J_{3,4}$ = $J_{4,5}$ = 7.5 Hz, H-4); 3.82 (dd, 1 H, $J_{5,6}$ = 2.3 Hz, $J_{6,6'}$ = 11

Hz, H-6); 3.78 (dd, 1 H, $J_{5,6'}$ = 2.3 Hz, $J_{6,6'}$ = 11 Hz, H-6'); 3.75 (t, 1 H, $J_{2,3}$ = $J_{3,4}$ = 7.5 Hz, H-3); 0.22, 0.20,

0.19, 0.12 (4 s, 36 H, [{CH$_3$}$_3$Si-O]$_4$). $^{13}$C NMR data (75 MHz, CDCl$_3$): δ 171.02 (C-1); 81.28, 75.77, 73.00,

70.71 (C-2 to C-5); 61.30 (C-6); 0.75, 0.55, 0.44, 0.26 (12 C, [{CH$_3$}$_3$Si-O]$_4$). DCI MS data: *m/z* 467 (MH$^+$).

**2,6-Anhydro-1-deoxy-1,1-difluoro-3,4,5,7-tetra-*O*-(trimethylsilyl)-D-*gluco*-hept-1-enitol (2.4)** (see

Motherwell et al., 1989). Freshly distilled CF$_2$Br$_2$ (obtained from Aldrich Chemical Co.) [4.5 g, 22 mmol, 5

equiv.] was weighed in ~15 mL of dry THF and then added to a dry 3-necked flask. The solution was cooled in

an ice bath, and then (Me$_2$N)$_3$P (obtained from Fluka Chemical Co.) [3.9 mL, 22 mmol, 5 equiv., dissolved in 5

mL of dry THF] was added dropwise from a dropping funnel under N$_2$. A white precipitate formed

immediately. The mixture was stirred at room temperature for 30 min. Freshly activated zinc [1.41 g, 21.5

mmol, 5 equiv.] (Zn was activated with 10% HCl for ~1 min, rinsed 3 times with acetone, 3 times with ether,

and then dried *in vacuo* for ~2 hours) was added, the dried lactone **2.3** [2.0 g, 4.3 mmol, dissolved in ~10 mL of

dry THF] was added by syringe, and then the reaction was stirred for 90 min at 70 °C. Heating was stopped, the

product was extracted three times into ether, and then the combined ether layer was washed with NaCl and $H_2O$.

The ether layer was dried over $MgSO_4$, the solvent was evaporated *in vacuo*, and then the residue was purified
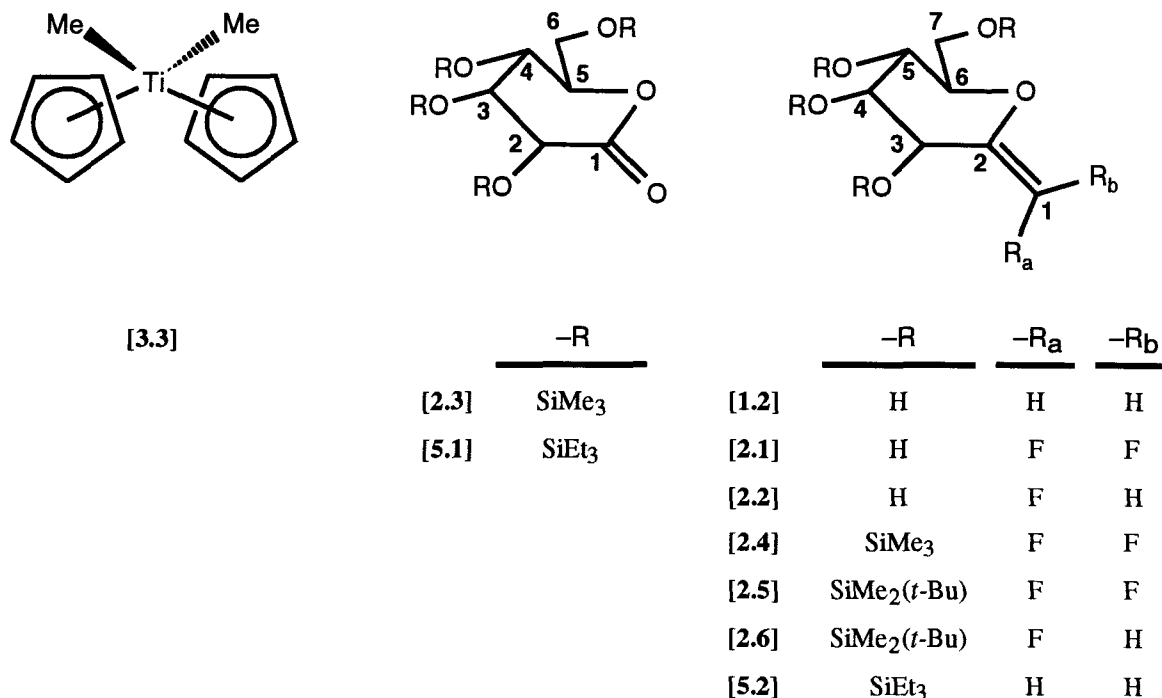
by column chromatography (1:1 $CHCl_3$:hex) to give an oil of **2.4** [0.64 g, 30%]. $^1H$ NMR data (200 MHz,

$CDCl_3$): δ 4.15 ($t$, 1 H, $J_{3,4} = J_{3,F} = 3.6$ Hz, H-3); 3.86 ($m$, 1 H, H-6); 3.82 ($dd$, 1 H, $J_{6,7} = 2$ Hz, $J_{7,7'} = 11.6$

Hz, H-7); 3.74 ($dd$, 1 H, $J_{6,7'} = 4$ Hz, $J_{7,7'} = 11.6$ Hz, H-7'); 3.70-3.65 ($m$, 2 H, H-4, H-5); 0.14 ($s$, 27 H,

[{$CH_3$}$_3$Si-O]$_3$); 0.12 ($s$, 9 H, {$CH_3$}$_3$Si-O). $^{19}F$ NMR data (188.3 MHz, $CDCl_3$): δ -103.03 ($d$, $J = 78.7$ Hz,

$F_b$); -117.75 ($d$, $J = 78.9$ Hz, $F_a$); **DCI MS data:** m/z 500 ($M^+$); 501 ($MH^+$).

**2,6-Anhydro-1-deoxy-1,1-difluoro-D-*gluco*-hept-1-enitol. (2.1).** The heptenitol **2.4** [3.4 g, 6.8 mmol]

was dissolved in ~20 mL of MeOH, $Me_4NF.3H_2O$ [8.8 g, 5 equiv.] was added, and then the mixture was stirred

for 60 min at room temperature. The $Li^+$ form of Dowex 50W X2 resin was added to remove the ammonium

salt ($Me_4N^+$). The mixture was stirred overnight at room temperature, and then the resin was filtered and

washed with MeOH. The solvent was evaporated *in vacuo*, and then the product was purified further by column

chromatography (27:2:1 EtOAc:MeOH:$H_2O$). Lyophilization of the eluate gave a white powder [0.90 g, 62 %]

of **2.1** (mp 67-70 °C). $^1H$ NMR data (400 MHz, $D_2O$): δ 4.18 ($m$, 1 H, H-3); 3.89 ($dd$, 1 H, $J_{7,7'} = 12.6$ Hz,

$J_{6,7} = 2$ Hz, H-7); 3.75 ($dd$, 1 H, $J_{7,7'} = 12.6$ Hz, $J_{6,7'} = 5.6$ Hz, H-7'); 3.62-3.50 ($m$, 3 H, H-6, H-5, H-4).

$^{13}C$ NMR data (125.8 MHz, $D_2O$): δ 154.2 ($t$, $J_{C,Fa} = J_{C,Fb} = 283$ Hz, C-1); 115.25 ($dd$, $J_{C,Fa} = 25$ Hz, $J_{C,Fb} =$

12.6 Hz, C-2); 82.19, 76.30, 69.12 ($s$, C-4, C-5, C-6); 68.13 ($d$, $J_{C,F} = 2.5$ Hz, C-3); 60.74 ($s$, C-7). $^{19}F$ NMR

data (188.3 MHz, $D_2O$): δ -97.36 ($d$, $J_{F,F} = 74.3$ Hz, $F_b$); -112.55 ($dd$, $J_{F,F} = 74.0$ Hz, $F_a$). **DCI MS data:** m/z

230 ($M+NH_4^+$). *Anal.* Calc. for $C_7H_{10}F_2O_5$ (212.15): C, 39.63; H, 4.75. Found: C, 39.72 H, 4.90.

**2,6-Anhydro-1-deoxy-1,1-difluoro-3,4,5,7-tetra-*O*-(*t*-butyldimethylsilyl)-D-*gluco*-hept-1-enitol**

**(2.5)** (see Corey & Venkateswarlu, 1972). The heptenitol **2.1** [0.374 g, 1.76 mmol, dissolved in ~10 mL of dry

DMF] was persilylated as described above using TBDMS chloride [2.25 g, 8.4 equiv.] and imidazole [1.9 g, 10

equiv.]. The reaction was stirred at room temperature for 2 hours under $N_2$, a condenser was attached to the

flask, and then the mixture was stirred at 100 °C for 2 hours until the reaction was complete. Work up of the product was as described above. The product was purified by column chromatography (5:1 hex:CHCl3) to yield

**2.5** [0.9 g, 76%]. $^1$**H NMR data** (400 MHz, CDCl3): δ 4.27 (m, 1 H, H-3); 4.02 (ddd, 1 H, $J_{5,6}$ = 7.6 Hz, $J_{6,7'}$ = 4.1 Hz, $J_{6,7}$ = 2.9 Hz, H-6); δ 3.89 (d, 1 H, $J_{5,6}$ = 7.9 Hz, H-5); 3.82 (dd, 1 H, $J_{7,7'}$ = 11.8 Hz, $J_{6,7}$ = 2.8 Hz, H-7); 3.79-3.73 (m, 2 H, H-4, H-7'); 0.87 (×3), 0.84 (2 s, 36 H, [(Me3C)Me2Si-O]4); 0.09, 0.08, 0.07 (×2), 0.05 (×2), 0.04, 0.03 (6 s, 24 H, [(Me3C)Me2Si-O]4). $^{13}$**C NMR data** (75 MHz, CDCl3): δ 152.23 (dd, $J_{C,Fb}$ = 268.9 Hz, $J_{C,Fa}$ = 287.2 Hz, C-1); 114.86 (dd, $J_{C,Fa}$ = 42.38 Hz, $J_{C,Fb}$ = 12.2 Hz, C-2); 78.29, 75.64, 71.68 (s, C-4, C-5, C-6); 66.90 (d, J = 2 Hz, C-3); 61.87 (s, C-7); 25.84, 25.82, 25.65, 25.55 (s, 12 C, [(Me3C)Me2Si-O]4); 18.30, 17.93, 17.88, 17.77 (s, 4 C, [(Me3C)Me2Si-O]4), -5.47, -5.11{x2}, -5.02{x2}, -4.73, -4.36, -4.12 (s, 8 C, [(Me3C)Me2Si-O]4). $^{19}$**F NMR data** (188.3 MHz, CDCl3): δ -104.90 (d, J = 85.0 Hz, Fb); -121.24 (dd, J = 85.0 Hz, Fa). **FAB MS data:** m/z 669 (MH$^+$).

**(E)-2,6-Anhydro-1-deoxy-1-fluoro-3,4,5,7-tetra-O-(t-butyldimethylsilyl)-D-gluco-hept-1-enitol**

**(2.6)** (see Hayashi et al., 1979). The dried heptenitol **2.5** [0.250 g, 0.37 mmol] was combined with 1.8 mL of Red Al$^{®}$ (obtained from Aldrich Chemical Co.) [0.89 M in toluene; diluted from a 3.4 M stock in toluene; an excess of Red Al$^{®}$ was needed for complete reaction] in a reaction flask at 0 °C. The mixture was stirred at 0 °C, allowed to warm slowly to room temperature, and stirring was continued until the reaction was complete. The reaction was quenched with ice, acidified with conc. HCl, the product was extracted four times into ether, and then the combined ether layer was washed with NaCl and then H2O. The ether layer was dried over MgSO4, the solvent was evaporated in vacuo, and then the residue was purified by column chromatography (20:1 hex:CH2Cl2) to yield an oil of **2.6** [0.11 g, 47%]. $^1$**H NMR data** (400 MHz, CDCl3): δ 6.82 (d, 1 H, $J_{H,F}$ = 81.3 Hz, H-1); 4.57 (dd, 1 H, $J_{3,4}$ = 3.1 Hz, $J_{3,F}$ = 2.2 Hz, H-3); 4.01 (ddd, 1 H, $J_{5,6}$ = 8 Hz, $J_{6,7'}$ = 4.4 Hz, $J_{6,7}$ = 2.5 Hz, H-6); 3.83 (d, 1 H, $J_{5,6}$ = 8 Hz, H-5); 3.80 (dd, 1 H, $J_{6,7}$ = 2.5 Hz, $J_{7,7'}$ = 11.7 Hz, H-7); 3.79 (m, 1 H, H-4); 3.72 (dd, 1 H, $J_{6,7'}$ = 4.3 Hz, $J_{7,7'}$ = 11.7 Hz, H-7'); 0.87 (×3), 0.83 (2 s, 36 H, [(Me3C)Me2Si-O]4); 0.10 (×2), 0.09, 0.08, 0.07 (×3), 0.03 (5 s, 24 H, [(Me3C)Me2Si-O]4). $^{13}$**C NMR data** (75 MHz, CDCl3): δ 143.27 (d, $J_{C-2,F}$ = 29.9 Hz, C-2); 138.42 (d, $J_{C-1,F}$ = 232.9 Hz, C-1); 77.90, 75.83, 72.27 (s, C-4, C-5, C-6); 65.24 (s, C-3); 62.33 (s, C-7); 25.89, 25.84, 25.70, 25.63 (s, 12 C, [(Me3C)Me2Si-O]4); 18.33, 17.95{x2}, 17.85

($s$, 4 C, [(Me₃C)Me₂Si-O]₄), -5.28, -5.15, -5.03, -4.99, -4.94, -4.70, -4.25, -4.02 ($s$, 8 C, [(Me₃C)Me₂Si-O]₄).
¹⁹F NMR data (188.3 MHz, CDCl₃): δ -181.5 ($d$, $J_{H-1,F}$ = 81 Hz).

($E$)-2,6-Anhydro-1-deoxy-1-fluoro-D-$gluco$-hept-1-enitol (2.2). The heptenitol 2.6 [0.230 g, 0.35 mmol] was dissolved in 1.75 mL [5 equiv.] of a 1 $M$ solution of TBAF in THF and then stirred for 60 min at room temperature. The Li⁺ form of Dowex 50W X2 resin was added to remove the ammonium salt (Bu₄N⁺). The mixture was stirred for several hours at room temperature, and then the resin was filtered and washed with MeOH. After removal of the solvent the residue was purified by column chromatography (27:2:1 EtOAc:MeOH:H₂O) to give an oil of 2.2 [0.060 g, 87%]. ¹H NMR data (400 MHz, D₂O): δ 7.01 ($dd$, 1 H, $J_{1,F}$ = 78.6 Hz, $J_{1,3}$ = 1.8 Hz, H-1); 4.18 ($ddd$, 1 H, $J_{5,6}$ = 7.5 Hz, $J_{6,7'}$ = 4.3 Hz, $J_{6,7}$ = 1.5 Hz, H-6); 3.81 ($dd$, 1 H, $J_{6,7}$ = 2.0 Hz, $J_{7,7'}$ = 12 Hz, H-7); 3.68 ($dd$, 1 H, $J_{6,7'}$ = 5.4 Hz, $J_{7,7'}$ = 12 Hz, H-7'); 3.54 ($t$, 1 H, $J_{4,5}$ = $J_{5,6}$ = 7.7 Hz, H-5); 3.42 ($m$, 1 H, H-4). NOTE: No resonance could be assigned to H-3, presumably because this signal was hidden by the resonance attributable to water (δ = 4.88-4.65 ppm). ¹⁹F NMR data (188.3 MHz, D₂O): δ -169.71 ($d$, $J_{H-1,F}$ = 78 Hz). Anal. Calc. for C₇H₁₁FO₅ (194.16): C, 43.30; H, 5.67. Found: C, 43.05; H, 5.70.

| | –R | –X | | R | | –R | –CX |
|---|---|---|---|---|---|---|---|
| [1.1] | H | H | [3.5] | H | [3.7] | Ac | CN |
| [3.12] | H | NHAc | [3.6] | Br | [3.8] | H | CN |
| [5.3] | SiMe₂($t$-Bu) | H | | | [5.4] | SiMe₂($t$-Bu) | CH₃ |
| [5.6] | Ac | CN | | | [5.5] | H | CH₃ |
| [5.7] | H | CN | | | | | |
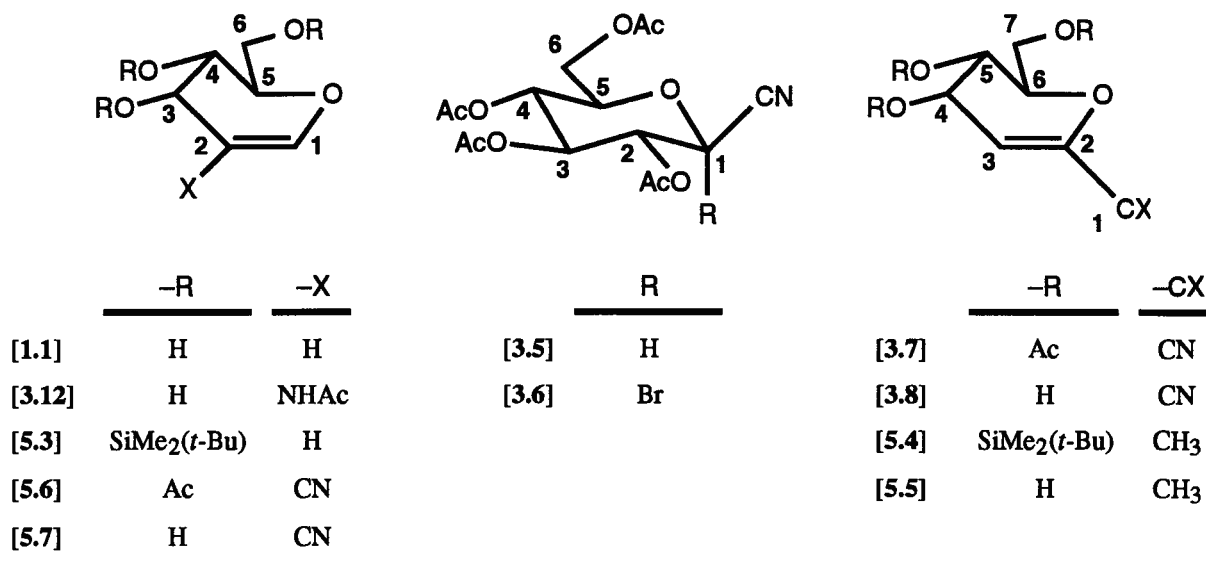
Figure 5.2. Structures of glucal derivatives and associated synthetic intermediates.

The numbering systems $used\ in\ this\ chapter$ for the various compounds are indicated.

*b. The synthesis of glucal and its derivatives.*

**1,5-Anhydro-2-deoxy-D-*arabino*-hex-1-enitol (1.1).** 1,5-Anhydro-2-deoxy-3,4,6-tri-*O*-acetyl-D-*arabino*-hex-1-enitol (Sigma Chemical Co.) was deacetylated using NaOMe/MeOH as described above (see Zemplen & Pacsu, 1929). The product was recrystallized from hot EtOAc to yield D-glucal **1.1** [99%] (mp 57-58 °C; lit. 57-59 °C, Roth & Pigman, 1963). $^1$H NMR data (400 MHz, D$_2$O): δ 6.42 (*dd*, 1 H, $J_{1,2}$ = 7.0 Hz, $J_{1,3}$ = 1.7 Hz, H-1); 4.82 (*dd*, 1 H, $J_{1,2}$ = 7.0 Hz, $J_{2,3}$ = 2.8 Hz, H-2); 4.23 (*dt*, 1 H, $J_{4,5}$ = 7.0 Hz, $J_{5,6}$ = $J_{5,6'}$ = 1.7 Hz, H-5); 3.94-3.84 (*m*, 3 H, H-3, H-6, H-6'); 3.69 (*dd*, 1 H, $J_{4,5}$ = 7.0 Hz, $J_{3,4}$ = 9.4 Hz, H-4).

**1,5-Anhydro-2-deoxy-3,4,6-tri-*O*-(*t*-butyldimethylsilyl)-D-*arabino*-hex-1-enitol (5.3)** (see Corey & Venkateswarlu, 1972). A dry 3-necked flask was charged with the glucal **1.1** [0.5 g, 3.4 mmol], which was persilylated as described above using TBDMS chloride [2.58 g, 17 mmol, 5 equiv.] and imidazole [2.33 g, 34 mmol, 10 equiv., dissolved in ~8 mL of dry DMF]. The reaction was stirred at room temperature for 2 hours under N$_2$, a condenser was attached to the flask, and then the mixture was stirred at 45 °C for 10 hours until the reaction was complete as determined by TLC. Work up of the product was as described above. The product was purified by column chromatography (3:1 hex:CHCl$_3$) to yield an oil of **5.3** [1.35 g, 81%]. $^1$H NMR data (300 MHz, CDCl$_3$): δ 6.33 (*d*, 1 H, $J_{1,2}$ = 6.4 Hz, H-1); 4.65 (*ddd*, 1 H, $J_{1,2}$ = 6.4 Hz, $J_{2,3}$ = 4.5 Hz, $J_{2,4}$ = 1.0 Hz, H-2); 3.99 (*m*, 1 H, H-5); 3.95 (*dd*, 1 H, $J_{5,6}$ = 3.7 Hz, $J_{6,6'}$ = 11 Hz, H-6); 3.89 (*m*, 1 H, H-3); 3.80-3.73 (*m*, 2 H, H-4, H-6'); 0.90, 0.89 (×2) (2 *s*, 27 H, [(Me$_3$C)Me$_2$Si-O]$_3$); 0.10 (×2), 0.08 (×2), 0.06, 0.05 (4 *s*, 18 H, [(Me$_3$C)Me$_2$Si-O]$_3$).

**2,6-Anhydro-1,3-dideoxy-4,5,7-tri-*O*-(*t*-butyldimethylsilyl)-D-*arabino*-hept-2-enitol (5.4)** (see Lesimple et al., 1986). The glucal **5.3** [1.30 g, 2.66 mmol] was combined with 1.5 mL of dry THF, and then the solution was cooled to -78 °C. Immediately after the addition of 4.4 mL of *t*-BuLi [1.84 *M* in pentane, 8 mmol, 3 equiv.] the colorless solution turned yellow (due to the formation of the *t*-BuLi-THF complex). The mixture was stirred at -78 °C for 15 min, then at 0 °C for 45 min. About 5 mL of THF was added at 0 °C to react with the excess *t*-BuLi, and then the solution was cooled to -78 °C. Methyl iodide [1.0 mL, 2.3 g, 16 mmol, 6 equiv., dried by passage through a pipette filled with flame-dried Al$_2$O$_3$] was added at -78 °C, and then the solution was stirred and slowly allowed to warm up to room temperature. The reaction was stopped by the addition of NH$_4$Cl

then H₂O, and then the product was extracted 4 times with ether. The combined organic layer was washed with H₂O, filtered, and then the solvent was evaporated *in vacuo*. ¹H NMR analysis showed that the reaction yielded a mixture of **5.3** and **5.4**, and it was not possible to purify the product by column chromatography, as the $R_f$ values of **5.3** and **5.4** were too similar.

**2,6-Anhydro-1,3-dideoxy-D-*arabino*-hept-2-enitol (5.5)**. The unpurified mixture from the preceding synthesis [0.90 g, ~1.8 mmol of a mixture of **5.3** and **5.4**] was cooled to 0 °C under N₂, 11 mL of *t*-Bu₄NF [1.0 M in THF, 11 mmol, 6 equiv.] was added, and the mixture was stirred under N₂ at 0 °C for 15 min and then at room temperature for 2 hours. The solvent was evaporated *in vacuo*, the residue was purified by column chromatography (4:1:2 CHCl₃:MeOH:hex) 3 times (to remove *t*-Bu₄N⁺), and then the final eluate was crystallized and recrystallized from ether, MeOH, and pet. ether to yield crystals of **5.5** [0.110 g, 27% from **5.3**] (mp 100-102 °C). **¹H NMR data** (300 MHz, D₂O): δ 4.58 (*dd*, 1 H, $J_{3,4}$ = 2.9 Hz, $J_{1,3}$ = 1.0 Hz, H-3); 4.14 (*ddd*, 1 H, $J_{1,4}$ = 1.7 Hz, $J_{3,4}$ = 2.9 Hz, $J_{4,5}$ = 6.7 Hz, H-4); 3.88 (*ddd*, 1 H, $J_{6,7}$ = 3.3 Hz, $J_{6,7'}$ = 4.8 Hz, $J_{5,6}$ = 8.4 Hz, H-6); 3.82 (*m*, 2 H, H-7, H-7'); 3.60 (*dd*, 1 H, $J_{4,5}$ = 6.7 Hz, $J_{5,6}$ = 8.4 Hz, H-5); 1.73 (*dd*, 3 H, $J_{1,4}$ = 1.7 Hz, $J_{1,3}$ = 1.0 Hz, H-1). **DCI MS data:** *m/z* 178 (M+NH₄⁺). *Anal.* Calc. for C₇H₁₂O₄ (160.2): C, 52.49; H, 7.55 Found: C, 52.29 H, 7.76.

**1,5-Anhydro-2-deoxy-2-acetamido-D-*arabino*-hex-1-enitol (3.12)**. The peracetylated precursor 1,5-anhydro-2-deoxy-2(*N*-acetylacetamido)-3,4,6-tri-*O*-acetyl-D-*arabino*-hex-1-enitol (**3.11**) was first purified by column chromatography (1:1 hex:EtOAc). Deacetylation of 0.44 g of this starting material using sodium methoxide in methanol (Pravdić & Fletcher Jr., 1967) removed one of the two *N*-acetyl groups and all three *O*-acetyl groups. The product was purified by column chromatography (25:10:4 EtOAc:EtOH:H₂O) [0.4 g, 91%] and then recrystallized from 2-PrOH, CH₃CN, and hexane to yield **3.12** [0.25 g, 57%] (mp 120-122 °C; lit. 124-125 °C, Pravdić & Fletcher Jr., 1967). **¹H NMR data** (300 MHz, D₂O): δ 6.71 (*d*, 1 H, $J_{1,3}$ = 1 Hz, H-1); 4.29 (*dd*, 1 H, $J_{1,3}$ = 1 Hz, $J_{3,4}$ = 6.4 Hz, H-3); 4.02 (*dt*, 1 H, $J_{5,6}$ = $J_{5,6'}$ = 4.2 Hz, $J_{4,5}$ = 8.5 Hz, H-5); 3.89 (*d*, 2 H, $J_{5,6}$ = $J_{5,6'}$ = 4.2 Hz, H-6, H-6'); 3.79 (*dd*, 1 H, $J_{3,4}$ = 6.4 Hz, $J_{4,5}$ = 9.0 Hz, H-4); 2.10 (*s*, 3 H, H₃CCONH-). **¹³C NMR data** (50 MHz, D₂O): δ 175.29 (H₃CCONH-); 142.46 (C-1); 113.97 (C-2); 79.32,

69.56, 69.15, 60.63 (C-3, C-4, C-5, C-6); 22.64 ($H_3$CCONH-). *Anal.* Calc. for $C_8H_{13}NO_5$ (203.20): C, 47.29; H, 6.45; N, 6.89. Found: C, 47.29; H, 6.39; N, 6.75.

**1,5-Anhydro-2-deoxy-2-cyano-3,4,6-tri-*O*-acetyl-D-*arabino*-hex-1-enitol (5.6)** (see Hall & Jordaan, 1973). 1,5-Anhydro-2-deoxy-3,4,6-tri-*O*-acetyl-D-*arabino*-hex-1-enitol (obtained from Sigma Chemical Co.) [0.50 g, 1.8 mmol] was dried *in vacuo* for a few hours, then dissolved in 5 mL of dry ether. A solution containing 5 mL of dry ether and 0.16 mL of chlorosulfonyl isocyanate was prepared, and then a dropping funnel was used to add this solution to the reaction at 0 °C over a period of 30 min. The reaction was stirred overnight at 0 °C, and then a solution containing 1.3 mL of dry $CH_2Cl_2$ and 0.24 mL of dry $Et_3N$ [0.19 g, 1 equiv., dried over KOH] was added at 0 °C. The reaction was slowly allowed to warm to room temperature, poured into 25 mL of $H_2O$, and then the organic solvent was evaporated with a stream of $N_2$. The aqueous residue was extracted 4 times with $CH_2Cl_2$, the combined organic layer was washed with $H_2O$, the solvent was evaporated *in vacuo*, and then the residue was purified by column chromatography (2:1 hex:EtOAc) to give **5.6** [0.15 g, 27%]. $^1$H NMR data (200 MHz, acetone-$D_6$): δ 7.58 (*s*, 1 H, H-1); 5.53 (*d*, 1 H, $J_{3,4}$ = 5 Hz, H-3); 5.23 (*dd*, 1 H, $J_{3,4}$ = 5 Hz, $J_{4,5}$ = 6 Hz, H-4); 4.70 (*td*, 1 H, $J_{4,5}$ = $J_{5,6}$ = 6 Hz, $J_{5,6'}$ = 3 Hz, H-5); 4.49 (*dd*, 1 H, $J_{5,6}$ = 6 Hz, $J_{6,6'}$ = 13 Hz, H-6); 4.28 (*dd*, 1 H, $J_{5,6'}$ = 3 Hz, $J_{6,6'}$ = 13 Hz, H-6'); 2.09, 2.05, 2.02 (3 *s*, 9 H, [AcO-]$_3$). $^{13}$C NMR data (50 MHz, CDCl$_3$): δ 170.21, 169.50, 169.11 (*s*, [$H_3$CCOO-]$_3$); 157.84 (*s*, C-1); 115.54 (*s*, conj. CN); 88.19 (*s*, C-2); 75.46, 65.20, 64.25 (3× *s*, C-3, C-4, C-5); 60.44 (*s*, C-6); 20.61{×2}, 20.57 (*s*, [$H_3$CCOO-]$_3$). IR data: $v_{max}$ (cm$^{-1}$): 2223 (conj. CN); 1757 (C=O); 1631 (conj. C=C). DCI MS data: *m/z* 315 (M+NH$_4^+$).

**1,5-Anhydro-2-deoxy-2-cyano-D-*arabino*-hex-1-enitol (5.7)**. The glucal **5.6** was dried *in vacuo* overnight prior to deacetylation using NH$_3$-saturated MeOH as described above. The reaction was left at 4 °C for a few hours until the reaction was complete as determined by TLC (27:2:1 EtOAc:MeOH:H$_2$O). The solvent was evaporated *in vacuo* to give a solid that was recrystallized from acetone and hexane to give colorless needles of **5.7** [0.17 g, 57%] (mp 123-125 °C). $^1$H NMR data (200 MHz, D$_2$O): δ 7.30 (*d*, 1 H, $J_{1,3}$ = 1 Hz, H-1); 4.29 (*dd*, 1 H, $J_{1,3}$ = 1 Hz, $J_{3,4}$ = 7 Hz, H-3); 4.12 (*ddd*, 1 H, $J_{5,6}$ = 3 Hz $J_{5,6'}$ = 4 Hz, $J_{4,5}$ = 9 Hz, H-5); 3.89 (*d*, 1 H, $J_{5,6}$ = 3 Hz, H-6); 3.86 (*d*, 1 H, $J_{5,6'}$ = 4 Hz, H-6'); 3.73 (*dd*, 1 H, $J_{3,4}$ = 7 Hz, $J_{4,5}$ = 9 Hz, H-4).

$^{13}$C NMR data (50 MHz, D$_2$O): δ 159.11 (*s*, C-1); 118.70 (*s*, CN); 91.10 (*s*, C-2); 80.89, 67.55, 67.39 (*s*, C-3,

C-4, C-5), 60.25 (C-6). **IR data:** $v_{max}$ (cm$^{-1}$): 2220 (conj. CN); 1627 (conj. C=C). **DCI MS data:** *m/z* 189

(M+NH$_4^+$). **Anal.** Calc. for C$_7$H$_9$NO$_4$ (171.15): C, 49.12; H, 5.30; N, 8.18. Found: C, 49.08; H, 5.38; N, 8.12.

**2,3,4,6-Tetra-*O*-acetyl-β-D-glucopyranosyl cyanide (3.5)** (see Fuchs & Lehmann, 1975). 2,3,4,6-

Tetra-*O*-acetyl-α-D-glucopyranosyl bromide (**3.4**, see Lemieux, 1963) [10 g, 24 mmol] and Hg(CN)$_2$ [13 g,

51 mmol, 2 equiv.] were dried in a dessicator *in vacuo* over P$_2$O$_5$ and KOH for 2 days. The starting materials

were ground in a mortar and mixed together, and then distributed evenly on the bottom of a 125-mL Erlenmeyer

flask. The mixture was heated at 80-85 °C under N$_2$ for 30 min, and then the melted solid was dissolved in

~100 mL of warm CHCl$_3$. The solution was filtered through a bed of Celite, the filtrate was washed 3 times

with 10% KBr (aq), the organic solvent was evaporated *in vacuo*, leaving a solid that was crystallized and

recrystallized from EtOH to give white crystals of **3.5** [5.2 g, 60%] (mp 113 °C; lit. 114-115 °C, Myers & Lee,

1984). $^1$**H NMR data** (200 MHz, CDCl$_3$): δ 5.30 (*t*, 1 H, $J_{1,2}$ = $J_{2,3}$ = 9 Hz, H-2); 5.24-5.03 (*m*, 2 H, H-3,

H-4); 4.30 (*d*, 1 H, $J_{1,2}$ = 9 Hz, H-1); 4.23 (*dd*, 1 H, $J_{5,6}$ = 4.8 Hz, $J_{6,6'}$ = 12 Hz, H-6); 4.10 (*dd*, 1 H, $J_{5,6'}$ =

2 Hz, $J_{6,6'}$ = 12 Hz, H-6'); 3.69 (*ddd*, 1 H, $J_{4,5}$ = 10 Hz, $J_{5,6}$ = 4.8 Hz $J_{5,6'}$ = 2 Hz, H-5); 2.09 (×2), 2.01, 2.00

(3 *s*, 12 H, [AcO-]$_4$). $^{13}$**C NMR data** (50 MHz, CDCl$_3$): δ 170.46, 170.02, 169.10, 168.69 (*s*, [H$_3$CCOO-]$_4$);

114.10 (conj. CN); 76.81, 72.80, 68.94, 67.25, 66.46, 61.41 (*s*, C-1, C-2, C-3, C-4, C-5, C-6); 20.64, 20.48 (×2),

20.36 (*s*, [H$_3$CCOO-]$_4$).

**2,3,4,6-Tetra-*O*-acetyl-1-α-bromo-β-D-glucopyranosyl cyanide (3.6)** (see Lichtenthaler & Jarglis,

1982). The glucosyl cyanide **3.5** [2.8 g, 7.8 mmol] was dried *in vacuo* overnight and then dissolved in 100 mL

of CCl$_4$. *N*-Bromosuccinimide [5.5 g, 31 mmol, 4 equiv., recrystallized from hot H$_2$O and then dried over P$_2$O$_5$

*in vacuo*] and a catalytic amount of BaCO$_3$ [0.6 g, 3 mmol] were added, and then a condenser and a drying tube

were connected to the reaction flask. The reaction was refluxed for ~90 min while it was irradiated with a

250 W tungsten lamp. The mixture was cooled on ice to give the product as a solid, which was collected by

filtration prior to further purification by column chromatography (3:1 hex:EtOAc) and recrystallization from

anhydrous ether and pet. ether to yield white needles of **3.6** [2.1 g, 60%] (mp 100-101 °C; lit. 92 °C,

Lichtenthaler & Jarglis, 1982). $^1$**H NMR data** (200 MHz, CDCl$_3$): δ 5.39 (*t*, 1 H, $J_{2,3}$ = $J_{3,4}$ = 9.6 Hz, H-3);

5.25 ($d$, 1 H, $J_{2,3}$ = 9.6 Hz, H-2); 5.16 ($t$, 1 H, $J_{3,4}$ = $J_{4,5}$ = 9.6 Hz, H-4); 4.31 ($dd$, 1 H, $J_{5,6}$ = 3 Hz, $J_{6,6'}$ = 12

Hz, H-6); 4.25 ($ddd$, 1 H, $J_{4,5}$ = 9.6 Hz, $J_{5,6'}$ = 1.6 Hz, $J_{5,6}$ = 3 Hz, H-5); 4.08 ($dd$, 1 H, $J_{5,6'}$ = 1.6 Hz, $J_{6,6'}$ = 12

Hz, H-6'); 2.16, 2.12, 2.04, 2.01 (4 $s$, 12 H, [AcO-]$_4$). **DCI MS data:** $m/z$ 455, 453 (M+NH$_4^+$).

**2,6-Anhydro-3-deoxy-4,5,7-tri-$O$-(acetyl)-D-$arabino$-hept-2-enononitrile (3.7)** (see Somsák et al., 1990). The brominated glucosyl cyanide **3.6** [2.82 g, 6.4 mmol] was dissolved in benzene, Zn [1.7 g, 29 mmol, 4.5 equiv.] was added, and then the mixture was stirred under N$_2$ and heated to reflux. Pyridine [0.50 mL, 6.4 mmol, 1 equiv.] was added to the refluxing suspension and then the reaction was continued for 30 min. The solid was evaporated by filtration and washed with ether. The filtrate was washed with KHSO$_4$ then H$_2$O, and then the organic layer was dried over MgSO$_4$. Evaporation of the solvent $in$ $vacuo$ gave a white solid which was purified further by column chromatography (2:1 hex:EtOAc) to give crystals of **3.7** [1.72 g, 90%]. **$^1$H NMR data** (400 MHz, CDCl$_3$): $\delta$ 5.68 ($d$, 1 H, $J_{3,4}$ = 4 Hz, H-3); 5.33 ($dd$, 1 H, $J_{3,4}$ = 4 Hz, $J_{4,5}$ = 5.5 Hz, H-4); 5.19 ($dd$, 1 H, $J_{4,5}$ = 5.5 Hz, $J_{5,6}$ = 6.4 Hz, H-5); 4.41-4.36 ($m$, 2 H, H-6, H-7); 4.15 ($dd$, 1 H, $J_{7,7'}$ = 15 Hz, $J_{6,7'}$ = 5 Hz, H-7'); 2.08, 2.04, 2.02 (3 $s$, 9 H, [AcO-]$_3$).

**2,6-Anhydro-3-deoxy-D-$arabino$-hept-2-enononitrile (3.8)** (see Fritz et al., 1983). The cyanoglucal **3.7** [2.82 g, 6.4 mmol] was dried $in$ $vacuo$ overnight prior to deacetylation using NH$_3$-saturated MeOH as described above. The reaction was left at 4 °C for 4.5 hours until the reaction was complete. The solvent was evaporated $in$ $vacuo$ to give a solid that was purified further by column chromatography (27:2:1 EtOAc: MeOH:H$_2$O) and recrystallized from acetone, ether and hexane to give **3.8** [0.20 g, 70%] (mp 95-97 °C). **$^1$H NMR data** (200 MHz, D$_2$O): $\delta$ 5.80 ($d$, 1 H, $J_{3,4}$ = 3 Hz, H-3); 4.30 ($dd$, 1 H, $J_{3,4}$ = 3 Hz, $J_{4,5}$ = 7 Hz, H-4); 4.05 ($ddd$, 1 H, $J_{5,6}$ = 9 Hz, $J_{6,7}$ = 2.8 Hz, $J_{6,7'}$ = 4 Hz, H-6); 3.88 ($d$, 1 H, $J_{6,7}$ = 2.8 Hz, H-7); 3.86 ($d$, 1 H, $J_{6,7'}$ = 4 Hz, H-7'); 3.71 ($dd$, 1 H, $J_{4,5}$ = 7 Hz, $J_{5,6}$ = 9 Hz, H-5). **$^{13}$C NMR data** (50 MHz, D$_2$O): $\delta$ 129.04 ($s$, C-2); 118.98 ($s$, C-3); 114.72 ($s$, CN); 81.03, 68.68, 68.02, 60.34 ($s$, C-4-7). **DCI MS data:** $m/z$ 189 (M+NH$_4^+$). **Anal.** Calc. for C$_7$H$_9$NO$_4$ (171.15): C, 49.12; H, 5.30; N, 8.18. Found: C, 49.42; H, 5.29; N, 8.26.

*5.2. ENZYME KINETICS.*

**5.2.1. Miscellaneous procedures and definition of enzyme activity units.**

Absorbance measurements were made using either a Perkin-Elmer Lambda 2 model, or a Pye-Unicam PU-8800 or PU-8700 model UV-VIS spectrophotometer, each of which was equipped with a circulating water bath and thermostatted cuvette holders. In all cases absorbance measurements were made using cuvettes with a 1.00-cm pathlength.

All pH measurements were performed using a Radiometer PHM 82 pH meter equipped with an Orion combination electrode (Model no. 8103). Prior to use this instrument was standardized using commercially obtained standard pH buffers.

In all cases, one unit (U) of enzyme activity represents an amount capable of catalyzing the formation of one micromole of product per minute under the conditions specified for each assay.

**5.2.2. Enzymes and enzyme assays used in this work.**

*a. Glycogen phosphorylase.*

Glycogen phosphorylase *b* (E.C. 2.4.1.1) was prepared from rabbit muscle by (now Dr.) William Stirtan of Prof. Withers' laboratory (see Stirtan, 1993). The concentration of this protein in stock solutions was determined from $A_{280}$ measurements using an $A_{280}^{0.1\%} = 1.32 \, \text{cm}^{-1}$ (Buc & Buc, 1968).

*b. The assay for glycogen phosphorylase activity.*

In most cases phosphorylase activity was assayed in the direction of glycogen synthesis, and in these cases initial rates were determined by measuring the amount of inorganic phosphate released in a 5-minute time period (Engers et al., 1970).

Except as noted, the buffer for all kinetic experiments using phosphorylase in the glycogen synthesis reaction contained 100 m$M$ KCl, 1 m$M$ EDTA, 1 m$M$ DTT, and 50 m$M$ triethanolamine hydrochloride pH 6.8. Reaction mixtures (0.500 mL) also contained 1 m$M$ AMP and 0.5-1% glycogen. Reactions were carried out at 30 °C for 5 min. In most cases the enzyme was preincubated with AMP and glycogen and then added to a

solution containing a substrate with or without an inhibitor. The enzyme concentration in the reaction mixture depended on the kinetic parameter under study, and is given in the figure legends.

When phosphorylase activity was assayed in the direction of glycogen phosphorolysis, initial rates were determined using a phosphoglucomutase/glucose-6-phosphate dehydrogenase coupled assay (Engers et al., 1969). The reaction buffer for these assays was adjusted to pH 6.8 and contained 35 m$M$ imidazole, 20 m$M$ sodium glycerophosphate, 10 m$M$ Mg(OAc)$_2$, 5 m$M$ DTT, 1 m$M$ EDTA, and also contained 1 m$M$ AMP, 0.5% glycogen, 1 m$M$ $\beta$NADP, 15 U/mL phosphoglucomutase, and 3.4 U/mL of glucose-6-phosphate dehydrogenase. In these coupled assays the reduction of NADP is quantitated by following the change in absorbance at 340 nm. These assays were performed by Ms. Karen Rupitz.

Technical assistance with the kinetics experiments using glycogen phosphorylase was also provided by (now Dr.) William Stirtan.

### c. Agrobacterium β-glucosidase.

The cloned *Agrobacterium* $\beta$-glucosidase pABG5 was prepared as described (Kempton & Withers, 1992). The concentration of this protein in stock solutions was determined from A$_{280}$ measurements using an $A_{280}^{0.1\%} = 2.184$ cm$^{-1}$ (Street, 1988).

### d. The assay for Agrobacterium β-glucosidase activity.

Except as noted, initial rates of $\beta$-glucosidase activity were measured by adding aliquots of the enzyme to a cuvette containing 1.00 mL of the substrate $\beta$GlcPNP in 50 m$M$ sodium phosphate buffer (pH 6.8) containing 0.1% BSA. The cuvette and its contents were equilibrated to 37 °C in the spectrophotometer just prior to addition of the enzyme. Absorbance readings at 400 nm (A$_{400}$) were measured to give initial rates in A$_{400}$ units per minute. Enzyme concentration and reaction times were chosen to ensure that <10% of the substrate was consumed, thus ensuring linear kinetics. The $\varepsilon_{400}$ of 4-nitrophenol at pH 6.8 and 37 °C is 7280 $M^{-1}$cm$^{-1}$ (Street, 1988).

*e. β-N-Acetylhexosaminidases.*

Sigma Chemical Company supplied β-*N*-acetylhexosaminidases (NAGases) isolated from jack bean (J-NAGase), bovine kidney (K-NAGase), and human placenta (H-NAGase). The catalogue numbers of these products were A-2264, A-2415, and A-6152, respectively.

*f. Assays for β-N-acetylhexosaminidase activity.*

Kinetic studies of hydrolysis reactions were performed by following changes in UV-VIS absorbance using a spectrophotometer equipped with a circulating water bath that maintained the 1.00-cm cuvettes at 25 °C. Except as noted, reaction buffers contained BSA (0.1%), NaCl (100 m$M$) and citrate buffer (50 m$M$), and were adjusted to pH 5.0 (used with jack bean NAGase) or pH 4.25 (used with human placenta or bovine kidney NAGase). Molar extinction coefficients for 4-nitrophenol and βGlcNAcPNP were determined at 25 °C by measuring the absorbance at 360 nm of carefully prepared stock solutions of each compound in the appropriate enzyme reaction buffer (pH 5.0 or 4.25). The molar extinction differences at 360 nm ($\Delta\varepsilon_{360}$) determined for βGlcNAcPNP and 4-nitrophenol at pH 5.0 and pH 4.25 were 2280 and 2150 $M^{-1}cm^{-1}$, respectively.

The initial rates of βGlcNAcPNP hydrolysis were determined by incubating the reaction buffer at 25 °C in the thermostatted cuvette-holder of the spectrophotometer. An appropriate volume of stock substrate solution was added to the cuvette ~4 min before the reaction (to ensure negligible spontaneous hydrolysis of the substrate during the pre-incubation and reaction periods). Reactions were initiated by the addition of enzyme (in BSA-containing buffer) by syringe, and the reactions were monitored at 360 nm. Initial rates were determined using 6-7 different substrate concentrations, which ranged from about one-third to (in most cases) three times the value of the $K_m$ ultimately determined. However, due to the high background absorbance of βGlcNAcPNP at 360 nm, its concentration was kept below 2 m$M$. The rates of βGlcDNP hydrolysis were determined using a comparable assay, except the reaction was monitored at 400 nm. In these (0.200-mL) reactions, 1.5 or 6.5 m$M$ βGlcDNP was incubated in the appropriate buffer for several hours at 25 °C with (or without) 6 μg of J-NAGase. The $\Delta\varepsilon_{400}$ determined for βGlcDNP and 2,4-dinitrophenol at pH 5.0 was 9750 $M^{-1}cm^{-1}$.

### 5.2.3. The determination of kinetic parameters for substrates.

*a. Determinations of $K_m$ and $V_{max}$ for various substrates.*

Approximate values of $K_m$ and $V_{max}$ were determined by measuring initial reaction rates using 3 different (and wide-ranging) concentrations of the substrate. Accurate values of these parameters were then determined by measuring initial reaction rates using 5-8 different concentrations of the substrate, concentrations that typically ranged between 0.3-5 times the approximately determined $K_m$ value (Lineweaver & Burk, 1934).

Values of $K_m$ and $V_{max}$, together with the errors associated with the scatter of the data, were calculated by fitting the data to a weighted nonlinear regression of the Michaelis-Menten equation using the computer program GraFit™ (Leatherbarrow, 1990).

Initial-rate data were also plotted according to the method of Lineweaver and Burk (1934), but this method was not used for calculating kinetic parameters due to inaccuracies associated with such plots. However, these plots are included in this thesis because they are a useful tool for recognizing deviations from linear behaviour caused by allostery or various types of inhibition.

*b. Determinations of reaction rates for the catalytic hydration of heptenitol.*

Eight 0.500-mL reaction buffer mixes containing sodium phosphate buffer (50 m$M$, pH 6.8), no BSA, and one of eight different concentrations of heptenitol were prepared. Appropriate control reactions (with the same concentrations of heptenitol but without enzyme) were also carried out. Reactions were pre-incubated and carried out at 37 °C, and were started by the injection of 30 µg of pABG5 (in 10 µL) into each solution. Reactions were carried out for 10 min.

The reaction product, 1-deoxy-D-*gluco*-heptulose, as well as standard solutions of the same, was assayed by a cuprimetric method (Hehre et al., 1980) with slight modifications. The basis of this method is the stoichiometric reduction of Cu(II) (by the reducing sugar) to Cu(I) oxide, which in turn reduces arsenomolybdate to molybdenum blue. The absorption at 540 nm of the latter is a measure of the sugar concentration. Each reaction was stopped by transferring 0.200 mL of the 0.500-mL reaction mixture into a fresh tube containing 2.00 mL of Somogyi's reagent (Somogyi, 1952). Each stopped reaction mixture was

placed in a boiling water bath for 10 min and then cooled. Nelson's reagent [2.00 mL] (Nelson, 1944) and 1.5

mL of double-deionized water were added per tube, each reaction was mixed, and then the absorbance at 540 nm

was measured on a Pye-Unicam PU-8700 spectrophotometer. Nine dilutions of stock 1-deoxy-D-*gluco*-

heptulose were used to construct the standard curve for the assay. There was a linear relationship between the

$A_{540}$ of the cuprimetric assay and the amount of 1-deoxy-D-*gluco*-heptulose over the range of 0.56 to 7.9 m$M$

(in the original 0.500-mL reactions).

Initial rates were calculated after correction for the rate of nonenzymatic hydration in appropriate

control reactions. Determinations of $K_m$ and $V_{max}$ values were as described above using the computer program

GraFit™ (Leatherbarrow, 1990). The standard curve was used to quantitate the reaction product.

*c. Determinations of reaction rates for the catalytic hydration of methylglucal.*

This assay utilized $^1$H NMR to quantitate the reaction product. Five 0.500-mL reaction buffer mixes

containing HEPES-NaOH (10 m$M$, pH 7.0), BSA (0.1%), and one of five different concentrations of

methylglucal were prepared. Reactions were pre-incubated and carried out at 37 °C, and were started by the

injection of 0.65 mg of pABG5 into each solution. Reactions were carried out for 110 hours and then stopped

by cooling to 0 °C. Water was removed by lyophilization and then several cycles of resuspension with D$_2$O and

lyophilization were carried out. The $^1$H NMR spectrum was obtained for each D$_2$O-exchanged reaction using a

400 MHz Brüker WH-400 instrument. The concentration of the reaction product was determined by integration

of the product methyl hydrogen peak (at $\delta = 1.43$ ppm), which was corrected by subtracting the integral of the

same peak in the appropriate control (reactions with the same concentration of methylglucal but without

enzyme). The number of micromoles of product formed was calculated from the $^1$H NMR data using the

equation shown below. Determinations of $K_m$ and $V_{max}$ values were as described above.

$$\begin{bmatrix} \mu\text{mol of} \\ \textbf{product} \\ \text{formed} \end{bmatrix} = \left\{ \cfrac{\left( \begin{array}{c} \text{Area of the } \textbf{product} \\ \text{methyl } ^1\text{H peak} \end{array} \right)}{\left( \begin{array}{c} \text{Area of the } \textbf{product} \\ \text{methyl } ^1\text{H peak} \end{array} \right) + \left( \begin{array}{c} \text{Area of the } \textbf{substrate} \\ \text{methyl } ^1\text{H peak} \end{array} \right)} \right\} \times \begin{bmatrix} \mu\text{mol of} \\ \textbf{substrate} \\ \text{originally} \\ \text{present in} \\ \text{the assay} \end{bmatrix}$$

### 5.2.4. The determination of kinetic parameters for inhibitors.

*a. Determinations of $K_i$ values (reversible inhibition).*

Approximate values for inhibition constants (range-finding or $RF$ $K_i$ values) for reversible inhibitors were determined by measuring initial reaction rates at a single substrate concentration (usually equal to the $K_m$) and 5 or 6 different concentrations of the inhibitor. An accurate $V_{max}$ value was then determined in a parallel experiment using several different concentrations of the substrate, but the same amount of enzyme as was used in the first experiment (i.e., with the inhibitor present). The data from the first experiment was then plotted as the inverse of the initial reaction rate vs. the inhibitor concentration (Dixon, 1972). The $RF$ $K_i$ value is easily obtained from the intercept ($-K_i$) of the line through the plotted data and a horizontal line drawn at $1/V_{max}$ (Dixon, 1972).

In some but not all cases, inhibition constants were determined accurately by measuring initial reaction rates at 4 or 5 substrate concentrations bracketing the $K_m$ value, at each of 4 or more inhibitor concentrations bracketing the 'range-finding' $K_i$ value, and also in the absence of inhibitor. The initial-rate data obtained at each substrate and inhibitor concentration were then fitted to equations describing different types of enzyme inhibition (and which yield a $K_i$ value for each case), using the nonlinear regression analysis computer program GraFit™ (Leatherbarrow, 1990). The $K_i$ value for the best fit of the data was reported in all cases, but in some cases more than one $K_i$ value was reported because the data fit well to equations describing different types of inhibition. Double-reciprocal (or Dixon) plots were also used as a convenient graphical method to show the pattern of inhibition.

*b. Determinations of $K_i$ values using glycogen phosphorylase.*

In most cases the inhibition of glycogen phosphorylase activity was assayed in the direction of glycogen synthesis (Engers et al., 1970). Initial rates were determined by measuring the amount of inorganic phosphate released in a 5-minute time period (Engers et al., 1970; described above). Inhibition constants were determined accurately by measuring initial reaction rates at 5 substrate concentrations, at each of 5 or more inhibitor concentrations. The data were then analyzed using Hill plots (i.e., plots of $\ln[v/\{V_{max} - v\}]$ vs. $\ln[S]$).

The $K_{m,app}$ values are easily obtained from the intercept ($\ln[K_{m,app}]$) of the line through the plotted data and the abscissa ($\ln[S]$ axis). Replots of the $K_{m,app}$ values vs. the inhibitor concentrations yielded the inhibition constant, $K_i$, from the intercept ($-K_i$) of the line through the plotted data and the abscissa ($[I]$ axis).

The inhibition of glycogen phosphorylase activity was also assayed in the direction of glycogen phosphorolysis for the fluoroheptenitol inhibitors. Initial rates were determined using a phosphoglucomutase/ glucose-6-phosphate dehydrogenase coupled assay (Engers et al., 1969; described above). In these cases $RF\ K_i$ values were determined using Dixon plots as described above.

*c. Irreversible inhibition (inactivation) tests: Experimental methods.*

F$_2$hept was tested as an inactivator of glycogen phosphorylase *b* by incubating 17 m$M$ F$_2$hept, 100 m$M$ KCl, 1 m$M$ EDTA, 1 m$M$ DTT, 50 m$M$ triethanolamine hydrochloride (pH 6.8), 1% glycogen, 5 m$M$ orthophosphate, 1.5 m$M$ AMP, and 0.6 mg of enzyme, for 5 days at room temperature. Over the course of this incubation period, small aliquots (10 μL) of the above reaction were removed, and then added to fresh tubes, each of which contained 0.500 mL of a reaction mixture containing a saturating concentration (16 m$M$) of αG1P, 1 m$M$ AMP, 1% glycogen, 100 m$M$ KCl, 1 m$M$ EDTA, 1 m$M$ DTT, and 50 m$M$ triethanolamine hydrochloride (pH 6.8). Initial reaction rates were then assayed in the direction of glycogen synthesis as described (Engers et al., 1970).

The following inactivation tests were performed with either β-glucosidase or NAGase, and in these cases the substrates employed were the chromogenic glycosides βGlcPNP and βGlcNAcPNP, respectively. In both cases the residual activity was determined by measuring the release of 4-nitrophenol spectrophotometrically as described earlier. In these inactivation tests, reaction mixtures were set up containing one of several different concentrations of the putative inactivator in the appropriate buffer for each enzyme (see above; in all cases these buffers contained 0.1% BSA), and then the reactions were incubated at the enzyme's optimal temperature. Equal aliquots of enzyme were added to each reaction, the reactions were incubated at the indicated temperature, and then the residual enzyme activity was measured at various time intervals. This was done by removing a 10-μL aliquot of the inactivation reaction mixture and then adding this aliquot to a fresh tube containing a much larger volume (typically 0.600 or 1.00 mL) of a saturating concentration of the substrate (as well as the appropriate

buffer for each enzyme; see above). For assays of residual β-glucosidase activity, ~1.0 m$M$ βGlcPNP was used ($K_m$ = 78 μ$M$, Kempton & Withers, 1992). For assays of residual NAGase activity, ~1.4 m$M$ βGlcNAcPNP was used ($K_m$ ~ 0.62 m$M$, Li & Li, 1970, and this work) due to the high background absorbance of the substrate at 360 nm.

*d. Irreversible inhibition (inactivation) tests: Theory and calculations.*

The inactivation of a glycosylase can be expressed by the following Scheme (5.1):

$$I + E \; \underset{\phantom{K_i}}{\overset{K_i}{\rightleftharpoons}} \; EI \; \overset{k_i}{\longrightarrow} \; E\text{—}I$$

**Scheme 5.1.** A kinetic model for the inactivation of an enzyme (E) by an inactivator (I).

Here the inactivator (I) and the free enzyme (E) are involved in a reversible, initial binding step ($K_i$), followed by an irreversible, rate-limiting, bond-forming step ($k_i$) that results in the formation of a covalent, glucosyl-enzyme complex (E—I). If

$$[I] \gg [E]; \qquad \text{i.e.,} \qquad \{[I] - [E]\} \approx [I],$$

then [I] is essentially constant over the course of the reaction, and the kinetics are pseudo first-order with respect to the enzyme concentration. The inactivation equation can then be written in Michaelis-Menten form as:

$$v = \frac{k_i \, [E]_o \, [I]}{K_i + [I]} \qquad\qquad \textit{Equation (1)}$$

where:      $k_i$ = rate constant of inactivation

           $K_i$ = the apparent dissociation constant for all species of enzyme-bound inactivator

$$K_i = \frac{[E]\,[I]}{\Sigma\,[EI]} \qquad\qquad \textit{Equation (2)}$$

If [I] is constant, Equation (1) becomes:

$$v = k_{obs} [E]_t \qquad Equation (3)$$

where:

$$k_{obs} = \frac{k_i [I]}{K_i + [I]} \qquad Equation (4)$$

In those cases where a time-dependent, first-order decay in activity (after correction for the control assay without the putative inactivator) was observed, the residual activity was plotted against time, and $k_{obs}$ was calculated at each inactivator concentration by fitting the initial rates (which measure [E]) to Equation (5), using the computer program GraFit™ (Leatherbarrow, 1990).

$$[E] = [E]_o e^{-\{k_{obs}t\}} \qquad Equation (5)$$

The pseudo first-order rate constant ($k_{obs}$) obtained at each concentration of the inactivator was fitted to Equation (4) above using the computer program GraFit™ (Leatherbarrow, 1990). This equation was used to calculate the binding constant, $K_i$, and the inactivation rate constant, $k_i$. These data were also presented in the form of a double-reciprocal plot for convenient visual inspection.

*e. The reactivation test for nitroglucal-inactivated pABG5.*

A sample (0.13 mg) of pABG5 was inactivated after incubation in a solution containing 16 m$M$ nitroglucal. This solution was placed in dialysis tubing, and then excess inactivator was removed by dialysis using three changes of a large volume of 50 m$M$ phosphate buffer (pH 6.8).

As a control, another sample (0.13 mg) of pABG5 went through the same procedure except that no inactivator was added. After the control sample was dialyzed, the retentate was divided into two equal-size aliquots. To one control aliquot was added BSA (to a final concentration of 0.1%) in 50 m$M$ phosphate buffer. To the second control aliquot was added BSA (to a final concentration of 0.1%) and cellobiose (to a final

concentration of 21 m$M$) in 50 m$M$ phosphate buffer. The final volume of each of these control "reactivation" reactions was 0.110 mL.

The "nitroglucal-free" retentate containing nitroglucal-inactivated pABG5 was divided into three equal-size aliquots. To one aliquot was added BSA (to a final concentration of 0.1%) in 50 m$M$ phosphate buffer. To the second aliquot was added BSA (to a final concentration of 0.1%) and cellobiose (to a final concentration of 21 m$M$) in 50 m$M$ phosphate buffer. To the third aliquot was added BSA (to a final concentration of 0.1%) and 1d$\beta$Glc$\phi$ (to a final concentration of 21 m$M$) in 50 m$M$ phosphate buffer. The volume of each of these reactivation reactions was 0.110 mL.

The five 0.110-mL reactions mentioned above were incubated at pH 6.8 at 37 °C. At various time intervals, aliquots were removed from each reaction, transferred to cuvettes containing 1.00 mL of $\beta$GlcPNP, and then assayed for enzymatic activity.

### 5.2.5. The determination of kinetic parameters by HPLC.

*a. Instrumentation.*

HPLC analyses were carried out using instrumentation from Waters®, including the HPLC apparatus, Model 712 WISP® auto-sampler (injector), Model 410 differential refractometer detector, Model 486 tunable absorbance detector, and an analytical DextroPak® column (100 × 8 mm; operated using water as the eluent; used to separate anomers of GlcNAc). A Guard-Pak® pre-column was used to remove protein before the sample entered the DextroPak® column. A Bio-Rad® Aminex® HPX-87H column was also used (300 × 7.8 mm; operated using 13 m$M$ H$_2$SO$_4$ as the eluant; used to separate GlcNAc and ManNAc). Data was collected using the Baseline® 810 chromatography workstation, and analytes were identified by their retention time in comparison with authentic standards. Chromatographs from the workstation were exported as ASCII data files to the computer program GraFit™ (Leatherbarrow, 1990) for printing.

*b. Determination of the product of NAGase-catalyzed $\beta$GlcNAcPNP hydrolysis.*

The stereochemical course of the enzymatic hydrolysis of $\beta$GlcNAcPNP was determined by HPLC analysis using a DextroPak® column. Assignment of peaks was achieved by loading a freshly prepared sample

of αGlcNAc onto the column and measuring its retention time. $^1$H NMR analysis of a similar, freshly prepared sample of αGlcNAc confirmed the identity of the sample, while similar analysis of an equilibrated mixture was used to determine which anomer was the major component. HPLC analysis was carried out using samples of βGlcNAcPNP (in 3 m$M$ citrate buffer without BSA) incubated for 7 min at 25 °C with one of each of the three types of NAGase under study. Control reactions (without βGlcNAcPNP or the enzyme) were also analyzed. The analyses of the enzymatic reactions were repeated using samples obtained after 1-3 days of incubation at 25 °C.

*c. Determination of the rate of NAGase-catalyzed reactions.*

The following procedures were used to determine kinetic parameters for NAGlucal hydration catalyzed by jack bean NAGase. Seven 1.00-mL reaction buffer mixes containing NaCl (100 m$M$), citrate (5 m$M$, pH 5.0), BSA (0.01%), and one of 7 different NAGlucal concentrations were prepared. Reactions (at 25 °C) were started by injecting 2 μg of jack bean NAGase into each solution. Reactions were incubated at 25 °C for 8 min, then stopped by boiling for 30 sec (the latter step irreversibly denatured the enzyme, but did not result in significant decomposition of other components of the reaction). Water was removed by lyophilization, and then the residue remaining in each reaction tube was resuspended with 0.100 mL of double-deionized water. Aliquots (0.080 mL) of each reaction were analyzed by HPLC using a Bio-Rad® Aminex® HPX-87H column (300 × 7.8 mm) with 13 m$M$ H$_2$SO$_4$ as the eluant, which separated GlcNAc and ManNAc. A GlcNAc standard curve was prepared by following the above procedure for the enzymatic reactions (but without addition of the enzyme) using 8 different concentrations of GlcNAc standard. The concentration of the enzyme reaction product was determined by measuring the area of the GlcNAc peak, which was corrected by subtracting the area of the GlcNAc peak in appropriate controls (reactions with the same concentration of NAGlucal but without enzyme), and then comparing the corrected peak area with the standard curve. Determinations of $K_m$ and $V_{max}$ values were as described above.

## 5.3. PROTEIN MASS SPECTROMETRY OF NITROGLUCAL-INACTIVATED pABG5.

Ion-spray protein mass spectrometry was carried out on a PE-Sciex API III triple quadrupole instrument (Sciex, Thornhill, Ontario) in the laboratory of Prof. R. Aebersold at the Biomedical Research Centre of the University of British Columbia. Spectra were collected in the LC-MS mode (single MS) by Dr. S. C. Miao. Prior to mass spectrometry the protein samples were centrifuged to remove insoluble matter. Low molecular mass compounds were removed by HPLC using a 1.00-mm microbore PLRP-S column (Michrom Bioresources Inc.). The following gradient was applied to elute the protein from the column: 20% solvent B in solvent A to 100% solvent B over 10 min, followed by 100% solvent B over 2 min. The composition of solvent A was 0.05% TFA, 2% acetonitrile in water. The composition of solvent B was 0.045% TFA, 80% acetonitrile in water.

The experimental conditions for the preparation of nitroglucal-inactivated pABG5 (0.100 mg, 2.5 mg/mL) were the same as those used in previous inactivation experiments (described above).

APPENDIX I: SUPPLEMENTARY DATA



(a)

(b)
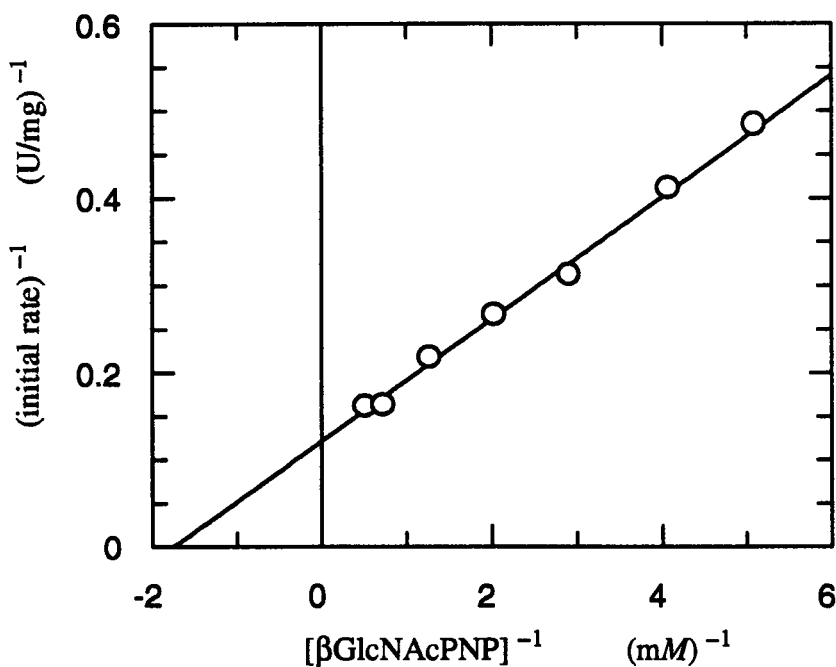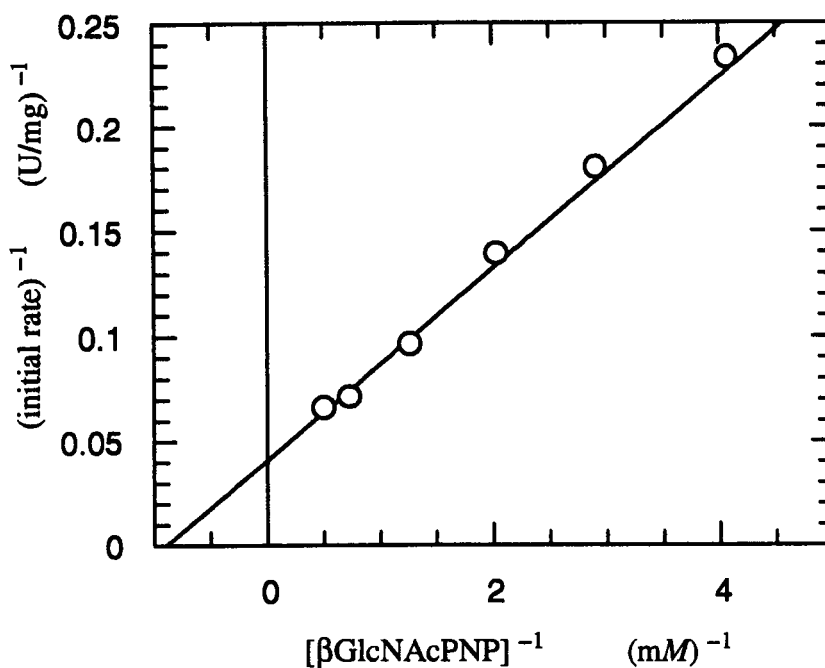
Figure A-I.1. Determination of $K_m$ and $V_{max}$ for βGlcNAcPNP hydrolysis by K-NAGase and H-NAGase.

Reactions were performed at pH 4.25 and 25 °C in 50 m$M$ citrate buffer containing 0.1% BSA, 100 m$M$ NaCl, and β-$N$-acetylhexosaminidase and βGlcNAcPNP as indicated below.

(a) K-NAGase (2.0 µg/mL). Reactions contained 0.25, 0.34, 0.49, 0.79, 1.38, or 1.96 m$M$ βGlcNAcPNP.
(b) H-NAGase (4.2 µg/mL). Reactions contained 0.20, 0.25, 0.34, 0.49, 0.79, 1.38, or 1.96 m$M$ βGlcNAcPNP.
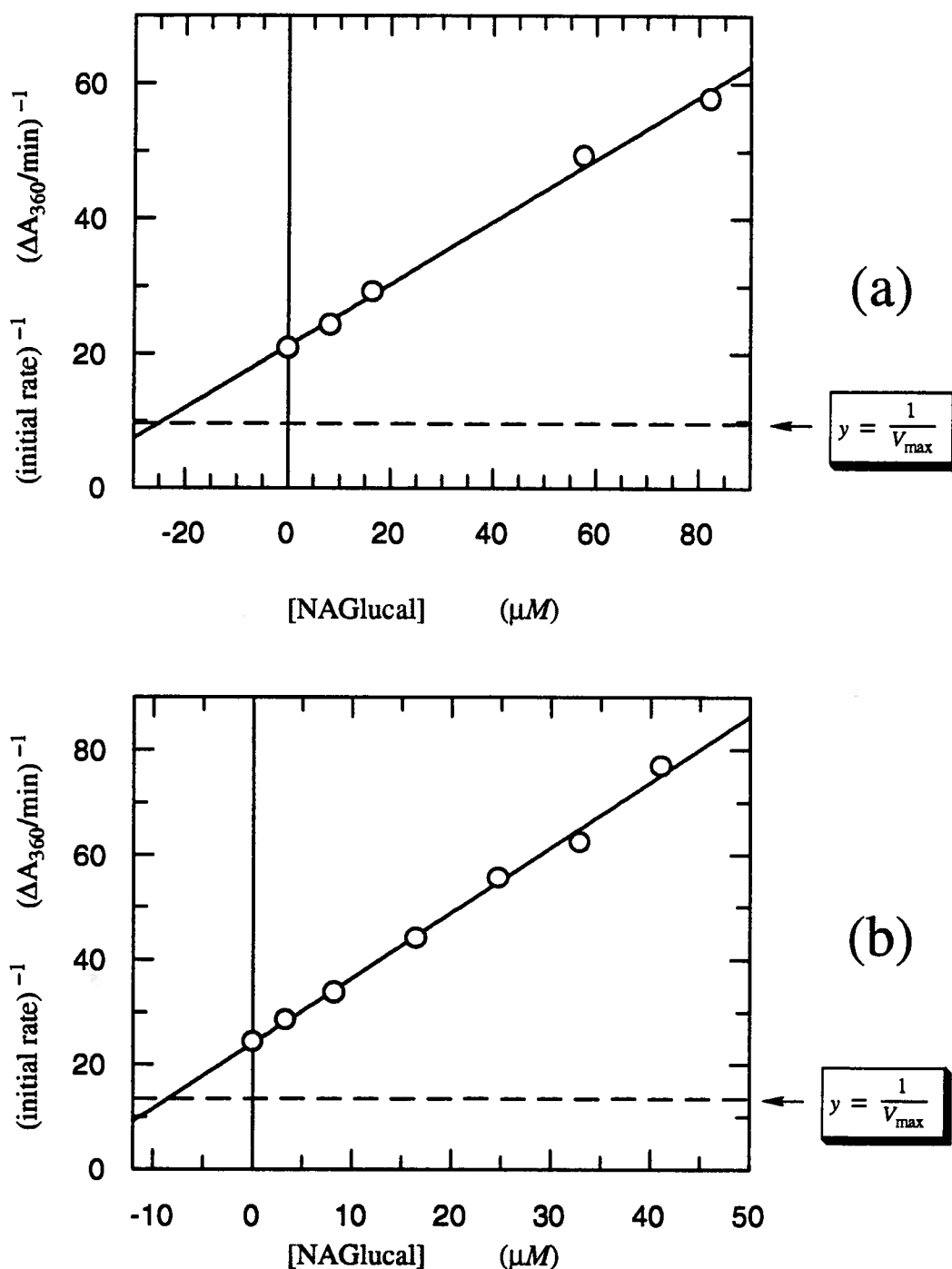
**Figure A-I.2.** Estimation of $K_i$ values for the inhibition of K-NAGase and H-NAGase by NAGlucal.

Reactions were performed at pH 4.25 and 25 °C in 50 m$M$ citrate buffer containing 0.1% BSA, 100 m$M$ NaCl, and β-$N$-acetylhexosaminidase, βGlcNAcPNP, and NAGlucal as indicated below.

(a) $RF$ $K_i$ determination for the inhibition of K-NAGase (2.0 μg/mL). The concentration of βGlcNAcPNP in the reactions was 0.98 m$M$. Reactions contained 0, 8.2, 16, 58, or 82 μ$M$ NAGlucal.

(a) $RF$ $K_i$ determination for the inhibition of H-NAGase (4.2 μg/mL). The concentration of βGlcNAcPNP in the reactions was 0.79 m$M$. Reactions contained 0, 3.3, 8.2, 16, 25, 33, or 41 μ$M$ NAGlucal.
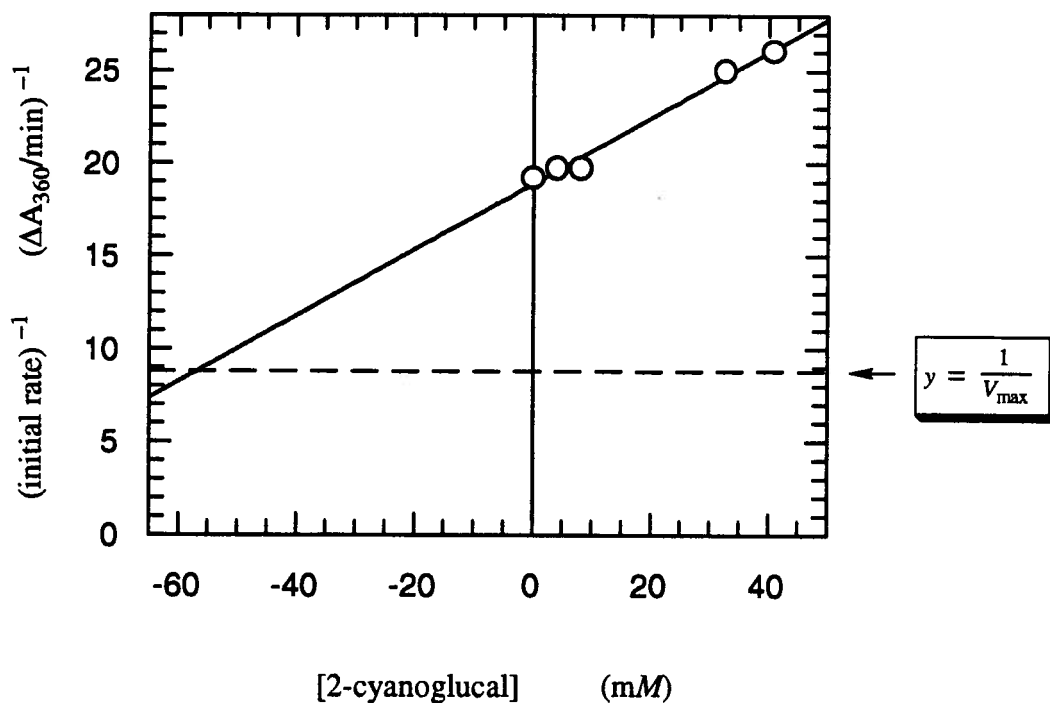
**Figure A-I.3.** Estimation of the $K_i$ for the inhibition of J-NAGase by 2-cyanoglucal.

Reactions were performed at pH 5.0 and 25 °C in 50 m$M$ citrate buffer containing 0.1% BSA and 1.0 $\mu$g/mL of $\beta$-$N$-acetylhexosaminidase from jack beans. The concentration of $\beta$GlcNAcPNP in the reactions was 0.58 m$M$. The concentrations of 2-cyanoglucal in the reactions were 0, 4.1, 8.2, 33, and 41 m$M$.

# APPENDIX II: SIMPLE THEORETICAL TREATMENT OF ENZYME CATALYSIS.

*A-II.1. ENZYME CATALYSIS IN THE ABSENCE OF INHIBITION.*

A general theory of enzyme action and kinetics was developed by Michaelis & Menten (1913), which

confirmed the earlier work of Henri (1902) (see Segel, 1975). Later, a more general treatment was given by

Briggs & Haldane (1925), who introduced the idea of the steady-state. In the absence of inhibition, a simple

reaction with *one* substrate and *one* enzyme (in this case a protein that acts as a catalyst) can be expressed as

shown below, where the free enzyme (E) first combines with the substrate (S) to form *one* distinct

enzyme-substrate complex (ES), which may then be converted to the free enzyme and *one* product (P).

$$E + S \underset{k_{-1}}{\overset{k_1}{\rightleftharpoons}} ES \xrightarrow{k_2} E + P$$

The other assumptions (in addition to those described above) underlying the Henri-Michaelis-Menten

treatment of enzyme catalysis are listed below (Segel, 1975):

(i) The concentration of the substrate is much greater than that of the enzyme, thus the formation of the enzyme-substrate complex does not significantly alter the concentration of the substrate.

(ii) The enzyme and the substrate react rapidly to form the enzyme-substrate complex.

(iii) The enzyme, substrate, and enzyme-substrate complex establish a *rapid equilibrium*, thus the rate at which the enzyme-substrate complex dissociates to form the free enzyme and the substrate ($k_{-1}$) greatly exceeds the rate of conversion of the enzyme-substrate complex to form the free enzyme and the product ($k_2$).

(iv) The rate-limiting step in the reaction is therefore the conversion of the enzyme-substrate complex to form the free enzyme and the product.

(v) Only the *initial* velocity of the reaction is considered, thus the reverse reaction (from the free enzyme and the product) to form the enzyme-substrate complex is ignored.

Under steady-state conditions (Briggs & Haldane, 1925):

$$\frac{d\,[ES]}{d\,t} = k_1[E][S] - k_{-1}[ES] - k_2[ES] = 0 \tag{1}$$

$$k_1[E][S] = k_{-1}[ES] + k_2[ES] \tag{2}$$

The *total* concentration of the enzyme, $[E]_o$, is the sum of the concentrations of free and substrate-bound enzyme species.

$$[E]_o = [E] + [ES] \tag{3}$$

Solving for [ES] using Equations 2 and 3, one obtains:

$$[ES] = \frac{k_1[E]_o[S]}{k_{-1} + k_2 + k_1[S]} \tag{4}$$

The initial velocity *(v)* of the reaction is equal to the initial rate of formation of the product:

$$v = \frac{d[P]}{dt} = k_2[ES] \tag{5}$$

Substituting Equation 4 into 5, one obtains:

$$v = \frac{k_2 k_1[E]_o[S]}{k_{-1} + k_2 + k_1[S]}$$

which can be expressed as the Michaelis-Menten (or Henri-Michaelis-Menten) equation:

$$v = \frac{k_{cat}[E]_o[S]}{K_m + [S]} \tag{6}$$

Some kinetic parameters derived from Equation 6 are given below:

| | | |
|---|---|---|
| **Catalytic constant:** | $k_{cat} = k_2$ | The first-order rate constant for the conversion of the enzyme-substrate complex to form the product. |
| **Michaelis constant:** | $K_m = \dfrac{k_{-1} + k_2}{k_1}$ | When $k_{-1} \gg k_2$, $K_m \approx K_s = k_{-1}/k_1$, the dissociation constant of the ES. |
| **Specificity constant:** | $\dfrac{k_{cat}}{K_m} = \dfrac{k_1 k_2}{k_{-1} + k_2}$ | A second-order constant that relates the reaction rate to the concentration of the *free* enzyme, [E], rather than that of the total enzyme, $[E]_o$. |
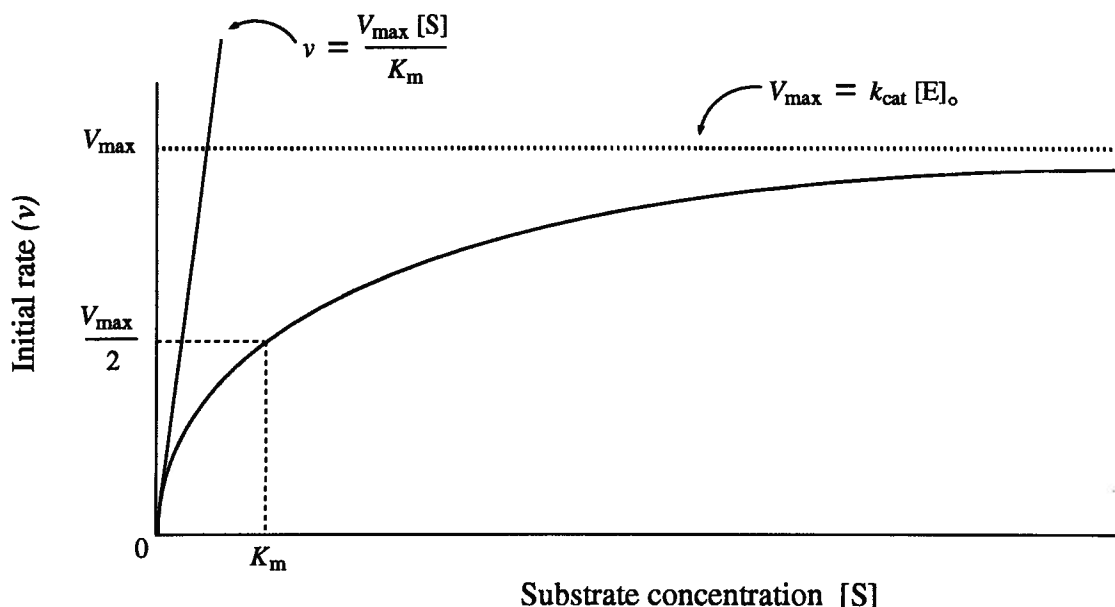
**Figure A-II.1.** Michaelis-Menten kinetics of an enzyme-catalyzed reaction.

The effect of substrate concentration on the rate of the enzyme-catalyzed reaction is shown in Fig. A-II.1. At low concentrations of substrate, where $[S] \ll K_m$, the initial rate of the reaction is proportional to the substrate concentration:

$$v = \frac{k_{cat}\,[E]_o\,[S]}{K_m} \tag{7}$$

In contrast, at saturating concentrations of the substrate, where $[S] \gg K_m$, the initial rate of the reaction becomes independent of the substrate concentration, and approaches a constant maximum rate, $V_{max}$:

$$v = k_{cat}\,[E]_o = V_{max} \tag{8}$$

It also follows from the above that when the initial rate of the reaction is equal to one-half of the maximal velocity ($v = V_{max}/2$), the substrate concentration is equal to the Michaelis constant, $K_m$. The value of $K_m$ gives a measure of the stability of the enzyme-substrate complex. An enzyme has a high affinity for a substrate with a low $K_m$.

The Henri-Michaelis-Menten equation is often transformed into a linear form for analyzing data graphically and detecting deviations from ideal behaviour. One of the most commonly used transformations is the double-reciprocal form introduced by Lineweaver & Burk (1934). This type of plot is shown in Fig. A-II.2, and the equation used to plot the data is obtained by simply taking the reciprocal of both sides of Equation 6:

$$\frac{1}{v} = \frac{1}{V_{max}} + \frac{K_m}{V_{max}} \left( \frac{1}{[S]} \right)$$
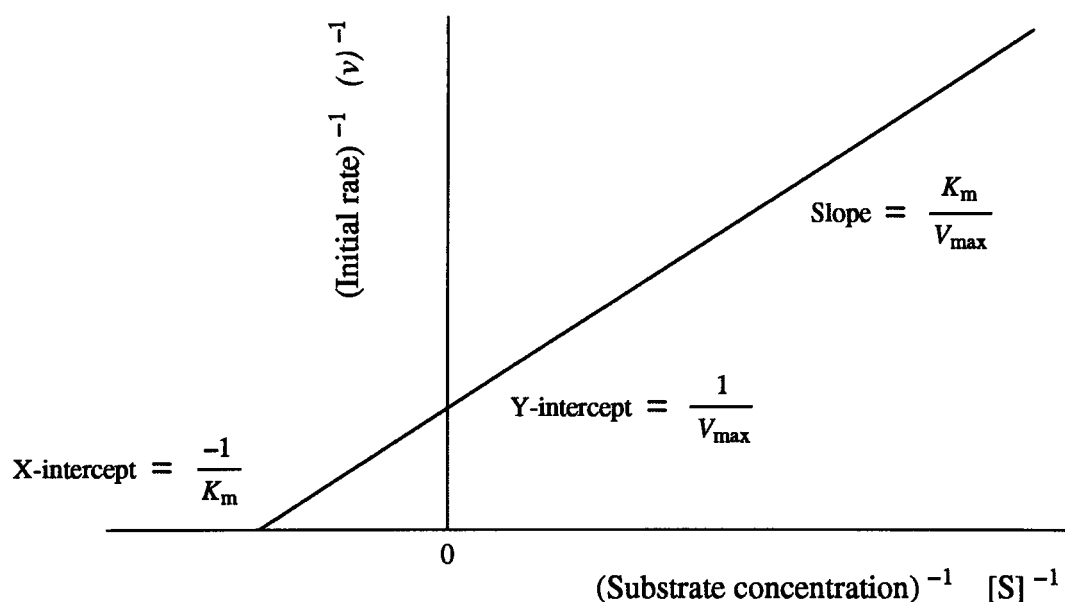


**Figure A-II.2.** Double-reciprocal (or Lineweaver-Burk) plot of the Henri-Michaelis-Menten equation.

*A-II.2. THE INHIBITION OF ENZYME CATALYSIS.*

**A-II.2.1. Irreversible inhibition.**

Irreversible inhibition (or inactivation) has already been dealt with in Section 5.2.4 (d) of Chapter 5.

### A-II.2.2. Reversible inhibition.

*a. The three types of reversible inhibition.*

There are three major types of reversible inhibition: competitive, noncompetitive, and uncompetitive. In each case the effects of these types of inhibition can be analyzed using the simple theoretical treatment discussed above.

*b. Competitive inhibition.*

A competitive inhibitor competes with the normal substrate for binding in the active site of the free enzyme. The binding of either the competitive inhibitor or the substrate in the active site is mutually exclusive. The reactions describing competitive inhibition are shown below:

$$\text{E} + \text{S} \xrightleftharpoons[\quad]{K_s} \text{ES} \xrightarrow{k_{cat}} \text{E} + \text{P}$$

$$+$$
$$\text{I}$$

$$K_i \updownarrow$$

$$\text{EI}$$

$$K_s = \frac{[\text{E}][\text{S}]}{[\text{ES}]} \qquad K_i = \frac{[\text{E}][\text{I}]}{[\text{EI}]}$$
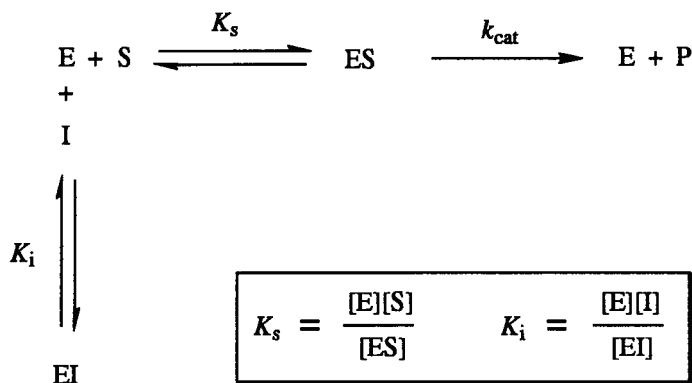
The substrate constant ($K_s$) is the dissociation constant for the enzyme-substrate complex, and the inhibition constant ($K_i$) is the dissociation constant for the enzyme-inhibitor complex. The catalytic constant ($k_{cat}$) is the rate constant for the conversion of the enzyme-substrate complex to form the free enzyme and the product.

$$[\text{E}]_o = [\text{E}] + [\text{ES}] + [\text{EI}] \qquad\qquad (9)$$

Using Equation 9, the steady-state assumption ($d$ [ES]/$d$ t = 0), and the expression $v = k_2[\text{ES}]$, one can derive the rate equation for competitive inhibition:

$$v = \frac{V_{max}\,[S]}{K_m \left(1 + \dfrac{[I]}{K_i}\right) + [S]}$$ (10)

A competitive inhibitor increases the apparent $K_m$ by a factor of $(1 + [I]/K_i)$. With a competitive inhibitor the factor $(1 + [I]/K_i)$ is a function of $[I]$ that reflects the statistical distribution of the enzyme between the E and EI forms. The value of $K_{m,app}$ increases as $[I]$ increases because the formation of the EI removes some of the free enzyme, which drives the first step of the reaction to the left. The value of $V_{max}$ does not change, but the substrate concentration necessary to achieve any fraction of $V_{max}$ increases as a result of the presence of the competitive inhibitor.

Four parameters affect the degree of competitive inhibition observed: $[S]$, $[I]$, $K_m$, and $K_i$. The degree of inhibition decreases as $[S]$ increases and $[I]$ remains constant, whereas the degree of inhibition increases as $[I]$ increases and $[S]$ remains constant. The degree of inhibition at any given $[S]$ and $[I]$ is larger with smaller values of $K_i$. When $[I] = K_i$, the slope of the double-reciprocal plot ($1/v$ vs. $1/[S]$) is twice that of the uninhibited reaction, and the value of $K_{m,app}$ is $2K_m$.

*c. Noncompetitive inhibition.*

A noncompetitive inhibitor can bind to the free enzyme or the ES. In both cases the inhibitor binds at a site *other* than the active site, thus the binding of a noncompetitive inhibitor and the substrate are independent events. The reactions describing noncompetitive inhibition are shown below:



$$K_s = \frac{[E][S]}{[ES]} = \frac{[EI][S]}{[ESI]}$$

$$K_i = \frac{[E][I]}{[EI]} = \frac{[ES][I]}{[ESI]}$$

$$[E]_o = [E] + [ES] + [EI] + [ESI] \tag{11}$$

Using Equation 11, the steady-state assumption ($d$ [ES]/$d$ t = 0), and the expression $v = k_2$[ES], one can derive the rate equation for noncompetitive inhibition:
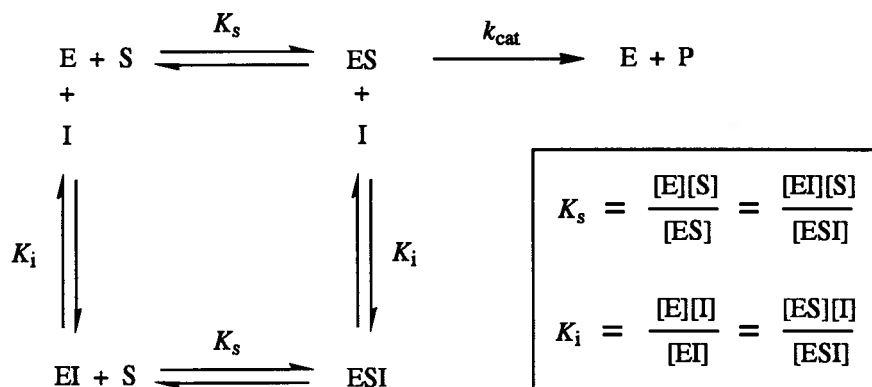
$$v = \frac{\left( \dfrac{V_{max}}{1 + \dfrac{[I]}{K_i}} \right) [S]}{K_m + [S]} \tag{12}$$

A noncompetitive inhibitor does not affect the value of $K_m$ because at any [I] both of the substrate-binding forms of the enzyme (E and EI) have equal affinities for the substrate. The inhibitor decreases the value of the apparent $V_{max}$ by a factor of $(1 + [I]/K_i)$. With a noncompetitive inhibitor the factor $(1 + [I]/K_i)$ is a function of [I] that reflects the statistical distribution of the enzyme-substrate complexes between the ES and ESI forms. In the presence of a noncompetitive inhibitor, the steady-state concentration of the ES is decreased at all [S], and can never approach $[E]_o$, no matter how high [S] may be. However, the value of $k_{cat}$ is unchanged. The overall effect of a noncompetitive inhibitor is to reduce the effective concentration of the enzyme.

With a noncompetitive inhibitor the degree of inhibition only depends on [I] and $K_i$. The degree of inhibition increases as [I] increases. For a given [I], the degree of inhibition is constant, regardless of the values of [S] or $K_m$. The degree of inhibition at any given [I] is larger with smaller values of $K_i$. The [I] that causes 50% inhibition (at all [S]) equals $K_i$.

*d. Uncompetitive inhibition.*

An uncompetitive inhibitor can only bind to the enzyme-substrate complex. The inhibitor is unable to bind to the free enzyme. This type of inhibition is rarely observed in one-substrate reactions, but is common in steady-state multireactant systems. The reactions describing uncompetitive inhibition are shown below:

$$E + S \; \overset{K_s}{\rightleftharpoons} \; ES \; \overset{k_{cat}}{\longrightarrow} \; E + P$$

$$+$$
$$I$$

$$\Big\updownarrow K_i$$

$$ESI$$

$$K_s = \frac{[E][S]}{[ES]}$$

$$K_i = \frac{[ES][I]}{[ESI]}$$

$$[E]_o = [E] + [ES] + [ESI] \tag{13}$$

Using Equation 13, the steady-state assumption ($d\,[ES]/d\,t = 0$), and the expression $v = k_2[ES]$, one can derive the rate equation for uncompetitive inhibition:
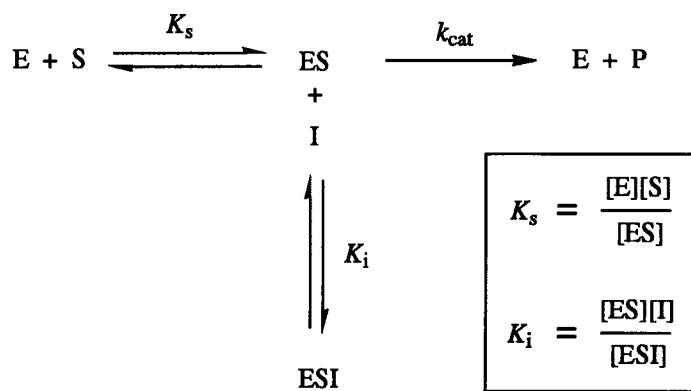
$$v = \frac{\left(\dfrac{V_{max}}{1 + \dfrac{[I]}{K_i}}\right)[S]}{\left(\dfrac{K_m}{1 + \dfrac{[I]}{K_i}}\right) + [S]} \tag{14}$$

An uncompetitive inhibitor decreases the values of both the apparent $V_{max}$ and the apparent $K_m$ by a factor of $(1 + [I]/K_i)$. With an uncompetitive inhibitor the factor $(1 + [I]/K_i)$ is a function of $[I]$ that reflects the statistical distribution of the enzyme-substrate complexes between the ES and ESI forms. In the presence of an uncompetitive inhibitor the value of $k_{cat}$ is unchanged, but the steady-state concentration of the ES is decreased at all $[S]$, and can never approach $[E]_o$, no matter how high $[S]$ may be. The value of $K_{m,app}$ decreases as $[I]$

increases because the formation of the ESI removes some of the ES, which drives the first step of the reaction to the right. Thus an uncompetitive inhibitor can be viewed as an *activator* with respect to $K_m$ (as $K_{m,app} < K_m$), and at low $[S]$ (i.e., first-order kinetics), the effects of the inhibitor on $K_m$ and $V_{max}$ essentially cancel, and little if any inhibition is observed.

Four parameters affect the degree of uncompetitive inhibition observed: [S], [I], $K_m$, and $K_i$. The

degree of inhibition increases as [I] increases and [S] remains constant. However, in contrast to the case of

competitive inhibition, with uncompetitive inhibition the degree of inhibition *increases* as [S] increases and [I]

remains constant. This is because the [ES] increases as the [S] increases, and an uncompetitive inhibitor can

only bind to the ES. For the same reason the degree of uncompetitive inhibition is inversely related to the value

of $K_m$, again in contrast to the case of competitive inhibition. The degree of inhibition at any given [S] and [I] is

larger with smaller values of $K_i$.

*e. Graphical methods for distinguishing different types of reversible inhibition.*

The three types of reversible inhibition discussed above can be identified and distinguished by

graphical methods. The two most commonly used graphical methods are double-reciprocal plots and Dixon

plots. These are shown in Fig. A-II.3, along with the appropriate forms of the rate equations used to plot the

data.

In this very brief Appendix, only the three "pure" types of reversible inhibition have been discussed.

Table A-II.1 provides a summary of some of the kinetic parameters that may be obtained for these three cases.

Intermediate (or mixed) inhibition behaviour may also occur. For a thorough treatment of these cases the work

of Segel (1975) is highly recommended.

---

**Figure A-II.3.** Some graphical methods for distinguishing different types of reversible inhibition.

---

This figure appears on the following page. Double-reciprocal plots (1) appear on the left, and Dixon plots (2) appear on the right. The appropriate form of the rate equation appears at the bottom of each panel.

(C) Competitive inhibition; (N) Noncompetitive inhibition; (U) Uncompetitive inhibition.

---

**C.1**

Increasing [I]

$\frac{1}{v}$

y-intercept $= \dfrac{1}{V_{max}}$

$\dfrac{-1}{K_m\left(1 + \dfrac{[I]}{K_i}\right)} = $ x-intercept

$0$

$\dfrac{1}{[S]}$

$$\frac{1}{v} = \frac{K_m}{V_{max}}\left(1 + \frac{[I]}{K_i}\right)\frac{1}{[S]} + \frac{1}{V_{max}}$$

**C.2**

Decreasing [S]

$\frac{1}{v}$

y-intercept $= \left(1 + \dfrac{K_m}{[S]}\right)\dfrac{1}{V_{max}}$

$y = \dfrac{1}{V_{max}}$

x-intercept $= -K_i\left(1 + \dfrac{[S]}{K_m}\right)$

$x = -K_i$

$0$

$[I]$

$$\frac{1}{v} = \left(\frac{K_m}{V_{max}K_i[S]}\right)[I] + \left(1 + \frac{K_m}{[S]}\right)\frac{1}{V_{max}}$$

**N.1**

Increasing [I]

$\frac{1}{v}$

y-intercept $= \dfrac{\left(1 + \dfrac{[I]}{K_i}\right)}{V_{max}}$

$\dfrac{-1}{K_m} = $ x-intercept

$0$

$\dfrac{1}{[S]}$

$$\frac{1}{v} = \frac{K_m}{V_{max}}\left(1 + \frac{[I]}{K_i}\right)\frac{1}{[S]} + \left(1 + \frac{[I]}{K_i}\right)\frac{1}{V_{max}}$$

**N.2**

Decreasing [S]

$\frac{1}{v}$

y-intercept $= \left(1 + \dfrac{K_m}{[S]}\right)\dfrac{1}{V_{max}}$

x-intercept $= -K_i$

$0$

$[I]$

$$\frac{1}{v} = \left[\frac{\left(1 + \dfrac{K_m}{[S]}\right)}{V_{max}K_i}\right][I] + \left(1 + \frac{K_m}{[S]}\right)\frac{1}{V_{max}}$$

**U.1**

Increasing [I]

$\frac{1}{v}$

y-intercept $= \dfrac{\left(1 + \dfrac{[I]}{K_i}\right)}{V_{max}}$

$\dfrac{-\left(1 + \dfrac{[I]}{K_i}\right)}{K_m} = $ x-intercept

$0$

$\dfrac{1}{[S]}$

$$\frac{1}{v} = \left(\frac{K_m}{V_{max}}\right)\frac{1}{[S]} + \left(1 + \frac{[I]}{K_i}\right)\frac{1}{V_{max}}$$

**U.2**

Decreasing [S]

$\frac{1}{v}$

y-intercept $= \left(1 + \dfrac{K_m}{[S]}\right)\dfrac{1}{V_{max}}$

$-K_i\left(1 + \dfrac{K_m}{[S]}\right) = $ x-intercept

$0$

$[I]$

$$\frac{1}{v} = \left(\frac{1}{V_{max}K_i}\right)[I] + \left(1 + \frac{K_m}{[S]}\right)\frac{1}{V_{max}}$$

**Table A-II.1.** Some kinetic parameters for different types of reversible inhibition.

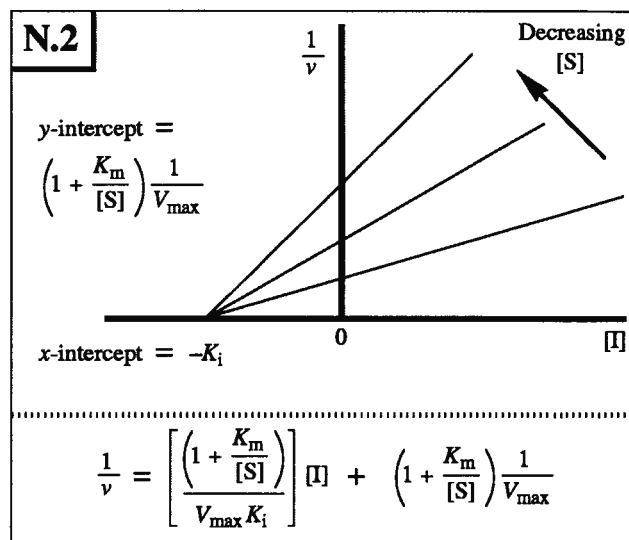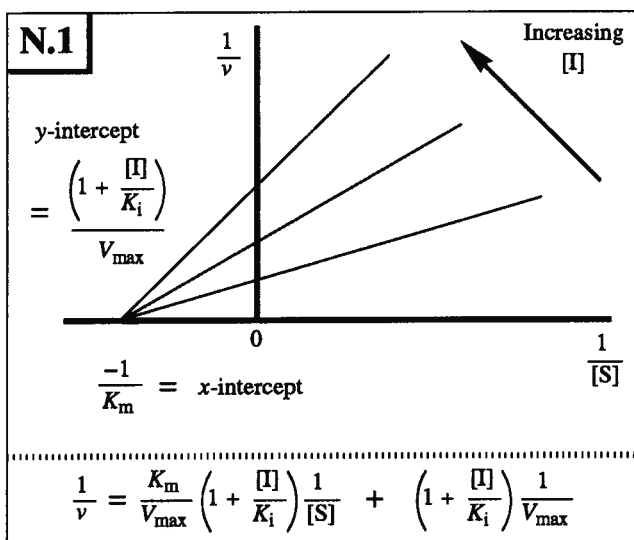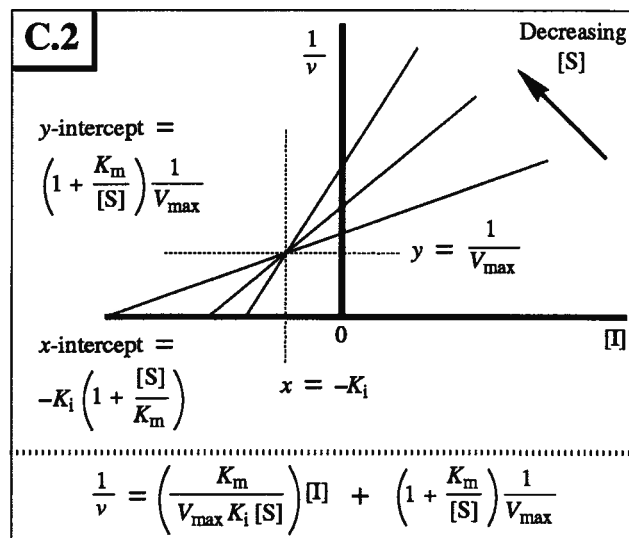| Type of inhibition | Apparent $V_{max}$ | Apparent $K_m$ | Degree of inhibition[a] |
|---|---|---|---|
| Competitive | $V_{max}$ | $K_m\left(1 + \dfrac{[I]}{K_i}\right)$ | $\dfrac{K_m\left(\dfrac{[I]}{K_i}\right)}{K_m\left(1 + \dfrac{[I]}{K_i}\right) + [S]}$ |
| Noncompetitive | $\dfrac{V_{max}}{1 + \dfrac{[I]}{K_i}}$ | $K_m$ | $\dfrac{[I]}{[I] + K_i}$ |
| Uncompetitive | $\dfrac{V_{max}}{1 + \dfrac{[I]}{K_i}}$ | $\dfrac{K_m}{1 + \dfrac{[I]}{K_i}}$ | $\dfrac{[S]\left(\dfrac{[I]}{K_i}\right)}{K_m + \left(1 + \dfrac{[I]}{K_i}\right)[S]}$ |

(a) The degree of inhibition, $i$, is defined by the equation $i = [v_o - v_i]/v_o$, where $v_o$ and $v_i$ are the velocities of (otherwise identical) reactions in the absence and presence of the inhibitor, respectively (Segel, 1975).

**REFERENCES**

Acharya, K. R., Stuart, D. I., Varvill, K. M., & Johnson, L. N. (1991). *Glycogen phosphorylase b.* World Scientific Publishers, Singapore.

Anderson, W. F., Grütter, M. G., Remington, S. J., Weaver, L. H., & Matthews, B. W. (1981). *J. Mol. Biol.* **147**, 523.

Atsumi, S., Iinuma, H., Nosaka, C., & Umezawa, K. (1990b). *J. Antibiot.* **43**, 1579-1585.

Atsumi, S., Umezawa, K., Iinuma, H., Naganawa, H., Nakamura, H., Itake, Y., & Takeuchi, T. (1990a). *J. Antibiot.* **43**, 49-53.

Banait, N. S., & Jencks, W. P. (1991). *J. Am. Chem. Soc.* **113**, 7951.

Barranger, J. A., & Ginns, E. I. (1989). In *The Metabolic Basis of Inherited Disease*, 6th ed. (Scriver, C. R., Beaudet, A. L., Sly, W. S., & Valle, D., Eds.) p 1677, McGraw-Hill, New York.

Barton, N. W., Brady, R. O., Dambrosia, J. M., DiBisceglie, A. M., Doppelt, S. H., Hill, S. C., Mankin, H. J., Murray, G. J., Parker, R. I., & Argoff, C. E. (1991). *N. Engl. J. Med.* **324**, 1464.

Baumberger, F., Beer, D., Christen, M., Prewo, R., & Vasella, A. (1986). *Helv. Chim. Acta* **69**, 1191.

Bause, E., & Legler, G. (1974). *Hoppe-Seyler's Z. Physiol. Chem.* **355**, 438.

Bearpark, T. M., & Stirling, J. (1978). *Biochem. J.* **173**, 997.

Beer, D., Bieri, J. H., Macher, I., Prewo, R., & Vasella, A. (1986). *Helv. Chim. Acta* **69**, 1172.

Berghem, L., & Pettersson, L. (1974). *Eur. J. Biochem.* **46**, 295.

Berghem, L., Pettersson, L., & Axiofedriksson, U. (1975). *Eur. J. Biochem.* **53**, 55.

Bernacki, R. J., Niedbala, M. J., & Korytnyk, W. (1985). *Cancer Metastasis Rev.* **4**, 81.

Beutler, E., Kay, A., Saven, A., Garver, P., Thurston, D., Dawson, A., & Rosenbloom, B. (1991). *Blood* **78**, 1183.

Blake, C. C. F., Mair, G. A., North, A. C. T., Phillips, D. C., & Sarma, V. R. (1967). *Proc. R.oyal Soc. London, Ser. B* **167**, 365.

Briggs, G. E., & Haldane, J. B. S. (1925). *Biochem. J.* **19**, 338.

Brockhaus, M., & Lehmann, J. (1977). *Carbohydr. Res.* **53**, 21.

Buc, M. H., & Buc, H. (1968). *Regulation of Enzyme Activity and Allosteric Interactions*, p 109. Academic Press, New York.

Bunton, C. A., & Humeres, E. (1969). *J. Org. Chem.* **34**, 572.

Chiba, S., Brewer, C. F., Okada, G., Matsui, H., & Hehre, E. J. (1988). *Biochemistry* **27**, 1564.

Claus, K., & Bestian, H. (1962). *Justus Liebigs Ann. Chem.* **654**, 8.

Conzelmann, E. & Sandhoff, K. (1987). *Adv. Enzymol.* **60**, 89.

Conzelmann, E., Burg, J., Stephan, G., & Sandhoff, K. (1982). *Eur. J. Biochem.* **123**, 455.

Corey, E. J., & Venkateswarlu, A. (1972). *J. Am. Chem. Soc.* **94**, 6190.

Cori, C. F., & Cori, G. T. (1936). *Proc. Soc. Exp. Biol. Med.* **34**, 702.

Coxon, B., & Fletcher Jr., H. G. (1963). *J. Am. Chem. Soc.* **85**, 2637.

Dale, M. P., Ensley, H. E., Kern, K., Sastry, K. A. R., & Byers, L. D. (1985). *Biochemistry* **24**, 3530.

Dance, N. E., Price, R. G., & Robinson, D. (1970). *Biochim. Biophys. Acta* **222**, 662.

Day, A. G., & Withers, S. G. (1986). *Biochem. Cell Biol.* **64**, 914.

Derome, A. E. (1988). *Modern NMR Techniques for Chemistry Research.* Pergamon, Oxford.

Dinur, T., Osiecki, K. M., Legler, G., Gatt, S., Desnick, R. J., & Grabowski, G. A. (1986). *Proc. Natl. Acad. Sci. U. S. A.* **83**, 1660.

Dixon, M. (1972). *Biochem. J.* **129**, 197.

Duerksen, J., & Halvorson, H. (1958). *J. Biol. Chem.* **233**, 1113.

Engers, H. D., Bridger, W. A., & Madsen, N. B. (1969). *J. Biol. Chem.* **244**, 5936.

Engers, H. D., Shechosky, S., & Madsen, N. B. (1970). *Can. J. Biochem.* **48**, 746.

Fallet, S., Grace, M. E., Sibille, A., Mendelson, D. S., Shapiro, R. S., Hermann, G., & Grabowski, G. A. (1992). *Pediatr. Res.* **31**, 496.

Fischer, E. H., & Krebs, E. G. (1955). *J. Biol. Chem.* **216**, 121.

Fleet, G. W. J., Smith, P. W., Nash, R. J., Fellows, L. E., Parekh, R. B., & Rademacher, T. W. (1986). *Chem. Lett.* 1051.

Friesen, R. W., Sturino, C. F., Daljeet, A. K., & Kolaczewska, A. (1991). *J. Org. Chem.* **59**, 1944.

Fritz, H., Lehmann, J., & Schlesselmann, P. (1983). *Carbohydr. Res.* **113**, 71.

Fuchs, E. F., & Lehmann, J. (1975). *Chem. Ber.* **108**, 2254.

Gaucher, P. C. E. (1882). M.D. thesis. University of Paris.

Gaudemer, A. (1977). In *Stereochemistry Fundamentals and Methods Vol. 1: Determination of Configurations by Spectrometric Methods* (Kagan, H. B., Ed.) pp 44-136, Georg Thieme Publishers, Stuttgart.

Gebler, J. G., Aebersold, R., & Withers, S. G. (1992). *J. Biol. Chem.* **267**, 11126.

Gold, A. M., Johnson, R. M., and Tseng, J. K. (1970). *J. Biol. Chem.* **245**, 2565.

Gold, A. M., Legrand, E., & Sanchez, G. R. (1971). *J. Biol. Chem.* **246**, 5700.

Gordon, A. J., & Ford, R. A. (1972). *The Chemist's Companion: A Handbook of Practical Data, Techniques, and References;* p 293. John Wiley & Sons, New York.

Grabowski, G. A. (1993). In *Advances in Human Genetics* (Harris, H., & Hirschhorn, K., Eds.) Vol. 21 p 377, Plenum, New York.

Grabowski, G. A., Gatt, S., & Horowitz, M. (1990). *CRC Crit. Rev. Biochem. Mol. Biol.* **25**, 385.

Greene, T. W., & Wuts, P. G. M. (1991). *Protective Groups in Organic Synthesis,* 2nd ed. John Wiley & Sons, New York.

Hajdu, J., Acharya, K. R., Stuart, D. I., McLaughlin, P. J., Barford, D., Oikonomakos, N. G., Klein, H., & Johnson, L. N. (1987). *EMBO J.* **6**, 539.

Hall, R. H., & Jordaan, A. (1973). *J. Chem. Soc. Perkin Trans. 1*, 1059.

Hall, R. H., Jordaan, A., & Lourens, G. J. (1973). *J. Chem. Soc. Perkin Trans. 1*, 38.

Han, Y., & Srinivasan, V. (1969). *J. Bacteriol.* **100**, 1355.

Hayashi, S. I., Nakai, T., Ishikawa, N., Burton, D. J., Neae, D. G., & Kessling, H. S. (1979). *Chem. Lett.*, 983.

Hehre, E. J., Brewer, C. F., Uchiyama, T., Schlesselmann, P., & Lehmann, J. (1980). *Biochemistry* 19, 3557.

Hehre, E. J., Genghof, D. S., Sternlicht, H., & Brewer, C. F. (1977). *Biochemistry* 16, 1780-1787.

Hehre, E. J., Kitahata, S., & Brewer, C. F. (1986). *J. Biol. Chem.* 261, 2147.

Helferich, B., & Iloff, A. (1933). *Hoppe-Seyler's Z. Physiol. Chem.* 221, 252.

Helmreich, E. J. M. (1992). *BioFactors* 3, 159.

Henri, V. (1902). *Acad. Sci., Paris* 135, 916.

Herrchen, M., & Legler, G. (1984). *Eur. J. Biochem.* 138, 527.

Holzapfel, C. W., Marais, C. F., & van Dyk, M. S. (1988). *Synth. Commun.* 18, 97.

Horton, D., & Priebe, W. (1981). *Carbohydr. Res.* 94, 27.

Hough, L., & Jones, J. K. N. (1962) In *Methods in Carbohydrate Chemistry* (Whistler, R., & Wolfrom, M., Eds.) Vol. I p 28, Academic Press, New York.

Houlton, J. S., Motherwell, W. B., Ross, B. C., Tozer, M. J., Williams, D. J., & Slavin, A. M. Z. (1993). *Tetrahedron* 49, 8087.

Hu, H. Y., & Gold, A. M. (1978). *Biochim. Biophys. Acta* 525, 55.

Hultson, G. (1964). *Biochem. J.* 92, 142.

Illingworth, B., Jansz, H. S., Brown, D. H., & Cori, C. F. (1958). *Proc. Natl. Acad. Sci. U. S. A.* 44, 1180.

Imoto, T., Johnson, L. M., North, A. C. T., Phillips, D. C., & Rupley, J. A. (1972). In *The Enzymes*, 3rd ed. (Boyer, P. D., Ed.) Vol. 7 p 665, Academic Press, New York.

Johnson, L. N. (1992). *FASEB J.* 6, 2274.

Johnson, L. N., Acharya, K. R., Jordan, M. D., & McLaughlin, P. J. (1990). *J. Mol. Biol.* 211, 645.

Kanda, T., Brewer, C. F., Okada, G., & Hehre, E. J. (1986). *Biochemistry* 25, 1159.

Kastenschmidt, L. L., Kastenschmidt, J., & Helmreich, E. J. M. (1968). *Biochemistry* 7, 3590.

Kempton, J. B., & Withers, S. G. (1992). *Biochemistry* 31, 9961.

Klein, H. W., Im, M. J., & Palm, D. (1986). *Eur. J. Biochem.* 157, 107.

Klein, H. W., Im, M. J., Palm, D., & Helmreich, E. J. M. (1984). *Biochemistry* 23, 5853.

Klein, H. W., Palm, D., & Helmreich, E. J. M. (1982). *Biochemistry* 21, 6675.

Kokesh, F. C., & Kakuda, Y. (1977). *Biochemistry* 16, 2467.

Koshland, D. E. (1953). *Biol. Rev.* 28, 416.

Leatherbarrow, R. J. (1990). *GraFit™ Version 2.0.* Erithacus Software Ltd., Staines, U. K.

Lee, Y. C. (1969). *Biochem. Biophys. Res. Commun.* 35, 161.

Legler, G. (1990). *Adv. Carbohydr. Chem. Biochem.* 48, 319.

Legler, G., & Bollhagen, R. (1992). *Carbohydr. Res.* 233, 113.

Legler, G., & Harder, A. (1978). *Biochim. Biophys. Acta* 524, 102.

Legler, G., & Hasnain, S. N. (1970). *Hoppe-Seyler's Z. Physiol. Chem.* **351**, 25.

Legler, G., & Julich, E. (1984). *Carbohydr. Res.* **128**, 61.

Legler, G., Lüllau, E., Kappes, E., & Kastenholz, F. (1991). *Biochim. Biophys. Acta* **1080**, 89.

Legler, G., Roeser, K. R., & Illig, H. K. (1979). *Eur. J. Biochem.* **101**, 85.

Legler, G., Sinnott, M. L., & Withers, S. G. (1980). *J. Chem. Soc. Perkin Trans.* 2, 1376.

Lehmann, J., & Schlesselmann, P. (1983). *Carbohydr. Res.* **113**, 93.

Lemieux, R. U. (1963). In *Methods in Carbohydrate Chemistry* (Whistler, R., & Wolfrom, M., Eds.) Vol. II p 221, Academic Press, New York.

Lesimple, P., Beau, J. M., Jaurand, G., & Sinay, P. (1986). *Tetrahedron Lett.* **27**, 6201.

Li, S. C., & Li, Y. T. (1970). *J. Biol. Chem.* **245**, 5153.

Lichtenthaler, F. W., & Jarglis, P. (1982). *Angew. Chem. Suppl.* 1449.

Lineweaver, M., & Burk, D. (1934). *J. Am. Chem. Soc.* **65**, 1965.

Ludolph, J., Paschke, E., Glöss, J., & Kresse, H. (1981). *Biochem. J.* **193**, 811.

Maddaiah, V. T., & Madsen, N. B. (1966). *J. Biol. Chem.* **241**, 3873.

Madsen, N. B., & Shechosky, S. (1967). *J. Biol. Chem.* **242**, 3301.

Madsen, N. B., & Withers, S. G. (1984). In *Chemical and Biological Aspects of Vitamin B6 Catalysis, Part A* (Evangelopolous, A. E., Ed.) p 116, Alan R. Liss, New York.

Madsen, N. B., & Withers, S. G. (1986). In *Vitamin B6 Pyridoxal Phosphate: Chemical, Biochemical, and Medical Aspects, Part B* (Dolphin, D., Poulson, R., & Avramovic, O., Eds.) Chapter 11, John Wiley & Sons, New York.

Martin, J. L., Veluraja, K., Ross, K., Johnson, L. N., Fleet, G. W. J., Ramsden, N. G., Bruce, I., Orchard, M. G., Oikonomakos, N. G., Papageorgiou, A. C., Leonidas, D. D., & Tsitoura, H. S. (1991). *Biochemistry* **30**, 10101.

McCarter, J. D., Adam, M., & Withers, S. G. (1992). *Biochem. J.* **286**, 721.

McLaughlin, P. J., Stuart, D. I., Klein, H. W., Oikonomakos, N. G., & Johnson, L. N. (1984). *Biochemistry* **23**, 5862.

Metzger, B., Helmreich, E., & Glaser, L. (1967). *Proc. Natl. Acad. Sci. U. S. A.* **57**, 974.

Miao, S., Ziser, L., Aebersold, R., & Withers, S. G. (1994). *Biochemistry* **33**, 7027.

Michaelis, L., & Menten, M. L. (1913). *Biochem. Z.* **49**, 333.

Motherwell, W. B., Tozer, M. J., & Ross, B. C. (1989). *J. Chem. Soc. Chem. Commun.*, 1437.

Myers, R. W., & Lee, Y. C. (1984). *Carbohydr. Res.* **132**, 61.

Namchuk, M. N. (1993). Ph.D. Thesis. University of British Columbia.

Nelson, N. (1944). *J. Biol. Chem.* **153**, 375.

Niwa, T., Inouye, S., Tsuruoka, T., Koaze, Y., & Niida, T. (1970). *Agric. Biol. Chem.* **34**, 966.

O'Connor, J. V., Nunez, H. A., & Barker, R. (1979). *Biochemistry* **18**, 500.

Okada, S. & O'Brien, J. S. (1969). *Science* **165**, 698.

Palm, D., Klein, H. W., Schinzel, R., Buehner, M., & Helmreich, E. J. M. (1990). *Biochemistry* 29, 1099.

Park, J., & Johnson, M. (1949). *J. Biol. Chem.* 181, 149.

Pauling, L. (1946). *Chem. Eng. News* 24, 1375.

Pauling, L. (1948). *Nature (London)* 161, 707.

Petasis, N. A., & Bzowej, E. I. (1990). *J. Am. Chem. Soc.* 112, 6392.

Pokorny, M., Zissis, E., & Fletcher, H. (1975). *Carbohydr. Res.* 43, 345.

Pravdić, N., & Fletcher Jr., H. G. (1967). *J. Org. Chem.* 32, 1806.

Pravdić, N., Franjic-Mihalic, I., & Danilov, B. (1975). *Carbohydr. Res.* 45, 302.

RajanBabu, T. V., & Reddy, G. S. (1986). *J. Org. Chem.* 51, 5458.

Reissig, J. L., Strominger, J. L., & Leloir, L. F. (1955). *J. Biol. Chem.* 217, 959.

Roeser, K. R., & Legler, G. (1981). *Biochim. Biophys. Acta* 657, 321.

Roth, W., & Pigman, W. (1963). In *Methods in Carbohydrate Chemistry* (Whistler, R., & Wolfrom, M., Eds.) Vol. II p 405, Academic Press, New York.

Sandhoff, K. (1968). *Hoppe-Seyler's Z. Physiol. Chem.* 349, 1095.

Sandhoff, K. D., Andreae, U., & Jatzkewitz, H. (1968). *Life Sci.* 7, 278.

Schlesselmann, P., Fritz, H., Lehmann, J., Uchiyama, T., Brewer, C. F., & Hehre, E. J. (1982). *Biochemistry* 21, 6606-6614.

Segel, I. W. (1975). *Enzyme Kinetics.* Wiley Interscience, New York.

Shenhav, H., Rappoport, Z., & Patai, S. (1970). *J. Chem. Soc. (B)*, 469.

Sinnott, M. L. (1978). *FEBS Lett.* 94, 1.

Sinnott, M. L. (1979). *Chem. Brit.* 15, 293.

Sinnott, M. L. (1987). In *Enzyme Mechanisms* (Page, M. I., & Williams, A., Eds.) pp 259-297, The Royal Society of Chemistry, London.

Sinnott, M. L. (1990). *Chem. Rev.* 90, 1171.

Somogy, M. (1952). *J. Biol. Chem.* 195, 19.

Somsák, L., Bajza, I., & Batta, G. (1990). *Liebigs Ann. Chem.*, 1265.

Sprang, S. R., & Fletterick, R. J. (1979). *J. Mol. Biol.* 131, 523.

Stirling, J. L. (1983). In *Methods of Enzymatic Analysis*, 3rd ed. (Burgmeyer, H. U., Ed.) Vol. IV p 269, Verlag Chemie, Weinheim.

Stirtan, W. G. (1993). Ph.D. Thesis. University of British Columbia.

Street, I. P. (1988). Ph.D. Thesis. University of British Columbia.

Street, I. P., Armstrong, C., & Withers, S. G. (1986). *Biochemistry* 25, 6021.

Street, I. P., Rupitz, K., & Withers, S. G. (1989). *Biochem.* 28, 1581.

Sweeley, C. C., Bentley, R., Makita, M., & Wells, W. W. (1963). *J. Am. Chem. Soc.* 85, 2497.

Tatsuta, K., Niwata, Y., Umezawa, K., Toshima, K., & Nakata, M. (1990). *Tetrahedron Lett.* 31, 1171.

Tebbe, F. N., Parshall, G. W., & Reddy, G. S. (1977). *J. Am. Chem. Soc.* **100**, 3611.

Titani, K., Koide, A., Hermann, J., Ericsson, L. H., Kumar, S., Wade, R. D., Walsh, K. A., Neurath, H., & Fischer, E. H. (1977). *Proc. Natl. Acad. Sci. U. S. A.* **74**, 4762.

Wakarchuck, W. W., Kilburn, D. G., Miller, R. C., & Warren, R. A. J. (1986). *Molec. Gen. Genet.* **205**, 146.

Watanabe, K. (1936) *J. Biochem. (Tokyo)* **24**, 297.

Weiser, W., Lehmann, J., Chiba, S., Matzui, H., Brewer, C. F., & Hehre, E. J. (1988). *Biochemistry* **27**, 2294.

Wentworth, D. F., & Wolfenden, R. (1974). *Biochemistry* **13**, 4715.

Withers, S. G., & Rupitz, K. (1990). *Biochemistry* **29**, 6405.

Withers, S. G., & Street, I. P. (1988). *J. Am. Chem. Soc.* **110**, 8551.

Withers, S. G., & Umezawa, K. (1991). *Biochem. Biophys. Res. Commun.* **177**, 532.

Withers, S. G., Madsen, N. B., Sprang, S. R., & Fletterick, R. J. (1982). *Biochemistry* **21**, 5372.

Withers, S. G., Rupitz, K., & Street, I. P. (1988). *J. Biol. Chem.* **263**, 7929.

Withers, S. G., Warren, R. A. J., Street, I. P., Rupitz, K., Kempton, J. B., & Abersold, R. (1990). *J. Am. Chem. Soc.* **112**, 5887.

Wosilait, W. D., & Sutherland, E. W. (1956). *J. Biol. Chem.* **218**, 469.

Ya Khorlin, A., Zurabyan, S. E., Dubrovina, N. I., Bystrov, V. F., Vikha, G., & Kaverzneva, E. (1972). *Carbohydr. Res.* **21**, 316.

Zemplen, G., & Pacsu, E. (1929). *Chem. Ber.* **62**, 1613.